

Molecular Pathways Modulating the Severity of IgE-mediated Anaphylaxis

by

Amnah Nezar M. Yamani

A dissertation submitted in partial fulfillment
of the requirements for the degree of
Doctor of Philosophy
(Immunology)
in the University of Michigan
2021

Doctoral Committee:

Professor Simon P. Hogan
Professor David A. Antonetti
Associate Professor Katherine Ann Gallagher
Associate Professor J Michelle Kahlenberg
Professor Nicholas W. Lukacs

Amnah Nezar M Yamani

ayamani@umich.edu

ORCID iD: [0000-0002-5512-6220](https://orcid.org/0000-0002-5512-6220)

© Amnah Nezar M Yamani 2021

Acknowledgment

Writing this dissertation gave me the chance to reflect on all the people who made all kinds of contributions that have carried me to this point. I would like to thank my dissertation advisor, Dr. Simon Hogan, for allowing me to join his laboratory and all of his guidance. I arrived in Ohio with passion but as a white canvas in science. To the extent that I am a capable scientist today, it is because of the foundation Simon provided through his guidance and support. Simon created the culture for me to grow and become a scientist of my own. For all of this, I owe a sincere debt of gratitude.

Would also like to thank my dissertation committee: Drs David Antonetti, Katherine Gallagher, Michelle Kahlenberg and Nicholas Lukacs. Our meetings and emails have helped shape this dissertation and have been invaluable for my personal development. I value all of the time that you gave to my education.

The Hogan Lab, past and present, has also been immensely helpful in my scientific training. I appreciate all of the help, conversations, and support of my scientific development and well-being. I wish my colleagues the best of luck in their futures, and I know they will be respected for their work and kindness. Special thank you to Taeko Noah, Varsha Ganesan, Sahiti Marella, Gila Idelman, and Ankit Sharma for their contribution in performing experiments for this work.

The Graduate Program in Immunology created a great community throughout my time in Michigan, which I am very blessed to be part of. I will always remember the time Dr. Beth Moore welcomed us to the University of Michigan and made our move from Ohio so easy.

I am also appreciative of the directors of the program: Drs. Malani Raghavan, Gary Huffnagle, and Durga Singer for their hard work and dedication to the Immunology community. Our wonderful administrator, Zarinah Aquil, has also been extremely supportive and considerate. She has made the logistics of Ph.D. training seamless.

I would like to thank my friends in the Immunology Graduate program who have been a constant support and made my time in Michigan enjoyable. I feel blessed to have met hard-working, intelligent, kind classmates who will be cherished friends well beyond the bounds of grad school. I am particularly appreciative of Judy Chen, Alex Ethridge, Francisco Gomez-Rivera, Ranjitha Uppala, Emily Yarosz and Sahiti Marella for their friendship and all the editing they made on this dissertation.

Finally, I would like to express my deepest gratitude towards my family for their unconditional love, patience, and understanding throughout the toughest years of my life. My friends for sharing stress and frustration with me, for not forgetting me even though we were in different time zones. Your messages and calls meant the world to me.

Table of Contents

Acknowledgment	ii
List of Tables	vii
List of Figures	viii
List of Appendices	x
List of Abbreviations	xi
Abstract	xii
Chapter 1 Introduction	1
1. 1. Anaphylaxis	1
1. 1. 1 Food allergy prevalence:	1
1. 1. 2 Challenges in the management of food allergy and food-induced anaphylaxis:	1
1. 1. 3 Clinical manifestations of food-allergic reactions and anaphylaxis:	2
1. 1. 4 Severity grading of anaphylaxis:	3
1. 1. 5 Immunological mediators in food-induced anaphylaxis:	4
1. 1. 6 Pathways of systemic anaphylaxis:	5
1. 1. 7 Immunologic modulators of anaphylactic severity in mice:.....	7
1. 1. 8 The role of cytokines and MC-mediators in driving cardiovascular changes during severe food-induced anaphylaxis:.....	9
1. 2. Vascular Endothelial Barrier Function	10
1. 2. 1 Endothelial barrier:	10
1. 2. 2 Signaling pathways driving histamine-induced VE barrier disruption:	13
Figure 1.2 Summary for signaling pathways driving histamine-induced endothelial barrier disruption	16
1. 3. IL-4 and histamine signaling on vascular endothelial cells	16
1. 3. 1 IL-4 Signaling pathways:	16
1. 3. 2 Biological effects of IL-4 on vascular endothelial cells:	20
1. 3. 3 Histamine signaling:	22
1. 4. Summary	23
Chapter 2 Vascular Endothelial Specific IL-4Rα-ABL1 Kinase Signaling Axis Regulates Severity of IgE-mediated Anaphylactic Reactions	25
2. 1. Abstract	25
2. 2. Introduction	27
2. 3. Material and methods	28
2. 3. 1 Animals:	28
2. 3. 2 Oral Antigen-Induced Anaphylaxis:	29
2. 3. 3 Passive Anaphylaxis:	29

2. 3. 4 IL-4 and Histamine-Induced Anaphylaxis:	29
2. 3. 5 Passive Oral Antigen-Induced Anaphylaxis:.....	29
2. 3. 6 Anaphylaxis Assessments:.....	30
2. 3. 7 Mast Cell Quantification:	30
2. 3. 8 ELISA Measurements:	30
2. 3. 9 Cell Lines and Culture:.....	30
2. 3. 10 ABL Kinase Activity Assay:	30
2. 3. 11 <i>In Vitro</i> Permeability:	30
2. 3. 12 Lentiviral Transduction:	31
2. 3. 13 Flow Cytometry:	32
2. 3. 14 Immunofluorescent Assay:	32
2. 3. 15 Statistical Analysis:	32
2. 4. Results.....	33
2. 4. 1 IL-4 enhances histamine-induced hypovolemic shock via vascular endothelium–dependent IL-4R α chain signaling:	33
2. 4. 2 Vascular endothelial IL-4R α chain deletion attenuated hypovolemic shock induced by passive oral antigen–induced anaphylaxis:.....	37
2. 4. 3 Histamine and IL-4 modulation of paracellular leakage in the human vascular endothelial cell line (EA.hy926) is ABL1 kinase-dependent:.....	39
2. 4. 4 VE ABL1 kinase involvement in passive anaphylaxis in iIL-9Tg VE Δ ABL1 mice:..	41
2. 4. 5 ABL kinase inhibitor attenuated passive oral antigen–induced anaphylaxis:	41
2. 4. 6 ABL kinase inhibitor attenuated pre-existing oral antigen–induced anaphylaxis:	44
2. 5. Discussion.....	45
2. 6. Acknowledgment and Contributions	50
Chapter 3 Vascular Endothelial Cell IL-4-STAT3 Axis Modulates Severity of IgE-mediated Anaphylaxis Through Sustaining Vascular Endothelial Dysfunction	51
3. 1. Abstract	51
3. 2. Introduction.....	53
3. 3. Material and methods	55
3. 3. 1 Animals:	55
3. 3. 2 IL-4 and Histamine-Induced Anaphylaxis:.....	55
3. 3. 3 Passive Anaphylaxis:	55
3. 3. 4 ELISA Measurements:	56
3. 3. 5 Mouse endothelial cells isolation and sorting:	56
3. 3. 6 RNA Isolation and sequencing:	56
3. 3. 7 RNA sequencing data analysis:	56
3. 3. 8 Cell specific expression profile:	57
3. 3. 9 Endothelial Cell Resistance Measurement:.....	57
3. 3. 10 Cell Lines and Culture:.....	58
3. 3. 11 Lentiviral Transduction:	58
3. 3. 12 <i>In vitro</i> intracellular calcium measurement:	58
3. 3. 13 Western blot:	59
3. 3. 14 Rho GTPase assay:	59
3. 3. 15 Immunohistochemistry staining:	60
3. 3. 16 Statistical Analysis:	60

3. 4. Results	60
3. 4. 1 IL-4 amplified the magnitude and extended histamine-induced VE barrier dysfunction in EA.hy926 cell line:.....	60
3. 4. 2 IL-4 enhancement of histamine-induced VE barrier dysfunction is dependent on gene transcription in EA.hy926:	64
3. 4. 3 IL-4 enhancement of IgE-induced hypovolemic shock is associated with modulation of endothelium transcriptome with putative STAT-3 binding motif:	66
3. 4. 4 VE STAT3 is required to sustain IL-4 enhancement of histamine-induced VE barrier dysfunction in EA.hy926 cells:	70
3. 4. 5 IL-4 signaling on VE cells induces the expression of various STAT3 dependent genes that are involved in barrier integrity and barrier signaling:	73
3. 4. 6 Loss of VE STAT3 attenuated histamine-induced hypovolemic shock and IL-4 enhancement of histamine response:	78
3. 4. 7 Characterization of IgE-mediated anaphylaxis in C57/B6 mice:.....	80
3. 4. 8 Loss of VE STAT3 attenuated IgE-MC-induced anaphylaxis and IL-4 enhancement of histamine response:	81
3. 5. Discussion	83
Chapter 4 Dysregulation of Intestinal Epithelial CFTR-dependent Cl⁻ Ion Transport and Paracellular Barrier Function Drives Gastrointestinal Symptoms of Food-induced Anaphylaxis in Mice	90
4. 1. Abstract	90
4. 2. Introduction	91
4. 3. Methods	92
4. 3. 1 Animals:	92
4. 3. 2 Oral antigen-induced intestinal anaphylaxis:	92
4. 3. 3 Passive Anaphylaxis:	93
4. 3. 4 Solutions and drugs:	93
4. 3. 5 Ussing chambers:	93
4. 3. 6 Intestinal epithelial cells (IEC) preparation:	94
4. 3. 7 Immunofluorescence:.....	94
4. 3. 8 Statistical analysis:.....	95
4. 4. Results	95
4. 4. 1 Food antigen exposure is restricted to the small intestine (SI) during a food-induced anaphylactic reaction:	95
4. 4. 2 Antigen challenge stimulated intestinal epithelial CFTR-dependent Cl ⁻ transport and paracellular leak:	97
4. 4. 3 Direct exposure of OVA to jejunal SI preparations is sufficient to promote epithelial transcellular and paracellular dysfunction:	98
4. 4. 4 Dissection of mechanisms of oral antigen-induced transcellular and paracellular permeability:	102
4. 5. Discussion	106
4. 6. Acknowledgements and Contributions	110
Chapter 5 Discussion and Future Directions	111
Appendices	122
Bibliography	180

List of Tables

Table 1: Grading system for generalized hypersensitivity reactions.....	4
Table 2: Biological markers distinguishing IgE- from IgG-mediated anaphylaxis	7
Table 3: Histamine effect on hemodynamic	9
Table 4: Types and characteristics of histamine receptors.....	23
Table 5: Validated IL-4/STAT3 axis deponent genes annotation	78
Supplementary table 3- 1:cell specific subpopulation in sorted mouse pulmonary endothelial cells.....	138
Supplementary table 3- 2: IL-4C induced DEGs in lung endothelial cells	140
Supplementary table 3- 3: GO analysis of IL-4 up regulated genes	141
Supplementary table 3- 4: GO analysis of IL-4 down regulated genes	141
Supplementary table 3- 5: TF program from endothelial cells	142
Supplementary table 3- 6: TF and motif information	146
Supplementary table 3- 7: IL-4 DEGs in EA.hy926 ^{PLKO-1} cells.....	156
Supplementary table 3- 8: GO analysis based on the biological process on IL-4–up-regulated genes in EA.hy926 ^{PLKO-1}	158
Supplementary table 3- 9: GO analysis based on the biological process on IL-4–down-regulated genes in EA.hy926 ^{PLKO-1}	159
Supplementary table 3- 10: TF binding by IL-4 DEGs in EA.hy926 ^{PLKO-1}	166
Supplementary table 3- 11: GO on biological process by IL-4 DEGs with STAT3 TFBM in EA.hy926 ^{PLKO-1}	169
Supplementary table 3- 12: IL-4 induced DEGs in EAhy.926 ^{STAT3 KD}	176
Supplementary table 3- 13: Gene list identified by comparison and in silico analysis .	178
Supplementary table 3- 14: GO analysis based on the biological process on IL-4-dyregulated and STAT3 dependent genes.....	178
Supplementary table 3- 15: GO analysis on IL-4-dyregulated and STAT3 dependent genes	179

List of Figures

Figure 1.1 Overview of the molecular structure of the VE barrier	13
Figure 1.2 Summary for signaling pathways driving histamine-induced endothelial barrier disruption	16
Figure 1.3 IL-4 STATs and IRF signaling pathways.....	20
Figure 2.1: IL-4 enhancement of histamine-induced shock negatively correlates with fluid extravasation.	34
Figure 2.2: IL-4 amplifies histamine-induced VE barrier dysfunction.....	34
Figure 2.3: Loss and amplification of VE IL-4Ra signaling alters IL-4 enhancement of histamine-induced hypovolemic shock.....	36
Figure 2.4: VE IL-4Ra chain deletion attenuated hypovolemic shock in a passive oral antigen anaphylaxis model.....	38
Figure 2.5: Histamine- and IL-4–induced VE barrier dysfunction is ABL1 kinase dependent	40
Figure 2.6: Pharmacologic inhibition of ABL kinases attenuated IgE-mediated hypovolemic shock in a passive oral antigen anaphylaxis model.....	43
Figure 2.7: Established food-induced anaphylaxis is attenuated with ABL kinase inhibitor.....	45
Figure 3.1: IL-4 amplified histamine-induced VE barrier dysfunction and prevented barrier restoration in EA.hy926 cell line and this was associated with decrease VE-Cadherin expression	63
Figure 3.2: IL-4 enhanced histamine-induced calcium flux and modulated the kinetic of histamine-induced Rho GTP activity in EA.hy926 cell line	64
Figure 3.3: IL-4 enhancement of histamine-induced VE barrier dysfunction in EA.hy926 is cycloheximide dependent	66
Figure 3.4: IL-4 <i>in vivo</i> treatment dysregulated genes from endothelial cells that are enriched with STAT3 TFBS.....	69
Figure 3.5: VE STAT3 KD attenuated both IL-4 enhancement of histamine and histamine-induced barrier dysfunction.....	72
Figure 3.6: IL-4 induces the expression of STAT3 dependent genes that are involved in barrier integrity and barrier signaling.....	77
Figure 3.7: IL-4 induces the expression of STAT3 dependent genes that are involved in barrier integrity and barrier signaling.....	80
Figure 3.8: Deletion of VE STAT3 attenuated IgE-MC-induced hypovolemic shock and IL-4 enhancement of histamine response	82

Figure 3.9: Proposed mechanisms of IL-4 driven STAT3 dependent transcriptome alteration in VE cell that lead to barrier dysfunction	89
Figure 4.1: Eliciting antigen is restricted to the SI during the onset of food-induced anaphylactic symptoms	97
Figure 4.2: Oral antigen challenge induced SI epithelial transcellular and paracellular barrier dysfunction.....	98
Figure 4.3: Oral antigen-induced SI para-cellular dysfunction is associated with degradation of adherence and tight junction proteins.....	100
Figure 4.4: Oral antigen exposure leads to temporal loss of epithelial transcellular and paracellular dysfunction.....	102
Figure 4.5: SI transcellular the paracellular permeability was associated with the development of oral antigen-induced secretory diarrhea.....	103
Figure 4.6: Inhibition of Cl- secretory activity and proteolysis attenuated oral antigen-induced SI transcellular the paracellular permeability.	105
Figure 4.7: Inhibition of Cl- secretory activity and proteolysis was associated with inhibition of GI symptoms of food-induced anaphylaxis.....	106
Figure 5.1: Summary for major findings	112
Supplementary Figure 2- 1:VE ^{ΔIL-4Rα} mice lack IL-4Rα expression on VE cells.....	123
Supplementary Figure 2- 2: IL-4C is biologically active in VE ^{ΔIL-4Rα} mice.	124
Supplementary Figure 2- 3: Effect of the VE IL-4Rα chain on hypovolemic shock is MC and immunoglobulin independent.	125
Supplementary Figure 2- 4: Histamine-induced VE permeability in EA.hy926 cells is inhibited by imatinib.....	126
Supplementary Figure 2- 5: Hypovolemic shock induced by EM95 is dependent on VE ABL1.	127
Supplementary Figure 3- 1:IL-4 and histamine modulated the resistance between the cells and not the resistance underneath the cells in VE cells.....	128
Supplementary Figure 3- 2: Sorted EP-CAM – CD31 hi Hematopoietic markers – cells show a distinct transcriptome profiles for endothelial cells.	129
Supplementary Figure 3- 3: Histamine 1 receptor expression in EA.hy926 cells following IL-4 treatment.....	130
Supplementary Figure 3- 4: Anti-IgE challenge in C57/B6 mice increase serum histamine levels.....	131

List of Appendices

Appendix 1: Chapter 2 Supplemental Figures.....	123
Appendix 2: Chapter 3 Supplemental Figures and Table.....	128

List of Abbreviations

Ag	Antigen
AJs	Adherens junctions
CFTR	Cystic fibrosis transmembrane conductance regulator
EA.hy 296	Human Vascular Endothelial cells
GI	Gastrointestinal
HRP	Horseradish peroxidase
i.p.	Intraperitoneal
i.v.	Intravenous
IL-4C	Interleukin-4 complex
Isc	Short circuit current
KD	Knock-down
mAb	Monoclonal antibody
MCs	Mast cells
mHEVC	Murine high endothelial venules cells
mMCPT-1	Mouse mast cell protease-1
OIT	Oral immunotherapy
OVA-TNP	Ovalbumin- 2,4,6-trinitrophenol
PAF	Platelet-activating factor
RT	Room Temperature
SD	Standard deviation
shRNA	Short hairpin RNA
SI	Small intestine
TER	Transendothelial resistance
TJs	Tight junctions
VE	Vascular endothelial
VE	Vascular endothelium
WT	Wild type

Abstract

Food allergic reactions can involve cardiovascular, respiratory, cutaneous, gastrointestinal (GI) and neurologic organ systems. Clinical and experimental studies have provided corroborative evidence that upon food exposure, dietary antigens cross-link the IgE- Fc ϵ RI complex on mast cells (MC) and basophils surface to stimulate the release of mediators that drive the clinical manifestations of food allergy. However, the cellular and molecular processes that contribute to the organ involvement and severity of the reaction are unknown. Herein, we define: 1) the interaction between the cytokine Interleukin-4 (IL-4) and histamine in the regulation of vascular endothelial (VE) barrier function; 2) IL-4 receptor α (IL4R α) / Signal Transducer and Activator of Transcription 3 (STAT3) signaling pathways in the regulation of VE barrier function; 3) the role of MC-derived mediators in the GI symptoms of food-induced anaphylaxis in mice.

We show that IL-4 increased histamine-induced fluid extravasation, and this increase positively correlated with anaphylaxis severity in mice. Genetic deletion of the IL-4R α chain on VE cells showed that IL-4-enhancement of histamine and IgE/MC-induced anaphylaxis symptoms were dependent on the VE IL-4R α chain. Mechanistically, we show that IL-4 enhanced histamine-induced VE ABL1 activation. IL-4-enhancement and histamine-induced VE barrier dysfunction, histamine-induced anaphylaxis and hypovolemia were ABL1 dependent. Collectively, these data implicate an important contribution by the VE compartment in the severity of IgE-mediated anaphylaxis.

We next show that IL-4 enhancement of histamine-induced VE barrier dysfunction in VE cells was associated with histamine-mediated VE-Cadherin degradation. The enhancement of histamine-induced VE barrier dysfunction was dependent on IL-4-induced gene transcription. RNAseq analyses revealed enrichment of differentially expressed genes (DEGs) that possessed a putative STAT3 motif. *In silico* and *in vitro* approaches identified an IL-4-induced and STAT3 dependent VE transcriptome that was

characterized by barrier integrity and signaling genes. Indeed, IL-4-induced exacerbation of histamine- or anti IgE mAb- induced anaphylaxis was in part STAT3-dependent. Collectively, these data implicate an important role of the IL-4/ STAT3 signaling axis in the priming of VE cells, which results in modulating the severity of IgE-and histamine-induced anaphylaxis.

Finally, we defined the intestinal epithelial response during a food-induced anaphylaxis. We show that oral allergen challenge stimulates a rapid dysregulation of intestinal epithelial transcellular and paracellular transport that was associated with the development of secretory diarrhea. Allergen-challenge induced a rapid intestinal epithelial *Cftr*-dependent Cl⁻ secretory response, and a paracellular macromolecular leak that was associated with modification in epithelial adherence and tight junction proteins. Blockade of both the proteolytic activity and Cl⁻ secretory response was required to alleviate intestinal symptoms of food-induced anaphylaxis. Collectively, these data suggest that the GI symptom of food-induced anaphylactic reaction, secretory diarrhea, is a consequence of CFTR-dependent Cl⁻ secretion and proteolytic activity.

Collectively, these studies have unveiled a role for the IL-4-STAT3-histamine axis in dysregulation of VE barrier function of the systemic symptoms of food-induced anaphylaxis, and MC-derived proteases in the regulation of the GI symptoms of food-induced anaphylaxis.

Chapter 1 Introduction

1. 1. Anaphylaxis

1. 1. 1 Food allergy prevalence:

Food allergy is an immune-based disease that has become a serious health concern. Prevalence in allergic disease has been continually increasing in the industrialized world for more than 50 years^{1,2}. In the United States (US), around 10%, of the population³. Various studies from different countries across the world (e.g., Australia, Canada, United Kingdom and US) indicate that peanut allergy now affects at least 1% of school-aged children, and its prevalence appears to be increasing⁴⁻⁶. Evidence from pediatric studies indicates that there is an 18% increase in pediatric food allergy over the past decade⁷.

Severe food-allergic reactions (food-induced anaphylaxis), can be life-threatening and are responsible for 30,000–120,000 emergency department visits, 2,000–3,000 hospitalizations and approximately 150 deaths per year in the US^{8,9}. Based on clinical studies from emergency departments, reactions to food allergens account for 30–75% of anaphylactic cases in North America, Europe, Asia and Australia^{8,10,11}. Databases of hospital discharges indicate that admissions for food-induced anaphylaxis in children aged <18 years more than doubled from 2000 to 2009 in the US¹². A review of anaphylaxis fatalities and hospital admissions in Australia from 1997 to 2005 revealed a 350% increase in food-induced anaphylaxis admissions over this period^{12,13}. Furthermore, from 1993–1994 to 2004–2005 there was an 8.8% continuous annual increase in the rate of anaphylaxis hospital admissions in Australia.

1. 1. 2 Challenges in the management of food allergy and food-induced anaphylaxis:

Food allergies constitute a significant financial burden for the US. It costs US families nearly \$25 billion annually to care for children with food allergies¹⁴. Currently, Food and Drug Administration (FDA) approved treatments for food allergy are limited, leaving food avoidance as the main way to prevent an allergic reaction. However, studies have shown

that a significant number of children and adults are accidentally exposed to allergens^{15,16}. As a result, the quality of life of allergic individuals is affected due to fear and anxiety from accidental ingestion. A large cohort study showed that out of 1941 children with physician-confirmed peanut allergy, 369 children had accidental exposures, and some even had multiple exposures¹⁵. Moreover, 13% of children in this cohort had a severe allergic reaction that included wheeze and cyanosis (a sign of inadequate oxygenation of the blood)¹⁵.

Oral immunotherapy (OIT) can be effective in increasing the amount of food that can be tolerated by a food allergic individual; however; adverse allergic reactions, including anaphylaxis, are frequently observed during desensitization protocols; More than 90 % of patients undergoing milk OIT develop reactions, and 10-20 % of patients have a severe reaction¹⁷. Therefore, there is a need to develop adjunctive therapy to prevent severe adverse reactions during immunotherapy.

To prevent cardiovascular collapse and to enhance blood flow during anaphylactic shock, epinephrine is administrated¹⁸; the α -adrenergic vasoconstrictive effects of epinephrine reverse peripheral vasodilation, which alleviates hypotension and also reduces angioedema¹⁹. The β -adrenergic properties of epinephrine increase myocardial output and contractility. However, epinephrine is not always effective in severe allergic shock, and patients may still die¹⁹⁻²². A study showed that the administration of epinephrine during peanut-induced anaphylaxis although improved symptoms, it had a limited effect on the cardiovascular parameter, which is the decreased stroke volume²³. Therefore, there is a need to understand factors modulating cardiovascular response during anaphylaxis.

1. 1. 3 Clinical manifestations of food-allergic reactions and anaphylaxis:

In general, symptoms of anaphylaxis involve the skin, gastrointestinal tract, respiratory tract and cardiovascular systems²⁴. Anaphylactic symptoms may develop within seconds to a few hours after the ingesting of a food allergen; however, most reactions develop within the first hour. The most common symptoms are cutaneous symptoms (e.g., urticaria and angioedema), which occur in more than 80% of cases in both adults and children²⁵. GI symptoms (e.g., vomiting and diarrhea) and respiratory

symptoms (e.g., chest tightness and wheezing) are relatively common^{26,27}. Cardiovascular symptoms only appear in 39% of food-allergic reactions and are mostly associated with respiratory arrest^{28,29}. It is hypothesized that cardiovascular and respiratory collapse result from a hypotensive state and this drives the subsequent presentation of symptomologies such as vomiting, dyspnea and hypoxia^{30,31}.

Clinical observations support the possible involvement of a mixed hypovolemic and distributive shock in anaphylaxis³², and mounting evidence identifies hypovolemic shock as an important contributor to the cardiovascular collapse that leads to the life-threatening anaphylactic shock³². An altered vascular permeability during hypovolemic shock facilitates the delivery of protein to tissues, which decreases protein levels in the blood and creates an imbalanced pressure between intravascular and interstitial spaces³³. Due to the imbalance of pressure between the two compartments and the increased proteins concentration in interstitial space, intravascular fluid is sequestered into interstitial space to follow the proteins leaving red blood cells behind in the blood vessels³³. Consistent with this, Black and Kemp demonstrated an increase in the relative density of blood in patients experiencing a ragweed-induced anaphylaxis³⁴, and 5 of 26 patients with idiopathic anaphylaxis had elevated erythrocyte sedimentation rates³⁵. Fisher and colleagues showed that there was up to a 35% decrease in circulating blood volume following allergen exposure in anaphylactic patients under anesthesia, and aggressive fluid resuscitation was an effective treatment^{30,36}. During hypovolemic shock, the sequestered vascular fluid leads to inadequate blood volume, which in turn leads to hypotension. Consistent with this, drug-induced anaphylaxis was characterized by a decrease in cardiac output and blood pressure parameters, which also respond to fluid resuscitation³⁰. Recently, Ruiz-Garcia and colleagues showed that changes in the cardiovascular system were observed during a double-blind, placebo-controlled food challenge (DBPCFC)²³. Specifically, allergic patients showed a decrease in stroke volume (volume of blood pumped from the left ventricle per beat) and venous return upon allergen exposure, suggesting a decrease in vascular resistance and loss of peripheral blood volume. Administration of intravenous fluids significantly increased stroke volume and venous return compared with baseline.

1. 1. 4 Severity grading of anaphylaxis:

Aiming to develop a simple grading system, Brown *et al.* performed a retrospective analysis on 1125 cases (Table 1)³⁷. This grading system was based on hypotension (the results of decreased cardiac output) and hypoxia (the results of failed oxygenation and carbon dioxide elimination) since cardiovascular and respiratory involvement indicate a severe reaction^{37,38}. Symptoms that define a severe reaction, such as confusion and collapse, strongly correlated with hypotension and hypoxia³⁷. Symptoms that define a moderate reaction, such as vomiting and dizziness, correlated with hypotension and hypoxia as well but were less closely associated. Finally, skin features, such as erythema and urticarial, did not correlate with hypotension and hypoxia and therefore were included in the mild reaction.

Grade	Defined by
Mild (skin and subcutaneous tissues only)	Generalized erythema, urticaria, periorbital edema, or angioedema
Moderate (features suggesting respiratory, cardiovascular, or gastrointestinal involvement)	Dyspnea, stridor, wheeze, nausea, vomiting, dizziness (presyncope), diaphoresis, chest or throat tightness or abdominal pain
Severe (hypoxia, hypotension, or neurologic compromise)	Cyanosis or SpO ₂ 92% at any stage, hypotension (SBP < 90 mm Hg in adults), confusion, collapse, LOC or incontinence

Table 1: Grading system for generalized hypersensitivity reactions

SBP, Systolic blood pressure; LOC, loss of consciousness; SpO₂, peripheral capillary oxygen saturation (an estimate of the amount of oxygen in the blood).

Several risk factors have been linked to severe anaphylactic reactions. Factors that place patients with food allergy at greater risk for a fatal anaphylactic episode include the following: being a teenager or young adult, not carrying epinephrine, mastocytosis, late or absent treatment, exercise and lack of information from health care providers^{39,40}. In addition, studies and case reports demonstrated that preexisting lung disease, mainly asthma, appears to be the major determinant of reaction severity and fatalities^{11,37,39}. Peanuts, tree nuts and seafood are shown to be implicated in most fatal food-allergic reactions more than any other food allergy²².

1. 1. 5 Immunological mediators in food-induced anaphylaxis:

IgE, Mast cells (MCs) and basophils have long been thought to be the primary effector pathway in anaphylaxis⁴¹. MC activation by antigen (Ag) cross-linking of Ag-specific IgE bound to FcεRI on the MC surface leads to a rapid release of preformed

mediators (e.g., histamine, proteoglycans, serotonin and tryptases) and newly synthesize mediators (e.g., platelet-activating factor (PAF), prostaglandin-D₂ (PGD₂))⁴²⁻⁴⁴. Indeed, evidence of MC activation is observed in clinical settings; MC mediators such as PAF, lipoxygenase products (leukotriene -C₄ (LTC₄) and leukotriene-D₄ (LTD₄)), cyclooxygenase products (PGD₂), tryptase, chymase, histamine and cytokines (IL-6, IL-10 and IL-2) have been reported to be elevated in the blood of human patients with anaphylaxis^{32,44,45}.

An emergency department-based study showed that histamine levels were raised in almost 50% of patients presenting with acute allergic reactions⁴⁶. Interestingly, histamine elevation was associated more strongly with gastrointestinal symptoms than tryptase elevation⁴⁶. Notably, histamine can be measured from patients' serum within 5-10 min of its release but only remains elevated for 30–60 min⁴⁷, therefore, histamine levels might be underestimated in patient serum due to its short half-life. Tryptase is the most widely used anaphylaxis marker due to its longer half-life compared to histamine^{46,47}. Tryptase levels peak at 15–120 minutes with a half-life of 1.5–2.5 hours⁴⁷⁻⁴⁹. Increased tryptase levels have been shown after anaphylaxis triggered by food challenge as well as other anaphylaxis triggers such as penicillin and exercise^{49,50}.

Other MC-derived mediators have also been shown to correlate with anaphylaxis severity⁴⁴. The severity of the initial reaction has been correlated with urinary LTE₄ excretion and peak serum concentrations of IL-2, IL-6, IL-10 and TNFRI. Delayed deterioration of anaphylaxis symptoms in some patients has been shown to be associated with an increase in MCT, histamine, IL-6, IL-10 and TNFRI.

1. 1. 6 Pathways of systemic anaphylaxis:

In mice, anaphylaxis can be rapidly induced through two distinct pathways: IgE-dependent or IgE-independent. In the first pathway, IgE cross-links FcεR1 and activates MCs, leading to the release of mediators such as histamine and PAF, that drive allergic response^{43,51}. In addition to MC activation, IgE cross-linking FcεRI on basophils leads to the rapid secretion of large quantities of IL-4 that act on non-immune cells such as mucosal epithelial cells^{52,53}. The second pathway depends on IgG binding to the low-affinity receptor FcγRIII on macrophages. Both pathways were shown to be complement-independent, as complement depletion did not change the severity of anaphylaxis⁴³.

Different markers have been studied to distinguish between IgE- and IgG-mediated anaphylaxis (Table 2)⁵⁴.

1. 1. 6. 1 IgE-mediated anaphylaxis:

Experimental evidence from murine studies supports that food and oral antigen-induced anaphylaxis is IgE-MC-dependent⁵⁵⁻⁵⁷. Targeting MC activity and MC numbers (MC-stabilizing agent and neutralizing antibodies) or blocking IgE and its signaling (FcεRI^{-/-} mice or mice treated with anti-IgE antibodies) prevented systemic and gastrointestinal symptoms of oral antigen-induced anaphylaxis in sensitized mice⁵⁵⁻⁵⁷. On the contrary, targeting IgG (IgG1^{-/-} mice) did not affect systemic and gastrointestinal symptoms of oral antigen-induced anaphylaxis⁵⁵. Similar to MC, eosinophil numbers are increased in food allergen sensitized mice, however, eosinophils are thought to have no role in gastrointestinal symptoms of oral antigen-induced anaphylaxis, and this has been shown by targeting eosinophils (IL-5 transgenic or IL-5/ eotaxin-1^{-/-} mice with elevated or depressed level of eosinophils)⁵⁸. Targeting histamine and histamine signaling (H1R and H2R antagonists, and histidine decarboxylase gene knockout mice that lack histamine) showed that histamine is the primary mediator driving the systemic but not the GI symptoms in IgE-MC-mediated anaphylaxis^{43,58,59}. The primary gastrointestinal symptom (diarrhea) is dependent on both serotonin and PAF (inhibited by 5-HT and PAF receptor antagonist)⁵⁸.

1. 1. 6. 2 IgG-mediated anaphylaxis

This pathway was demonstrated in IgE-deficient mice. Sensitized IgE-deficient mice became anaphylactic upon Ag challenge in a manner that was dependent on PAF and independent of histamine^{43,60}. In IgG-mediated anaphylaxis, MCs are not important for Ag-induced anaphylaxis⁴³. Although IgG-mediated anaphylaxis has been demonstrated in mice, this pathway may have a role in human anaphylaxis because human macrophages express FcγRIII⁴³.

Jönsson *et al.* showed a requirement for neutrophils in systemic anaphylaxis in C57BL/J6 mice⁶¹. This pathway appeared to be FcγIV- and IgG-dependent and PAF was involved^{61,62}. In contrast, Strait *et al.* showed that monocytes/macrophages, and not neutrophils, are responsible for systemic anaphylaxis in BALB/C mice^{43,63}. Together, these data support the idea that IgG is capable of inducing anaphylactic reactions and

that neutrophils may contribute to the reaction by engaging FcγR-bearing cells in mice⁶⁴. Basophils have been shown to play a major role in IgG-induced systemic anaphylaxis, which is FcγRIII-dependent^{62,64-66}. Upon capturing of IgG-allergen complexes, basophils release PAF, which increases vascular permeability, leading to anaphylactic shock⁶². Since anaphylaxis is complements independent this suggests the involvement of IgG1 in the IgG-dependent pathway because IgG1 does not activate complement^{43,67}.

1. 1. 6. 3 Role of IgG in food allergy.

Serum IgE level might persist in patients with food allergy even without showing any signs of allergy, suggesting the existence of a suppressive mechanism⁶⁸. Milk, eggs and peanuts specific IgGs is increased following OIT and have also been associated with successful immunotherapy and tolerance to food allergens⁶⁹⁻⁷¹. Food-specific IgG4 can be gained without immunotherapy. Several studies showed that children with positive IgE against cow's milk (CM) showed a natural increase in serum CM-specific IgG and this correlated with loss or clinical reactivity⁷²⁻⁷⁴. Therefore, food-specific IgG is thought to contribute to oral tolerance. Murine studies showed that IgG signaling through its inhibitory receptor FcγRIIB can inhibit IgE-dependent activation. Moreover, a high concentration of IgG can bind allergen before the allergen comes in contact with IgE on the MC surface (steric inhibition)⁶⁸.

Biological markers	IgE-mediated anaphylaxis	IgG-mediated anaphylaxis
Peripheral blood basophils and monocyte	decrease	decrease
Peripheral blood neutrophils	increase	increase
Serum IL-4 sIL-4Rα IL-4Rα expression on CD4+ T-cells	10000-fold increase 60-70% increase 40-70% increase	< 100-fold increase no change no change
Mouse Mast Cell Protease 1 (mMCP-1)	10000-fold increase	no change
FcγRIII expression on neutrophils	no significant change	28-60% reduction

Table 2: Biological markers distinguishing IgE- from IgG-mediated anaphylaxis

1. 1. 7 Immunologic modulators of anaphylactic severity in mice:

The different molecular mechanisms that lead to severe anaphylaxis have not yet been delineated⁶⁷. Research aiming to identify the specific immune functions regulating

the severity of IgE-MC-induced anaphylaxis showed that IL-4 and intestinal MC levels can modulate the severity of anaphylaxis⁵⁶.

Strait *et al.* showed that IL-4/IL-4R α signaling enhanced anaphylaxis through increasing sensitivity to vasoactive mediators including histamine, PAF, serotonin and leukotriene⁷⁵. In addition, using *T.spiralis* infection as a source of endogenous IL-4 showed that IL-4R α -deficient mice are protected from anti-Fc γ RII/RIII mAb-induced shock⁷⁵. IL-4 pretreatment increased vascular leak in mice injected with vasoactive mediators leading to hypovolemic shock and as a consequence of this, the mice became hypothermic⁷⁶. Given that vasoactive mediator levels, including histamine, were not increased after IL-4 exposure, the authors postulated that IL-4 increases vasoactive mediator sensitivity through an effect on the vascular endothelium (VE). The effect of IL-4 on the histamine-induced shock is not fully delineated.

Ahrens *et al.* showed that density of intestinal MC controls the severity of oral Ag-induced anaphylaxis⁵⁷. By employing an active Ovalbumin (OVA) model the author showed that the severity of anaphylaxis, as indicated by an increase in systemic (hypothermia) and intestinal (diarrhea) symptoms, correlated with intestinal MC levels. In contrast, anaphylaxis severity did not correlate with Ag-specific IgE levels. This is consistent with human data indicating that specific IgE levels do not predict the severity of food-induced anaphylaxis^{77,78}. In a second model, Ahrens *et al.* showed that mice with increased intestinal MC levels experienced an increased in the severity of anaphylaxis in both passive and active IgE models⁵⁷. These findings correlate with human data showing a much higher prevalence of severe and sometimes fatal anaphylaxis in patients with mastocytosis compared to the general population⁷⁹.

It is postulated that intestinal MCs modulate the severity of oral Ag-induced anaphylaxis through increasing oral Ag absorption⁶⁷. Transgenic mice (intestinal IL-9 Tg mice) with increased numbers of MCs in the intestines but not in other tissues predisposes the mice to oral Ag sensitization⁵⁷. These mice have an increase in Gastrointestinal paracellular permeability, which leads to increased systemic Ag absorption and dissemination hence, the increased IgE/Fc ϵ RI MC degranulation and increased severity of anaphylaxis⁶⁷.

1. 1. 8 The role of cytokines and MC-mediators in driving cardiovascular changes during severe food-induced anaphylaxis:

The capillary bed is the shock organ in the mouse. In anaphylaxis, mediators from both pathways act on target cells to increase capillary bed dilatation and fluid extravasation. This leads to hypovolemic shock and fatal tissue hypoxia^{80,81}. IgE-mediated -MC activation promotes the secretion of vasoactive amines (histamine and serotonin) and, lipid mediators (leukotrienes, prostaglandins) that are thought to induce VE dysfunction and hypovolemic shock^{82,83}. Histamine injection into mice increased hemoconcentration and induces hypovolemic shock, therefore, it induces the systemic symptoms of anaphylaxis⁷⁵; However, antihistamines drugs lack the life-saving capacity and are used as the second-line supportive therapy following epinephrine⁸⁴.

Histamine strongly increases vascular permeability, but its precise mechanism of action *in vivo* remains unknown. Ashina *et al* closely studied the effect of histamine on the ear’s blood vessels⁸⁵. Intravital imaging showed that histamine increased blood flow in arteries, while increased permeability in veins and venules. Histamine-induced vasodilation in both arteries and veins (Table 3).

	Diameter	Dye extravasation	Blood flow
Artery	Increase	No affect	Increase
Vein	Increase	Increase	No changes
Venulae	Not measured	increase	Not measured
Capillary	Not measured	No affect	Not measured

Table 3: Histamine effect on hemodynamic

In addition, pro-inflammatory responses driven by TNF-like weak inducer of apoptosis (TWEAK) released from MCs play a role in passive-induced and histamine-induced anaphylaxis and vascular leakage through an interplay with endothelial cells; TWEAK signal through its receptor, FN-14, on VE cells and leads to vascular leakage. In addition, the TWEAK receptor FN14 on VE cell lines is also needed in histamine-induced and bone marrow mononuclear cell (BMMC)-induced barrier dysfunction. However, these *in vivo* studies were done using FN-14 global KO mice and TWEAK global KO mice, therefore, more studies are needed to show the role of VE specific Fn14 in MC-induced shock. Also, while histamine increases the expression of VE cell FN-14, it is unclear if VE cells are capable of secreting TWEAK⁸⁶.

1. 2. Vascular Endothelial Barrier Function

The hallmark of hypovolemic shock during anaphylaxis is an increase in vascular permeability. Under homeostatic conditions, VE cells line the inner blood vessel walls to form a barrier separating the blood from the tissue and actively regulating the exchange of cells and solute between these compartments⁸⁷. The components of the VE barrier and the mechanisms histamine utilizes to target these components are summarized below:

1. 2. 1 Endothelial barrier:

A complex of protein-protein networks, called junctional complexes, mechanically connect VE cells (Figure 1.1, A)⁸⁸. These networks maintain endothelial integrity and serve as a selective barrier to fluid, solutes and cells going in and out of the circulation. The VE junctional complexes comprise of tight junctions (TJs), adherens junctions (AJs)⁸⁹. Gap junction (GJs) also contribute to endothelial barrier regulation. These junctional proteins are bound to the actin cytoskeleton to control intercellular contact and permeability⁹⁰. Notably, the morphology of the intercellular cleft in the endothelium generally differs from that of epithelium, as TJs are not only located on the apical side but may also be intermingled with AJs⁹¹. Moreover, AJs are the key regulator of vascular permeability and barrier function^{88,92}. One of the exceptions to these roles is VE barrier in the nervous system vasculature that are rich in well-developed TJs^{91,93,94}.

1. 2. 1. 1 Adherens Junctions (AJs):

AJs are formed by cadherin-catenin complexes^{87,89}. Several cadherins are expressed in endothelial cells such as N-cadherin, P-cadherin and T-cadherin. The most prominent cadherin at the endothelial cells' AJ is the vascular endothelium (VE)-cadherin, which is also solely expressed in endothelial cells (both lymphatic and vascular endothelial cells)⁹⁰. Murine studies targeting VE-cadherin (blocking mAb (BV13) and conditional genetic deletion) showed a major role of VE-cadherin in regulating basal vascular permeability in the heart and the lungs but not the brain and the skin^{92,95}. This supports the concept that endothelial barrier function and composition differ among organs.

Vascular permeability can be modulated by targeting the extracellular or the intracellular structure of VE-cadherin. The extracellular domain of VE-cadherin mediates a homophilic interaction in a Ca²⁺ dependent manner, creating a zipper-like structure that maintains stable adhesion between vascular cells (Figure 1.1, B)^{96,97}. This

extracellular domain is susceptible to degradation by enzymes such as metalloproteases and cathepsin G which can promote leukocyte and fluid extravasation^{98,99}. The cytoplasmic tail of VE-cadherin binds to a couple of adaptor proteins including β -catenins that in turn bind α -catenins and link VE-cadherin to the actin cytoskeleton and thus control cell-to-cell adhesion (Figure 1.1, C)^{96,97}. Consistent with this, loss of β -catenin decreased the association of α -catenin with VE-cadherin, and resulted in less organized actin filaments at cell borders.¹⁰⁰ Furthermore, direct phosphorylation of VE-cadherin is associated with weak junction⁸⁸. Permeability inducing factors phosphorylates Tyr 685 of VE-cadherin in cultured VE cells^{90,101}. Consistent with that, mice with Tyr 685-VE cadherin point mutation showed an impaired induction of vascular permeability¹⁰². Notably, *in vivo*, VE-cadherin is constitutively phosphorylated at Tyr 685 and Tyr 658 in mouse veins and capillaries but not in the arteries¹⁰³. Therefore, more studies are needed to understand the physiological relevance of phosphorylation events at the VE-cadherin complex.

1. 2. 1. 2 Tight Junctions (TJs):

The quantity and complexity of TJs are inversely proportional to permeability. In general, arterial and arteriole endothelial cells have continuous and elaborated TJs and this is suitable to limit the exchange of fluid and mass between blood and tissues^{91,104}. The capillary endothelial cells have loose TJs. Interestingly, the postcapillary venules have loosely organized and discontinuous TJs. This junctional protein structure serves to maintain immune cells trafficking and plasma protein extravasation, and has a greater capacity to mediate inflammatory responses¹⁰⁵. The more developed venous endothelial cells in veins have loss and disorganized TJs.

TJs consist of different families of transmembrane proteins including integral membrane proteins (e.g., claudin, junctional adhesion molecule A [JAM-A]) and intracellular proteins (e.g., zona occludens proteins). Among the claudin family of proteins, claudin-5 is restricted to endothelial cells⁸⁹. Other claudins have also been reported to be expressed on VE cells such as claudin 1, 3 and 10¹⁰⁶. In brain capillary endothelial cells, claudin-5 mRNA levels are almost 600-fold higher than claudin-3. Claudin-5 plays an important role in the blood-brain barrier¹⁰⁷. Mice deficient in claudin-5 showed rapid extravasation of small-molecule tracers into the brain and spinal cord

parenchyma. Interestingly, claudin-5 expression is necessary but insufficient for establishing VE barrier function in cultured VE cells¹⁰⁸. Specifically, claudin-5 controlled barrier formation of microvascular cells but not venous cells¹⁰⁸.

Junctional Adhesion Molecule-A (JAM-As) are another type of TJ protein composed of an extracellular region, a transmembrane segment and a short cytoplasmic tail⁸⁹. Genetic deletion of JAM-A in mice significantly increased vascular permeability, as JAM-A maintain VE barrier function by inducing claudin-5 expression¹⁰⁹. JAM-C is an independent group but homologous to JAM-A. JAM-C are localized in high endothelial venules, lymphatic vessels of lymphoid organs, and in vascular structures of the kidney¹¹⁰. JAM-C roles in permeability were demonstrated using an ectopically expressed JAM-C where it localized closely to the TJs of transfected epithelial cells and increased paracellular permeability.

1. 2. 1. 3 Gap Junction:

Gap junctions mediate cell-to-cell communication⁸⁷. These junctions are composed of connexin (Cx) (Figure 1.1, C). Each gap junction channel is composed of two connexins, which form passages that allow various molecules, ions and electrical impulses to directly pass between cells¹¹¹. Endothelium expresses Cx43, Cx40 and Cx37. Cx43 expression inversely correlates with VE-Cadherin and permeability in endotoxin-induced vascular leakage in the lungs¹¹¹. Cx40 interacts with cytoskeleton proteins during acute lung injury and contributes to vascular leakage¹¹².

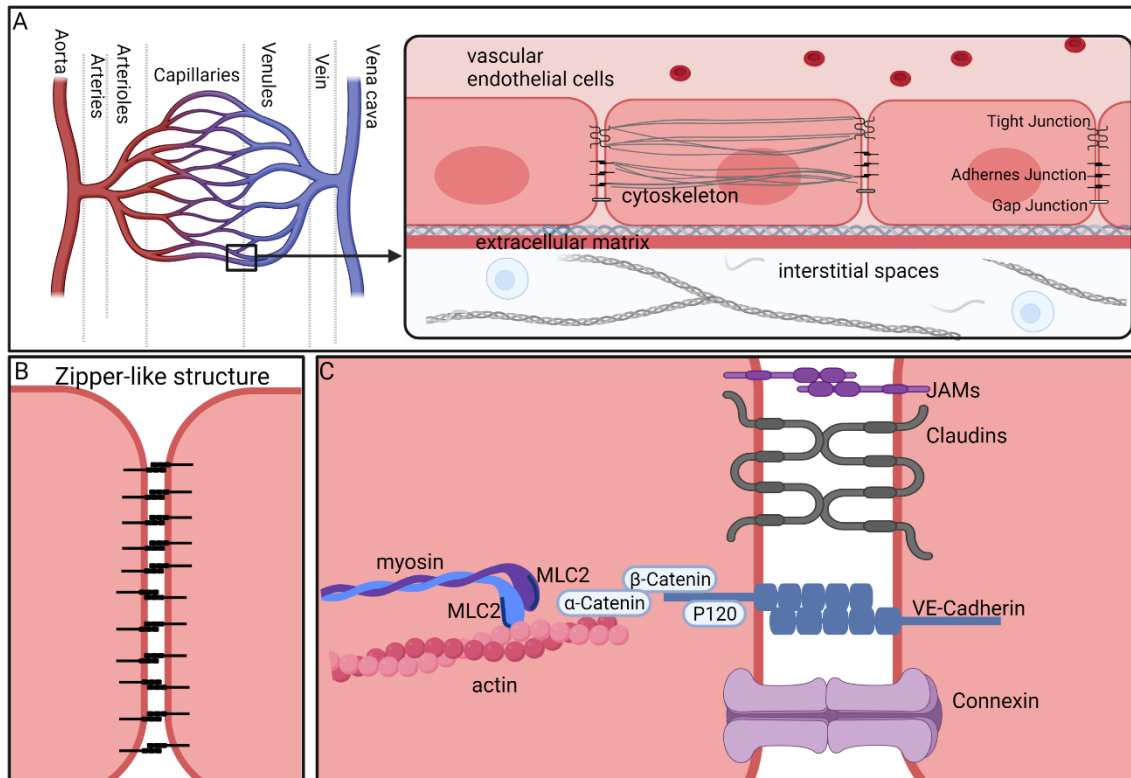


Figure 1.1 Overview of the molecular structure of the VE barrier

Schematic for the arrangement of blood vessels along with magnified part showing VE cells separating intravascular and interstitial space (A). Schematic for zipper-like structure between VE cells (B). Schematic for Junctional components that connect to cytoskeleton proteins (C).

Figure created with BioRender.com

1. 2. 2 Signaling pathways driving histamine-induced VE barrier disruption:

Generally, VE barrier-destabilizing agents target junctional proteins to create space between VE cells to allow cells and fluids to pass from blood vessels into the extravascular space⁸⁹. Junctional proteins can be disassembled or internalized from the cell membrane⁸⁹. Changes in phosphorylation of AJ proteins can regulate the integrity of AJs^{88,89}. Histamine has been shown to promote phosphorylation of Tyr-658 on VE-cadherin that results in its dissociation from the cellular anchor catenins and alters VE-cadherin localization from cell-cell contact to the cytoplasm, leading to disruption of the VE barrier^{102,101}. The effect of the acute histamine response on TJ proteins is unknown. A few studies have shown that long-term histamine stimulation decreases the expression of endothelial ZO-1 and Claudin-5^{113,114}. In addition, myosin-actin contraction can generate a force that pulls junctional proteins inward, thus disturbing the endothelial barrier by opening cell-cell junctions¹¹⁵. The endothelial isoform myosin light chain kinase

(MLCK) phosphorylates myosin light chain 2 (MLC2) which enables myosin to be activated to slide over actin myofilaments. Below is a summary of the known molecular pathways that histamine drives to induce VE barrier dysfunction:

1. 2. 2. 1 Histamine activation of RhoA and phospholipase C β :

Histamine acts through H1R ($G\alpha_q$ -coupled GPCR) to activate two major pathways¹¹⁶. The first pathway activates the classical phospholipase C β (PLC β) cascade and yields the consequent Calmodulin (CaM)-dependent activation of MLCK, leading to the disruption of endothelial barrier and vascular leakage(Figure 1.2). PLC β hydrolyzes phosphatidylinositol 4,5-bisphosphate to produce two second messengers: inositol 1,4,5-trisphosphate (IP3) and diacylglycerol (DG) ¹¹⁷. IP3 raises intracellular Ca^{2+} levels, which stimulates multiple Ca^{2+} -regulated mechanisms, and acts together with DG, to activate classic protein kinase C isozymes (PKCs)¹¹⁸. Finally, PKC contributes to the disruption of junctional protein complexes by phosphorylating the junctional protein or its adaptor molecules¹¹⁹.

In the second pathway, a $G\alpha_q$ downstream targets the Guanine nucleotide exchange factors (GEFs) Trio to initiates the activation of RhoA GTPase and the consequent stimulation of Rho-associated protein kinase (ROCK)(Figure 1.2)¹¹⁶. MLCK is also activated by ROCK¹¹⁶. This leads to disruption of the endothelial barrier by VE-cadherin forming zigzag-like structures known as focal adherens junctions (FAJs)¹¹⁶; histamine results in a rapid transition from stable junctions to the zigzag-like structure in which VE-cadherin is localized perpendicular to radial actin bundles¹¹⁶. Histamine does not transiently remodel the AJs through endocytosis of VE-cadherin complexes, unlike the VE growth factor (VEGF)¹²⁰.

1. 2. 2. 2 AKT/eNOS axis:

Treatment of human umbilical vascular endothelial cells (HUVEC) with Cap NO (Nitric oxide donor) decreases permeability, while *in vivo* Cap NO decreases canine heart rate and blood pressure ¹²¹. Later on, histamine has been shown to promote activation and phosphorylation of endothelial nitric oxide synthase (eNOS) in a Ca^{2+} and PKA-dependent manner but independent of PKC ¹²²(Figure 1.2). In addition, histamine-induced permeability was reduced in eNOS S1176A (loss of function) mice ¹²³. Using AKT1 deficient mice, it was shown that the histamine-induced vascular leakage is partially

dependent on AKT¹²⁴. However, histamine was injected dermally and not systemically in these studies. Therefore, it's unclear if histamine-induced eNOS activation targets endothelial cells systemically and whether it affects dilation or permeability.

1. 2. 2. 3 Non-receptor tyrosine kinases:

Tyrosine kinases have various roles in histamine-induced VE barrier dysfunction^{103,125}. For example, histamine induced-tyrosine phosphorylation of the VE-cadherin complex correlated with a rapid dissociation from β -catenins and VE-cadherin degradation^{103,125}. Indeed, inhibition of the ABL or the SRC family of non-receptor tyrosine kinases attenuated histamine-induced VE barrier dysfunction^{101,126}.

The ABL family of non-receptor tyrosine kinases include both ABL1 and ABL2 (also known as ABL1 and ABL2, respectively)¹²⁷. Histamine activates ABL kinases in VE cells which contributed to Ca^{2+} mobilization (Figure 1.2). Although it is not clear how ABL kinases activation by histamine mechanistically disrupts barriers, activation of ABL kinases by thrombin and VEGF signaling disrupt VE-cadherin complexes at cell border via positively regulating phosphorylation of MLC2 and Ca^{2+} mobilization¹²⁶. Furthermore, the role of ABL kinases in barrier function is supported by the presence of a unique, C-terminal actin-binding domain, supporting a role in the generation of actomyosin contractility^{127,128}.

Histamine signaling also activates SRC kinase in VE cells, which partially contribute to VE-cadherin dissociation from β -catenins¹⁰¹(Figure 1.2). Inhibition of SRC kinase activity, by PTEN, stabilizes the VE barrier and inhibits histamine-induced VE barrier dysfunction¹⁰¹.

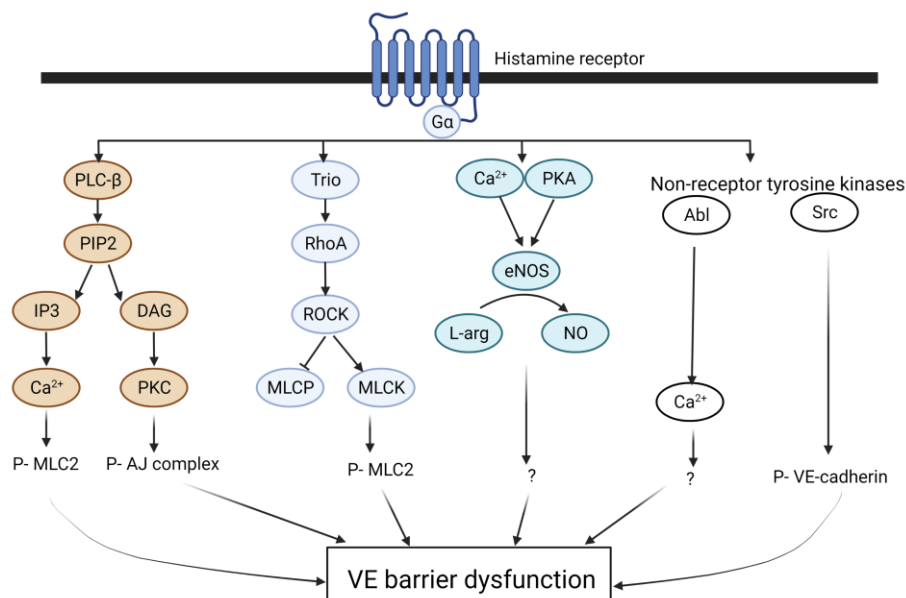


Figure 1.2 Summary for signaling pathways driving histamine-induced endothelial barrier disruption
Figure created with BioRender.com

1. 3. IL-4 and histamine signaling on vascular endothelial cells

1. 3. 1 IL-4 Signaling pathways:

IL-4 plays a fundamental role in both the sensitization and effector phases of anaphylaxis through promoting IgE and IgG1 class switching, mastocytosis and vascular permeability¹²⁹. IL-4 is part of the IL-2 family that signals through type I cytokine receptors¹³⁰. These receptors lack intrinsic kinase activity and have constitutively associated JAKs, which facilitate the recruitment of downstream signaling molecules. IL-4 can signal through 2 types of receptors containing the IL-4R α chain and can activate the signal transducer and activator of transcription STAT6 and STAT3 (Figure 1.3, A)^{130,131}. The type I receptor is composed of IL-4R α and the common γ chain (γ c). The type II receptor is used by IL-4 and shared with IL-13 as it is composed of an IL-4R α chain and IL-13R α 1 chain^{132,133}.

IL-4 binds the IL-4R α chain with very high affinity (KD = 20–300 pM), then recruits the second chain¹³⁰. It is postulated that second chain recruitment is governed by the second receptor chain's availability on the cell surface. Human and mouse hematopoietic and non-hematopoietic cells show a broad distribution of the IL-4R α chain^{134,135}. Since γ c is highly expressed on lymphocytes, IL-4 and IL-4R α chain complex recruits the γ c forming the type I IL-4 receptor. Non-hematopoietic cells generally lack or express low levels of

the γ_c , while the IL-13R α 1 chain is widely expressed on the surface of many cells, therefore the general consensus is that IL-4 signals through type II receptors in non-hematopoietic cells¹³⁶. Myeloid cells express both IL-13R α 1 and γ_c chains, therefore, myeloid cells express both type I and type II IL-4 receptors.

The γ_c is essential for the type I receptor signaling even though it does not bind to IL-4 or to IL-13¹³⁰. The IL-4R α /IL-4 complex has a weak affinity for the γ_c , possibly because the γ_c interacts with IL-4R α transiently to initiate signal transduction¹³⁷. On naïve T cells, IL-4 signals through the type I IL-4R α /STAT6 axis, which results in the upregulation of the T helper-2 (Th₂) master transcription factor GATA3¹³⁸. On B cells, IL-4 promotes IgE class switching through type I receptor signaling

Type II IL-4/IL-13 receptor is a heterodimer receptor composed of IL-13R α 1 and IL-4R α chains¹³⁹. IL-4 first binds to IL-4R α with high affinity, then the ligand-receptor complex recruits and associates with the IL-13R α 1 chain¹³⁷. The first evidence for the existence of type II receptors came from B cells derived from immune-deficient human patients (X-SCID), which demonstrates that B cells retain their ability to proliferate and secrete IgE in response to IL-4 without the presence of γ_c ¹⁴⁰.

1. 3. 1. 1 IL-4 STATs pathways:

Ligand binding to IL-4R α results in the activation of two pathways. The first is the Janus kinase (JAK)/STAT pathway, which results in gene activation. IL-4 engagement to the type I receptor results in JAK1 (associated with IL-4R α) and JAK3 (associated with γ_c) activation^{130,141}. JAK1 activates STAT6, which in turn promotes transcription of several genes, including immunoglobulin heavy constant epsilon (IGH ϵ), immunoglobulin heavy constant gamma 1 (IGHG1) and immunoglobulin heavy constant gamma 4 (IGHG4)^{142,143}. The amino acids sequence between 557 and 657 in the IL-4R α is vital for phosphorylation and activation of STAT6 and hence gene expression (Figure 1.3, B)^{144,145}. Specifically, the tyrosines Y575, Y603 and Y633 act as a docking site for STAT6.

IL-4 engagement with the type II receptor also leads to activation of STAT3. Forcing the expression of the IL13R α 1 chain in the cells that lack the IL13R α 1 enables STAT3 phosphorylation by IL-4. In addition, STAT3 has been shown to bind the phosphorylated IL-13R α 1¹³¹. The JAKs linked to the type II receptor are JAK1, JAK2 and TYK2¹⁴⁶. On the IL13R α 1 chain, the tyrosine Y402, but not Y399, acts as a docking site for STAT3

^{131,147,148}. Although STAT3 activation promotes gene transcription, the genes regulated by the IL-4/STAT3 axis are ill-defined.

1. 3. 1. 2 STAT3 activity and function in disease pathogenesis:

Many cytokines signal through STAT3, leading to STAT3 involvement in diverse pathways such as metabolism, MC degranulation, apoptosis and proliferation¹⁴⁹. STAT3 is well known to have oncogenic properties as it is shown to increase myeloid cell proliferation and inhibit apoptosis. In stem cells, STAT3 pathways maintain the stem cells phenotype. STAT3 genetic deletion in mice is lethal, therefore, STAT3 is essential for the early development of mouse embryos¹⁵⁰. Specific deletion of STAT3 within the gut epithelium showed a role STAT3 in controlling inflammatory immune response by inducing IL-22 production and by protecting against injury induced by dextran sodium sulfate (DSS) in drinking water¹⁵¹. In the context of immune cells, STAT3 is required for mast cell degranulation and production of IL-17 from CD4+ T cells¹⁴⁹. A dominant-negative STAT3 mutation in humans is associated with dermatitis, increased serum IgE levels and inability to clear microbial infection¹⁵².

STAT3 phosphorylation at Y705 residue leads to dimerization of STAT3 molecules that bind DNA with high affinity¹⁵³. Phosphorylated STAT3 dimer enters the nucleus, where it acts as a transcription factor to initiate the expression of selected genes. Maximal activation of gene transcription is achieved by additional STAT3 phosphorylation at the serine residue (S727). STAT3 bind gene promoters related to angiogenesis and cell adhesion such as VEGFC and β -catenin, innate immune response genes such as JAK3 and NLRC5, NIK/NF-kappa β signaling genes such as RELB and NFKB2; cytokines signaling genes such as IL6ST and STAT2^{153,154}.

Interestingly, a small pool of STAT3 modulates homeostatic mitochondrial function in a transcription-independent manner¹⁵⁵. In normal conditions, STAT3 is localized in the mitochondrial and this is dependent on STAT3 phosphorylation on S727 and not Y705 residues¹⁵⁵. Mitochondria lacking STAT3 expression show reduced ATP cellular levels, reduced oxidation rate and less complex I and II activity¹⁵⁵. Therefore, phosphorylated STAT3^{S727} is thought to be essential for optimal mitochondrial function and cell survival¹⁵⁵. The mitochondria have been shown to contribute to endothelium function by the generation of NO and reactive oxygen species (ROS) and regulation of the dynamics of

intracellular $[Ca^{2+}]$ signaling¹⁵⁶. Both NO, ROS and Ca^{2+} signaling contribute to permeability¹⁵⁷. However, the role of the IL-4/STAT3 axis in regulating mitochondrial function in VE cells is unknown.

1. 3. 1. 3 IL-4; IRS-1/IRS-2 pathway:

Insulin receptor substrate-1/-2 (IRS-1/IRS-2) pathway is the second pathway, besides the STAT pathways, that can be activated by IL-4 signaling. IRS-2 is predominantly found in hematopoietic cells, whereas IRS-1 is expressed in non-hematopoietic cells¹⁵⁸. By activating IRS molecules, IL-4 activates various signaling pathways, independent of STAT6, including activating phosphatidylinositol 3 kinase (PI3K), mitogen-activated protein kinase (MAPK), Protein kinase B (PKB) and mechanistic target of rapamycin (mTOR)(Figure 1.3, B)^{130,159}. The amino acid sequence in the IL-4R α between 437 and 557 mediates the phosphorylation of IRS molecules. Specifically, tyrosine Y497 is required for recruiting IRS molecules to the IL-4R α chain^{160,161}. In B and T cells, IRS molecules activate the PI3K and MAPK pathways to mediate IL-4 proliferative activity and to prevent apoptosis. IRS-2-deficient naïve CD4+ T cells fail to respond to IL-4 induced proliferation and IL-4 induced activation of survival mediators such as BCL-2 and PKB¹⁶². IL-4 also signals through IRS to activate the mTOR pathway to regulate signaling pathways contributing to Th₂ and M2 (alternatively activated macrophage)-type inflammation. The IL-4/IRS-1 axis effect on VE cells is ill-defined; however, VE cell specific IRS activation by insulin increases endothelial nitric oxide (eNOS) and vascular endothelial growth factor (VEGF) expression^{163,164}.

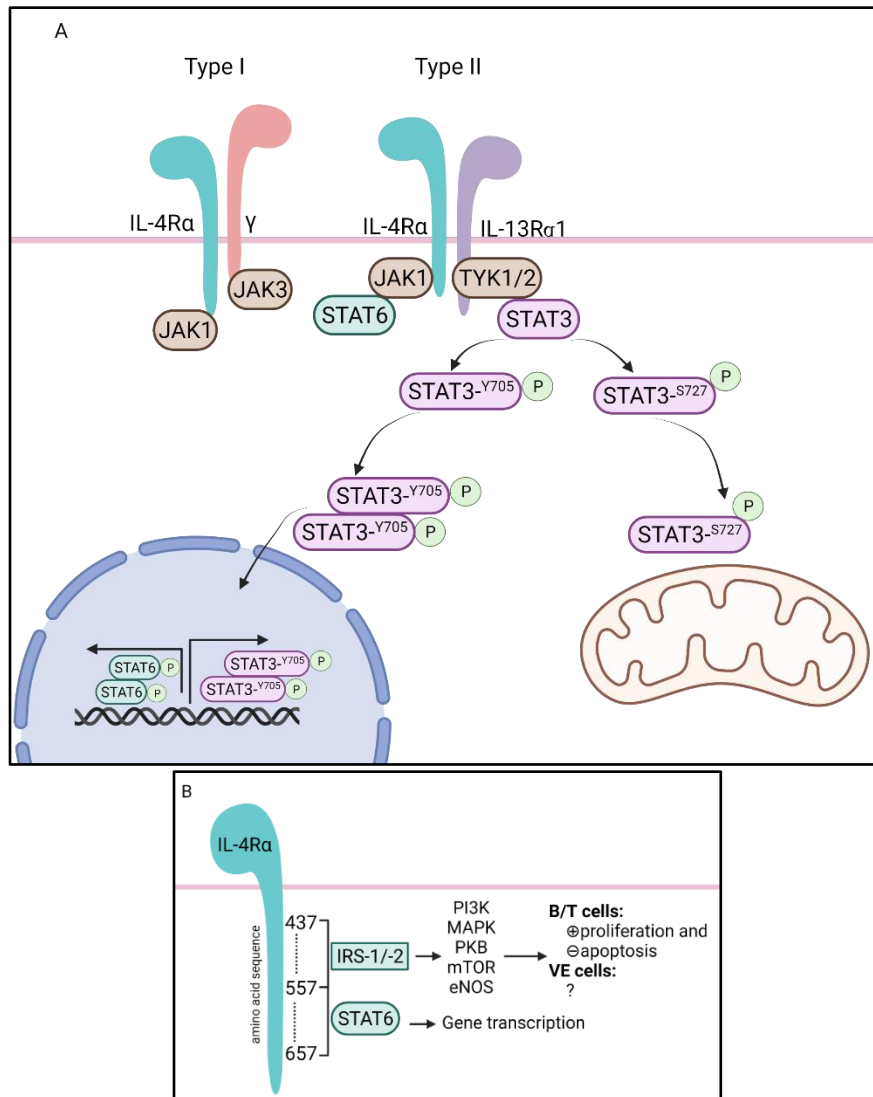


Figure 1.3 IL-4 STATs and IRF signaling pathways
 Figure created with BioRender.com

1. 3. 2 Biological effects of IL-4 on vascular endothelial cells:

1. 3. 2. 1 IL-4 increases adhesion molecules expression on endothelial cells:

VE cells play a dynamic role in regulating inflammatory and immune reactions. IL-4 signaling on VE cells modulates circulating leukocyte access to inflamed tissue¹⁶⁵. Studies *in vitro* with cultured human vascular endothelial cells (HUVEC) show that IL-4 signaling increases adhesion of monocyte and T cells by increasing the expression of vascular cell adhesion molecule-1 (VCAM-1). Interestingly, VCAM-1 is significantly increased in IL-4-positive asthma patients, compared with IL-4-negative asthma patients¹⁶⁶. VCAM-1 binding to its ligand, $\alpha 4\beta 1$ integrin, on leukocytes mediate the rolling and firm adhesion of leukocytes to the endothelium, as well as leukocyte

transmigration^{167,168}. VCAM-1 cross-linking generates ROS via Rac GTPase activation, and actin stress fiber formation via Rho GTPase signaling, both increase VE permeability to facilitates leukocyte transendothelial migration during inflammation^{166,169,170}. Indeed, anti-VCAM-1 antibody treatment in murine allergic asthma model attenuated leukocytes recruitment¹⁶⁶.

1. 3. 2. 2 IL-4 induces endothelial cell apoptosis or proliferation:

IL-4 has been long shown to be a mitogen for endothelial cells *in vitro*. IL-4 increased cell number and thymidine incorporation in HUVEC sub confluent monolayers¹⁷¹. Notably, IL-4 did not affect thymidine incorporation once cells reached confluence, suggesting that IL-4 might support the proliferation of immature endothelial cells¹⁷²; however, it is unclear if growth factors were used in these studies. In contrast, IL-4 has been shown to attenuate the FGF-and VEGF-induced VE cells proliferation, cell cycle progression and tube formation¹⁷³. Indeed, IL-4 increased the number of apoptotic cells through upregulating genes responsible for apoptosis such as caspase-3^{165,174}. These opposite results suggest that IL-4 signaling to VE cells depends on whether culture conditions permit efficient proliferation. Notably, many *in vitro* studies are done with HUVEC that are obtained from the immune naïve fetal tissue and do not represent the heterogeneity of different endothelial cells in the vasculature (Vein, venule, capillary etc.). There is a paucity of studies to determine IL-4 effects on VE cell proliferation and apoptosis *in vivo*.

1. 3. 2. 3 IL-4 induced endothelial cell barrier dysfunction:

The first signs showing that IL-4 is associated with increase vascular leakage and permeability came from human cancer patients undergoing IL-4 therapy. Atkins and his colleague showed that patients with refractory malignancies who took seven days of IL-4 treatment had an increased hematocrit, decreased albumin and capillary leak syndrome¹⁷⁵. Several other studies showed that side effects of IL-4 treatment included transient hypotension and capillary leak syndrome manifested as either periorbital edema or edema of the hands and fingers¹⁷⁶⁻¹⁷⁸.

Murine studies showed that the long-acting formulation of IL-4 by itself did no affect hematocrit percentage, suggesting minimum or no effect of IL-4 on vascular permeability *in vivo*; however, IL-4 enhanced anaphylactic shock induced by MC mediators⁷⁵.

Many *in vitro* studies indicate that IL-4 might cause vascular leakage by acting directly on VE cells to increase permeability. Indeed, IL-4 promoted an increase in the permeability of HUVECs which was evident following 3-6 hours of IL-4 treatment, and lasted for up to 24 hours^{179,180}; Besides HUVECs, IL-4 also induces increase in the permeability of adult human coronary artery endothelial cells (HCAEC), 3 hours after treatment and this lasted for 8 hours; however, the IL-4 effect was not examined following 24 hours¹⁸¹.

1. 3. 3 Histamine signaling:

Histamine exerts signal through four G protein-coupled receptors: H1R, H2R, H3R and H4R (Table 4)¹⁸². Although these receptors share certain key residues that are involved in activation and histamine binding, their sequence homology at the protein level is only 16-31%^{182,183}.

Histamine receptors signal through coupling and activating specific G proteins (Table 4). For example, H1R couples to G_q proteins, leading to phospholipase C β activation, inositol phosphate production and Ca²⁺ mobilization^{182,183}. H2R activates G_s and increases cAMP formation.

The contributions of the subtypes of histamine receptors to histamine response have been examined using specific receptor knockout (KO) mice. H1R and H2R are expressed in numerous cells such as vascular smooth muscle DC, T and B cells¹⁸⁴. H1R and H2R double KO mice were completely protected from IgE-mediated systemic anaphylaxis, whereas, H1R and H2R single KO mice had only attenuated anaphylactic shock¹⁸⁵. On VE cells monolayer, histamine signaling induced VE barrier dysfunction¹⁸⁶. This was associated with an increase in cAMP and free calcium and was inhibited by the H1R blocker (diphenhydramine) and the H2R blocker (famotidine)¹⁸⁶. Aside from the role of H2R in anaphylaxis, the main function of the H2R on parietal cells is mediating the release of gastric acid¹⁸⁷. This function led to the development of H2R antagonists such as cimetidine and ranitidine for the treatment of gastric acid disorders. H3R is found exclusively on neuronal cells where it controls brain histamine levels and can modulates the release of other neurotransmitters such as dopamine^{187,188}. H3R KO mice showed increased severity of neuroinflammation, behavioral state abnormalities, reduced locomotion, late-onset obesity and increased insulin levels¹⁸⁹. Therefore, the H3R is a

major target for the development of drugs against various brain disorders. H4R is largely expressed on hematopoietic cells¹⁸². H4R contributes to the regulation of the immune system through its chemotactic properties¹⁹⁰. Moreover, H4R is present in low amounts in the human lung, where it is expressed on bronchial epithelial, smooth muscle cells and microvascular endothelial cells¹⁹¹. H4R may contribute to inflammatory disorders such as asthma. Studies showed that H4R-deficient mice or those given H4R antagonists during sensitization exhibited reductions in lung inflammation, Th₂ and inflammatory cytokines and decreases eosinophil and lymphocytes infiltration into the lung^{183,192}.

	H1 Receptor	H2 Receptor	H3 Receptor	H4 Receptor
Best characterized function	Acute allergic reactions	Gastric acid secretion	Neurotransmitter modulation	Immunomodulator
G-protein coupling	Gα _{q/11}	Gα _s	Gα _{i/o}	Gα _{i/o}
Major signaling pathway	Increases in Ca ²⁺	Increases in cAMP	Inhibition of cAMP	Increases in Ca ²⁺
Expression in human	Multiple cell types including monocytes, vascular smooth muscle, DCs, T, B and endothelial cells ^{183,184}	Many cell types including Th ₂ , brain, vascular smooth muscle, DCs, T, B and parietal cells ¹⁸³⁻¹⁸⁵	Nervous system ¹⁸⁸	DCs MCs, eosinophils, monocytes, basophils and T cells ^{192,193}

Table 4: Types and characteristics of histamine receptors

1. 4. Summary

Scientific premise:

- Severe food-induced anaphylaxis is associated with movement of vascular fluid to the interstitial space and inadequate blood volume resulting in hypovolemic shock.
- Anaphylaxis in humans is associated with increased immune mediators and cytokines including IL-4 and histamine.
- Serum histamine levels were found to be associated with the severe anaphylactic phenotype.

- Histamine signaling on vascular endothelium (VE) leads to disrupting VE barrier function and to increased vascular permeability
- The non-hematopoietic Type II IL-4 receptor pathways are composed of the IL-4R α chain and IL-13R α 1 chain and signaling through STAT3.
- Histamine receptor signaling in VE cells activates non-receptor ABL kinases and induces vascular leakage.
- In VE cells STAT3 regulates permeability induced by growth factors and inflammatory mediators such as VEGF, IL-6 and histamine.
- Clinical data indicating a link between GI manifestations with the severe anaphylactic phenotype including hypotension and hypoxia.

Gaps in knowledge:

1. The underlying molecular processes that modulate the severity of food allergic reaction.
2. The mechanisms that regulate fluid extravasation in food-induced anaphylaxis.
3. The molecular process underlying the interaction between IL-4 and histamine signaling on VE cells barrier function and signaling pathways in food-induced anaphylaxis.
4. The molecular process underlying the GI symptoms in food-induced anaphylaxis.

Central hypothesis IL-4 and histamine synergize at VE STAT3 signaling to induce enhanced endothelial barrier dysfunction and as a result, triggers a severe IgE-MC-induced anaphylaxis and hypovolemic shock.

The specific aims of this dissertations are:

1. Identify the cellular target of IL-4–enhancement of anaphylaxis and the underlying IL-4 receptor α chain (IL-4R α)–dependent signaling processes involved in the amplification of histamine-induced VE barrier dysfunction.
2. Define the requirement of VE ABL1 in IL-4 enhanced histamine- and IgE-MC-induced anaphylaxis and associated hypovolemic shock.
3. Define the requirement of VE STAT3 in IL-4 enhanced histamine- and IgE-MC-induced anaphylaxis and associated hypovolemic shock.
4. Define the intestinal epithelial response associated with GI symptoms of food-induced anaphylactic reaction.

Chapter 2 Vascular Endothelial Specific IL-4R α -ABL1 Kinase Signaling Axis Regulates Severity of IgE-mediated Anaphylactic Reactions

2. 1. Abstract

Severe IgE-mediated, food-induced anaphylactic reactions are characterized by pulmonary venous vasodilatation and fluid extravasation, which is thought to lead to cardiovascular collapse and the severe, life-threatening anaphylactic phenotype. Animal-based studies suggest an interaction between the cytokine IL-4 and mast cell- and basophil-derived mediators in driving fluid extravasation; however, the molecular basis of this process is not fully elucidated. We aimed to define the interaction and requirement of IL-4 and vascular endothelial (VE) IL-4R α chain signaling in histamine-ABL1-mediated VE dysfunction and fluid extravasation in the severity of IgE-mediated anaphylactic reactions in mice. We show that IL-4 treatment exacerbated histamine-induced hypothermia and vascular leakage in mice. The IL-4-mediated amplification of hypothermia and vascular leakage was dependent on VE-specific expression of the IL-4R α . *In vitro*, VE cell analyses revealed that IL-4 and histamine induced ABL1 activation in EA.hy926 cells. Pharmacologic (imatinib) and shRNA ablation of *ABL1* revealed that IL-4- and histamine-induced VE barrier dysfunction was ABL1 dependent. Consistent with this observation, employing an IgE-induced model of anaphylaxis revealed a requirement for VE-restricted ABL1 expression in the development of hypovolemia and shock. Importantly, treating mice with a history of food-induced anaphylaxis with the ABL kinase inhibitor imatinib protected the mice from developing severe IgE-mediated anaphylaxis after allergen exposure. Our data indicate that IL-4 amplifies IgE- and histamine-induced VE dysfunction, fluid extravasation, and severity of anaphylaxis via a VE IL-4R α -ABL1-dependent mechanism. These studies implicate an important contribution by the VE compartment in the severity of anaphylaxis and identify a new

pathway for therapeutic intervention and prevention of IgE-mediated, food-induced anaphylaxis.

2. 2. Introduction

Anaphylaxis is a severe, life-threatening allergic reaction that affects both children and adults and males and females in the United States². The most common inciting agents (33.2% of reactions) are foods, particularly peanuts and nuts, and food-induced anaphylaxis (FIA) hospitalization rates for children in US have more than doubled from 2000 to 2009¹².

A food-induced anaphylactic reaction encompasses a variety of symptoms that may affect one or more target organs including those of the gastrointestinal, cutaneous, respiratory, and cardiovascular systems^{25,77,194}. In humans, compromise of either the cardiovascular or respiratory system defines a severe reaction^{25,77}, and it is postulated that basophil- and mast cell (MC)-derived mediators, through inducing pulmonary venous vasodilatation and fluid extravasation, cause the respiratory and cardiovascular collapse that leads to the severe, life-threatening anaphylactic phenotype¹⁹⁵. Fluid extravasation in patient with anaphylaxis is thought to be consequence of capillary fluid leak due to loss of the vascular endothelial (VE) barrier integrity, leading to the movement of fluids, electrolytes, and proteins from the vascular compartment into the interstitial spaces^{30,32,196}.

The VE barrier is maintained by adherens junction (AJ) and tight junction (TJ) proteins¹⁹⁷. The AJ proteins are the most ubiquitously expressed endothelial cell-cell junctional proteins and act as mechanical anchoring points that promote endothelial TJ protein-protein interactions and interjunctional integrity and barrier architecture¹⁹⁸. The TJ proteins are tethered to the actin cytoskeleton and seal the intercellular space, establishing the dense “fence” barrier preventing the bilateral apical-basolateral passage of ions, proteins, and lipids¹⁹⁸. VE-cadherin is one of the first endothelial cell-specific molecules expressed and required for endothelial survival, blood vessel assembly, and stabilization^{199,200}. VE-cadherin forms Ca²⁺-dependent homophilic interactions with adjacent endothelial cells, and the intracellular domains directly interact with actin-linking catenin family proteins and the actin cytoskeleton, establishing the vascular barrier integrity¹⁹⁸. The stability of the VE-cadherin–catenin–cytoskeleton complex is essential to maintaining endothelial barrier function²⁰¹. Disruption of these processes through receptor signaling pathways, including non-receptor kinases such as SRC, ABL1 and

ARG and myosin light chain kinase (MLCK), leads to VE-cadherin-mediated AJ disorganization or VE-cadherin internalization and loss of endothelial barrier integrity^{126,127,202}.

The cellular and molecular pathways that directly contribute to the severe anaphylaxis phenotype are unclear. Clinical studies have reported increased levels of IL-4 and histamine in the sera of human patients with severe anaphylaxis^{203,204}. While histamine, but not IL-4 levels were associated with severe disease, there is likely involvement of both of these molecules in expression of the severe disease phenotype. We and others have demonstrated that symptoms of food-induced anaphylaxis in mice are dependent on IgE/MC and histamine type I receptor signaling and that the severity of the reaction positively correlates with an increase in hemoconcentration (an indication for fluid extravasation and hypovolemic shock)^{43,56,76,205}. *In vitro* experimental evidence suggests that IL-4 modulates VE barrier properties, and we have demonstrated that IL-4 can interact with vasoactive mediators to increase hemoconcentration and the severity of anaphylaxis. However, the cellular target of these IL-4-mediated effects and the underlying IL-4 receptor α chain (IL-4R α)-dependent signaling processes involved in the amplification of histamine-induced VE barrier dysfunction and fluid extravasation in IgE-mediated reactions are not yet fully understood.

Here we examine the relationship between IL-4 and histamine in IgE-mediated VE leak and hypovolemic shock. We show that IL-4 amplifies histamine-induced hypovolemic shock through VE IL-4R α chain-dependent process. Furthermore, we show that IL-4 and histamine stimulate ABL1 kinase activity in VE cells and VE barrier dysfunction was inhibited by pharmacologic and genetic ablation of ABL1 activity. Importantly, by using both passive and active models of food-induced anaphylaxis, treating mice with the ABL kinase inhibitor imatinib protected the mice from the severe IgE-mediated anaphylactic phenotype after allergen exposure. These studies implicate an important contribution by the IL-4R α /ABL1 signaling pathway in the VE compartment in the severity of IgE- and histamine-induced anaphylaxis.

2.3. Material and methods

2.3.1 Animals:

Intestinal IL-9 transgenic (iIL9Tg) mice were generated as previously described⁵⁷. WT

BALB/c mice were originally provided by Charles River laboratories, (Wilmington, MA, USA) and bred in-house at Cincinnati Children's Hospital Medical Center (CCHMC) (Cincinnati, OH, USA). IL-4R α ^{Y709F} mice were obtained from Fred Finkelman, CCHMC²⁰⁶. Cadherin-5^{Cre} mice (purchased from Jackson Laboratory) (Bar Harbor, ME, USA) and IL-4R α ^{f/f} mice (generously provided by Frank Brombacher, University of Cape Town, South Africa) and iIL9Tg were used to generate mice lacking IL-4R α in VE²⁰⁷. Tie2^{Cre} mice (generously provided by Joseph E. Qualls, CCHMC) and ABL1^{f/f} mice (generously provided by Dawn Wetzel, University of Texas Southwestern, TX, USA) and iIL-9Tg mice were used to generate mice lacking ABL1 in VE²⁰⁸. Age-, sex-, weight-matched littermates were used as controls in all experiments. The mice were maintained and bred in a clean barrier facility and were handled under an approved Institutional Animal Care and Use Committee protocols at CCHMC animal facility.

2. 3. 2 Oral Antigen–Induced Anaphylaxis:

Six- to 8-week-old mice were sensitized and challenged as previously described⁵⁶. In some experiments, mice received imatinib mesylate (Santa Cruz Biotechnology, TX, USA) intraperitoneally (i.p.) (1.25 or 1.75 mg / 100 μ L distilled water per mouse) 2 hours prior to OVA challenge.

2. 3. 3 Passive Anaphylaxis:

Mice were injected intravenously (i.v.) with 20 μ g / 200 μ L of anti-IgE (IgG2a mAb to mouse IgE; EM95) (Obtained from Fred Finkelman, CCHMC)²⁰⁹. EM95 cross-linking to Fc ϵ R1 lead to MC and basophil activation and degranulation⁴³.

2. 3. 4 IL-4 and Histamine-Induced Anaphylaxis:

Twenty-four hours before the experiments, mice were injected i.v. with IL-4C (recombinant, IL-4–neutralizing, anti–IL-4 monoclonal antibody [mAb] complex, 1:5 weight) (anti–IL-4 mAb was obtained from Fred Finkelman, CCHMC) followed by histamine biphosphate monohydrate (Sigma–Aldrich, St. Louis, MO, USA) (0.4 or 2 mg / 200 μ L saline per mouse)^{75,210}.

2. 3. 5 Passive Oral Antigen-Induced Anaphylaxis:

Mice were primed and challenged as previously described⁵⁶. Mice received imatinib mesylate (Santa Cruz Biotechnology, TX, USA) i.p.(1.25-1.75 mg / 100 μ L distilled water per mouse) 2 h prior to OVA–2, 4, 6-trinitrophenyl hapten (TNP) challenge.

2. 3. 6 Anaphylaxis Assessments:

Hypothermia (significant loss of body temperature) and hypovolemia (increased in hemoconcentration) were used as an indication of anaphylactic reaction. Rectal temperature was taken with a rectal probe and a digital thermocouple thermometer (Model BAT-12; Physitemp Instruments, Clifton, NJ, USA). Temperature was taken prior to the challenge and then every 15 min for 30 or 60 min. For hemoconcentration assessment, blood was drawn by retro-orbital bleeding into heparinized capillary tubes and centrifuged for 5 min at 10,000 rpm. Hematocrit (percentage of packed red blood cell [RBC] volume) was calculated as previously described⁷⁵.

2. 3. 7 Mast Cell Quantification:

Jejunum and ileum were collected and processed for MC quantification by chloroacetate esterase (CAE) staining, as described previously⁵⁶.

2. 3. 8 ELISA Measurements:

Mouse MC protease 1 (mMCPT-1) serum levels were measured by ELISA according to the manufacturer's instructions (eBioscience, San Diego, CA, USA).

2. 3. 9 Cell Lines and Culture:

EA.hy926 cell line (human VE cell line) (ATCC, Manassas, VA, USA) were cultured in Dulbecco's Modified Eagle Medium (DMEM) supplemented with 10% fetal bovine serum (Atlanta Biological), nonessential amino acids (0.1 mM), sodium pyruvate (1 mM), HEPES (10 mM), and 1X penicillin and streptomycin (50 µg / mL) in a humidified incubator (5% CO₂, 37°C)^{211,212}. All reagents were obtained from Gibco, Life Technologies (Waltham, MA, USA) unless stated otherwise.

2. 3. 10 ABL Kinase Activity Assay:

3x10⁶ cells/well were plated in a 6-well plate and grown for 24 h. Cells were pretreated with IL-4 (10 ng for 24 h; Peprotech, Rocky Hill, NJ, USA) before imatinib treatment (10-100 µM for 3 h; Santa Cruz Biotechnology, TX, USA) followed by histamine (10 µM for 30 min; Sigma–Aldrich, St. Louis, MO, USA) stimulation. To assess for ABL1 kinase activity, ABL1 was immunoprecipitated from treated EA.hy926 cells for a subsequent measurement of CRK-GST phosphorylation. The ABL1 activation assay was performed as describe by Dudek *et al.*²¹³.

2. 3. 11 In Vitro Permeability:

EA.hy926 were plated on transwells (12-mm diameter, 0.4- μm pore; Polyester Membrane Insert, Corning, NY, USA), cells were seeded and cultured until a monolayer formed. Transendothelial resistance (TER) was monitored with an EVOM/Endohm (WPI Inc, Sarasota, FL, USA), and endothelial monolayers with a TER $>100 \Omega/\text{cm}^2$ were used for all experiments. Monolayers were mounted between the hemi-chambers of an Ussing apparatus (P2300 Ussing chamber, Physiologic instruments, CA, USA), and 0.33 cm^2 of cell monolayer was exposed to 6 mL of Krebs buffer at 37°C . The transendothelial potential difference was detected with two paired electrodes that contain 4% agar in 3M KCl. The electrodes were connected to a voltage clamp amplifier (VCC MC8, multichannel voltage/current clamp, Physiologic instruments, CA, USA). The electrode potential difference and fluid resistance were compensated before mounting the monolayer onto the chamber. To establish equilibrium, the potential difference was continuously monitored under open-circuit conditions for 15 min. Thereafter, the monolayers were voltage-clamped at 0 mV while continuously measuring the short circuit current (Isc). Voltage pulses (10-mV square waves sustained for 200 ms) were delivered every 20 s to yield a current response for calculating resistance across a mucosa (resistance) using Ohm's law. IL-4- (100 ng / mL; 24 h), histamine- (100 mM; 30 min), and vehicle-stimulated endothelial monolayers were placed in Ussing chambers, where TER was measured as described previously²¹⁴. To measure paracellular flux, HRP solution was left for 30 min at room temperature (RT) before the assay. The assay was started by adding 4 μg / mL of horse radish peroxidase (HRP) to the apical side of the monolayers to measure flux from the apical to the basolateral direction. Afterward, aliquots of 250 μL from the basolateral side were collected at 30, 60, 90, 120, 150, and 180 minutes. HRP was assayed colorimetrically (BD OptEIA™, CA, USA) according to the manufacturer's instructions.

2. 3. 12 Lentiviral Transduction:

Bacterial glycerol stock (Sigma–Aldrich, St. Louis, MO, USA) containing shRNA plasmid DNA was used to generate lentiviral particles containing target shRNA. In brief, to expand the bacterial glycerol stock 1 μL was incubated at 37°C for 30 minutes in terrific broth (TB) without antibiotic then cultured in Luria broth (LB) agar with ampicillin (100 $\mu\text{g}/\text{ml}$). After an overnight incubation, a single colony was expanded by incubating with 3 mL of LB plus

ampicillin for 8-10 h and then moved to 300 mL LB with ampicillin and incubated overnight. ShRNA plasmid DNA was extracted using QIAGEN Plasmid Maxi Kit (Hilden, Germany). Afterward, the lentivirus partials were produced by CCHMC's Viral Vector Core. Cells were transduced with 5 μ L of concentrated lentiviral particles or control shRNA lentiviral particles containing an empty vector (PLKO.1). Transduction was carried out with media in the presence of 10 μ g/mL of polybrene (Sigma–Aldrich, St. Louis, MO, USA). The cells were incubated for 24 h at 37°C, and then the media was replaced with fresh media. Cells were selected with 10 μ g/mL puromycin (Gibco, Grand Island, NY, USA) two days after transduction.

2. 3. 13 Flow Cytometry:

Mice were injected with IL-4C (1 μ g of IL-4 + 5 μ g anti–IL-4 mAb) or vehicle. Twenty-four hours later, mice were sacrificed, and the spleen was harvested. To prepare a single-cell suspension, the spleen was homogenized, and then the suspension was filtered with a 40- μ m pore cell strainer. Afterward, the cell solution was centrifuged (5 minutes/1200 rpm). Red blood cells (RBCs) were lysed with RBC lysing buffer (Sigma-Aldrich, St. Louis, MO, USA) and incubated for 2 minutes at 37°C; the reaction was stopped using 30 mL 1X HBSS buffer (Gibco, Grand Island, NY, USA). Cells were centrifuge and re-suspended with 200 μ L FACS buffer (0.1% sodium azide, 2 % fetal calf serum, and 1X PBS) at 2×10^6 cells/mL and then stained with anti-mouse MHC II (I-A) FITC and PerCP/Cy5.5 anti-mouse/human CD45R/B220 antibody (BioLegend, San Diego, CA, USA). Following fixation with 1% paraformaldehyde (30 minutes at 4°C), the cells were re-suspended in 200 μ L FACS buffer. Flow cytometry data acquisition and analysis were performed on BD LSRFortessa using FACS Diva software (BD Biosciences, Mountain View, CA, USA).

2. 3. 14 Immunofluorescent Assay:

Antibodies and concentrations used were as follows: anti–IL-4R α at 1:400 (Santa Cruz, # sc-28361), anti-MECA32 at 1:100 (Novous Biologicals, # NB100-77668). Immunofluorescence was done as previously described ²¹⁵, except that the antigen retrieval step was done using a decloaking chamber for 30 s at 125°C.

2. 3. 15 Statistical Analysis:

Data are expressed as mean \pm standard deviation (SD), unless otherwise stated. In experiments comparing multiple experimental groups, statistical differences between

groups were analyzed using the one/two-way ANOVA parametric test. In experiments comparing two experimental groups, statistical differences between groups were determined using a Student's t-test. A $P < 0.05$ was considered significant. Correlation analysis was performed using the Spearman's rank correlation coefficient. All analyses were performed using Prism 7.0 software (GraphPad Software Inc., San Diego, CA, USA).

2. 4. Results

2. 4. 1 IL-4 enhances histamine-induced hypovolemic shock via vascular endothelium–dependent IL-4R α chain signaling:

We first examined the effect of IL-4 on histamine-induced increase in hemoconcentration (as an indication for fluid extravasation and hypovolemic shock) and hypothermia (as an indication for anaphylactic shock severity). WT mice were i.v. injected with IL-4C (a long-acting formula IL-4 complexed with anti-IL-4²¹⁰) or vehicle and 24 h later received an i.v. challenge of histamine. We show that IL-4C alone had no effect on hemoconcentration nor on mice body temperature. Histamine alone induced an increase in hemoconcentration that was associated with hypothermia (Figure 2.1). Notably, this response was potentiated by pretreatment with IL-4, suggesting that IL-4 amplifies histamine-induced hypovolemic shock (Figure 2.1). To determine whether IL-4 amplification of the histamine response was via direct modulation of VE barrier function, we examined the effect of histamine and IL-4 on the human VE cell line EA.hy926^{211,212}. We show that TER decreased and flux of HRP (40 kDa) increased in histamine-stimulated compared to unstimulated EA.hy926 cells (Figure 2.2, A-B). Importantly, the histamine-induced increase in endothelial cell permeability was enhanced by pretreatment with IL-4 (Figure 2.2, A-B). Collectively, these data suggest that IL-4 amplifies histamine-induced VE permeability through a direct activation of VE cells.

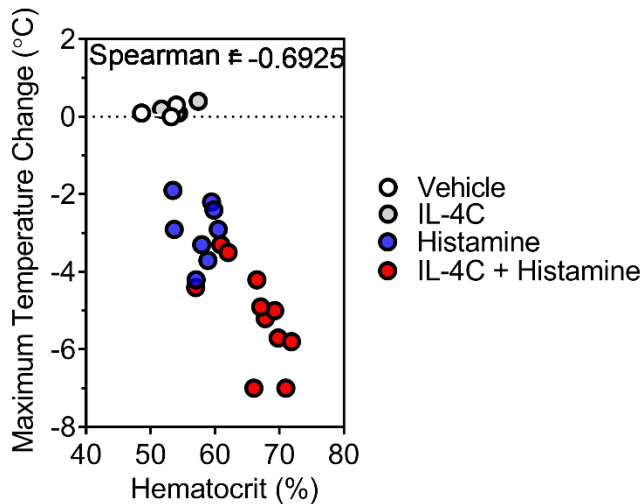


Figure 2.1: IL-4 enhancement of histamine-induced shock negatively correlates with fluid extravasation. $VE^{IL-4R\alpha^{WT}}$ ($iIL-9^{WT}$ $cadherin-5^{WT}$ $IL-4R\alpha^{fl/fl}$) mice were injected intravenously with 0.2 mL of vehicle or IL-4C (1 mg of IL-4 plus 5 mg of anti-IL-4 mAb) and then challenged intravenously 24 hours later with vehicle or histamine (0.4 mg/200 mL). Shown is the Spearman rank correlation coefficient between hematocrit percentage and the maximum temperature change from 0 to 30 minutes. Each circle represents an individual mouse ($n = 3-11$ mice per group).

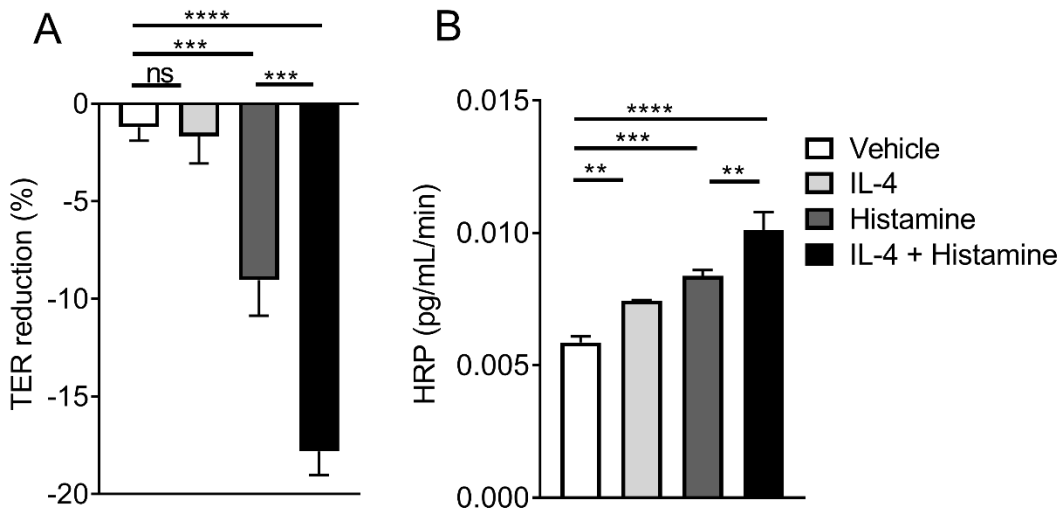


Figure 2.2: IL-4 amplifies histamine-induced VE barrier dysfunction.

A Percentage reduction in TER, B HRP flux of vehicle- or IL-4-treated EA.hy926 cells after histamine stimulation. EA.hy926 monolayers were pretreated with vehicle or IL-4 (100 ng / mL) for 24 hours and stimulated with histamine (100 mmol / L for 30 minutes) or vehicle, and TER and HRP flux were measured, as described in the methods section.

Data are represented as means \pm SDs ($n = 3$ wells per group from $n = 2$ independent experiments. **P < .01, ***P < .0001, and ****P < .0001. ns, P > .05).

To identify the requirement of IL-4 signaling on VE cells in the exacerbation of histamine-induced hypovolemic shock *in vivo*, we took a transgenic approach using the VE-specific promoter of the junction protein cadherin 5 (also called VE-cadherin)²⁰⁷. Cadherin-5^{Cre} IL-4R $\alpha^{fl/fl}$ mice (referred to as $VE^{\Delta IL-4R\alpha}$) lack the expression of the IL-4R α

chain on the VE compartment, whereas Cadherin-5^{WT} IL-4R α ^{fl/fl} mice (referred to as VE^{IL-4R α WT}) were used as a WT control (Supplementary Figure 2- 1). Mice received an i.v. injection of either IL-4C or vehicle and 24 hours later received an i.v. injection of histamine; evidence of hypovolemic shock and hypothermia were evaluated (Figure 2.3, A). I.v. administration of histamine induced hypothermia and increased hemoconcentration in both VE^{IL-4R α WT} and VE ^{Δ IL-4R α} (Figure 2.3, B-C). Pretreating VE^{IL-4R α WT} with IL-4C enhanced histamine-induced hypothermia and hemoconcentration (Figure 2.3, B-C). However, the IL-4C amplification of the histamine-induced hypovolemic shock was ablated in VE ^{Δ IL-4R α} mice (Figure 2.3, B-C). Consistent with previous studies, we found that IL-4C alone had no effect on body temperature nor on hemoconcentration⁷⁵ (Figure 2.3, B-C). To confirm IL-4C activity in VE ^{Δ IL-4R α} mice, we evaluated the expression of MHC II on B cells (B220⁺) after IL-4C treatment. We showed that the expression of MHC II on B cells increased in IL-4C–treated compared to vehicle-treated mice (Supplementary Figure 2- 2). Notably, IL-4C treatment induced a comparable increase in MHC II expression in the VE IL-4R α ^{WT} and VE ^{Δ IL-4R α} mice (Supplementary Figure 2- 2). These studies indicate that IL-4 amplification of histamine-induced hypovolemic shock was dependent on IL-4 signaling on the VE compartment.

Interestingly, clinical and experimental studies indicate that gain-of-function mutations in the IL-4R α chain have been associated with increased susceptibility to atopic disease and enhanced allergic inflammatory responses²¹⁶⁻²²¹. Given the observation that IL-4/IL-4R α signaling plays an important role in histamine-induced hypovolemic shock, we hypothesized that mice with a gain-of-function in IL-4 receptor signaling would have increased severity of histamine-induced hypovolemic shock. To test this, we employed IL-4R α ^{Y709F} mice, which have an activating variant IL-4R α chain (Figure 2.3, D). Histamine challenge of IL-4R α ^{Y709F} mice induced a hypovolemic shock response equivalent to that observed in WT mice (Figure 2.3, F). Notably, IL-4C treatment amplified histamine-induced hypothermia and hypovolemic shock in both IL-4R α ^{Y709F} and WT BALB/c mice (Figure 2.3, E and F). Moreover, we observed a significantly greater IL-4C–induced amplification of the histamine-induced hypothermic response in the IL-4R α ^{Y709F} mice than BALB/c mice, and this increased hypothermic response was associated with increased

hemoconcentration (Figure 2.3, E and F). These data indicate that enhanced IL-4R α signaling can exacerbate histamine- and IL-4-induced hypovolemic shock.

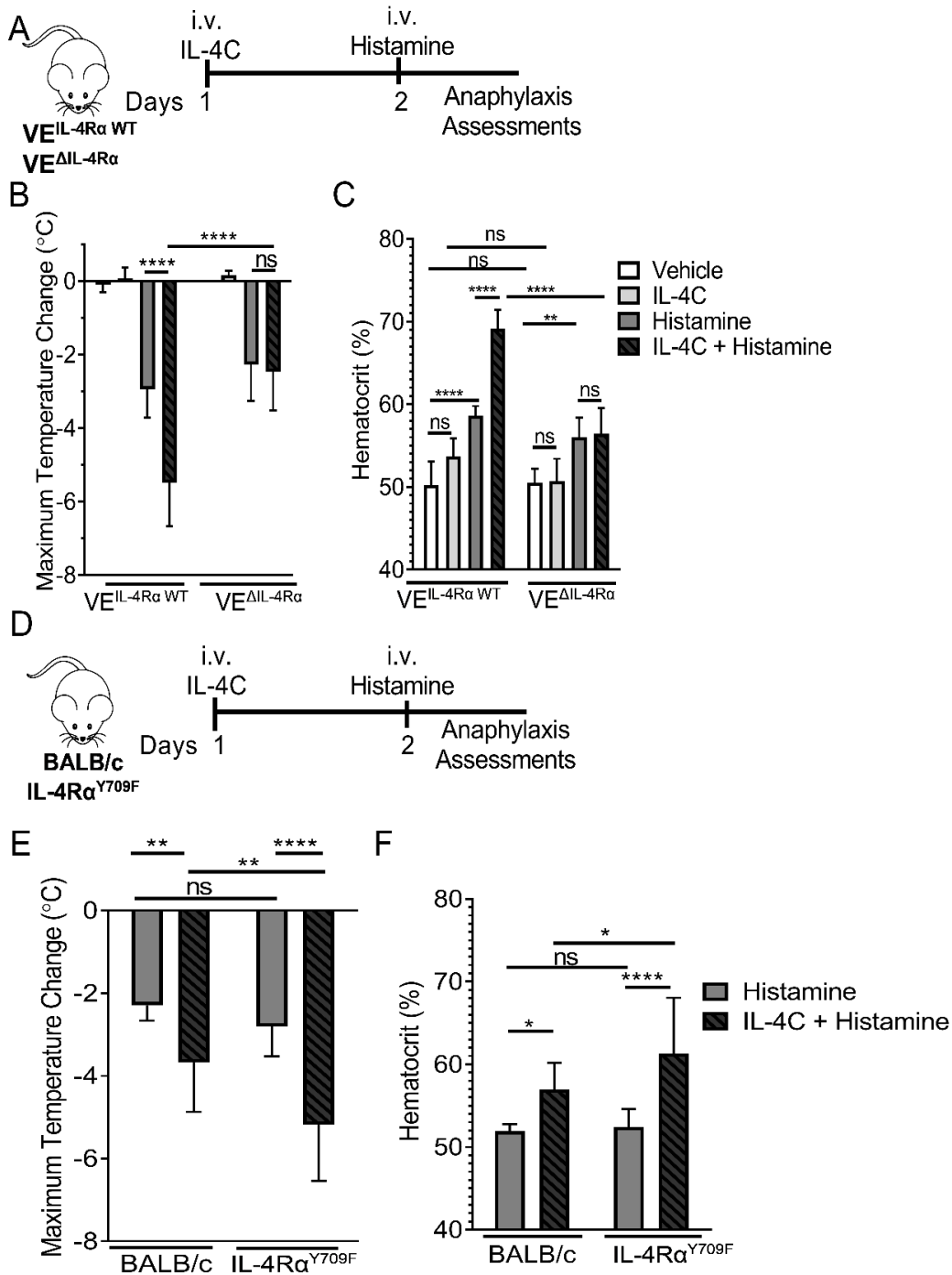


Figure 2.3: Loss and amplification of VE IL-4R α signaling alters IL-4 enhancement of histamine-induced hypovolemic shock

A and D Experimental regimen, B and E maximum temperature change, C and F and hematocrit percentage in **VE^{IL-4R α}** and **VE^{IL-4R α WT}** mice (A-C) and **IL-4R α ^{Y709F}** and **IL-4R α ^{WT}** mice (D-F) after intravenous (i.v.) injection with vehicle or IL-4C and intravenous challenge with histamine (0.4 mg).

Data are represented as means \pm SDs (n = 3-10 mice [Fig 3, B], 3-6 mice [Fig 3, C], and n= 9-13 mice [Fig 3, E and F] per group from n= 3-4 independent experiments). *P < .05, **P < .01, and ****P < .0001. ns, P > .05.

2. 4. 2 Vascular endothelial IL-4R α chain deletion attenuated hypovolemic shock induced by passive oral antigen–induced anaphylaxis:

To confirm the requirement of IL-4R α chain expression on VE in IgE/MC-mediated anaphylaxis, we used a passive oral antigen–triggered IgE-mediated anaphylaxis model⁵⁶. Cadherin-5^{Cre} IL-4R α ^{fl/fl} mice were backcrossed on the iIL-9Tg background (referred to as iIL-9Tg VE Δ IL-4R α). iIL-9Tg VE Δ IL-4R α mice and iIL-9Tg VE^{IL-4R α WT} mice were injected with anti-TNP IgE with IL-4C and then administered TNP-OVA 24 h later (Figure 2.4, A). Oral gavage of TNP-OVA increased hemoconcentration and induced shock in both iIL-9Tg VE^{IL-4R α WT} and iIL-9Tg VE Δ IL-4R α mice treated with anti-TNP IgE (Figure 2.4, B-C). Notably, pretreatment of the iIL-9Tg VE^{IL-4R α WT} mice with IL-4C exacerbated hypothermia and hemoconcentration; however, the IL-4 enhancement was absent in iIL-9Tg VE Δ IL-4R α mice (Figure 2.4, B-C). The reduced disease in iIL-9Tg VE Δ IL-4R α mice could not be explained by decreased MC activation or levels or immunoglobulin levels, as serum mMCPT-1 levels, intestinal MC levels, and immunoglobulin (Ig) (IgE and IgG1) were comparable between groups (Figure 2.4, D; Supplementary Figure 2- 3, A-E). Collectively, these data indicate that IL-4 enhancement of passive oral antigen–triggered anaphylaxis is dependent on the VE IL-4R α chain.

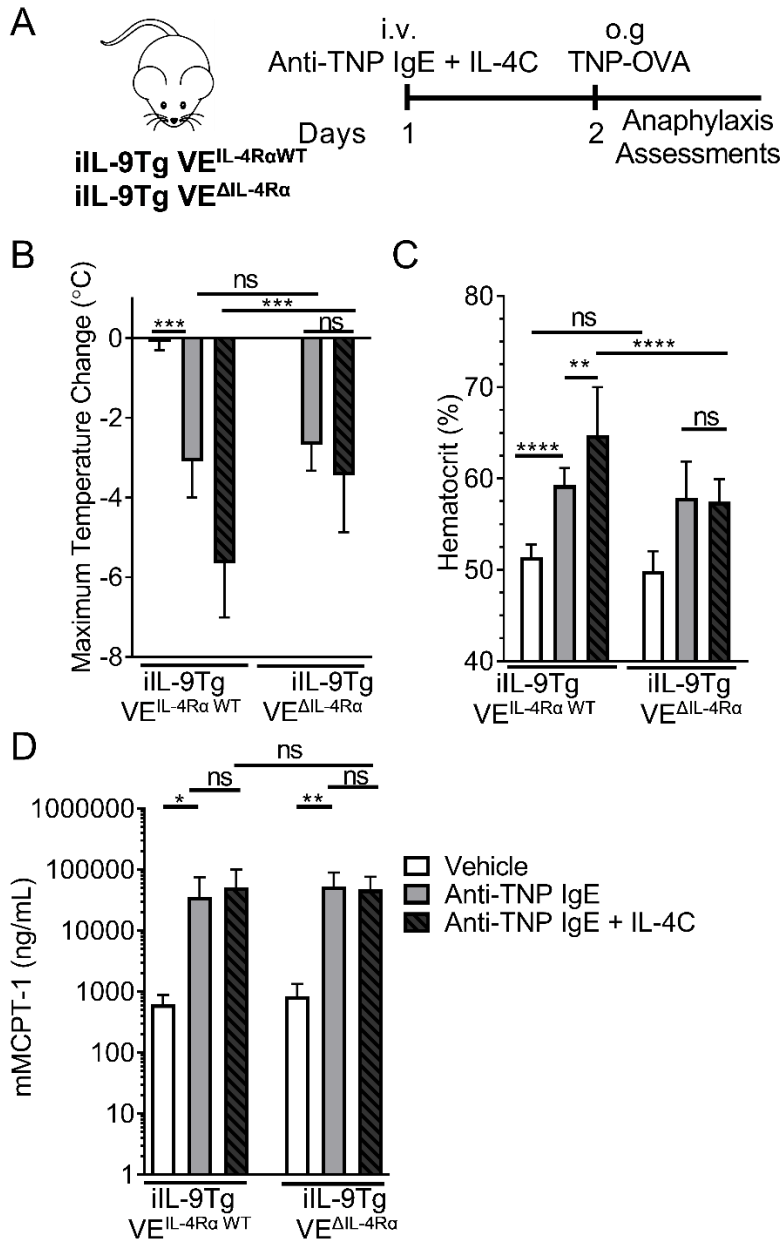


Figure 2.4: VE IL-4Ra chain deletion attenuated hypovolemic shock in a passive oral antigen anaphylaxis model.

A Experimental regimen maximum, B Maximum temperature change, C hematocrit percentage, D serum mMCPT-1 level in iIL-9^{Tg} VE^{IL-4Ra} and iIL-9^{Tg} VE^{IL-4Ra} WT mice injected intravenously (i.v.) with IL-4C mixed with anti-TNP IgE and then orally gavaged (o.g.) the next day with TNP-OVA.

Data are represented as means ± SDs (n= 3-13 mice per group from n= 4 independent experiments). *P < .05, **P < .01, ***P < .0001, and ****P < .0001. ns, P > .05.

2. 4. 3 Histamine and IL-4 modulation of paracellular leakage in the human vascular endothelial cell line (EA.hy926) is ABL1 kinase-dependent:

We were next interested in defining the signaling pathways involved in IL-4C amplification of the histamine-induced VE dysfunction. Recent studies have identified roles for members of the ABL family of non-receptor tyrosine kinases (ABL1 and ARG) and RhoA and ROCK in histamine-induced VE leakage; therefore, we examined histamine and IL-4 induction of ABL1 kinase activity^{116,126}. Employing the immortalized human endothelial cell line (EA.hy926), we firstly examined ABL1 kinase activity after histamine and IL-4 stimulation. We found that histamine and IL-4 alone stimulated ABL1 kinase activity as indicated by GST-CRK (a known ABL1 substrate) phosphorylation (Figure 2.5, A). Notably, EA.hy926 cell costimulation with both histamine and IL-4 amplified ABL1 kinase activity (Figure 2.5, A). To determine the requirement of ABL1 kinase in the histamine/IL-4–induced barrier function, we used a pharmacologic (imatinib) and shRNA ABL1 kinase knockdown approach. We show that pretreating EA.hy926 cells with imatinib blocked IL-4 amplification of histamine-induced VE barrier dysfunction in a dose-dependent manner (Figure 2.5, C-D; Supplementary Figure 2- 4). Notably, the decreased VE response in the presence of imatinib was associated with decrease of ABL1 kinase activity (Figure 2.5, B). Consistent with these observations, pretreating shRNA *ABL1*–transduced EA.hy926 cells with histamine or histamine and IL-4 did not induce VE barrier dysfunction (Figure 2.5, F-G). Taken together, these findings suggest that histamine-induced, IL-4–enhanced paracellular leakage is dependent on VE ABL kinases, possibly through ABL1 kinase.

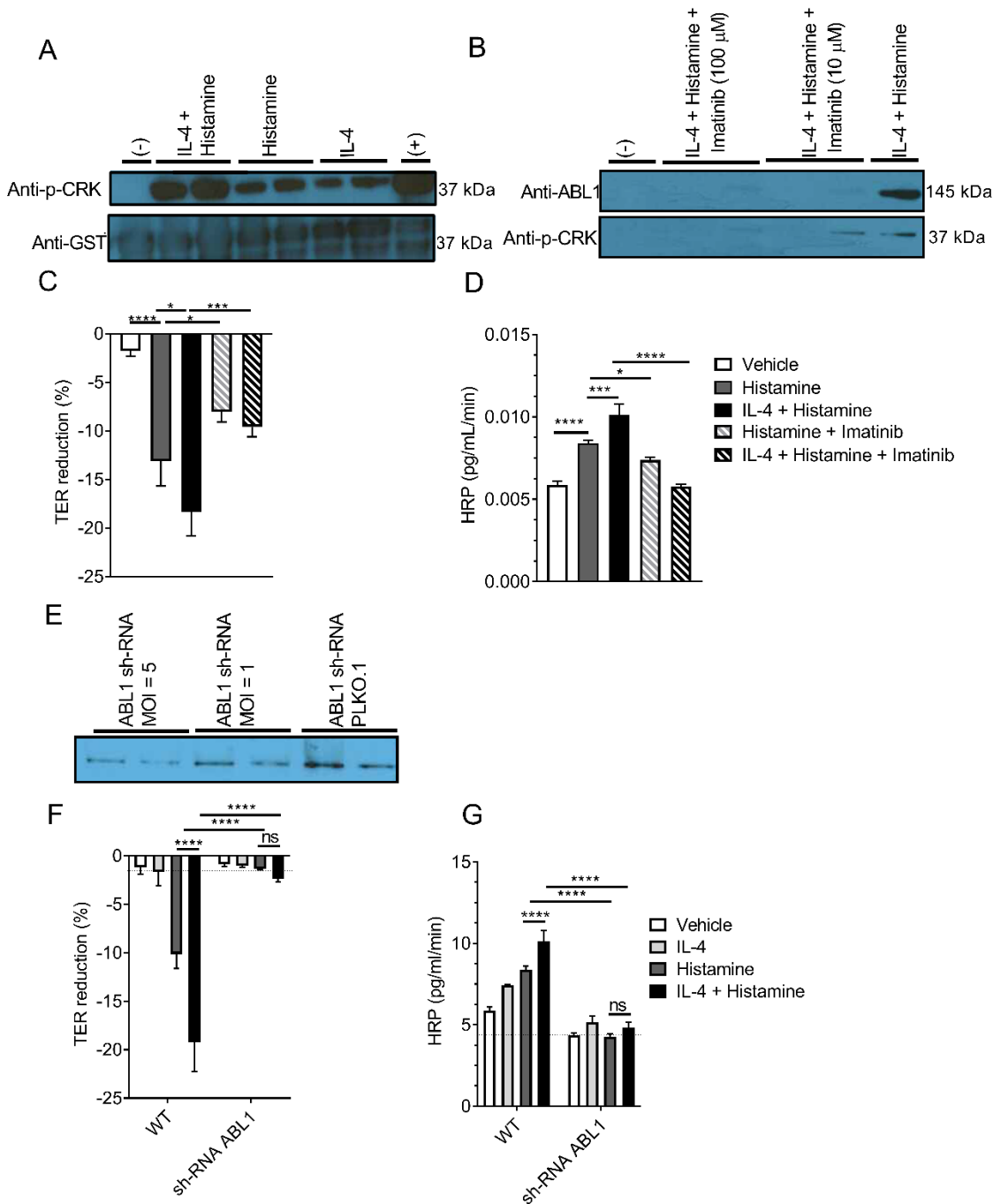


Figure 2.5: Histamine- and IL-4-induced VE barrier dysfunction is ABL1 kinase dependent

A and B, ABL1 kinase activity in vehicle- or IL-4 stimulated EA.hy926 cells after histamine stimulation (A) and in the presence of imatinib (B).

C and F TER, D and G HRP flux of EA.hy926 cells and EA.hy926 cells transduced with ABL1 shRNA or empty vector (PLKO-1) pretreated with IL-4 (10 ng/mL) and stimulated with histamine in the presence and absence of imatinib (100 mmol/L).

E ABL1 levels in EA.hy926 cells transduced with ABL1 shRNA lentiviral particles or an empty vector (PLKO-1) detected by using Western blotting.

Data are represented as means \pm SDs (n= 3 wells per group from 2 representative experiments). *P < .05, ***P < .0001, and ****P < .0001. ns, P > .05.

2. 4. 4 VE ABL1 kinase involvement in passive anaphylaxis in iIL-9Tg VE^{ΔABL1} mice:

We next examined the requirement of the VE ABL1 kinase in passive anaphylaxis by employing mice lacking ABL1 expression in the VE compartment. Tie2^{Cre} transgenic mice have been used as a genetic tool for the analyses of endothelial cell-specific gene targeting ²⁰⁸. Therefore, we employed Tie2^{Cre} ABL1^{fl/fl} mice on an iIL9Tg background (referred to as iIL-9Tg VE^{ΔABL1}) and WT control iIL9Tg Tie2^{WT} ABL1^{fl/fl} (referred to as iIL-9Tg VE^{ABL1 WT}). iIL-9Tg VE^{ΔABL1} mice and iIL-9Tg VE^{ABL1 WT} mice received an i.p. injection with vehicle or imatinib 30 minutes before i.v. injection with anti-IgE mAb (EM95) (Supplementary Figure 2- 5, A). In iIL-9Tg VE^{ABL1 WT} mice, i.v. anti-IgE mAb induced hypothermia and increased hemoconcentration, with these changes being sensitive to imatinib inhibition (Supplementary Figure 2- 5, B-C). Importantly, iIL-9Tg VE^{ΔABL1} mice showed an attenuated hypothermia that was comparable to the hypothermia observed in iIL-9Tg VE^{ABL1 WT} treated with imatinib (Supplementary Figure 2- 5). Importantly, levels of MC activation and degranulation were similar between groups (Supplementary Figure 2- 5, D). Collectively, these data indicate a requirement for VE ABL1 in hypovolemic shock induced by IgE.

2. 4. 5 ABL kinase inhibitor attenuated passive oral antigen-induced anaphylaxis:

To determine whether the ABL kinase inhibitors could suppress the development of symptoms of oral antigen-induced IgE/MC-mediated reactions in mice, we examined the effect of imatinib in a passive oral antigen-triggered, IgE-mediated anaphylaxis model. Evidence of anaphylaxis was evaluated in iIL-9Tg mice who received an i.v. injection of anti-TNP IgE and 24 hours later received either vehicle or imatinib (16-70 μg / kg per mice; 2 hours) and subsequently received oral gavage with TNP-OVA (Figure 2.6, A). In vehicle-treated mice, oral challenge of TNP-OVA induced shock, which was associated with an increase in hemoconcentration (Figure 2.6, B-C). Pretreating mice with imatinib prior to TNP-OVA administration protected the mice from hypothermia and hemoconcentration (Figure 2.6, B-C). Importantly, imatinib-mediated protection was not associated with reduced MC activation as levels of the mMCPT-1 were comparable between all groups (Figure 2.6, D).

Imatinib is known to target c-KIT, which is required for optimum MC degranulation^{222,223}. Although mMCPT-1 levels were not significantly different between group, mcpt-1 levels in imitinab-treated mice were lower than those vehicle-treated mice (Figure 2.6, D). To confirm that the imatinib-mediated protective effects were not due to decreased MC degranulation, we examined the relationship between mMCPT-1 levels and the onset of hypothermic response (Figure 2.6, E). We show that 10 out of 11 mice in the vehicle-treated, TNP-OVA–challenged group with mMCPT-1 >10,000 ng/mL were hypothermic ($\geq 1.5^{\circ}\text{C}$ temperature loss) and that no mice (0/6) with <10,000 ng/mL mMCPT-1 had hypothermia (Figure 2.6, E-F). Therefore, if we set a cut-off threshold of $\geq 10,000$ ng / mL mMCPT-1 as a level of MC degranulation sufficient to induce symptoms of anaphylaxis, this provides us with $\geq 90\%$ confidence that mice with $\geq 10,000$ ng / mL mMCPT-1 will develop evidence of anaphylaxis. Examining mMCPT-1 levels from the imatinib-treated, TNP-OVA–challenged group revealed that 10/13 mice had $\geq 10,000$ ng / mL mMCPT-1 and were protected from hypothermic response ($\geq 1.5^{\circ}\text{C}$ temperature loss) (Figure 2.6, E-F). Therefore, the protection from hypothermia in those mice is unlikely due to an effect on MC degranulation.

mMCPT-1 is a surrogate for MC activation and the hypothermic response is histamine-dependent; we therefore examined histamine levels after TNP-OVA administration in anti-TNP IgE–primed mice treated with vehicle or imatinib. TNP-OVA administration induced a significant increase in histamine levels in the vehicle-treated group, which was comparable with histamine levels in the imatinib-treated group (Figure 2.6, G). These studies suggest that imatinib protection is mainly via inhibiting ABL kinase activity independent of MC degranulation. Collectively, these data indicate that imatinib can reduce the severity of IgE/MC-driven anaphylaxis and that this effect is independent of MC degranulation.

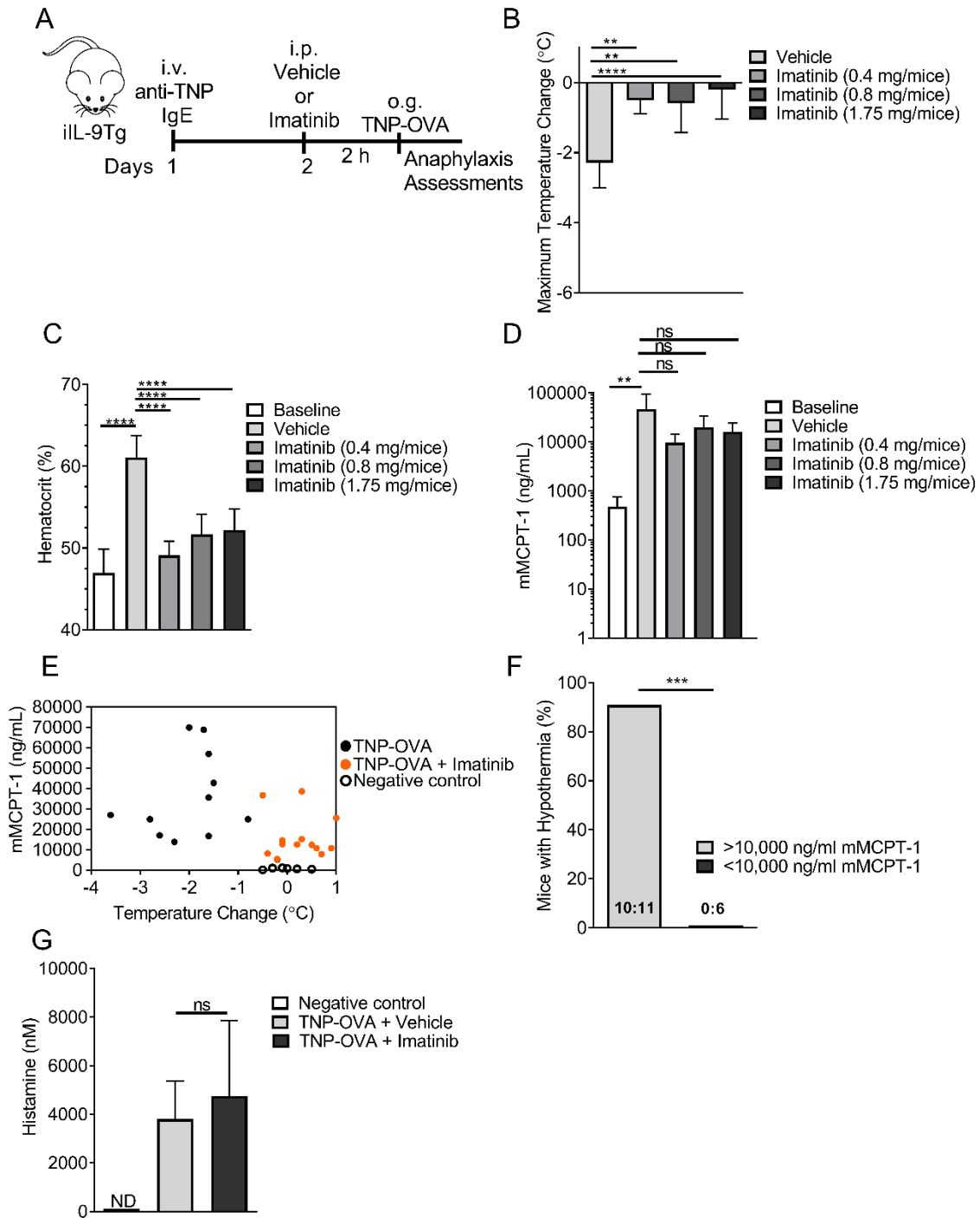


Figure 2.6: Pharmacologic inhibition of ABL kinases attenuated IgE-mediated hypovolemic shock in a passive oral antigen anaphylaxis model.

A Experimental regimen, B maximum temperature change, C hematocrit percentage, D and serum mMCPT-1 level in iIL-9^{Tg} mice injected intravenously (i.v.) with anti-TNP IgE (20 mg) and undergoing oral gavage (o.g.) with TNP-OVA. i.p., Intraperitoneal. E and F, mMCPT-1 values versus temperature change after oral challenge and Fisher exact test analysis. G Serum histamine levels in iIL 9^{Tg} mice after anti-TNP IgE and oral gavage (o.g.) with TNP-OVA in the presence and absence of imatinib. ND, Not detectable.

Data are represented as means \pm SDs (n= 3-9 mice per group [Fig 6, B-D] from n= 3 experiments and n= 5-6 mice per group [Fig 6, G]). *P < .05, **P < .01, ***P < .0001, and ****P < .0001. ns, P > .05.

2. 4. 6 ABL kinase inhibitor attenuated pre-existing oral antigen–induced anaphylaxis:

Next, we examined the effect of the ABL kinases pharmacologic antagonist, imatinib, on mice with established food allergy⁵⁶. BALB/c WT mice were primed i.p. with OVA-alum and subsequently challenged by repeated oral gavage with OVA (Figure 2.7, A). By the 6th allergen challenge, mice developed symptoms of food induced-anaphylaxis, including hypothermia and diarrhea⁵⁵⁻⁵⁷. Prior to the 7th challenge, mice were stratified into two groups, with some mice receiving vehicle while others were pretreated with imatinib (50-75 µg/kg i.p.; 2 hours) and then subsequently challenged with OVA (Figure 2.7, A). Oral antigen challenge induced hypothermia in vehicle-treated mice (Figure 2.7, B-C). In contrast, pretreating mice with imatinib protected the mice from anaphylactic shock; the level of hypothermia and diarrhea were significantly reduced in the imatinib-treated mice compared to the vehicle-treated mice (Figure 2.7, B-D). Notably, the protection from hypothermia was associated with reduced hemoconcentration (Figure 2.7, E) in the presence of comparable MC activation (mMCPT-1 levels) (Figure 2.7, F), suggesting that imatinib attenuates histamine-induced fluid extravasation. Collectively, these studies indicate that pretreating mice with imatinib can protect from the development of a severe food-induced reaction in mice with a previous history of severe reactions.

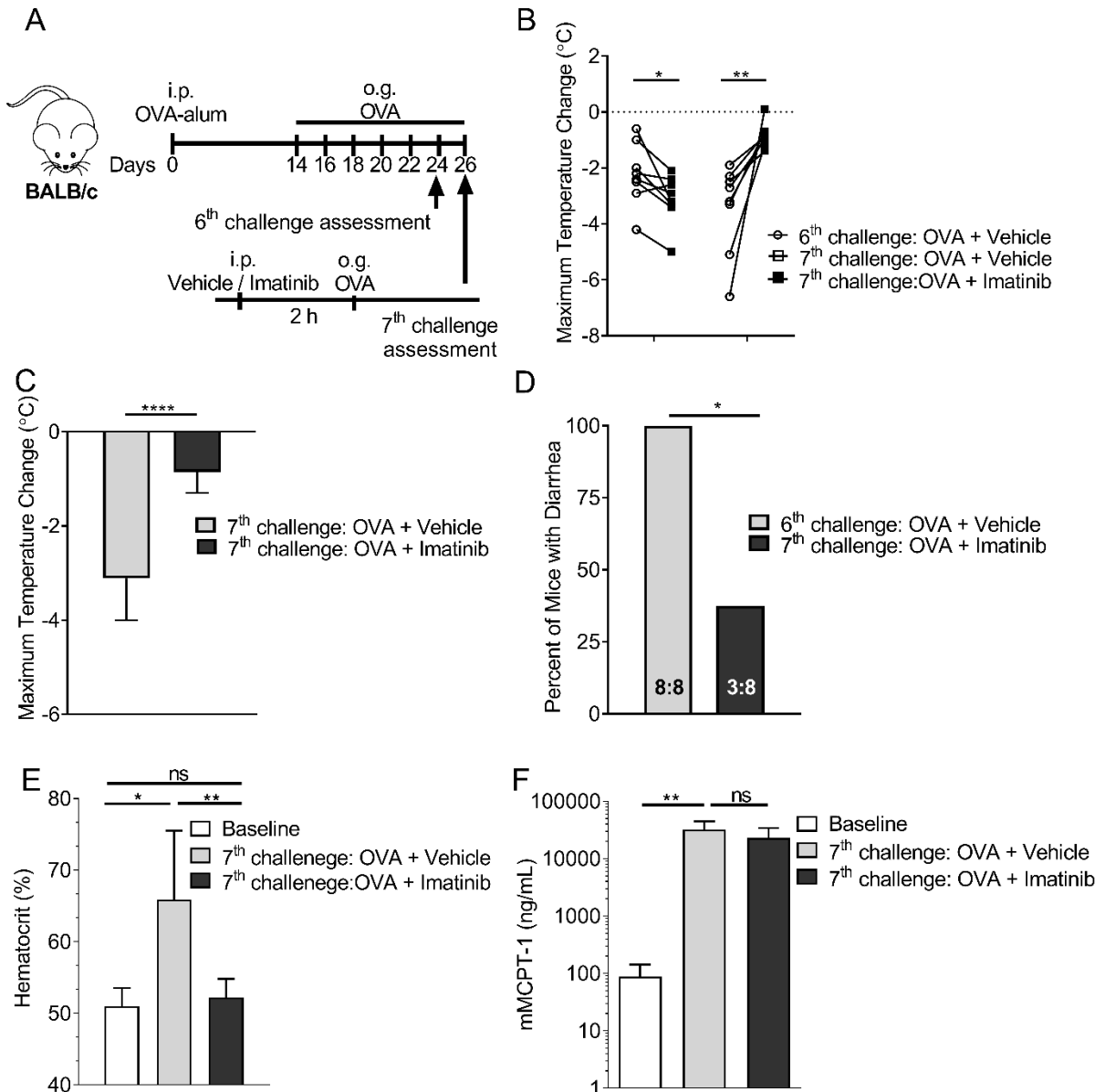


Figure 2.7: Established food-induced anaphylaxis is attenuated with ABL kinase inhibitor

A Experimental regimen, B maximum temperature changes at the sixth and seventh challenges (with or without imatinib; B and the seventh challenge (with or without imatinib; C), percentage of mice with diarrhea (D), hematocrit percentage (E), and serum mMCPT-1 level (F) of OVA-sensitized WT BALB/c mice treated with or without imatinib (1.27-1.75 mg per mouse).

Data are represented as means \pm SDs ($n = 8$ mice per group [Fig 7, D] and $n = 7-8$ per group except baseline $n = 3$ mice per group [Fig 7, E and F] from $n = 2$ experiments). In Fig 7, D, the ratio indicates the number of mice with diarrhea/total number of mice. * $P < .05$, ** $P < .01$, and **** $P < .0001$. ns, $P > .05$.

2. 5. Discussion

Clinical studies suggest a relationship between increased IL-4 and histamine levels and the severity of anaphylaxis^{203,204,224}. This was supported by animal-based studies indicating that IL-4 can exacerbate IgE-mediated reactions.³¹ IL-4 alone has been shown

to induce VE barrier dysfunction *in vitro*^{179,181}. However, the cellular target of IL-4 action and the underlying IL-4R α -dependent signaling processes involved in amplification of the IgE/MC-histamine-driven VE barrier dysfunction and fluid extravasation was not previously fully understood.

Herein, we show that: 1) IL-4 increased histamine-induced fluid extravasation, and this increase positively correlated with anaphylaxis severity (hypovolemic shock); 2) IL-4 enhancing histamine- and IgE/MC-induced systemic anaphylaxis symptoms was dependent on signaling through the VE IL-4R α chain; 3) IL-4 enhanced histamine-induced ABL1 activity and VE barrier dysfunction in human VE cells, which could be antagonized by ABL kinase inhibition; and 4) pharmacologic inhibition of ABL kinases by imatinib protected mice from passive and established oral antigen-induced anaphylaxis via suppressing VE barrier dysfunction and fluid extravasation.

Clinical evidence supporting possible involvement of hypovolemia and distributive and cardiogenic shock in human anaphylaxis³²; however, mounting evidence identifies hypovolemic shock as an important contributor to the cardiovascular collapse that leads to the severe, life-threatening anaphylactic phenotype. Consistent with these observations, aggressive fluid resuscitation has been shown to be an effective treatment for anaphylaxis occurring under anesthesia^{30,36}. Similarly, anaphylaxis in mice causes fluid extravasation, leading to severe hypovolemia and fatal tissue hypoxia^{80,81}. IgE-mediated MC activation promotes the secretion of vasoactive amines (histamine and serotonin) and lipid mediators (leukotrienes, prostaglandins) that are thought to induce VE dysfunction and the hypovolemic shock^{82,83}. Consistent with these observations, histamine treatment of mice increased hemoconcentration and hypovolemia-induced shock⁷⁵, and conversely, treating mice with H1R antagonists with or without concurrent H2R blockade attenuated IgE/MC-mediated hypovolemic shock^{59,185,205}.

Herein, we demonstrate that IL-4 can amplify the IgE-mediated, histamine-induced fluid extravasation through priming of the vascular endothelial compartment. Previous studies have revealed an important role for IL-4 and IL-4R α signaling in IgE-mediated anaphylaxis; however, this was predominantly thought to be through its effect on the hematopoietic compartment driving IgE-isotype switch and the associated CD4⁺ Th2 response in anaphylaxis⁷⁵. We show that IL-4 also acts on the non-hematopoietic

compartment, namely the VE to increase the sensitivity of the VE to histamine. This is supported by our observation levels of mMCPT-1 were comparable between iIL-9Tg VE Δ IL-4R α and iIL-9Tg VE^{IL-4R α WT} even though the iIL-9Tg VE^{IL-4R α WT} mice experienced greater hypovolemic. Notably, the mice lacking the expression of the IL-4R α chain on their VE developed histamine-induced anaphylactic shock; however, they were protected from the IL-4–induced amplification of anaphylaxis symptoms, suggesting that VE IL-4R α chain signaling is not required for histamine-induced hypovolemia but exacerbates the histamine-mediated component.

IL-4 can signal through either the type I (IL-4R α chain and γ c chain) and type II (IL-4R α chain and IL-13R α 1 chain) IL-4 receptor pathways. The previous demonstration of IL-4–enhanced anaphylaxis in RAG2/ γ c–deficient mice (which lack B cells, T cells, MCs, eosinophils, and NK cells) indicates the involvement of the IL-4 type II receptor and not the IL-4 type I receptor ⁷⁵. Interestingly, mutations in the *IL4RA* gene have been associated with susceptibility to atopic disease ²¹⁶⁻²²¹. Importantly, gain-of-function mutations in the IL-4R α chain (E375A, S478P, or Q551R) have been linked with enhanced allergic inflammatory responses including increased MCs and elevated IgE levels ²¹⁶⁻²²¹; Consistent with these observations, murine-based studies have revealed that mutations in the IL-4R α that promote gain-of-function (IL-4R α ^{Y709F}, IL-4R α ^{Q576R}, and IL-4R α ^{Y500F}) led to enhanced allergic inflammatory phenotypes including asthma, IgE-mediated responses, and food allergy ^{206,225-228}. We show that pretreating IL-4R α ^{Y709F} mice with IL-4 enhanced histamine-induced hypovolemic shock in, suggesting that gain-of-function mutations can increase severity of food-induced anaphylaxis.

Relevant to this study, Burton *et al.* and Mathias *et al.* demonstrated that IL-4R α ^{Y709F} mice have an enhanced sensitivity to food allergens and that the enhanced IgE/MC-mediated systemic anaphylaxis in IL-4R α ^{Y709F} mice is due to a direct effect on MCs ^{226,229}. Of note, Burton *et al.* showed that IL-4R α ^{Y709F} mice had a similar responsiveness to histamine to that of WT mice, suggesting no role for gain-of-function mutations in the IL-4R α chain in severity of anaphylaxis²²⁹. However, these studies were performed in the absence of IL-4 treatment. We show enhanced histamine-induced anaphylaxis with exogenous IL-4 treatment in IL-4R α ^{Y709F} mice, suggesting that gain-of-

function mutations in IL-4R α signaling can affect not only hematopoietic cell function but also non-hematopoietic cell function and severity of food-induced reactions.

Previously, we have previously demonstrated that the onset of a severe food-induced anaphylaxis in mice requires increased type 2 cytokines, food-specific IgE, and an intestinal mastocytosis⁵⁶. Antigen sensitization and repeated food antigen challenge of sensitized mice promotes an intestinal antigen-specific CD4⁺ Th2 cell / ILC2 response, which is thought to drive IL-9 producing mucosal MCs (MMC9 cells) and lead to the intestinal mastocytosis^{230,231}. We speculate that the repeated antigen challenge promotes heightened IL-4 levels, leading to the increased sensitivity of the VE compartment to MC-derived mediators. The cellular source of IL-4 during these allergic conditions is likely to be CD4⁺ T cells and basophils^{232,233}. Repeated oral antigen exposure drives the antigen-specific CD4⁺ type 2 response and generation of IL-4–dependent, antigen-specific IgE and mastocytosis^{230,231,234}. Concurrently, oral antigen exposure will also lead to IgE-Fc ϵ RI ligation on basophils and MCs, and the demonstration that IgE-mediated IL-4 responses are dependent on Fc ϵ RI and can occur independently of MCs but not basophils suggest that basophils are another likely source of IL-4^{52,232,233}.

Studies of mediators in human anaphylaxis revealed that in patients with anaphylaxis, histamine levels peaked during emergency department arrival and that histamine levels correlated with reaction severity²⁰⁴. From our observations, one would predict that IL-4 levels should also correlate with reaction severity; however, IL-4 did not correlate with reaction severity. Interestingly, the most sensitive known *in vivo* effect of IL-4 is upregulation of B cell MHC II expression^{210,235}, and IL-4 doses barely capable of inducing an increase in B cell class II MHC expression have been shown to be sufficient to enhance anaphylaxis⁷⁵. These data suggest that incremental changes in IL-4 may be sufficient to enhance histamine-induced VE dysfunction and anaphylaxis severity and may explain the lack of association between IL-4 levels and severity of anaphylaxis in human subjects.

The mechanism by which IL-4 modulates histamine responses is not fully elucidated. We show that IL-4 amplifies histamine-induced ABL1 kinase activation and that blockade of ABL1 kinase genetically or pharmacologically abrogated histamine-induced VE dysfunction and leak, suggesting that IL-4 modulation of histamine-induced

responses is likely through increased ABL1 activity. The ABL family of non-receptor tyrosine kinases, including both ABL1 and ARG, have been implicated in the regulation of endothelial barrier function ¹⁹⁵. Notably, Chislock and Pendergast demonstrated a requirement for activation of the ABL kinases in endothelial permeability induced by thrombin and Vascular endothelial growth factor (VEGF) in human microvascular endothelial cells (HMVECs) ¹²⁶.

VE-cadherin is a critical requirement for assembly and stability of the VE-cadherin–catenin–cytoskeleton complex and maintenance of endothelial barrier function ^{199,200,236}. Histamine is thought to destabilize the VE-cadherin–catenin complex through activating protein kinase C (PKC) and Rho-associated protein kinase (ROCK) and subsequent downstream activation of myosin light chain (MLC), resulting in reduced endothelial cell adhesiveness and increased paracellular permeability ¹²⁵. Pharmacologic and genetic blockade of ABL1 has been shown to reduce myosin light chain kinase (MLCK) phosphorylation and VE barrier dysfunction after VEGF and thrombin stimulation ¹²⁶.

Collectively, our data suggest that inhibiting ABL1 kinase does not ablate anaphylaxis but rather dramatically reduces the severity of the IgE-mediated reaction. On the basis of these observations, we suggest that inhibiting ABL1 kinase might be a therapeutic target for diminishing or preventing severe IgE-mediated anaphylactic reactions and could be used in conjunction with desensitization such as sublingual immunotherapy and oral immunotherapy to minimize the risk of possible severe adverse reactions. Recently, there has been significant development of second- and third-generation tyrosine kinase inhibitors (TKIs) for chronic myeloid leukemia (CML), including second-generation TKIs (dasatinib, nilotinib, and bosutinib) and third-generation TKIs (Ponatinib and GNF-2, -5, and -7), which act as ATP-binding site competitive inhibitors and allosteric ABL inhibitors that have distinct efficacy, specificity, and long-term safety ^{237,238}. Given that TKIs, such as imatinib, bind and inhibit c-KIT dependent tyrosine kinase signaling, which is essential for MC development and maturation, an added advantage of these classes of inhibitors is that they can target both MC levels and the VE compartment to attenuate IgE/MC-mediated reactions.²³⁹⁻²⁴¹. Consistent with this argument, long-term treatment with imatinib caused a profound MC deficiency in mice and patients with (PH⁺) CML²⁴². Furthermore, a recent study examined the clinical use of imatinib for treatment

of patients with severe refractory asthma and demonstrated that imatinib had excellent efficacy, reducing MC counts and activation and asthma symptoms²⁴³.

In conclusion, we show that IL-4 enhances histamine responses through the VE IL-4R α chain by modulating VE function and amplifying vascular leakage and anaphylaxis phenotypes. We demonstrated that IgE-mediated fluid extravasation and hypovolemic shock in mice are mediated by a histamine-induced, VE ABL kinase–dependent mechanism, possibly via ABL1 kinase. These studies identify that targeting of the ABL1-sensitive VE compartment may be a new pathway for therapeutic intervention and prevention of food-induced severe and life-threatening anaphylaxis and that repurposing TKI inhibitors such as imatinib may prevent food-induced reactions.

2. 6. Acknowledgment and Contributions

This work was supported by National Institutes of Health grants R01 AI073553, R01 AI 112626, R01 DK090119 (to S.P.H.), P30DK078392, and U19A1070235 and a Food Allergy Research Education Award (to S.P.H.).

Amnah Yamani, David Wu and Lisa Waggoner performed experiments. Simon Hogan and Amnah Yamani analyzed the data and wrote the manuscript. Taeko Noah designed and assisted with some experiments. Taeko Noah and Fred Finkelman manuscript revision and discussion. Simon Hogan study supervision and funding acquisition.

Chapter 3 Vascular Endothelial Cell IL-4-STAT3 Axis Modulates Severity of IgE-mediated Anaphylaxis Through Sustaining Vascular Endothelial Dysfunction

3. 1. Abstract

Severe food-induced anaphylaxis is induced by IgE-mast cell (MC)-derived mediators, which induce vasodilatation and fluid extravasation, leading to cardiovascular collapse. We have previously revealed a synergistic interaction between the cytokine IL-4 and the MC-derived mediator histamine in modulating vascular endothelial (VE) dysfunction and inducing severe anaphylaxis. We were interested in understanding the IL-4 driven molecular processes in the enhancement of histamine-induced VE dysfunction and severe anaphylaxis. We show that IL-4 enhancement of histamine-induced VE barrier dysfunction was associated with amplification of histamine-mediated VE-Cadherin degradation, intracellular calcium flux and modulated kinetic of histamine-induced Rho-GTPase activity. IL-4 enhancement of histamine-induced barrier function was inhibited by cycloheximide (CHX) indicating a requirement for de novo protein synthesis and transcription. To understand the effect of IL-4 on VE cells, we performed RNAseq analyses on flow cytometric-isolated lung VE cells (CD326⁻, CD31^{hi}, hematopoietic markers⁻) from WT BALB/c mice administered vehicle or IL-4C (IL-4+ anti-IL-4 mAb). We show that IL-4 dysregulated 83 genes. Transcription factor motif analyses revealed that 46 / 83 genes possessed a putative STAT3 motif, and these genes included: cell-cell adhesion signaling genes and Guanylate-binding proteins (such as Thbs1, Gbp4, Gbp6). Consistent with this, IL-4 stimulation in EA.hy926 cells induced both STAT3^{Y705} and STAT3^{S727} phosphorylation. shRNA ablation of VE STAT3 in EA.hy926 cells revealed that IL-4 enhancement and histamine-induced VE barrier dysfunction was partially dependent on STAT3, and that STAT3 is required for a sustained and long IL-4 enhancement of histamine-induced VE barrier dysfunction. Utilizing both *in silico* and *in vitro* approaches

we identified an IL-4-induced and STAT3-dependent VE transcriptome that was characterized by barrier integrity and barrier signaling genes including *CAPN11*, *CLDN16* and *PTPN6*. Finally, employing histamine- and IgE- induced model of anaphylaxis revealed a requirement for VE-restricted STAT3 expression in the development of hypovolemic shock. VE-specific genetic deletion of STAT3 also attenuated the IL-4-mediated amplification of histamine-induced hypovolemic shock. These studies unveil a novel role of the IL-4/ STAT3 signaling axis in the priming of VE cells and that resulted in exacerbation of IgE- and histamine-induced anaphylaxis.

3. 2. Introduction

Food-induced anaphylaxis is a potentially life-threatening condition, and it can require hospitalization^{8,9}. A recent study suggests that at least 10.8% of the United States adults are food allergic²⁴⁴. Surveys from 2015-2016 indicate that 5.6 million children have food allergies¹⁴. Unfortunately, there is no curative medication for food allergy, leaving food avoidance as the primary management method to control the disease. However, accidental exposure to food allergens is common and impacts the quality of life¹⁵.

A food allergic reaction can affect several organ systems²⁴⁵. The involvement of the cardiovascular or respiratory system defines a severe allergic reaction which is commonly termed anaphylaxis^{25,77}. Indeed, changes in the cardiovascular system were observed during peanut-induced anaphylaxis²³. Specifically, anaphylactic patients showed a decrease in stroke volume (volume of blood pumped from the heart per beat) and venous return (flow of blood from the periphery back to the heart) suggesting a decrease in vascular resistance and loss of peripheral blood volume²³. Administration of intravenous fluids significantly improved stroke volume and venous return, which support the involvement of hypovolemic shock where fluid extravagates from blood vessels into interstitial space²³. A gap in our knowledge is the molecular pathway contributing to fluid extravasation in food-induced anaphylaxis.

Experimental evidence from murine studies supports that food and oral antigen-induced anaphylaxis is IgE-MC-histamine-dependent⁵⁵⁻⁵⁷. IgE-mediated MC activation promotes the secretion of mediators (e.g., histamine, serotonin and platelet activation factor (PAF)) that can induce vascular endothelial (VE) barrier dysfunction, which causes fluid extravasation and leads to hypovolemic shock observed in anaphylaxis^{80,81}. Systemic manifestations of anaphylaxis are histamine driven, and histamine is sufficient to stimulate increased hemoconcentration and hypovolemic shock in mice^{81,183,203}. Conversely, treatment of mice with histamine receptor (H1R) antagonists with or without concurrent H2R blockade attenuated IgE/MC-mediated hypovolemic shock^{185,205}. We previously demonstrated that IL-4 increases the severity of IgE-mediated anaphylaxis by priming the VE compartment to amplify the histamine-induced fluid extravasation²⁴⁶.

Indeed, histamine and IL-4 were increased in the serum of anaphylactic patients. However, histamine but not IL-4 levels correlated with anaphylaxis severity²⁰⁴. The knowledge gap is the IL-4-induced molecular pathways that amplify histamine-induced VE barrier dysfunction and anaphylaxis.

VE cells serve as a selective barrier between the blood and the surrounding interstitial tissue to regulate protein and cell trafficking in and out of the tissue⁸⁷. Histamine has been shown to increase the permeability of VE cells by targeting the adherence junction protein, VE-Cadherin²⁴⁷. VE-cadherin intracellular domain complex with adpater molecules, such as β -catenin, to facilitate VE-cadherin tethering to the actin cytoskeleton⁹¹. Histamine signaling increases intracellular Ca^{2+} , activates classic protein kinase C (PKC) and RhoA GTPase leading to cytoskeleton rearrangement and junctional protein phosphorylation¹¹⁶. The phosphorylation of the cytoplasmic tail of VE-cadherin modulates the AJs dynamics. Histamine also activates the non-receptor tyrosine kinases SRC and ABL that regulates the binding of VE-Cadherin to β -catenin^{101,126}. These pathways converge to promote the disassemble of VE-cadherin complexes to allow disruption of the endothelial cell-cell junction thus increasing vascular leakage^{85,101,116}. Although IL-4 has been shown to enhance histamine VE response, the molecular pathways driving this interaction are unclear²⁴⁶.

The non-hematopoietic Type II IL-4 receptor pathways (IL-4R α chain and IL-13R α 1 chain) can signal through STAT3^{130,131}. In VE cells, STAT3 regulates permeability induced by VEGF, IL-6 and histamine^{101,248,249}. However, the role that VE STAT3 plays in IL-4 amplification of the histamine-induced VE barrier dysfunction and IgE-MC mediated anaphylaxis remains unknown. Therefore, we aimed to define the requirement of VE STAT3 in severe IgE-MC-induced anaphylaxis, hypovolemic shock and VE dysfunction.

Herein, we show that IL-4 enhancement of histamine-induced VE barrier dysfunction was dependent on gene transcription. Consistent with this, IL-4 stimulates phosphorylation of STAT3 for maximum gene transcription in VE cells. We show that IL-4 enhancement of histamine-or IgE-mediated hypovolemic shock was associated with IL-4-induced changes in endothelial cells transcriptome characterized with enrichment of genes that possessed STAT3 motif. Utilizing both *in silico* and *in vitro* approaches we

identified an IL-4-induced VE transcriptome that was characterized by barrier integrity and barrier signaling genes. Interestingly, we find that IL-4 enhancement and persistence of histamine-induced VE barrier dysfunction required STAT3 signaling. Indeed, VE STAT3 was required for IL-4 enhancement of both histamine- and IgE-MC-induced hypovolemic shock. These studies implicate a key role of the VE-specific STAT3 signaling pathway in modulating the severity of IgE- and histamine-induced anaphylaxis.

3. 3. Material and methods

3. 3. 1 Animals:

Cadherin-5^{Cre} mice (Stock No: 006137 ;Jackson Laboratory) (Bar Harbor, ME, USA) and STAT3^{fl/fl} mice (generously provided by Dr. Patricia C. Fulkerson, Cincinnati Children's Hospital Medical Center (CCHMC) (OH, USA) and iIL9Tg were used to generate mice lacking STAT3 in VE compartment²⁵⁰. Intestinal IL-9 transgenic (iIL9Tg) mice were generated as previously described⁵⁷. Age-, sex-, weight-matched littermates were used as controls in all experiments. The mice were maintained and bred in a clean barrier facility, and were handled under an approved Institutional Animal Care and Use Committee protocols at University of Michigan animal facility.

3. 3. 2 IL-4 and Histamine-Induced Anaphylaxis:

Twenty-four hours before the experiments, mice were injected i.v. with IL-4C (recombinant, IL-4-neutralizing, anti-IL-4 monoclonal antibody [mAb] complex, 1:5 weight) (anti-IL-4 mAb was obtained from Fred Finkelman, CCHMC) followed by histamine biphosphate monohydrate (Sigma-Aldrich, St. Louis, MO, USA) (2 mg / 200 mL saline per mouse)²¹⁰. Anaphylaxis was assessed as previously described²⁴⁶.

3. 3. 3 Passive Anaphylaxis:

Mice were injected intravenously (i.v.) with 1-20 µg / 200 µL of anti-IgE (IgG2a mAb to mouse IgE; clone EM95) (Obtained from Fred Finkelman, CCHMC). EM95 cross-linking to FcεR1 lead to MC and basophil activation and degranulation²⁰⁹. Anaphylaxis was assessed as previously described²⁴⁶. For histamine measurements, serum was collected by retro-orbital bleeding in separate experiments 10-15 minutes following anti-IgE injection. Serum Histamine was measured by EIA (IM2015 kit; IMMUNOTECH; Beckman Coulter; Brea, CA, USA).

3. 3. 4 ELISA Measurements:

Mouse MC protease 1 (mMCPT-1) serum levels were measured by ELISA according to the manufacturer's instructions (eBioscience, San Diego, CA, USA).

3. 3. 5 Mouse endothelial cells isolation and sorting:

BALB/c mice were treated with IL-4 complex (IL-4C; 1µg of recombinant, murin IL-4 plus 1µg of anti-IL-4 mAb complex) or vehicle for 24 hours. Mice were anesthetized with Ketamine/Xylazine. A small incision was made into the atrium and a needle was inserted into the ventricle to flush the pulmonary circulation with phosphate-buffered saline (PBS). To maintain VE cell viability, Dispase (20.5 mg in 1.2 ml PBS) was delivered into the lungs through a catheter inserted into the trachea²⁵¹. Mouse lung cells were obtained by digestion of lung tissue with Liberase TL (0.25 mg / mL) and DNase I (0.5 mg / mL) for 30 minutes at 37 °C. Cells were suspended in FACS buffer and subsequent EP-CAM BV421, CD31 PE and hematopoietic markers (CD45.2, Ly-6G, CD11c, ST2, CD11b, CD4, CD8 and B220) PerCP-Cy5.5 antibodies. VE cells were sorted using FACS Aria II cells sorter (BD Biosciences) and FACSDiva software (BD Biosciences).

3. 3. 6 RNA Isolation and sequencing:

RNA was isolated using Zymogen Quick-RNA Kit. The purified RNA was amplified using the Ovation RNA-Seq System v2. The Nextera XT DNA Sample Preparation Kit, was then used to create DNA library templates from the double stranded cDNA. Libraries were sequenced at the Genetic Variation and Gene Discovery Core Facility (Cincinnati Children's Hospital Medical Center) on the Illumina HiSeq2500 and at the Advanced Genomic Core (University of Michigan) NovaSeq (S4) 300 cycle with single-reads sequencing and 35 million to 40 million depth of coverage, and.

3. 3. 7 RNA sequencing data analysis:

FASTQC program and Trimmomatic tool were used to examine the quality of raw reads and to filter poor quality reads. Genome indexing was performed using Bowtie2 and the reads were aligned to the mm9 mouse reference genome (GRCm38) and human reference genome (GRCh38) using HiSAT2 program with the default options. Read counts were generated using the feature-counts function from the subRead package. Downstream analysis was performed using IDEP 9.1 webtool and R (R Core Team,

Vienna, Austria) where the read counts were analyzed to identify the differentially expressed genes (DEGs). Differential expression analysis was performed using DESeq2. DEGs were filtered using $p\text{-adj} \leq 0.05$ and the heat map was generated using python script on the normalized scale. Gene ontology (GO) enrichment analysis of the differentially expressed RNA transcripts was performed using DAVID Bioinformatics Resources 6.8. A comprehensive database of human and mouse DNase-seq, and H3K27ac ChIP-seq profiles named The epigenetic Landscape In Silico deletion Analysis (LISA) was used to determine the transcription factors and chromatin regulators that are directly responsible for the perturbation of the differentially expressed genes set²⁵². Protein-protein interaction data was extracted using STRING database. Network analysis was performed in Cytoscape3.7.1.

3. 3. 8 Cell specific expression profile:

To identify the EC specific expression profile in data, genes/markers were used from publicly available data in the NCBI Gene Expression Omnibus database (accession numbers: GSE99235) The searchable database is available at <http://betsholtzlab.org/VascularSingleCells/database.html>. In brief, database was derived from single cells RNA sequencing on endothelial cells sorted using Cldn5 (BAC)-GFP mice. Transcriptional basis of the gradual phenotypic change (zonation) along the arteriovenous axis was based on using Nr2f2 as maker for venous cells and Bmx, Efnb2, Vegfc and Sema3g as makers for arterial cells²⁵³.

3. 3. 9 Endothelial Cell Resistance Measurement:

The EA.hy926 barrier function was assayed by measuring the resistance of a cell-covered electrode by using an Ztheta Electric Cell-substrate Impedance Sensing (ECIS) system (Applied BioPhysics, Troy, NY, USA). Readings were taking at 4000Hz for resistance and 64,000 Hz for capacitance. An 8W10E+ array was coated with 1 μg / 300 μl water / well human Fibronectin (R&D system, Minneapolis, MN, USA) overnight in 37°C. EA.hy296 cells were plated on the electrodes at 100,000 cells per well and medium was changed daily. The day after cell plating, 200 nM Hydrocortisone was added for 24 hours to stabilize the barrier. Afterward cells were treated with vehicle of recombinant human IL-4 (100 ng / mL; 24 hours; PeproTech Rocky Hill, NJ, USA). At the day of the experimnt, media without hydrocortisone was replace and Resistance

reading was left to stabilize for 1-1:30 hr, then cells were treated with vehicle or histamine (100 mM; 30 minutes; Sigma–Aldrich, St. Louis, MO, USA). The average baseline resistance readings varied between 1000 and 1500 Ω . For some experiments Cycloheximide (Sigma–Aldrich, St. Louis, MO, USA) stock was made in ethanol and diluted with cell culture medium as needed. In some experiments, we applied a published mathematical model to differentiate between the resistance between cells (R_b) and the resistance beneath the cells (α)²⁵⁴.

3. 3. 10 Cell Lines and Culture:

EA.hy926 cell line was originally derived by fusing human umbilical vein endothelial cells with the permanent human cell line A549 (ATCC, Manassas, VA, USA)^{206,212}. Cells were cultured in Dulbecco's Modified Eagle Medium (DMEM) supplemented with 10% fetal bovine serum (Atlanta Biological), nonessential amino acids (0.1 mM), sodium pyruvate (1 mM), HEPES (10 mM), and 1X penicillin and streptomycin (50 mg / mL) in a humidified incubator (5% CO₂, 37°C)^{211,212}. All reagents were obtained from Gibco, Life Technologies (Waltham, MA, USA) unless stated otherwise.

3. 3. 11 Lentiviral Transduction:

Bacterial glycerol stock (Sigma–Aldrich, St. Louis, MO, USA) containing shRNA plasmid DNA was used to generate lentiviral particles containing target shRNA. In brief, to expand the bacterial glycerol stock 1 mL was incubated at 37°C for 30 minutes in terrific broth (TB) without antibiotic then cultured in Luria broth (LB) agar with ampicillin (100 mg / mL). After an overnight incubation, a single colony was expanded by incubating with 3 mL of LB plus ampicillin for 8-10 hours and then moved to 300 mL LB with ampicillin and incubated overnight. shRNA plasmid DNA was extracted using QIAGEN Plasmid Maxi Kit (Hilden, Germany). Afterward, the lentivirus partials were produced by CCHMC's Viral Vector Core. Cells were transduced with 5 mL of concentrated lentiviral particles or control shRNA lentiviral particles containing an empty vector (PLKO.1). Transduction was carried out with media in the presence of 10 mg / mL of polybrene (Sigma–Aldrich, St. Louis, MO, USA). The cells were incubated for 24 h at 37°C, and then the media was replaced with fresh media. Cells were selected with 10 mg / mL puromycin (Gibco, Grand Island, NY, USA) two days after transduction.

3. 3. 12 *In vitro* intracellular calcium measurement:

For intracellular calcium ($[Ca^{+2}]_i$) measurement, 40.4 mm glass-bottom plates (Thermo Scientific, 15680) were coated with fibronectin 1 μ g/1cm² in 1X phosphate buffered saline and incubated at 37°C for 24 hours. EA.hy926 cells were plated at a density of 50,000 and incubated at 37°C overnight. Cells were loaded with Fluo-4, AM (Invitrogen, F14201) diluted in Pluronic F-127 and a baseline reading was recorded for 15 minutes. Following the baseline reading, cells were loaded with 100 μ M of histamine and intracellular calcium flux was measured for 30 minutes. Fluorescence images of Fluo-4 AM were acquired every 15 seconds with a Nikon N-SIM + A1R microscope and with a 20x objective. The fluorescent intensity from 10 representative areas was measured and normalized by subtracting an intensity of an area without cells by using FIJI Image J software. The area under the curve was determined by plotting the fluorescent intensity over 30 minutes with Prism software (GraphPad Software, La Jolla, Calif).

3. 3. 13 Western blot:

EA.hy926 cultures were lysed using Radioimmunoprecipitation Assay Buffer (RIPA) (Cell Signaling Technology, Danvers, MA, USA) supplemented with Halt protease inhibitor cocktail (Thermo Fisher Scientific Incorporated, Rockford, IL, USA) and PhosSTOP (Roche, Basel, Switzerland). Proteins were then quantified with BCA assay, and 5-20 μ g of protein extracted together with protein-reducing buffer was loaded and separated on a 4%-12% Bis-Tris gel and transferred to a nitrocellulose membrane (Life Technologies, Carlsbad, CA). Antibody of STAT3, VE-Cadherin (Abcam# 33168, 1:3000), STAT3 (sc#8019, 1:1000), phospho STAT3 Tyr705 (CST#9145, 1:1000), phospho STAT3 Ser705 (CST#9134, 1:1000) and GAPDH (1:50,000) were used for protein detection. Following incubation with appropriate secondary antibody, Super Signal™ West Pico PLUS Chemiluminescent Substrate Thermo Fisher Scientific, Waltham, MA, USA) was used to develop the assay and Amersham imager (GE Healthcare, Chicago, IL, USA) was used for imaging.

3. 3. 14 Rho GTPase assay:

Rho GTPase activity was measured using G-LISA RhoA Activation Assay Biochem Kit (Cytoskeleton, Denver, CO) according to the manufacturer's instructions. EA.hy926 cells were plated in the amount of 5×10^5 cells in 10 cm tissue culture dish. Next day, cells were treated with IL-4 (100 ng / mL) / Vehicle for 24 hours. Before stimulation

with the histamine, cells were serum starved for 6 hours (with the presence of IL-4). Then cells were stimulated with Histamine (10 μ M) for various time points. Cells then were lysed, centrifuged and lysate were frozen in aliquots immediately. Protein concentration was determined as instructed in the manufacturer protocol. To normalize the G-LISA results, Western Blot was performed using rabbit anti-RhoA (CST #2117;1:2000).

3. 3. 15 Immunohistochemistry staining:

Harvested Lungs were infiltrated and fixed with 4% paraformaldehyde in PBS for 24 hours before paraffin embedding. Five μ M-thick sections were dewaxed and rehydrated through an ethanol gradient before antigen retrieval in Tris/EDTA pH 9.0 buffer. The following antibodies and concentrations were used: anti-STAT3 (1:50, polyclonal H-190, Santa Cruz Biotechnology catalog #sc-7179). For immunohistochemistry, the Mouse on Mouse Immunodetection Kit, peroxidase (Vector Laboratories, Burlingame, CA, USA) was used for detection following the manufacturer's instructions. DAB Substrate Kit, peroxidase was used for developing (Vector Laboratories). Slides were counterstained with Hematoxylin, dehydrated with ethanol and mounted in CYTOSEAL 60 (Thermo Fisher Scientific).

3. 3. 16 Statistical Analysis:

Data are expressed as mean \pm standard deviation (SD), unless otherwise stated. In experiments comparing multiple experimental groups, statistical differences between groups were analyzed using the one/two-way ANOVA parametric test. In experiments comparing two experimental groups, statistical differences between groups were determined using a Student's t-test. P-value \leq 0.05 was considered significant. All analyses were performed using Prism 9.0 software (GraphPad Software Inc., San Diego, CA, USA).

3. 4. Results

3. 4. 1 IL-4 amplified the magnitude and extended histamine-induced VE barrier dysfunction in EA.hy926 cell line:

We have previously demonstrated that IL-4 directly signals through the IL-4R α chain on VE cells to enhance histamine-induced VE barrier dysfunction²⁴⁶. To better understand the temporal and spatial components of IL-4 enhancement of histamine-

induced VE barrier dysfunction, we monitored the resistance of vehicle or IL-4 pre-treated EA.hy926 cells (an immortalized human vascular endothelial cell line) following histamine stimulation for 120 minutes (Figure 3.1). Histamine stimulation of untreated EA.hy926 cells induced a rapid decrease in the VE resistance reaching maximal response ~ 20 minutes following histamine exposure (defined as immediate response) (Figure 3.1, A and B). The VE resistance returned to baseline levels at ~ 40 minutes following histamine exposure (defined as recovery phase) (Figure 3.1, A and C). Histamine stimulation of IL-4-pretreated EA.hy926 cells induced a rapid reduction in resistance that was significantly greater in amplitude (immediate response Figure 3.1, A and B). Furthermore, IL-4 pretreatment led to a more sustained response and the resistance remained significantly lower than that of vehicle-pretreated histamine-stimulated cells at 120 minutes following exposure (Figure 3.1, A). Notably, the recovery phase response in the IL-4-pretreated EA.hy926 cells was significantly tempered compared with vehicle-treated cells following histamine stimulation (Figure 3.1, C).

Resistance in the ECIS[®] Z-Theta system is defined as the sum of resistance between cells (R_b), resistance beneath the cells (α) and resistance coupled to cell membrane (C_m ; constant) (Supplementary Figure 3- 1, A). Analyses of the R_b values showed that histamine stimulation of EA.hy926 cells decreased R_b significantly, which was enhanced by IL-4 pretreatment (Supplementary Figure 3- 1, B and C). Histamine stimulation did not decrease α values compared to vehicle, and IL-4 pre-treatment had no significant effect on the α values (Supplementary Figure 3- 1, D and E). These data indicate that the observed changes in the VE resistance, induced by IL-4 and histamine stimulation, reflect changes in para-cellular resistance. Together, these data show that IL-4 synergize with histamine to modulate the magnitude and kinetic of histamine induced VE-barrier dysfunction.

The VE permeability relies on the opening and closing of endothelial cells-to-cell junction, mainly adherence junction (AJ)^{97,255}. Specifically, histamine disrupts VE-Cadherin at the cellular junction to increase VE permeability²⁵⁶; Therefore, we examined VE-cadherin protein level and cellular distribution in vehicle or IL-4 pre-treated EA.hy926 cells following histamine stimulation. Histamine stimulation of EA.hy926 cells decreased VE-cadherin levels within 5 minutes which returned to basal levels within 15

minutes compared to vehicle treated cells (Figure 3.1, D). Histamine stimulation of IL-4 pre-treated cells led to a significant and a sustained decrease in VE-cadherin expression upon 5, 15, 30, 60 and 120 minutes of histamine treatments (Figure 3.1, D). The maximum decrease in VE-cadherin was observed at 30 minutes and this was followed by a gradual recovery (Figure 3.1, D). Importantly, the kinetics of VE cadherin protein levels in IL-4 pre-treated histamine stimulated cells mirrored the kinetics of the amplified and sustained reduction in resistance (Figure 3.1, A). Using a polyclonal VE-cadherin Ab for immunoblotting showed that none of the treatments demonstrated low molecular weight products for VE-cadherin, suggesting that there was no endosomal degradation of VE-cadherin following treatments.

Immunofluorescence analysis for VE-Cadherin, demonstrated that 5 minutes of histamine treatment decreased localization of VE-Cadherin at the lateral membrane of the cells, compared to vehicle treated EA.hy926 cells (Figure 3.1, E). IL-4 pre-treatment dramatically modulate localization of VE-Cadherin expression upon histamine exposure for 5-30 minutes compared to cells treated with histamine alone (Figure 3.1, E).

Intracellular Calcium $[Ca^{+2}]_i$ and Rho GTPase signaling pathways are the major histamine-driven pathways that disrupt VE barrier function^{116,256}; Consistent with this, histamine stimulation of EA.hy926 cells rapidly increased $[Ca^{+2}]_i$ influx (Figure 3.2, A and B). IL-4 pre-treatment enhanced histamine-induced $[Ca^{+2}]_i$ influx compared to histamine treatment alone (Figure 3.2, A and B). IL-4 pretreatment alone had no effect on $[Ca^{+2}]_i$ influx (Figure 3.2, A and B).

Histamine stimulation of EA.hy926 cells rapidly increased Rho GTPase activity within 10 seconds and that went down rapidly with time (Figure 3.2, C). Histamine stimulation of IL-4 pre-treated cells led to a delayed and more sustained histamine-induced Rho GTPase activation with the response being sustained for up to 60 minutes (Figure 3.2, C). We concluded that, IL-4 enhancement of histamine-induced VE barrier dysfunction was associated with enhanced histamine-induced intracellular calcium flux and RhoA GTPase activity.

These data show that IL-4 enhancement of histamine-induced VE barrier dysfunction is associated with amplification of histamine-induced $[Ca^{+2}]_i$ flux, and modulating the kinetics of histamine-induced Rho GTPase activation.

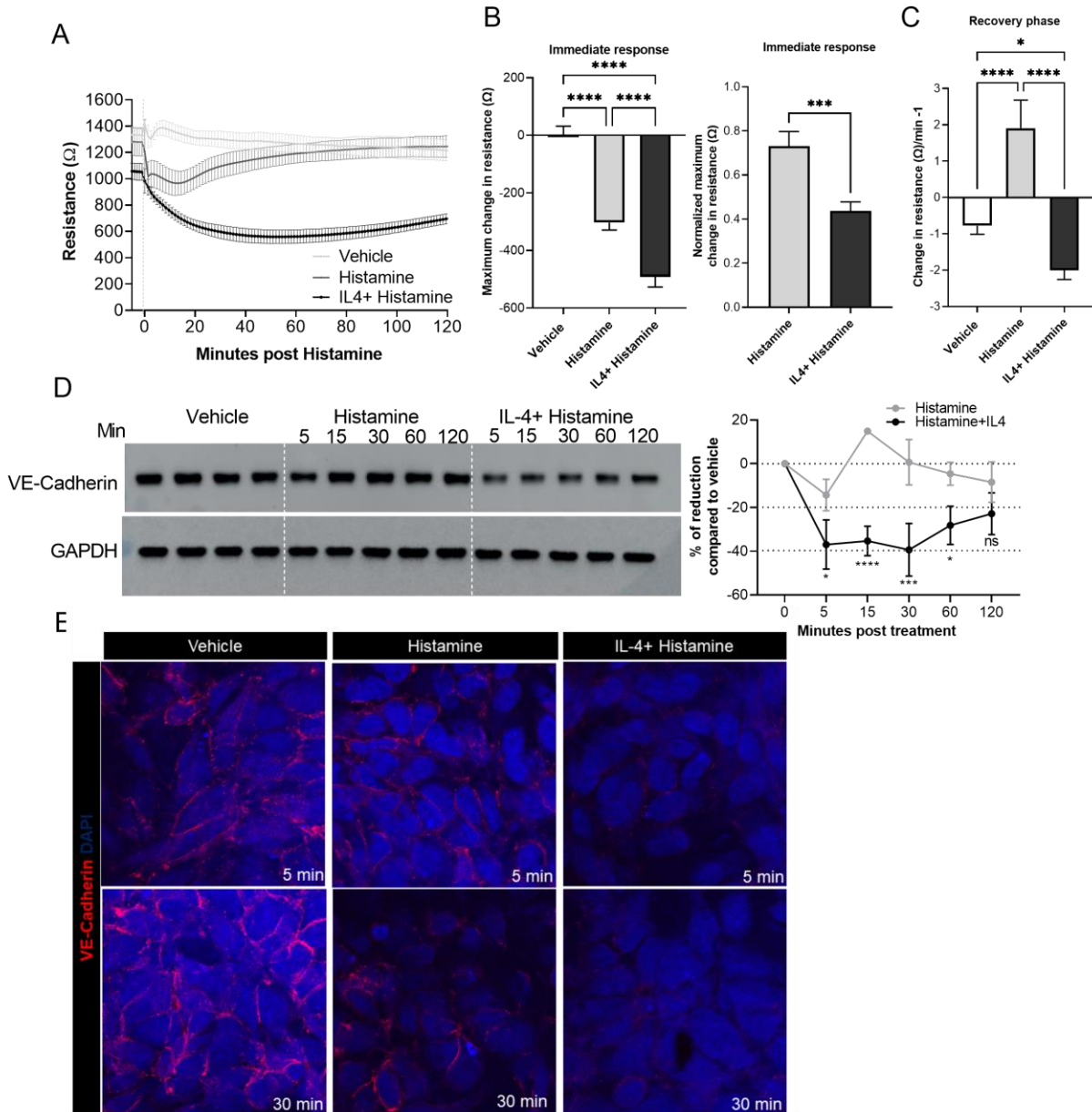


Figure 3.1: IL-4 amplified histamine-induced VE barrier dysfunction and prevented barrier restoration in EA.hy926 cell line and this was associated with decrease VE-Cadherin expression

A, Absolute resistance in ohms of post-confluent EA.hy926 cells monolayer pre-treated with Vehicle (PBS) or IL-4 (100 ng / mL; 24 hours) followed by removal of IL-4 then treatment with Vehicle (PBS) or histamine (100 μM; 2 hours) in ECIS® Z-Theta system.

B, Raw and normalized maximum change in resistance within 60 minutes of histamine treatment

C Recovery phase is the rate of resistance 20 minutes post maximum change in resistance

D Western blot analysis for VE-Cadherin from EA.hy926 cells treated with Vehicle (PBS) or IL-4 (100 ng / mL; 24 hours) followed by removal of IL-4 then treatment with Vehicle (PBS) or histamine (100 μM; 5-120 minutes), GAPDH was used as a loading control, lower graph showing quantification of Western blot analysis of VE-cadherin presented as percentage of reduction in VE-Cadherin level compared to vehicle treatment.

E Immuno-fluorescent analysis of VE-Cadherin of EA.hy926 monolayer on trans-well

Data are represented as the mean \pm SD; n = 3 samples per group from representative experiments (A-C). A represented blot from 3 independent biological replicates, data are presented as the mean \pm SD; n = 3 from 3 technical replicates (D). ****P < 0.0001, ***P < 0.001, **P < 0.01, *P < 0.05, ns > 0.05

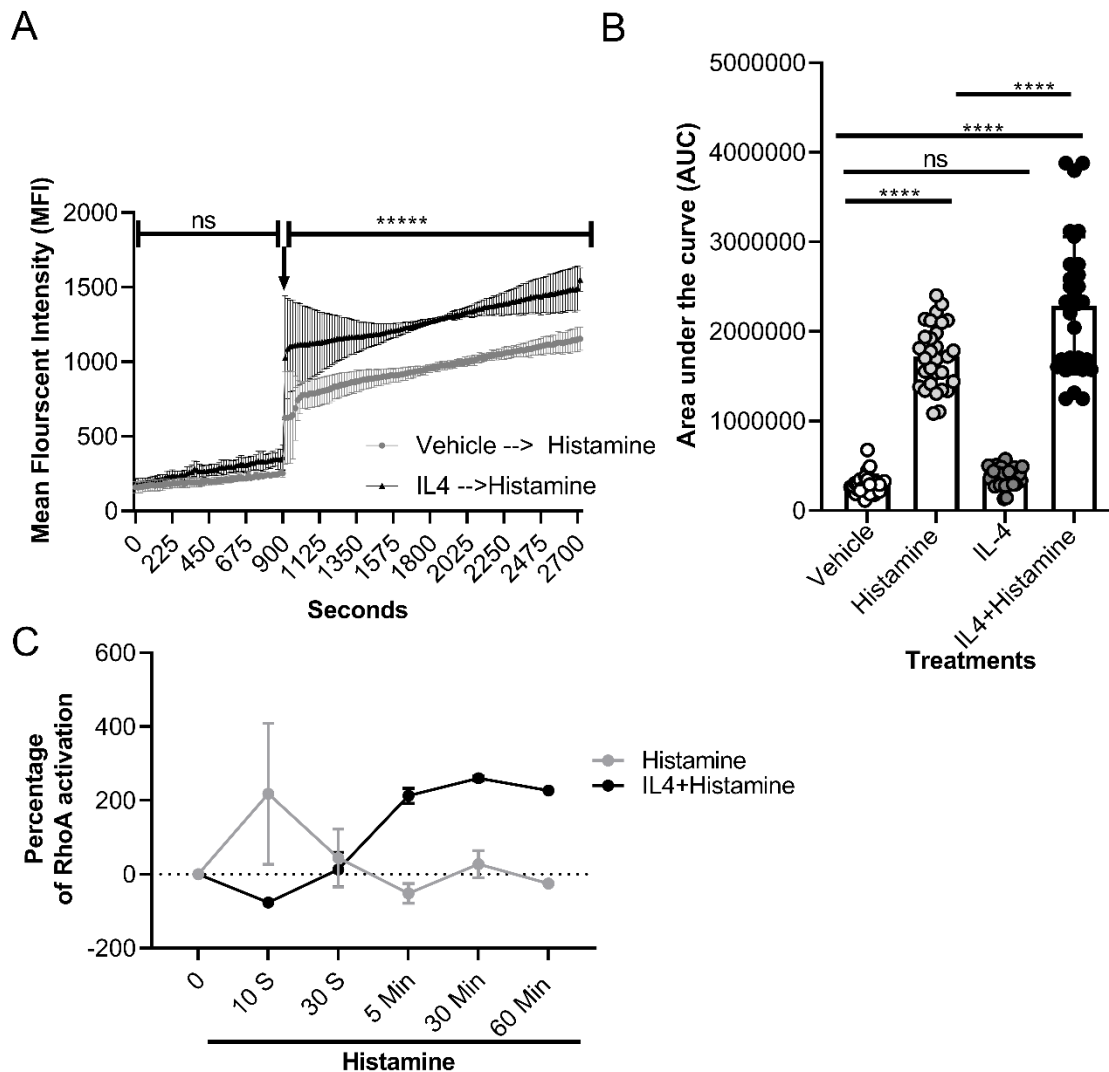


Figure 3.2: IL-4 enhanced histamine-induced calcium flux and modulated the kinetic of histamine-induced Rho GTP activity in EA.hy926 cell line

A graph showing $[Ca^{2+}]_i$ levels measured with Furo-4 AM in EA.hy926 cells over 2700 seconds (45 minutes), arrow indicated time of histamine (100 μ M) treatment.

B $[Ca^{2+}]_i$ levels quantified as area under the curve over 45 minutes

C the percentage of Rho GTPase activity over 0 time point.

Data are represented as the mean \pm SD; n = 3 fields per group (A) and n = 30 cells per group (B) and are representative of 4 independent experiments (A-B). n = 1-3 samples per group C

****P < 0.0001, ***P < 0.001, **P < 0.01, *P < 0.05, ns > 0.05

3. 4. 2 IL-4 enhancement of histamine-induced VE barrier dysfunction is dependent on gene transcription in EA.hy926:

To determine whether IL-4 enhancement of histamine-induced VE barrier dysfunction involved gene transcription and protein translation, EA.hy926 cells were

treated with cycloheximide (CHX), an inhibitor of protein synthesis and gene transcription^{257,258}. We then measured the resistance of vehicle or IL-4 pre-treated EA.hy926 cells following histamine stimulation. We show that CHX exposure did not impact histamine-induced VE barrier dysfunction (Figure 3.3, A). Moreover, we observed no difference in histamine-induced VE barrier dysfunction in vehicle or CHX-exposed EA.hy926 cells (Figure 3.3, A). Consistent with previous datasets, IL-4-pretreatment of EA.hy926 cells amplified histamine-induced VE barrier dysfunction. Importantly, CHX inhibited IL-4 amplification of histamine-induced VE barrier dysfunction (Figure 3.3, A).

Consistent with previous datasets, in the control-vehicle cells, IL-4-pretreatment significantly tempered the recovery response compared with histamine only treated cells. Intriguingly, CHX improved the recovery phase for histamine-treated cells compared to vehicle-histamine-treated cells (Figure 3.3, B, gray bar). In IL-4 primed and histamine-treated cells, the resistance in CHX-pretreated cells was recovering at $2.8 \pm 2.2 \Omega / \text{minutes}$ (mean \pm SD) while resistance in vehicle-treated cells was continuing to decline at $-1.9 \pm 0.4 \Omega / \text{minutes}$ (mean \pm SD) (Figure 3.3, B, black bar). Collectively, these data indicate that IL-4 exacerbation of histamine-induced VE barrier dysfunction is dependent on transcription.

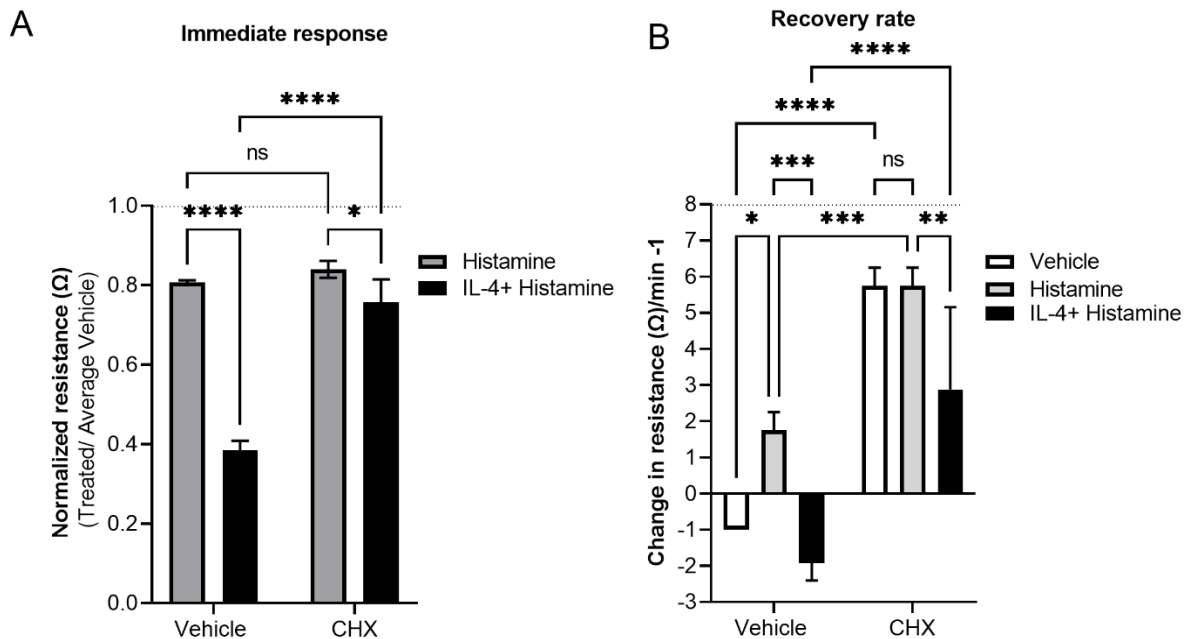


Figure 3.3: IL-4 enhancement of histamine-induced VE barrier dysfunction in EA.hy926 is cycloheximide dependent

A Normalized resistance measurements of a post-confluent EA.hy926 Cells monolayer that was pre-treated with Vehicle (PBS) or IL-4 (100 ng / mL; 24 hours) followed by removal of IL-4 then treatment with Vehicle (PBS) or histamine (100 μM; 2 hours) in ECIS® Z-Theta system. EA.hy926 Cells monolayer were treated with CHX (5 μg / mL; 24 hours).

B Recovery phase which is the rate of resistance 20 minutes post maximum change in resistance

Data are represented as the mean ± SD; n = 4 samples per group from 1 representative experiment run in triplicates (A-B).

****P < 0.0001, ***P < 0.001, **P < 0.01, *P < 0.05, ns > 0.05

3. 4. 3 IL-4 enhancement of IgE-induced hypovolemic shock is associated with modulation of endothelium transcriptome with putative STAT-3 binding motif:

To begin identifying IL-4-mediated transcriptional changes in the vascular endothelial compartment, we performed RNA sequencing analyses on flow cytometric-isolated lung endothelial cells (CD326⁻, CD31^{hi}, hematopoietic markers⁻) from WT BALB/c mice administered vehicle or IL-4C (Supplementary Figure 3- 2, A). Sorted pulmonary endothelial cells were confirmed for enrichment of the endothelial cells specific genes Von Willebrand factor (VWF) and VE-Cadherin compared to lung epithelial cells (EP-CAM⁺) and lungs hematopoietic cells (hematopoietic markers⁺) (Supplementary Figure 3- 2, B).

To determine the VE cell composition of the purified mouse lung endothelial cells, we took VE cell population-specific transcriptome from mouse lung vascular and vessel-associated cell database (GSE99235) that is derived from scRNA sequencing

analysis²⁵³; then we mapped the VE cell population-specific transcriptome onto the expressed genes (RPKM > 1) from CD326⁻, CD31^{hi}, hematopoietic markers- lung endothelial cells from vehicle-treated mice. We demonstrate that the sorted pulmonary endothelial cell transcriptome consisted of genes expressed by multiple endothelial populations (Supplementary Figure 3- 2, C). We observed significant enrichment of highly expressed genes specific to various endothelial cells population including arterial endothelial cells (aEC), capillary endothelial cells (CapillEC), endothelial cells type 1 and 2 (EC1-2), continuous endothelial cells (cEC1-3; clusters with wide range of arteriovenous markers) and lymphatic endothelial cells (LEC) (Supplementary table 3- 1 and Supplementary Figure 3- 2, C). Together, these data indicate that the purified mouse lung endothelial cells predominantly consisted of aECs, capillEC and cEC1-3.

Comparison of gene expression of vehicle and IL-4C-treated pulmonary endothelial cells revealed that IL-4- dysregulated 83 genes (70 upregulated genes and 13 down regulated genes), including: cell-cell adhesion signaling genes (Thbs1, Mink1, Hecw2), GTPase and GTPase signaling genes (Rgs4, Cdc42ep2, Gbp4, Tgtp2, Irgm2, Igtp), protease inhibitors (SerpinA3g, SerpinA3f), post translation modification (Dusp16, Herc6, Arpp21, Ppt1, Spsb1), vasomodulator (EDN1) and endothelial cells specific gene (Esm1) (Supplementary table 3- 2, FC ≥ 0.5, FDR-corrected p < 0.05) (Figure 3.4, A).

Gene Ontology (GO) analysis based on the biological processes of the IL-4–upregulated genes revealed that the most significant individual GO biological process nodes included cellular response to cytokines including IFN β and IFN γ , innate immune response and immune system process (Figure 3.4, B) (Supplementary table 3- 3, FDR-corrected p < 0.05). GO analysis based on the biological processes of the IL-4–down regulated genes revealed that the most significant individual GO biological process nodes included positive regulation of cell migration and proliferation, response to hypoxia and positive regulation of protein phosphorylation (Figure 3.4, C) (Supplementary table 3- 4, FDR-corrected p < 0.05). RT-qPCR analysis on the purified lung endothelial cells confirmed the specific differentially expressed genes (DEGs) detected by the RNA sequencing analysis. RNA sequencing data (presented as RPKM) showed a consistent trend as RT-PCR data (presented as relative gene expression) for both the IL-4Ra and SerpinA3 gene (Supplementary Figure 3- 2, D).

To determine the transcriptional programs that regulated the IL-4 DEGs we used the LISA cisrome database and algorithm²⁵². We identified the significant enrichment of genes that possess transcription factor binding motifs (TFBM) for inflammatory transcription regulators including: STAT1, STAT2, STAT3, RelA and the Interferon regulatory factors (IRF1, IRF2, IRF8) (Supplementary table 3- 5 and Supplementary table 3- 6) (Figure 3.4, D). Examining the gene expression level of these transcription regulators showed that STAT3 was one of the highest TF genes expressed in purified lung endothelial cells (Figure 3.4, D).

Given the enrichment of IL-4 DEGs that possess STAT3 motif and that STAT3 is activated by IL-4 type II receptors¹³¹, we focused our analysis on STAT3. *In silico* analysis showed that out of the 83 DEGs, 37 genes possessed a putative STAT3 motif, including SerpinA3g (protease inhibitor), thrombospondin-1 (Thbs1; adhesive glycoprotein), plasmolipin (Plip; ion channel), Stat1, and Guanylate-binding proteins (Gbp4, Gbp6, Gbp7) (Figure 3.4, E). Gene ontology analysis based on the molecular function showed that the STAT3 related genes grouped into 4 nodes related to GTPase activity, GTP Binding, 2'-5' oligoadenylate synthase activity and serine type endopeptidase inhibitor activity (Figure 3.4, F, FDR-corrected $p < 0.05$). To validate the *in silico* analysis, we examined the role of STAT3 in IL-4-induction of human SerpinA3 expression in human microvessel cell line (HMEC-1^{PLKO-1} cells; WT; transduced with the empty vector PLKO-1) and HMEC-1^{shRNA STAT3} cells (lentiviral particles with shRNA STAT3 knockdown). Notably, the mice genome possesses multiple SerpinA3 genes due to chromosomal duplication, while human expresses a single SerpinA3 gene. We show that IL-4 stimulation increased huSerpinA3 gene expression in HMEC-1^{PLKO-1} cells but not in HMEC-1^{shRNA STAT3}, indicating that IL-4 induced huSerpinA3 expression in VE cells in STAT3 dependent (Supplementary Figure 3- 2, E).

Collectively, these data identify an IL-4-induced VE transcriptome that is characterized by genes involved in antiviral immune responses, modulation of cell-cell signaling adhesion, down-regulated hypoxic and vasoactive mediators. Moreover, a significant proportion of the IL-4 induced DEGs possessed putative STAT-3 binding motif.

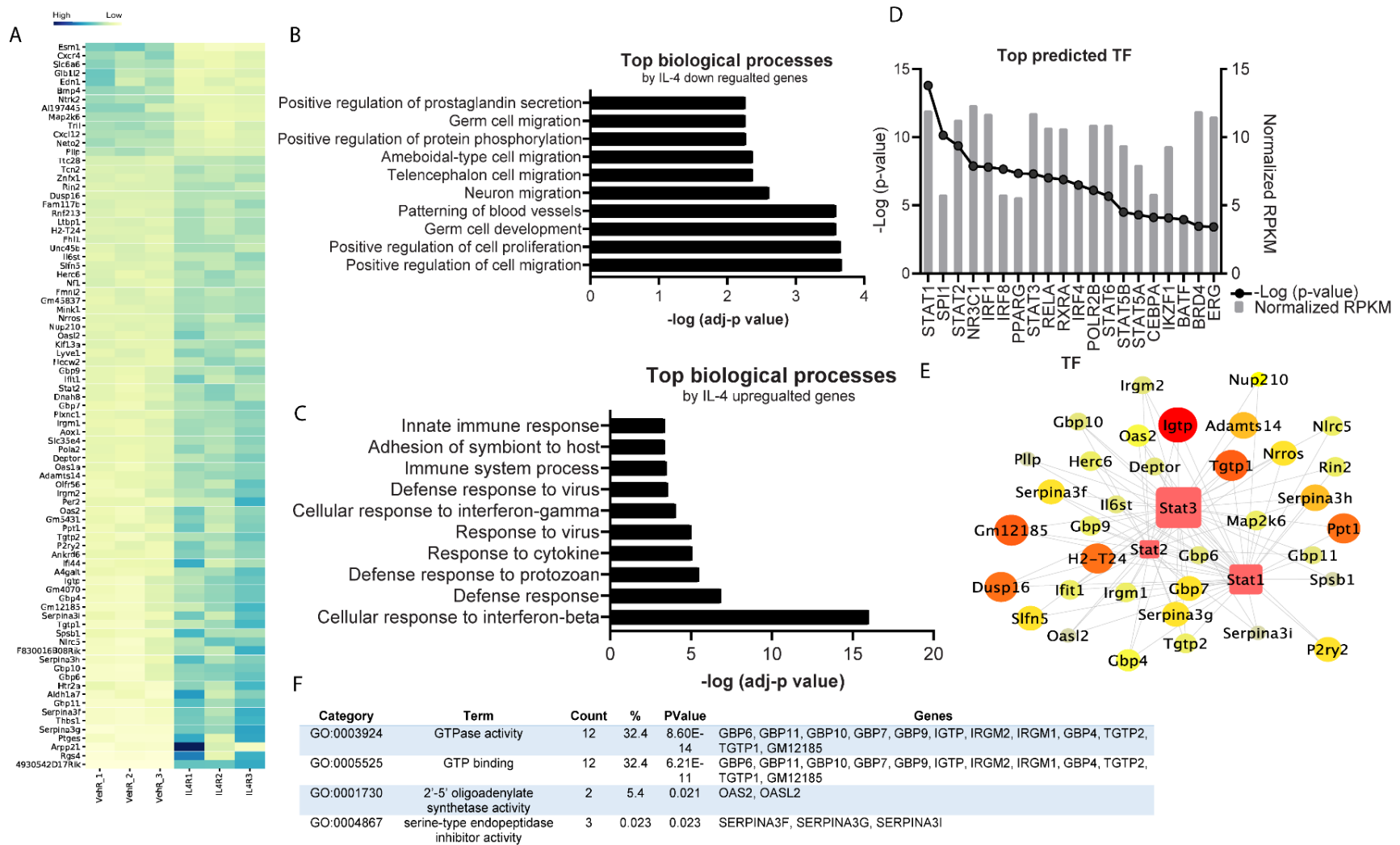


Figure 3.4: IL-4 *in vivo* treatment dysregulated genes from endothelial cells that are enriched with STAT3 TFBS

A Heatmap depicting the expression level of significantly 83 dysregulated genes by IL-4C in sorted mice EC compared to vehicle treated mice (adjusted $P \leq 0.05$).
B and C Bar graphs show top biologic processes enriched for upregulated and downregulated genes (FDR $P < .05$).
D Bar graph shows top Transcription factors enriched for dysregulated genes defined by LISA CISTROME algorithm, and the TF expression in sorted mouse endothelial cells
E String analysis showing IL-4 dysregulated genes that is known to be potentially regulated by Stat3, genes that are shown in square shape are also transcription factors targeted by Stat3.
F Table showing the molecular function of Stat3 targets genes identified using DAVID analysis. BALB/c mice were treated with vehicle or IL-4C (1 μg of IL-4 + 5 μg BVD4 anti IL-4 mAb) for 24 hours, then Endothelial cells were sorted from lung for RNA sequencing analysis (A-F).

3. 4. 4 VE STAT3 is required to sustain IL-4 enhancement of histamine-induced VE barrier dysfunction in EA.hy926 cells:

Next, we examined the effect of IL-4 on STAT3 activity and levels in EA.hy926 cells. STAT3 activation is associated with phosphorylation of STAT3 at residue Y705 and S727¹⁵³. STAT3^{Y705} residue stimulates receptor dimerization and nuclear translocation of STAT3 molecules, and the STAT3^{S727} residue stimulates maximal activation of gene transcription¹⁵³. Histamine stimulation of EA.hy926 cells led to STAT3^{S727} phosphorylation (Figure 3.5, A) within 5 minutes and reached a maximum at 60 minutes before returning to basal levels by 120 minutes. IL-4 stimulation alone induced both STAT3^{Y705} and STAT3^{S727} phosphorylation within 5 minutes and that returned to basal levels by 60 minutes (Figure 3.5, A). Histamine stimulation of IL-4 pretreated cells led to both STAT3^{Y705} and STAT3^{S727} phosphorylation. Notably, histamine stimulation of STAT3^{S727} phosphorylation in IL-4 pretreated cells appeared to be stronger and more sustained than that observed in histamine stimulation alone (Figure 3.5, A). Importantly, we observed no significant difference in total STAT3 protein levels between treatment groups. This is consistent with the observed no different in STAT3 mRNA expression levels in EA.hy926 treated with IL-4, and in mouse lung endothelial cells following IL-4C treatment (Figure 3.6, B and C). Therefore, we concluded that IL-4 maximally activates STAT3 for gene transcription in VE cells.

To determine the involvement of VE STAT3 in IL-4 amplification of the histamine-induced VE barrier dysfunction, we transduced EA.hy926 cells with lentiviral particles possessing STAT3 shRNA. Transduction of EA.hy926 cells with STAT3 shRNA and not control (PLKO-1) lentiviral particles led to > 75% reduction in STAT3 protein and mRNA levels (Figure 3.5D and E). As expected, histamine stimulation of EA.hy926^{PLKO-1} cells (WT; transduced with the empty vector PLKO-1) induced a rapid decrease in resistance

that was amplified by IL-4 pretreatment (Figure 3.5, F and G). Genetic knockdown of STAT3 in EA.hy926 attenuated the histamine-induced and IL-4 enhancement of histamine-induced immediate response, compared to EA.hy926^{PLKO-1} (Figure 3.5, H). EA.hy926^{shRNA STAT3} cells showed a notable difference in the IL-4-mediated enhancement of histamine response 20 minutes post-histamine treatment, as evident by the increase in resistance during the recovery phase (Figure 3.5, F and I). Moreover, the resistance in EA.hy926^{PLKO-1} cells was decreasing at -1.92 ± 0.24 ohm / minute whereas EA.hy926^{shRNA STAT3} cells was decreasing at -0.6 ± 0.09 ohm / minute ; $p = 0.04$ (Figure 3.5, I), suggesting that knockdown of STAT3 was associated with improved restoration of VE barrier. Collectively, these data suggest that STAT3 knockdown was associated with a reduction in both IL-4 and histamine-induced barrier dysfunction and that STAT3 is also required to sustain IL-4 enhancement of histamine response in VE cells.

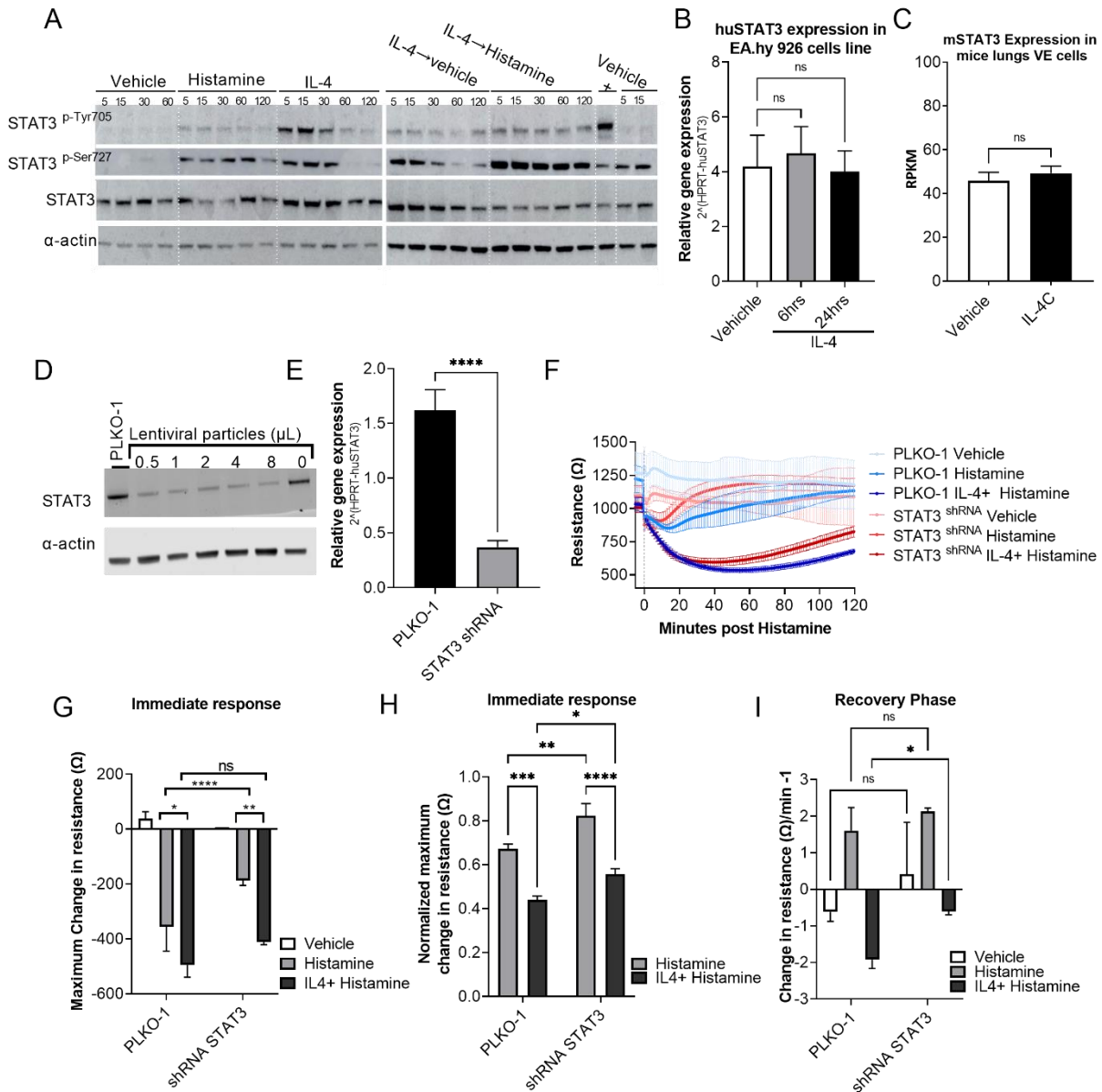


Figure 3.5: VE STAT3 KD attenuated both IL-4 enhancement of histamine and histamine-induced barrier dysfunction

A Western blot analysis for phosphorylated STAT3 on Tyr 705 (first row), Ser 727 (second row) and total STAT3 (third row). Actin was used as a loading control. Cell lysates were collected from EA.hy926 cells treated with vehicle, Histamine only (100 μM; 5-120 minutes), IL-4 only (100 ng / mL; 5-120 minutes), IL-4 for 24 hours followed by removal of IL-4 then treatment with Vehicle (PBS) or histamine (100 μM; 5-120 minutes). IL-6 was used as a positive control for STAT3 phosphorylation. B Relative gene expression of STAT3 genes normalized to the housekeeping gene HPRT from EA.hy926 Cells treated with IL-4 (100 ng / mL; 0-6-24 hours).

C mouse STAT3 RNA expression levels expressed as RPKM from sorted lung endothelial cells following treatment with vehicle or IL-4C (1 μg of IL-4 + 5μg BVD4 anti IL-4 mAb) for 24 hours.

D Western blot analysis for confirmation of KD of total STAT3 in EA.hy 926 cells transduced with various amounts of lentiviral particles carrying STAT3 shRNA.

E Relative gene expression of STAT3 normalized to the housekeeping gene HPRT from EA.hy 926^{PLKO-1} and EA.hy 926^{shRNA STAT3}

F Absolute resistance in ohms of post-confluent EA.hy926 cells transduced with lentiviral particles carrying empty vector (PLKO-1; WT control) or lentiviral particles carrying STAT3 shRNA. Cell were pre-treated with Vehicle (PBS)

or IL-4 (100 ng / mL; 24 hours) followed by removal of IL-4 then treatment with Vehicle (PBS) or histamine (100 μ M; 2 hours) in ECIS[®] Z-Theta system.

G and H Raw and normalized maximum change in resistance within 60 minutes of histamine treatment

I the resistance recovery rate for the first 20 minutes post maximum change in resistance.

Western blot images are from one experiment (A). Data are represented as the mean \pm SD; n = 3 samples per group from one experiment (B), n= 5-11 from 3 independent experiments (C), n= 4 wells per group (E), n = 2-3 samples per group from a representative experiment that was done in triplicate (F-1). ****P < 0.0001, ***P < 0.001, **P < 0.01, *P < 0.05, ns > 0.05

3. 4. 5 IL-4 signaling on VE cells induces the expression of various STAT3 dependent genes that are involved in barrier integrity and barrier signaling:

To determine the gene transcription programs dysregulated by the IL-4/STAT3 axis in VE cells, we performed RNA sequencing analyses on EA.hy926^{PLKO-1} cells and EA.hy926^{shRNA STAT3} cells treated with either vehicle or IL-4 for 24 hours. We show that IL-4 stimulation of EA.hy926^{PLKO-1} cells dysregulated 382 genes, of which 213 genes were upregulated and 169 genes were downregulated (Supplementary table 3- 7, FC \geq 2, FDR-corrected p < 0.05) (Figure 3.6, A). The DEGs were enriched with genes related to tight junction and cytoskeleton protein including: junctional adhesion molecule 2 (JAM2), calpain 11 (CAPN11), claudin 5 (CLDN5), claudin 16 (CLDN16), crumbs cell polarity complex component (PATJ), actin filament associated protein 1 like 2 (AFAP1L2) and the apoptotic protein Caspase 3 (CASP3) (Supplementary table 3- 7). Among the significantly upregulated DEGs was the histamine receptor 1 gene (HRH1) with 2 folds increase in RPKM following IL-4 treatment (Supplementary Figure 3- 3, A). RT-qPCR analysis on EA.hy926 WT cells treated with IL-4 for 24 hours showed that IL-4 did not increase HRH1 expression (Supplementary Figure 3- 3, B).

Functional annotation analyses of the IL-4–up-regulated genes identified enrichment of GO biological processes involved in the regulation of vascular biology (extracellular matrix, permeability, sodium ion transport, response to hypoxia), response to cytokines (such as TNF, IL-1, IFN γ , TGF β) and signaling pathways (NF-kappaB, SMAD, peptidase activity, serine/threonine kinase, ERK1-2 cascade, proteolysis) (Supplementary table 3- 8, p value \leq 0.05) (Figure 3.6, B). Functional annotation analyses of the IL-4–down-regulated genes identified enrichment of GO biological processes involved in the regulation of cardiovascular system (Heart contraction and vasodilatation), mesoderm signaling, cell-cell adhesion and signaling, immune response (T cell costimulation and chemokine signaling), and signaling pathways (oxidation-

reduction process and MAPK) (Supplementary table 3- 9, p value ≤ 0.05) (Figure 3.6, C). Therefore, IL-4 stimulation of VE cells genes that contribute to barrier integrity.

To determine the transcriptional programs that regulated the IL-4 DEGs, we examined the enrichment of the transcription factor binding motif (TFBM) using the Database for Annotation, Visualization and Integrated Discovery (DAVID)²⁵⁹. Similar to the observed enrichment of STAT3 regulated genes from mouse pulmonary endothelial cells, the top identified TF were STATs and NFkB (Supplementary table 3- 10, expression in EA.hy926^{PLKO-1} cells baseline >1 RPKM, FDR-corrected p- value < 0.05)(Figure 3.6, D). Further *in silico* analysis using LISA Cistrome database tool identified enrichment of STAT1, STAT3 and STAT6 TFBMs in the 382 IL-4-dysregulated genes in EA.hy926^{PLKO-1} cells, with 168 of 382 genes possessing a STAT3 motif (Figure 3.6, E and F). Functional annotation analyses of the 168 genes identified enrichment of GO biological processes involved in extracellular matrix organization, inflammatory response and calcium ion transmembrane transport (Supplementary table 3- 11) (Figure 3.6, G).

In EA.hy926^{shRNA STAT3} Cells, IL-4 dysregulated 290 genes, of which 201 genes were upregulated and 89 genes were down regulated (Supplementary table 3- 12, FC > 2 , FDR-corrected p < 0.05). Comparison analyses of the IL-4 dysregulated genes in EA.hy926^{PLKO-1} and EA.hy926^{shRNA STAT3} cells revealed 151 DEGs that were unique to EA.hy926^{PLKO-1} cells (significantly dysregulated in EA.hy926^{PLKO-1} group but not in EA.hy926^{shRNA STAT3} cells, P-adj ≤ 0.05 , FC ≥ 2); 60 genes were unique to EA.hy926^{shRNA STAT3} group (significantly dysregulated in EA.hy926^{shRNA STAT3} but not in EA.hy926^{PLKO-1}, P-adj ≤ 0.05 , FC ≥ 2) and 231 DEGs that were common in both EA.hy926^{PLKO-1} and EA.hy926^{shRNA STAT3} cells (P-adj ≤ 0.05 , FC ≥ 2) (Supplementary table 3- 13) (Figure 3.6, H). Within the 231 common DEGs, 21 genes were differentially expressed by FC ≥ 1.25 in EA.hy926^{PLKO-1} vs EA.hy926^{shRNA STAT3} group, which we designated as STAT3 dependent genes. Therefore, IL-4 dysregulated a total of 172 STAT3 dependent genes (Figure 3.6, H and I) (Supplementary table 3- 13).

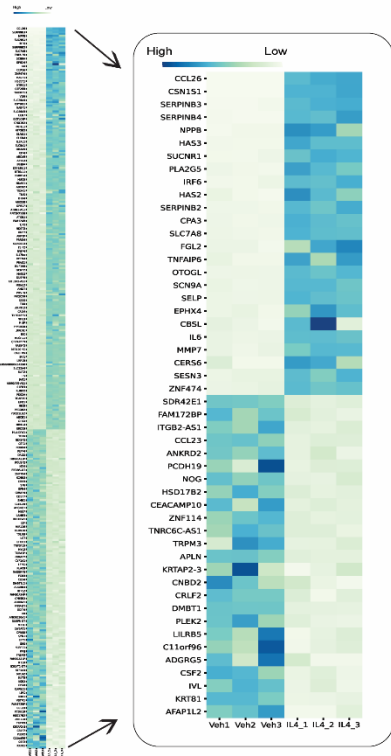
GO analysis based on the biological processes of the IL-4-dysregulated and STAT3 dependent genes revealed the most significant individual GO biological process nodes were associated with immune response, cell development, cardiac muscle

contraction, positive regulation of interferon-gamma production and oxidation-reduction process (Supplementary table 3- 14, $p < 0.05$) (Figure 3.6, J). GO analysis based on the molecular function showed that the IL-4-dyregulated STAT3-dependent genes included nodes related to oxygen binding and oxidoreductase activity. Both the KEGG pathway and cellular component analysis showed a number of genes (CLDN16, AMOT, PATJ, MYL2, JAM2) related to tight junction (Supplementary table 3- 15, $p < 0.05$) (Figure 3.6, K).

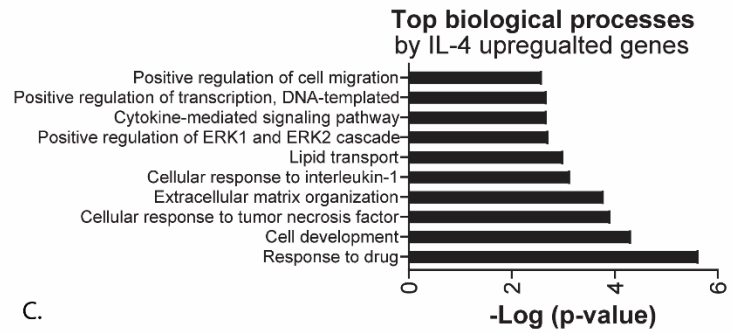
As validation analyses, the 172 DEGs (identified by *in vitro*-validated analyses to be STAT-3-dependent in Figure 3.6, I) were mapped onto the 168 DEGs (identified *in silico* to possess a STAT3 motif using the LISA Cistrome database in Figure 3.6, F) and we identified 55 DEGs that were common between the *in silico* and *in vitro* analyses (Supplementary table 3- 13) (Figure 3.6, L). Among the *in silico* and *in vitro*-validated DEGs were related to tight junction and cytoskeleton protein including: calpain 11 (CAPN11), claudin 16 (CLDN16), calpain small subunit 2 (CAPNS2) and protein tyrosine phosphatase non-receptor type 6 (PTPN6). GO terms manual text mining clustered most genes into 10 groups including apoptosis, cellular adhesion or/and extracellular matrix organization, cells signaling:(GPCR, GTPase, Wnt) (Table 5).

Collectively, these data identify that , in VE cells, IL-4 induces dysregulation of STAT-3 dependent genes that are related to junctional proteins, cellular adhesion, oxidation and apoptosis.

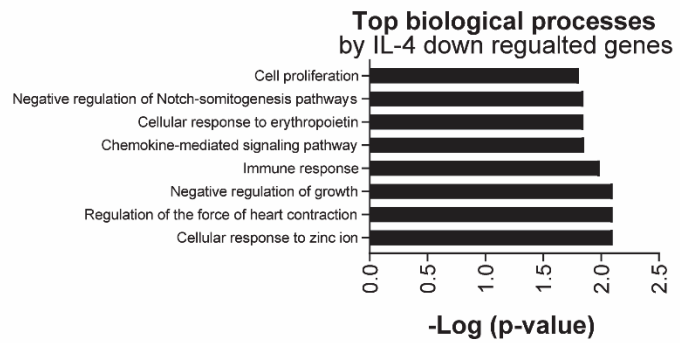
A.



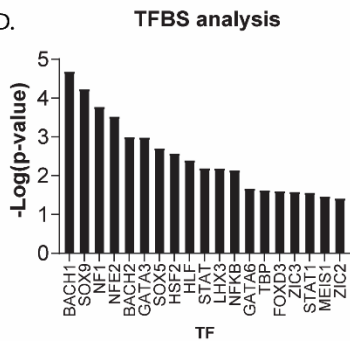
B.



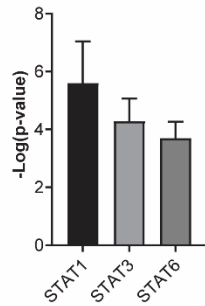
C.



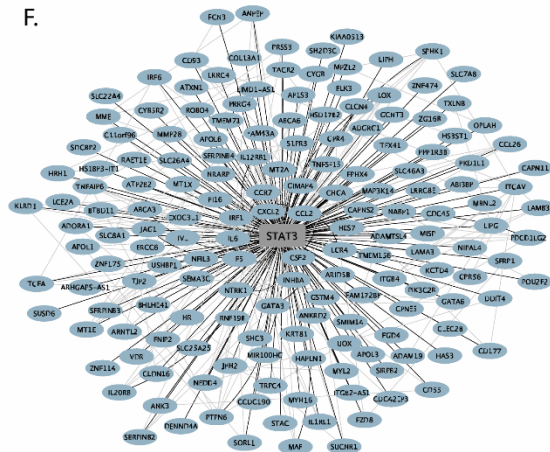
D.



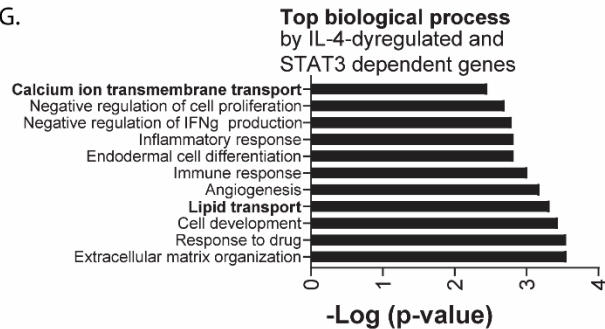
E.



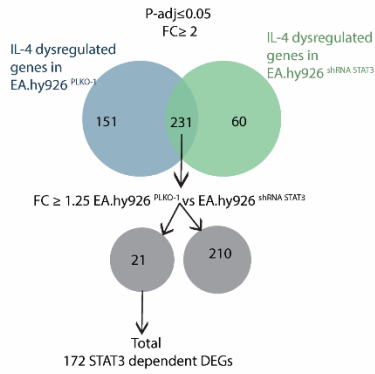
F.



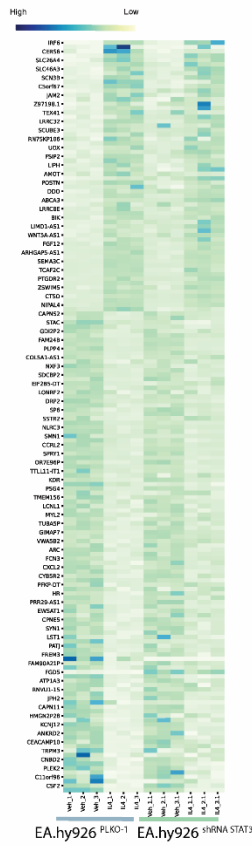
G.



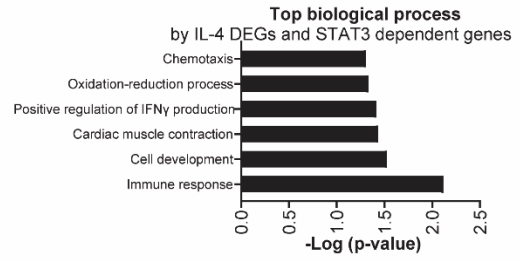
H.



I.



J.



K.

Category	Term	count	%	p-value	Genes
GOTERM_CC_DIRECT	GO:0005923~ bicellular tight junction	4	2.4	0.04	PATJ, CLDN16, JAM2, AMOT
KEGG_PATHWAY	hsa04530: Tight junction	4	2.4	0.02	PATJ, MYL2, CLDN16, JAM2
GOTERM_MF_DIRECT	GO:0008201~ heparin binding	5	3.0	0.02	POSTN, ADGRG1, LIPH, SLIT3, FGF12
GOTERM_MF_DIRECT	GO:0019825~ oxygen binding	3	1.8	0.03	CBSL, CYP1A1, CYGB
GOTERM_MF_DIRECT	GO:0016491~ oxidoreductase activity	5	3.0	0.04	CYB5R2, BDH1, CYP1A1, HR, HSD17B6

L.

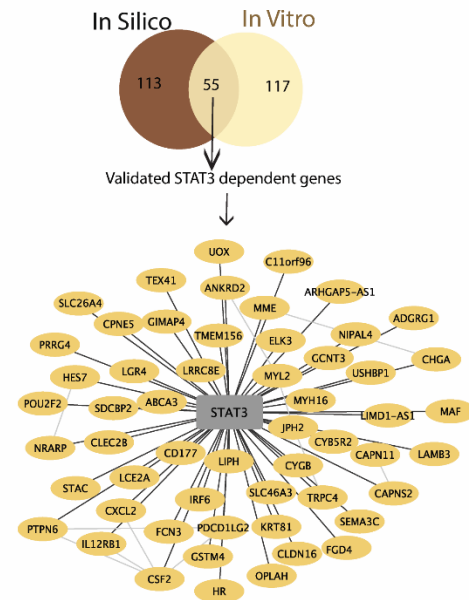


Figure 3.6: IL-4 induces the expression of STAT3 dependent genes that are involved in barrier integrity and barrier signaling

A Heatmap depicting the expression level of significantly 382 dysregulated genes by IL-4 in EA.hy 926^{PLKO-1}, magnified heatmap depict the top 50 upregulated and downregulated genes.

(FC>2, FDR-corrected p < 0.05)

B and C Bar graphs show top biologic processes enriched for upregulated and downregulated genes (P < .05).

D and E Bar graph shows top transcription factors and specific STATs enriched for dysregulated genes 382 dysregulated genes by IL-4 in EA.hy 926^{PLKO-1} defined by DAVID TFBM (D) and LISA Cistrome algorithm (E). F String analysis and G top biologic processes enriched for 168 IL-4 dysregulated genes from EA.hy 926^{PLKO-1} with STAT3 binding motif

H Venn diagram describing altered gene expression within by IL-4 EA.hy 926^{PLKO-1} and EA.hy 926^{shRNA STAT3} to identify common STAT3 dependent DEGs

I Heatmap depicting the expression level of the STAT3 dependent 172 IL-4-dysregulated genes that was extracted from comparison of EA.hy926^{PLKO-1} and EA.hy926^{shRNA STAT3} DEGs.

J and K GO analysis showing top pathways for the STAT3 dependent 172 IL-4-dysregulated genes.

L Venn diagram describing validation process of STAT3 dependent genes as identity by *in silico* analysis (LISA Cistrome) and DEGs (*in vitro* RNA sequencing) and string analysis of the resulted 55 genes.

EA.hy 926^{PLKO-1} and EA.hy 926^{shRNA STAT3} were cultured in 6 wells plate and treated with IL-4 (100 ng / mL; 24 hours), then RNA was collected and isolated for sequencing. n=3 wells per group. ****P < 0.0001, ***P < 0.001, **P < 0.01, *P < 0.05, ns > 0.05.

Gene ontology terms	Genes increased by IL-4	Genes decreased by IL-4
Electrolytes transport: (calcium, chloride, magnesium)	SLC26A4, SLC46A3, NIPAL4, TRPC4, LRRC8E	STAC, JPH2, PTPN6, CLDN16
Cardiac muscle contraction or pressure regulation		STAC, JPH2, MYL2, ANKRD2, CHGA
Apoptosis	PDCD1LG2	PTPN6, CSF2, FCN3, ANKRD2
Proteolysis	CAPNS2, MME	CAPN11, FCN3
Cellular adhesion or/and extracellular matrix organization	CAPNS2	CLDN16, PTPN6, ADGRG1, LAMB3
Cells signaling: (GPCR, GTPase, Wnt)	IRF6, FGD4, LGR4	NRARP, CXCL2, PTPN6, CHGA, ADGRG1, CSF2
Oxidation, carbohydrate or/and fat metabolism	OPLAH, LIPH, ABCA3, GCNT3	HR, CYB5R2, GSTM4, CYGB, ANKRD2
Plasma membrane	MME, TRPC4, ABCA3, PDCD1LG2, CAPNS2, LIPH, IL12RB1, SLC26A4, LRRC8E, LGR4	SDCBP2, JPH2, CLEC2B, CLDN16, CD177, ADGRG1

Table 5: Validated IL-4/STAT3 axis dependent genes annotation

3. 4. 6 Loss of VE STAT3 attenuated histamine-induced hypovolemic shock and IL-4 enhancement of histamine response:

To identify the requirement of VE STAT3 cells in the IL-4-exacerbation of histamine-induced hypovolemic shock *in vivo*, we took a transgenic approach using the VE-specific promoter of the junction protein cadherin-5 (also called VE-cadherin). Cadherin-5^{Cre} STAT3^{fl/fl} mice (referred to as VE^{ΔSTAT3}) lack expression of STAT3 on the VE compartment, whereas cadherin-5^{WT} STAT3^{fl/fl} mice (referred to as VE^{STAT3 WT} mice) were used as a WT control (Figure 3.7, A). Immunohistochemically staining confirmed the specific deletion of STAT3 in VE cells (Figure 3.7, B); We observed positive brown staining within the single layer of VE cells of the blood vessel within the lungs of VE^{STAT3WT} mice whereas, the VE cells lining the blood vessel within the lungs of VE^{ΔSTAT3} mice were negative (Figure 3.7, B). Analyses of the VE^{ΔSTAT3} mice revealed

the mice breed consistent with Mendelian inheritance. Analyses of hemoconcentration of these mice revealed that basal hematocrit (hct) levels were significantly lower than that observed in $VE^{STAT3\ WT}$ mice (Figure 3.7, C). $VE^{STAT3\ WT}$ and $VE^{\Delta STAT3}$ mice received an intravenous injection of either vehicle or IL-4C (a long-acting formula IL-4 complexed with anti-IL-4), and 24 hours later received an intravenous injection of histamine and evidence of anaphylaxis (hypovolemic shock and hypothermia) were evaluated (Figure 3.7, A). Consistent with our previous observations, histamine injection induced a drop in body temperature and increased hematocrit percentage in $VE^{STAT3\ WT}$, and IL-4C pretreatment exacerbated histamine-induced hypothermia and hemoconcentration in $VE^{STAT3\ WT}$ mice (Figure 3.7, D and E).

Histamine challenge of $VE^{\Delta STAT3}$ mice induced hypothermia that was comparable with $VE^{STAT3\ WT}$ mice (Figure 3.7, D). The IL-4C amplification of the histamine-induced hypothermia was ablated in $VE^{\Delta STAT3}$ mice (Figure 3.7, D). Histamine challenge increased hemoconcentration in $VE^{\Delta STAT3}$ mice compared to baseline, and IL-4 enhanced that response (Figure 3.7, E). Although $VE^{\Delta STAT3}$ mice were not protected from histamine-induced hypothermia, $VE^{\Delta STAT3}$ mice demonstrated a significant attenuation in hemoconcentration following histamine challenge, compared to $VE^{STAT3\ WT}$ mice (Figure 3.7, E). Moreover, IL-4 amplification of histamine-induced hemoconcentration was significantly attenuated in $VE^{\Delta STAT3}$ mice compared to $VE^{STAT3\ WT}$ mice (Figure 3.7, E).

Collectively these data suggest that VE STAT3 is required for histamine-induced hypovolemic shock and IL-4 enhancement of histamine induced-hypovolemic shock.

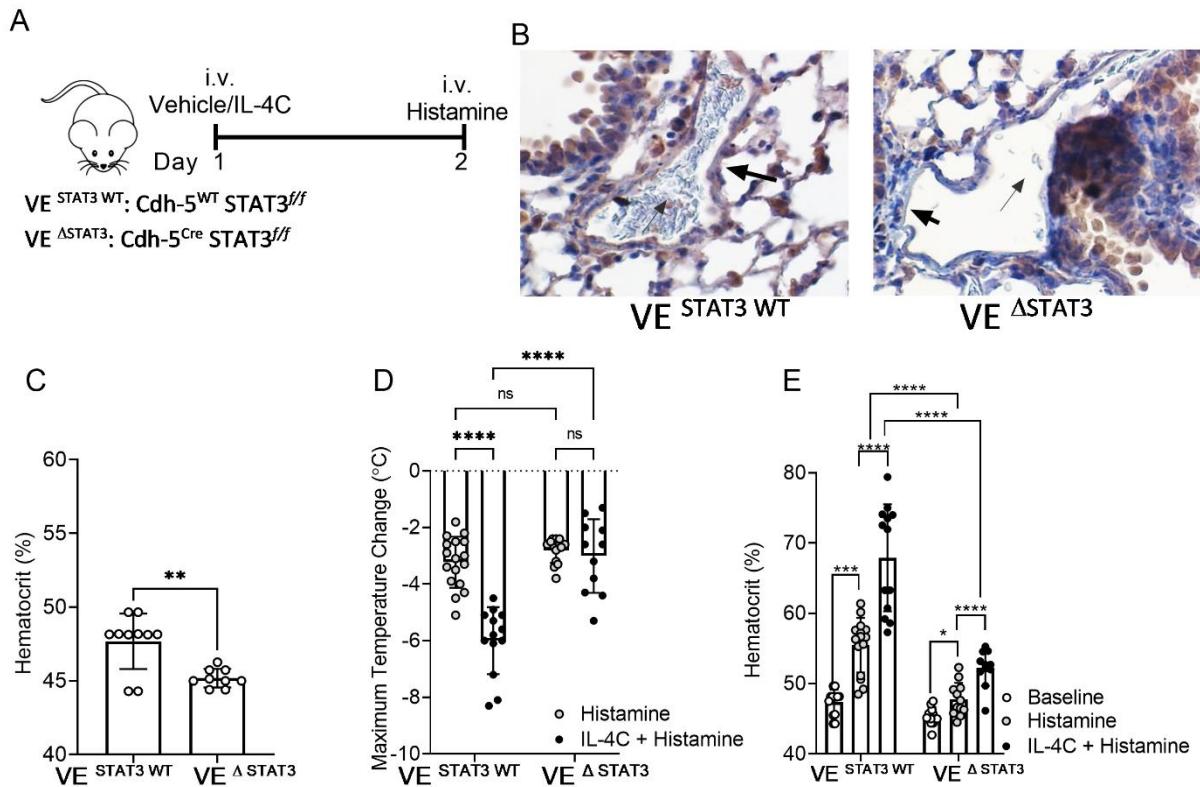


Figure 3.7: IL-4 induces the expression of STAT3 dependent genes that are involved in barrier integrity and barrier signaling

A Experimental regimen.

B Immunohistochemistry staining for STAT3 in lungs section from VE^{ΔSTAT3} and VE^{STAT3} WT mice, thick arrow point to VE cells lining blood vessels while thin arrow point in red blood cells inside blood vessels.

C Baseline hematocrit percentage from untreated mice,

D Maximum temperature change, and E hematocrit percentage

from VE^{ΔSTAT3} and VE^{STAT3} WT mice after intravenous (i.v.) injection with vehicle or IL-4C and intravenous challenge with histamine (2 mg / mice).

Data are represented as means ± SD; n=9-10 mice per group (C) n=11-17 mice pre group (D) n=11-15 mice pre group (E) from n=3-4 independent experiments. ****P < 0.0001, ***P < 0.001, **P < 0.01, *P < 0.05, ns > 0.05.

3. 4. 7 Characterization of IgE-mediated anaphylaxis in C57/B6 mice:

To begin examining the role of VE STAT3 in the IgE-MC-induced anaphylaxis, we performed a dose response of the anti-IgE mAb on the VE^{STAT3} WT mice. We found that the standard dose of anti-IgE mAb (10-20 μg / mice) induced a strong hypothermic response at a mean of 4.8-5.4-point temperature lost (Supplementary Figure 3- 4, A). This hypothermia response was stronger than what we observe usually in BALB/c mice^{56,260}. A lower dose of anti-IgE mAb (1 μg / mice) was sufficient to induce hypothermia at a mean of 2.7-point temperature lost (Supplementary Figure 3- 4, A). Consistent with this anti-IgE mAb increased hemoconcentration in dose dependent manner

(Supplementary Figure 3- 4, B). Since the $VE^{STAT3\text{ WT}}$ are on C57/B6 mice background, these studies suggests that anti-IgE mAb have a strain dependent response.

Serum Mouse MC protease 1 (mMCPT-1) levels, traditionally used as a surrogate marker for mucosal MC degranulation, were undetectable or low (0 - < 60 ng / mL) in $VE^{STAT3\text{ WT}}$ (data not shown). We examined anaphylaxis parameters on C57/B6 mice. Similar to $VE^{STAT3\text{ WT}}$ littermates, we observed that WT C57/B6 mice showed signs of anaphylaxis with 1 and 10 μg of anti-IgE mAb in a dose dependent manner (Supplementary Figure 3- 4, C and D), but had serum mMCPT undetectable or low < 10 ng / mL (Supplementary Figure 3- 4, E). Another serum marker for MC degranulation is histamine. We observed that both 1 and 10 μg of anti-IgE mAb dose induce high serum histamine level (> 8000 nM), indicating that 1 μg of anti-IgE mAb induce sufficient MC degranulation in WT mice (Supplementary Figure 3- 4, F). Indeed, these histamine level mimic what we previously observed in BALB/c mice and correlated with anaphylactic phenotype²⁴⁶. Therefore, for these studies we used 1 μg of anti-IgE mAb to induce anaphylaxis. Moreover, we used serum histamine as a marker for MC activation and degranulation.

3. 4. 8 Loss of VE STAT3 attenuated IgE-MC-induced anaphylaxis and IL-4 enhancement of histamine response:

We next examined the requirement of the VE STAT3 in IgE-MC-induced anaphylaxis. $VE^{STAT3\text{ WT}}$ and $VE^{\Delta\text{STAT}3}$ mice were pre-treated with vehicle or IL-4C then intravenously challenged the next day with anti-IgE mAb (Figure 3.8, A). As expected, anti-IgE mAb intravenous injection induced hypothermia and increased hemoconcentration in $VE^{STAT3\text{ WT}}$ mice, and IL-4C pre-treatment enhanced anti-IgE induced hypothermia and hemoconcentration (Figure 3.8, B and C). Importantly, $VE^{\Delta\text{STAT}3}$ mice were protected from anti-IgE induced hypothermia and hemoconcentration and from IL-4C enhancement (Figure 3.8, B and C). Serum histamine levels were comparable between groups, indicating that the reduced disease in $VE^{\Delta\text{STAT}3}$ mice was not due to decreased in MC activation and degranulation (Figure 3.8, D).

Collectively these data suggest that VE STAT3 is required for IgE-MC-induced anaphylaxis and associated hypovolemic shock and possibly IL-4 enhancement of IgE-MC-induced VE dysfunction.

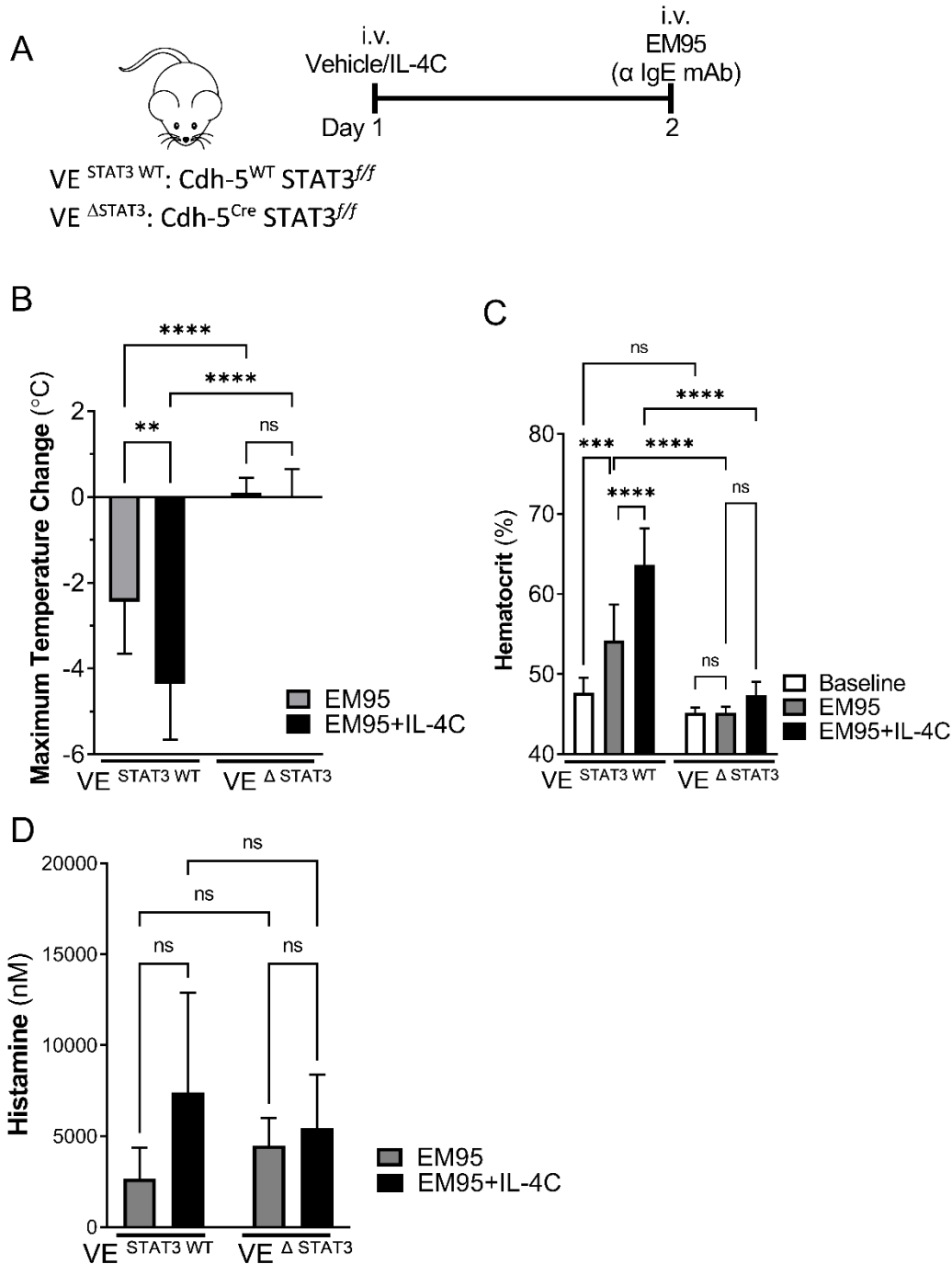


Figure 3.8: Deletion of VE STAT3 attenuated IgE-MC-induced hypovolemic shock and IL-4 enhancement of histamine response

A Experimental regimen.

B Maximum temperature change, and C hematocrit percentage from VE^{ΔSTAT3} and VE^{STAT3 WT} mice after intravenous (i.v.) injection with vehicle or IL-4C and intravenous challenge with anti-IgE mAb clone EM95 (1 µg / mice).
D Serum histamine levels in mice 10 - 15 minutes post anti-IgE mAb injections.
Data are represented as means ± SD; n=6-10 mice per group (B and C) n=4-12 mice pre group (D) from n=3-4 independent experiments (B-D).
****P < 0.0001, ***P < 0.001, **P < 0.01, *P < 0.05, ns > 0.05.

3. 5. Discussion

Herein we demonstrate that: 1) IL-4 priming of VE cells enhanced the immediate phase of histamine-induced-VE barrier dysfunction and prevented recovery of barrier strength in a gene transcription-dependent manner; 2) IL-4-induced lung endothelial cell transcription was characterized by genes that possess putative STAT3 binding motif; 3) *In vitro* analyses revealed that STAT3 is required for IL-4 enhancement of histamine induced-VE barrier dysfunction; 4) in VE cells, IL-4/STAT3 dysregulates genes involved in barrier integrity and barrier signaling; 5) VE STAT3 is required for histamine- and IgE-MC-induced hypovolemic shock and IL-4 enhancement of VE compartment.

Hypovolemic shock has been implicated in food-induced anaphylaxis²³. Hypovolemic shock is a consequence of altered vascular permeability leading to leakage of the intravascular fluid into the interstitial space³³. This fluid leakage from blood vessels into tissue is governed by mechanisms that controls VE barrier function^{96,97}. Consistent with other studies, we showed that histamine-induced a rapid and a transient increase in vascular permeability^{97,116}. Histamine signal in VE cells via G_{αq/11} protein-coupled receptor histamine receptors 1 (HR1) to disrupt the hemophilic interacting VE-Cadherin complexes at the cell-cell junction, which leads to loss of cell-cell anchorage and an increase in space between VE cells^{92,97,116}. The increased paracellular space causes an increase in vascular permeability. Histamine disrupt VE cadherin complexes via two molecular processes: 1) inducing phosphorylation of VE-Cadherin or its adaptor molecules (e.g β-catenin) that lead to dissociation of the complex and hence losing its anchoring ability¹²⁵. 2) inducing the Myosin light chain 2 (MLC2) phosphorylation to form actomyosin that pull junctional proteins from lateral cell membrane¹¹⁶. VE-Cadherin can be phosphorylated by histamine-induced SRC kinase^{101,126}. β-catenin can be phosphorylated by the classical phospholipase C- β (PLC-β) activation^{101,126}. MLC2 can be phosphorylated by histamine either by

Calmodulin (CaM)-dependent myosin light chain kinase (MLCK) activation¹¹⁶, or RhoA GTPase axis-dependent MLCK activation²⁶¹.

We show that IL-4 synergizes with histamine and increases the magnitude and kinetics of histamine-induced VE-barrier dysfunction. We observed 2-fold increase in *HR1* transcription following IL-4 *in vitro* treatment in a human venous cell line (EA.hy926)²⁶². IL-4 is unlikely inducing a significant increase in HR1 expression in 24 hours as PCR analysis showed no significant difference in HR1 expression between vehicle and IL-4 treated cells. Other studies performed using human arterial and venous cell lines also did not observe IL-4 induction of *HR1* transcription^{165,181}. Furthermore, we did not see dysregulation of mouse *Hr1* transcription *in vivo*, indicating that increase histamine receptor expression by IL-4 can be organ-specific or species-specific as endothelial barrier function differs greatly among organs⁹⁷. Notably, targeting histamine receptors during anaphylaxis in clinical setting do not relieve airway obstruction nor hypotension. Our studies demonstrated downstream signal molecules of HR1 that can attenuate histamine-induced anaphylaxis. We also show additional IL-4-induced pathways that can contribute to histamine-induced vascular leakage as shown by the RNA sequencing.

We show that IL-4 priming enhanced $[Ca^{2+}]_i$ intracellular signaling induced by histamine. We cannot exclude that this might be due to increased HR1 gene expression, however, RNA sequences also showed IL-4 induced DEGs related to $[Ca^{2+}]_i$, such as, *NIPAL4*, *TRPC4* and *STAC*. Therefore, IL-4 can be priming VE cells for phosphorylation events by providing signals transduction via $[Ca^{2+}]_i$. Calcium also is known to activate S100 proteins that induce F-actin disorganization in human umbilical vein endothelial cells (HUVEC) and induce barrier dysfunction through the p38 and ERK1/2 signaling pathways²⁶¹.

Interestingly we saw that IL-4 priming inhibited the initial histamine-induced Rho GTPase activation but activated Rho GTPase at a later time point which indicates that IL-4 may regulate other GTPase to enhance histamine initial response. Therefore, we speculate that the IL-4/STAT3 axis modulates VE cell sensitivity through various GTPase-related genes.

IL13R α is part of the type II IL-4 receptor and can utilize TYK2 kinase activity to phosphorylate STAT3^{Y705} residue (needed for STAT3 dimerization and transcription factor activity) and STAT3^{S727} (needed for maximum gene transcription and mitochondrial translocation)^{139,263,148,153}. We show that IL-4 phosphorylated STAT3 at Y705 and S727 residues, which indicates that IL-4 induces maximal STAT3 activity and gene transcription in VE cells. Consistent with this, we show in both a human VE cell line and sorted mouse lung endothelial cells that IL-4 dysregulated genes possessed a putative STAT3 motif. Notably, STAT3 has been shown to form a functional heterodimer with STAT1²⁶⁴. We observed that IL-4 DEGs were enriched for genes that possessed putative STAT3 and STAT1 motif. This may suggest possible upregulation of STAT1-dependent pathways. Indeed, we show that IL-4 dysregulation of the endothelial transcriptome was characterized by innate and IFN signaling pathways. Phosphorylation of STAT1 is induced by Type I IFNs via TYK2, IL-4 can utilize TYK2 as well via IL-13R α chain. However, it is unclear if IL-4 can utilize the IL-13R α chain to act as a docking site for STAT1 to be phosphorylated by TYK2.

Consistent with other studies we show that histamine induced phosphorylation of STAT3 on S727 residue in VE cells. Studies suggest that STAT3 signaling drives histamine-mediated VE-Cadherin phosphorylation and dissociation from β -catenin, but the role of histamine mediated STAT3^{S727} phosphorylation during the acute histamine response was not investigated¹⁰¹. We show that IL-4 pretreatment enhanced histamine-induced STAT3^{S727} phosphorylation. Previous studies have reported that mitochondria S727-STAT3 is required for optimal ATP levels and oxidation rate¹⁵⁵. The mitochondria contribute to endothelial function through the generation of (nitric oxide) NO and regulation of the dynamics of intracellular [Ca²⁺]_i signaling¹⁵⁶. Both NO and [Ca²⁺]_i signaling contribute to histamine-induced permeability^{116,121,123}. It is unclear if histamine-induced S727-STAT3 phosphorylation drive permeability through NO and [Ca²⁺]_i signaling.

Using both *in vivo* and *in vitro* approaches, we identified possible gene pathways where the IL-4/STAT3 axis can prime VE cells and enhance histamine induce VE-barrier dysfunction (Figure 3-9). Mechanistically, we show that IL-4 decreases VE-cadherin expression possibly through degradation of the VE-cadherin extracellular part.

By RNA sequencing, we observed in both mice and human that IL-4 increased expression of proteolytic metalloproteinases enzymes (*ADAM19*, *ADAMTSL4* and *Adamts14*) that are involved in “ectodomain shedding”. ADAM10 and ADAM12 cleaved the E-cadherin extracellular domain leading to less cellular adhesion and β -catenin at the cell membrane^{265,266}. Other studies showed that histamine released active matrix metalloproteinase 9 (MMP-9) from astrocyte and keratinocyte^{267,268}.

We show that IL-4/STAT3 dependent genes were related to oxidation and apoptosis. It is postulated that when VE cells are deprived of oxygen, mitochondria respond by increasing reactive oxygen species (ROS) and apoptogenic protein²⁶⁹. This hypoxic response in VE cells, activates caspase-3 leading to disruption of AJs junction complex and barrier function²⁶⁹. IL-4 increases transcription of caspase 3 leading to apoptosis²⁷⁰. Consistent with this, we show that IL-4 increases transcription of caspase 3, in a STAT3 independent manner. Moreover, Childs and colleagues showed that a hypoxic environment activated the mitochondrial intrinsic pathway which increase VE permeability²⁷¹. Therefore, apoptosis contributes to barrier dysfunction.

The small and large family of GTPase are involved in barrier function and cytoskeleton rearrangement^{116,272,273}, Specifically, we show that IL-4-induced DEGs in lung endothelium that are known to be involved in barrier integrity such as Thrombospondin-1, *GBPs*, *Mink1* and *Ankrd6*. Thrombospondin-1 increases permeability of Bovine artery endothelial cells through tyrosine phosphorylation of AJ Proteins paxillin, γ -catenin, and p120²⁷⁴. *Mink1* and *Ankrd6* localize to cell-cell junctions and interact with β -catenin and ZO-1 respectively^{275,276}. GBP-1 is localized at the TJs in the human salivary gland and intestinal epithelial cells where it mediates barrier protection effect against inflammatory cytokines^{277,278}. GBP-1 belongs to a family of large GTPases which also include the IL-4 dysregulated GBP-4, -6, -7, -9, -10 and -11²⁷⁹; however, it is unclear if these GBPs in VE cells confer a barrier stability effect or, similar to RhoA GTPase, drive phosphorylation events that drive AJ and cytoskeleton rearrangement and therefore barrier dysfunction.

Our data suggest the involvement of tight junction proteins such as *Calpin* genes and *ANKRD2*. *ANKRD2* is known to interact with ZO-1 and is dysregulated in atopic

dermatitis²⁸⁰. Calpain-1 mediated IL-1 β -induced blood-brain barrier dysfunction by promoting the dislocation of ZO-1 and disorganization of cytoskeletal assembly²⁸¹.

Consistent with the concept of IL-4 inhibiting recovery response of VE barrier strength, we observed that IL-4 downregulated Endothelin-1 which is known to be vasoconstrictive and to attenuate inflamed microvascular permeability^{282,283}. In addition, we found that IL-4 upregulated the *Cdc42ep2* gene, an inhibitor of the barrier protector GTPase CDC42²⁸⁴. Following thrombin-induced microvessels permeability, CDC42 is activated to initiate restoration of VE-Cadherin at AJ²⁸⁵. Interestingly, we observed that IL-4 decreased the phosphatase gene *PTPN6*, suggesting that IL-4 may prime VE cells by maintaining phosphorylation of AJs complex. Loss-of-function mutations in the *PTPN2* locus are associated with barrier function diseases such as IBD, celiac disease, and type 1 diabetes²⁸⁶.

We have previously shown that, systemic symptoms in IgE-mediated anaphylaxis is histamine driven⁴³. Herein, we show that histamine induced-hypovolemic shock was attenuated in VE Δ STAT3 (strain C57BL6) mice. Therefore, we would anticipate seeing an attenuated phenotype in VE Δ STAT3 mice following anti-IgE challenge, however, we did not observe IgE-induced hypothermia in VE Δ STAT3 mice. Notably, during our analyses we observed that IgE-mediated responses in mice was strain-dependent. Anti-IgE (20 μ g) treatment of C57/B6 mice induced a strong response where it caused $\sim 6^{\circ}\text{C}$ temperature loss and caused death (Supplementary figure 3-4, C). We were therefore required to use a lower concentration (1 μ g) of anti-IgE in experiments with transgenic mice on C57/BL6 background. However, at this dosage of anti-IgE, we observed no treatment effect on the VE Δ STAT3 mice (Figure 3.8). This is not a consequence of total protection from IgE-mediated responses as higher dose of anti-IgE (10 μ g) did promote hypothermia in VE Δ STAT3 mice at attenuated levels compared to VE^{STAT3 WT} (Data not shown). Currently, more experiments are being performed with anti-IgE dose response that include VE Δ STAT3 mice.

Hox *et al* showed a role of STAT3 in histamine-induced vascular leakage through preventing expression of phosphatase and tensin homolog (PTEN) that target SRC kinase, thus allowing for SRC kinase to dissociate VE-Cadherin and β -catenin¹⁰¹. Moreover, STAT3 inhibition delayed VE-cadherin phosphorylation during

histamine stimulation¹⁰¹. Our data is consistent with Hox *et al* in showing that histamine-induced vascular leakage and anaphylaxis are partially dependent on STAT3. Notably, Hox *et al* utilized STAT3 pharmacological inhibitor and globe mutant STAT3, which would affect VE cells and other blood vessels associated cells such as pericyte and vascular smooth muscle. Pericytes are known to contribute to vascular permeability *in vivo*²⁸⁷. We used specific endothelial cells STAT3 genetic deletion. We extended the knowledge by investigating how IL-4 can increase the severity of histamine-induced hypovolemic shock through VE STAT3 dependent pathways. Currently, transgenic mice are being developed to also examine the role of VE STAT3 in Oral-antigen induced anaphylaxis.

Mechanistically, we did not observe dysregulation of PTEN expression following IL-4 stimulation, Further studies are needed to understand the effect of IL-4 on PTEN activity and histamine-induced SRC kinase activity. Nevertheless, IL-4/STAT3 axis can enhance VE response through different pathways other than SRC kinase/PTEN transcription. For example, with IL-4 decreasing PTPN6 in a STAT3 dependent manner. We speculate that this allows for longer VE-cadherin phosphorylation which also leads to dissociation from β -catenin²⁸⁸. The different cellular pathways in each study can be contributed to different cell lines or degrees and methods of STAT3 inhibition. We used a short hairpin that decreased total STAT3. Hox *et al* used a small molecules inhibitor (C188-9; targets the phosphotyrosyl peptide binding site within the STAT3 SRC homology 2 (SH2) domain) and endothelial cells from patients with mutant STAT3 (mutation decreases phosphorylation and DNA binding)²⁸⁹.

In conclusion, we show that IL-4 enhances histamine responses through the VE STAT3 axis gene modification to modulate barrier integrity and barrier signaling. VE IL-4/STAT3 pathways possibly extend barrier dysfunction and prevent the recovery mechanism of barrier strength.

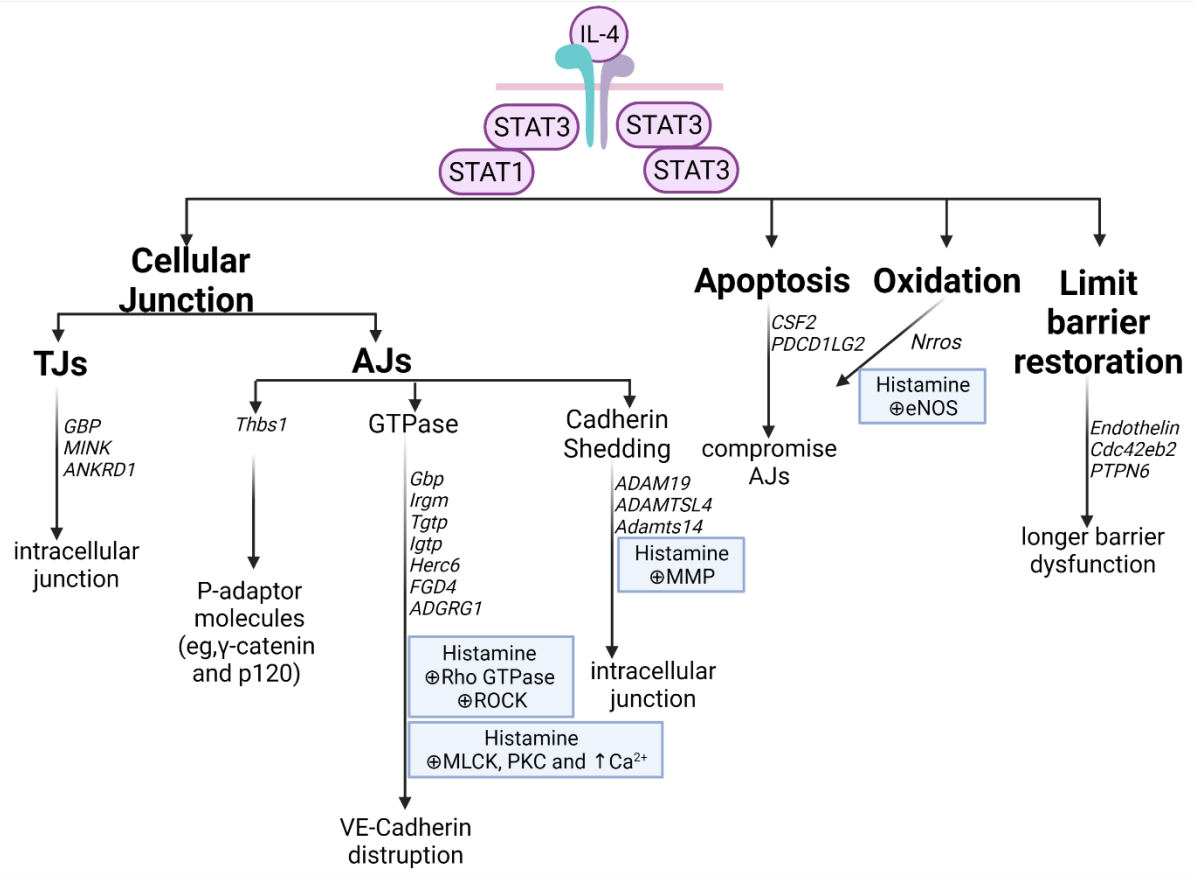


Figure 3.9: Proposed mechanisms of IL-4 driven STAT3 dependent transcriptome alteration in VE cell that lead to barrier dysfunction

Chapter 4 Dysregulation of Intestinal Epithelial CFTR-dependent Cl⁻ Ion Transport and Paracellular Barrier Function Drives Gastrointestinal Symptoms of Food-induced Anaphylaxis in Mice

4. 1. Abstract

Food-triggered anaphylaxis can encompass a variety of systemic and intestinal symptoms. Murine-based and clinical studies have revealed a role for histamine and H1R and H2R-pathway in the systemic response, however, the molecular processes that regulate the gastrointestinal (GI) response are not as well defined. In the present study, by utilizing an IgE-mast cell (MC)-dependent experimental model of oral antigen-induced anaphylaxis, we define the intestinal epithelial response during a food-induced anaphylactic reaction. We show that oral allergen-challenge stimulates a rapid dysregulation of intestinal epithelial transcellular and paracellular transport that was associated with the development of secretory diarrhea. Allergen-challenge induced (i) a rapid intestinal epithelial *Cftr*-dependent Cl⁻ secretory response and (ii) paracellular macromolecular leak that was associated with modification in epithelial intercellular junction proteins claudin-1, 2, 3 and 5, E-cadherin and desmosomal cadherins. OVA-induced *Cftr*-dependent Cl⁻ secretion and junctional protein degradation was rapid occurring and was sustained for 72 hours following allergen-challenge. Blockade of both the proteolytic activity and Cl⁻ secretory response was required to alleviate intestinal symptoms of food-induced anaphylaxis. Collectively, these data suggest that the GI symptom of food-induced anaphylactic reaction, secretory diarrhea, is a consequence of CFTR-dependent Cl⁻ secretion and proteolytic activity.

4. 2. Introduction

Severe food allergy-related reactions, termed food-triggered anaphylaxis, are serious life threatening reactions responsible for 30,000-120,000 emergency department visits, 2,000 - 3000 hospitalizations, and approximately 150 deaths per year in the United States^{8,9}. The onset of symptoms are variable, occurring within seconds to a few hours following exposure to the casual dietary allergen, and often affects multiple organ systems including gastrointestinal (GI), cutaneous, respiratory and cardiovascular²⁹⁰. Cutaneous symptoms (urticaria and angioedema) are the most common, occurring in approximately 80% of cases and GI symptoms occur in as much as 40% cases, which include cramping, abdominal pain, nausea, emesis and diarrhea²¹. Recently, there has been emerging clinical data indicating a link between GI manifestations with the more severe anaphylactic phenotype including hypotension and hypoxia²⁹¹⁻²⁹⁵. Clinical and experimental analyses have identified a central role for IgE/FcεRI cross linking on the surface on mast cells (MC) in promoting the clinical manifestations associated with food-triggered anaphylaxis^{43,51,75,296-299}. MCs upon IgE cross linking release an array of preformed mediators including histamine, PAF, serotonin, proteases (tryptase and chymase), and lipid-derived mediators (prostaglandins [PGD₂] and leukotrienes [LTC₄, LTD₄ and LTE₄]) which are thought to drive the systemic and GI symptoms^{43,51,298-300}. Genetic or pharmacological blockade of MC activity prevents the GI and systemic involvement in oral antigen-induced anaphylaxis^{57,58}. Notably, experimental investigations have revealed that histamine via histamine receptor (HR) HR1, HR2 and HR4 signaling drives the systemic manifestations of IgE-mediated anaphylaxis in mice^{58,185,301}, however the GI symptoms, while MC and IgE-dependent, remain unabated by HR1 and HR2 antagonism⁵⁸ indicating a role for other MC-derived mediators in the induction of the GI symptoms of oral antigen-induced anaphylaxis.

Herein, we describe the temporal molecular processes associated with GI symptoms of food-induced anaphylaxis in mice. We show that oral antigen-challenge induces a rapid dysregulation of small intestine (SI) transcellular *Cftr*-dependent Cl⁻ secretion and paracellular macromolecular leak. The paracellular macromolecular flux was linked with modification of transmembrane proteins in the tight junction (claudin-1,2,3, 5 and junctional adhesion molecule-A) and epithelial cadherins in the adherens

junction (E-cadherin) and desmosomes (DM) (Desmoglein 2 and desmocollin 2), and was mediated by IgE/MC activation. We show that GI manifestations such as secretory diarrhea was antigen-induced and persisted for 72 hours and was abated by abrogation of proteolytic activity and Cl⁻ secretion. Collectively, these studies suggest that MC-driven proteolytic activity and Cl⁻ secretory response is required for the development of secretory diarrhea response during a food-induced anaphylactic reaction in mice.

4. 3. Methods

4. 3. 1 Animals:

6-8-week-old BALB/c wild type (WT) mice were obtained from the National Cancer Institute (Bethesda, MD, USA) and bred in-house at Cincinnati Children's Hospital Medical Center (CCHMC) (Cincinnati, OH, USA) and at the University of Michigan (UM) (Ann Arbor, MI, USA). Intestinal IL-9 transgenic (iIL9Tg) mice were generated as previously described⁵⁷. Age-, sex-, weight-matched littermates were used as controls in all experiments. The mice were maintained and bred in a clean barrier facility and were handled under an approved Institutional Animal Care and Use Committee protocols at CCHMC and UM animal facility.

4. 3. 2 Oral antigen-induced intestinal anaphylaxis:

4-8-week-old mice were sensitized to ovalbumin (OVA) (50 µg of OVA / 1 mg of alum in sterile saline by intraperitoneal (i.p.) injection) and received repeated oral gavage (o.g.) challenge with OVA (250 µl of OVA (50 mg) in saline or 250 µl of saline (vehicle)) as previously described⁵⁶. Prior to each o.g. challenge, mice were deprived of food for 4-5 h. Rectal temperatures were measured prior to challenge and then every 15 minutes for 60 minutes. Diarrhea was assessed by visually monitoring mice for up to 60 minutes following o.g. challenge and mice demonstrating profuse liquid stool were recorded as diarrhea-positive. Evidence of secretory diarrhea was assessed by determination of short-circuit current (I_{sc}) of SI segments ex vivo in a Ussing chamber system up to 60 minutes following o.g. challenge. Mice were considered allergic if they demonstrated symptoms of anaphylaxis (hypothermia > 1.5 °C Temperature loss and diarrhea) following the 6th or 7th challenge. In Some experiments, mice were o.g. with 0.5 mM N-(2-naphthalenyl)-[(3,5-dibromo-2,4-dihydroxyphenyl) methylene] glycine hydrazide (GlyH101) (EMD Millipore #219671) 15 minutes before the 7th OVA-challenge. 500 µg 4-benzenesulfonyl fluoride

hydrochloride (AEBSF) (Sigma# A8456) were giving intravenous (i.v.) 2 hours prior to the 7th OVA the challenge. To track food allergen passage in the GI tract, Mice were administered OVA (200 mg / mL) with 5×10^5 FITC-labelled FluoSpheres™ Polystyrene Microspheres (10 μ M size) (Thermo Fisher, Waltham, MA, USA) by oral gavage and monitored for 30 minutes. The mice were euthanized, the GI tract surgically removed and segmented into anatomical compartments of the GI tract (stomach, duodenum, jejunum, ileum, caecum and colon). The duodenum was divided into 1.5 cm segments, jejunum into 4 cm segments, ileum into 2 cm segments and colon into 4 cm segments. The duodenum was defined as 3 cm GI segment distal to pyloric sphincter. The jejunum was defined as the ~16 cm GI segment distal of the duodenum and 10 cm proximal from the ileocecal valve. The ileum was defined as the GI segment 10 cm proximal from the ileocecal valve. The caecum was defined as the pouch connecting to the junction of the proximal ileum and distal colon. The colon segment was ~ 8 cm connecting the proximal caecum to the distal rectum. The luminal contents of the segments were flushed with Phosphate-buffered saline (PBS) centrifuged and suspended in 200 μ l PBS and the fluorescence of the total contents of each segment was measured using a Biotek multi-mode plater reader (Synergy H1) with Gen5 software.

4. 3. 3 Passive Anaphylaxis:

Mice were injected i.v. with 20 μ g / 200 μ L of anti-IgE (IgG2a mAb to mouse IgE; EM95) and evidence of anaphylaxis was examined as previously described^{209,43}.

4. 3. 4 Solutions and drugs:

The Krebs buffer used on each side of the Ussing chamber contained 4.70 mM KCl, 2.52 mM CaCl₂, 118.5 mM NaCl, 1.18 mM NaH₂PO₄, 1.64 mM MgSO₄ and 24.88 mM NaHCO₃. The tissues were allowed to equilibrate for 15 minutes in Krebs buffer containing 5.5 mM glucose. All reagents were obtained from Sigma-Aldrich (St. Louis, MO, USA) unless stated otherwise.

4. 3. 5 Ussing chambers:

1 cm, freshly isolated, serosal-stripped segments of jejunum were mounted between the hemi-chambers of an Ussing apparatus (U2500 Dual Ussing chamber, Warner instruments, Hamden, CT), and 0.112 cm² of tissue was exposed to 10 ml Krebs buffer at 37 °C. The transepithelial potential difference (PD) was detected with two paired

electrodes that contained 4% agar in 3 M KCl. The electrodes were connected to a voltage clamp amplifier (EC-800, Epithelial voltage clamp, Warner Instruments, Hamden, CT). The electrode potential difference and fluid resistance were compensated before mounting tissue segments into the chamber. To establish equilibrium, PD was continuously monitored under open-circuit conditions for 15 minutes. Thereafter, the tissues were voltage-clamped at 0 mV while continuously measuring Short circuit current (Isc). Voltage pulses (3-mV square waves sustained for 5 seconds) were delivered every 50 seconds to yield a current response for calculation of transepithelial resistance (TER) from Ohm's law. For ion conductance experiments, changes in Isc were determined for the cumulative addition of forskolin and acetylcholine to the serosal reservoir. After the peak response to the final concentration of each agonist was recorded, the Krebs buffer on each side of the chamber was replaced, and the tissue was allowed to equilibrate for 30 minutes. Immediately following re-equilibration, tissue was pre-incubated with ion channel blockers 4,4'-Diisothiocyanatostilbene-2,2'-disulfonate (DIDS) (100 μ M) or CFTR^{Inh172} (20 μ M) to mucosal reservoir. Changes in Isc were measured in response to the addition of forskolin to the mucosal side. To study effects of direct allergen application, 1% OVA or equal volume of PBS was directly added into apical side of the dissected jejunum mounted in the Ussing Chamber and Isc, TER were recorded as previously described⁵⁷.

4. 3. 6 Intestinal epithelial cells (IEC) preparation:

5 cm segment of the jejunum was washed with cold PBS and 2% fetal bovine serum (FBS) and 5 mM DTT (20 minutes at 37°C with shaking). Afterward, IEC were isolated by washing tissue 3 times with PBS and 2% FBS and 5 mM EDTA (10 minutes at 37°C with shaking), then the washing solution was collected then centrifuged (400g for 10 minutes at 4°C) and pellet was suspended in PBS for cells quantification and lysis. For cell lysis, isolated IEC were resuspended in RIPA buffer (0.5% Triton X-100, 0.5% NP-40, 0.5% deoxycholic acid, 0.1% SDS, 150 mM NaCl, 1 mM EGTA [pH 8.0], 1 mM EDTA, 0.2 mM sodium orthovanadate, 20 mM Tris [pH 7.4]) supplemented with protease and phosphatase inhibitors. Immunoblotting was performed as previously described³⁰².

4. 3. 7 Immunofluorescence:

5 cm segment of the jejunum was fresh frozen in O.C.T. Tissues were fixed in 95% cold ethanol for 30 minutes, followed by 1 minutes of pure acetone fixation at room temperature. For ZO-1 staining, tissues were fixed in 4% PFA, followed by permeabilization with 0.5% Triton X-100. Primary antibody staining was performed in Hank's balanced salt solution with 3% bovine serum albumin (BSA) for overnight. Secondary antibodies were incubated in 3% BSA and for 1h. Antibodies for WB were as follows: Rabbit anti-claudin-1 #51-9100 (Thermo Fisher, Waltham, MA, USA), rabbit anti-claudin-2 #51-6100 (Thermo Fisher, Waltham, MA, USA), rabbit anti-claudin-3 #SAB4500434 (Sigma Aldrich, St. Louis, MO, USA), mouse anti-claudin-5 #35-2500, rabbit anti-ZO-1 #617300 (ThermoFisher, Waltham, MA, USA), goat anti-E-Cadherin #AF748, goat anti-mouse JAM-A #AF1077 (R&D Systems, Minneapolis, MN, USA), rabbit anti-cytokeratin-8 #ab53280, rabbit anti-desmoglein-2 #ab124683 (Abcam, Cambridge, United Kingdom), mouse anti-desmocollin-2 #32-6200 (Thermo Fisher, Waltham, MA, USA), rabbit anti-GADPH #G9545 (Sigma Aldrich, St. Louis, MO, USA), rabbit anti-calnexin #C4731 (Sigma Aldrich, St. Louis, MO, USA). Antibodies for immunofluorescence were as following: rat anti-E-cadherin #53-3249-82, rabbit anti-claudin-1 #51-9000, rabbit anti-claudin-2 #516100 (Thermo Fisher, Waltham, MA, USA). Nucleus were detected with DAPI. Confocal microscopy was performed using a Leica SP5 inverted microscope (Wetzlar, Germany) Leica SP5 software.

4. 3. 8 Statistical analysis:

Data are expressed as mean \pm standard deviation (SD), unless otherwise stated. Statistical significance comparing different sets of mice was determined by Student's t test. In experiments comparing multiple experimental groups, statistical differences between groups were analyzed using the one-way, nonparametric ANOVA and a Bonferroni post-test. $P < 0.05$ was considered significant. All analyses were performed using Prism 7.0 software (GraphPad Software Inc., San Diego, CA, USA).

4. 4. Results

4. 4. 1 Food antigen exposure is restricted to the small intestine (SI) during a food-induced anaphylactic reaction:

We have previously demonstrated that OVA-sensitized mice demonstrate systemic and gastrointestinal symptoms including diarrhea within 30 minutes of the 7th

oral OVA challenge^{56,228}. To ascertain the localization of dietary antigen in the GI tract during the onset of the symptoms of food-induced anaphylaxis, mice received o.g. of fluorescent-OVA and the transit of dietary antigen along the GI tract was monitored for 30 minutes (Figure 4.1A). We show that dietary antigen was predominantly localized in the SI, in particularly the jejunum-ileum region, with the highest concentration localized to the proximal ileum region (Figure 4.1B). We observe minimal evidence of dietary antigen in the caecum and colon from the ileocecal junction to distal colon. OVA-sensitized and challenged mice possess a heightened GI CD4⁺ Th₂, ILC2 immune response in the SI, which can alter GI peristalsis³⁰³⁻³⁰⁷. To determine the localization of antigen in the GI compartment following IgE-MC activation independent of the Type-2 immune response we employed the passive-oral IgE mediated model of anaphylaxis using transgenic mice with intestinal mastocytosis and no Th2 activation (iIL-9Tg)^{56,57}. Notably, fluorescent OVA in iIL-9Tg mice 30 minutes following MC activation was similar to that observed in WT mice that experienced food-induced anaphylaxis (Figure 4.1B). Furthermore, the dietary antigen was restricted to the distal jejunum and jejunoileal region in naïve WT mice and iIL-9Tg mice that received isotype control and did not experience anaphylaxis, suggesting that anaphylaxis does not significantly alter dietary antigen translocation (Figure 4.1B). These studies indicate that the eliciting dietary antigen is predominantly restricted to the murine jejunoileal region and not in the caecum or colon at the corresponding time these mice experience symptoms of anaphylaxis.

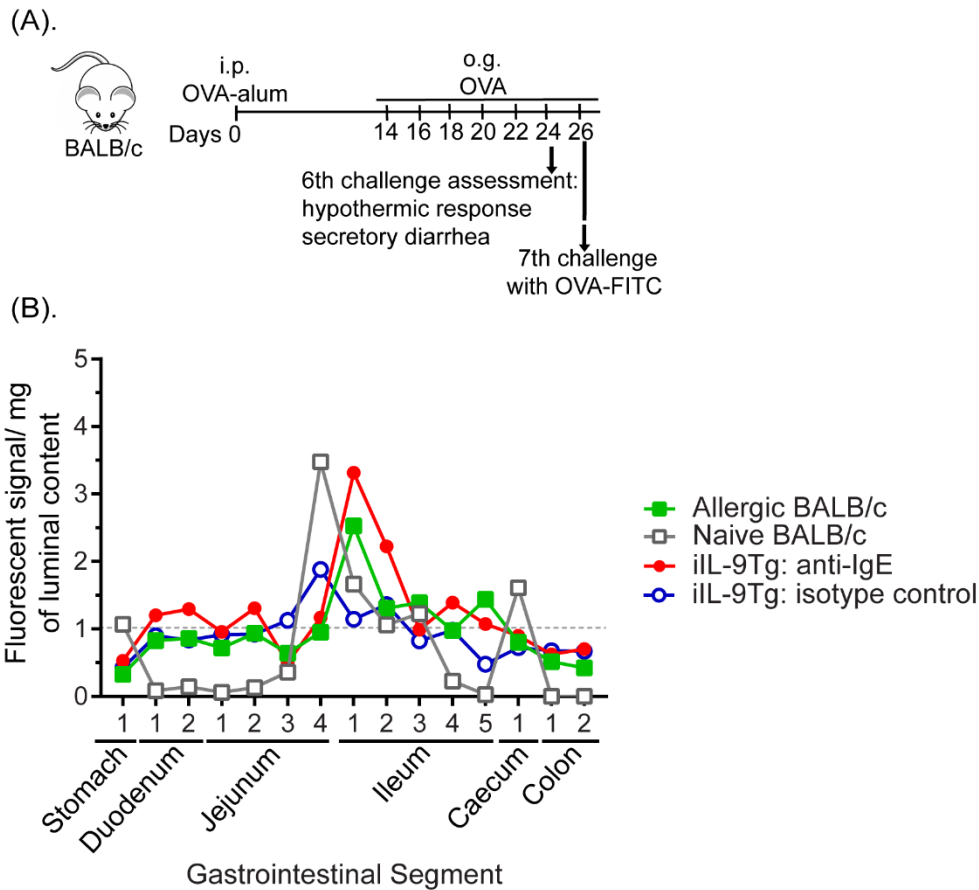


Figure 4.1: Eliciting antigen is restricted to the SI during the onset of food-induced anaphylactic symptoms

A Experimental regimen,

B Localization of OVA-fluorescence in the GI tract segments of naïve or food allergic WT and iIL-9Tg mice following anti-IgE treatment. OVA-sensitized BALB/c mice were repeatedly challenged with OVA and on the 7th challenge received 5×10^5 FITC-labelled FluoSpheres™ Polystyrene Microspheres and localization of FluoSpheres in the GI segments were examined by fluorescence within 30 minutes. Naïve mice and iIL-9Tg mice challenged with either anti-IgE (20 μ g / 200 μ l i.v.) or vehicle received oral gavage of 5×10^5 FITC-labelled FluoSpheres™ Polystyrene Microspheres and localization of FluoSpheres in the GI segments were examined within 30 minutes.

Data are represented as the mean fluorescence signal detected in luminal contents (per mg) of the respective GI segments from $n = 5$ mice.

4. 4. 2 Antigen challenge stimulated intestinal epithelial CFTR-dependent Cl⁻ transport and paracellular leak:

Given our observation that dietary antigen was restricted to the SI, we examined epithelial ion transport (Short circuit current; I_{sc}) of the SI from control and food-allergic mice (within 30 minutes of food-challenge) to determine whether anaphylaxis was associated with altered intestinal epithelial permeability. Basal I_{sc} and forskolin-induced ΔI_{sc} of the SI of food allergic mice was significantly increased compared to vehicle-treated mice (Figure 4.2A and B). Pre-exposure of the SI epithelium to the CFTR inhibitor (CFTR^{inh172}) and not DIDS, a potent inhibitor of calcium activated Cl⁻ transporters (Cl-

/HCO₃⁻ exchanger and potassium/chloride co-transporter), abrogated the Forskolin-induced Δ Isc indicating that increased current is predominantly mediated by CFTR-dependent Cl⁻ transport activity (Figure 4.2C). Assessment of the paracellular epithelial function of the jejunum from OVA-treated mice revealed decreased Transepithelial resistance (TER) and increased macromolecular flux (FITC-Dextran flux; apical to basolateral) compared with jejunal preparations from vehicle-treated mice (Figure 4.2D and E). Collectively, these studies suggest that dietary antigen induced a rapid SI epithelial CFTR-dependent Cl⁻ secretory response and paracellular permeability within 30 minutes of antigen challenge.

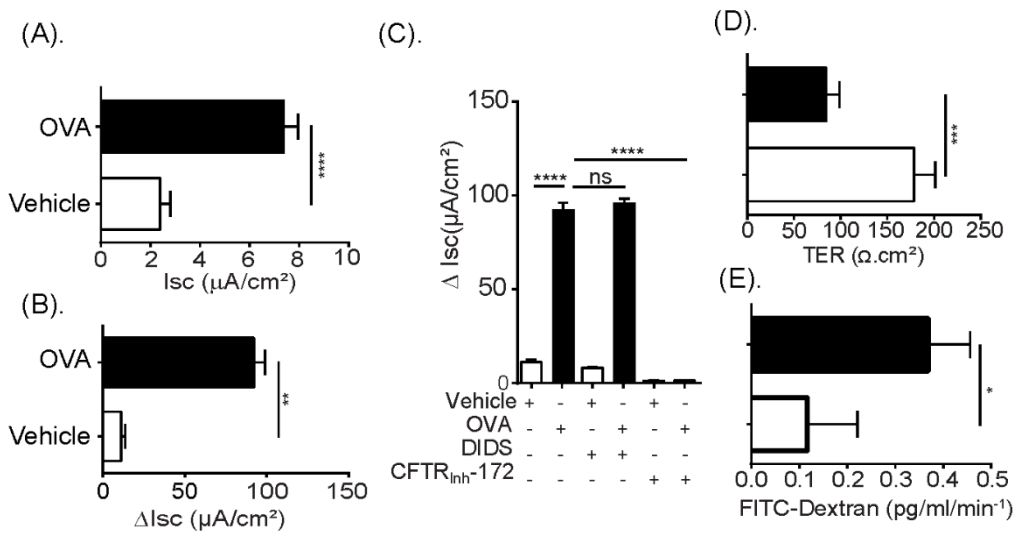


Figure 4.2: Oral antigen challenge induced SI epithelial transcellular and paracellular barrier dysfunction.

A Isc baseline,

B Forskolin-induced short-circuit current response (Δ Isc) of jejunum segments from Vehicle- and OVA-treated BALB/c WT mice within 60 minutes of the 7th OVA challenge.

C Forskolin-induced Short-circuit current response of jejunum segments from Vehicle- and OVA-treated mice following exposure to the ion channel blockers DIDS (100 µM) or CFTR^{inh}172 (20 µM) in the mucosal reservoir inside Ussing chambers system.

D TER and E FITC-dextran flux of jejunum segments from Vehicle- and OVA-treated BALB/c WT mice within 60 minutes of the 7th OVA challenge. OVA-treated mice were sensitized with OVA-alum and received seven o.g. OVA challenges. Vehicle-treated mice are OVA-sensitized mice that were challenged with vehicle (Saline) and did not develop anaphylaxis symptoms.

Data are represented as the mean \pm SD; n = 3 - 7 mice per group from 2 - 3 representative experiments (A-E). **** P < 0.0001, *** P < 0.001, ** P < 0.01, * P < 0.05, ns > 0.05.

4. 4. 3 Direct exposure of OVA to jejunal SI preparations is sufficient to promote epithelial transcellular and paracellular dysfunction:

Next, we examined whether the food-induced macromolecular leak was associated with changes in intercellular junctional proteins (JP). To do this, we examined SI epithelial AJ and TJ proteins from naïve mice and mice that demonstrated symptoms

of anaphylaxis (≥ 1.5 °C Temperature loss and diarrhea) 30 minutes following the 7th food allergen challenge. We observed a significant reduction in the level of full length transmembrane proteins in the TJ, Claudin -1, -2, -3 and -5 AJ, E-cadherin and DM, Desmoglein-2 (Dsg-2) and Desmocollin-2 (Dsc-2) in SI epithelial extracts from food allergic mice compared with naïve mice (Figure 4.3A and B, control (CTL) vs. food-challenge #7). Intriguingly, we identified the presence of cleaved fragments of the AJ protein, E-cadherin (~55 kDa) and Dsg-2 (22 kDa) and Dsc-2 (75 kDa) in SI epithelial extracts from anaphylactic mice (Figure 4.3B, food-challenge #7). The food allergic reaction was not associated with a decrease in all intestinal JP as the SI TJ protein occludin was unaffected by repeated dietary food-challenge (Figure 4.3A challenge #7). Keratin-8 (CK-8) immunoblotting reveals comparable level of intestinal epithelial cells and Actin and GAPDH shows similar protein loading (Figure 4.3A and B). Immunofluorescence analyses of the jejunum revealed a similar pattern of decreased proteins in the TJ, Claudin-1, Claudin-2 and E-cadherin in the apical junctional complex of the intestinal epithelium of allergic mice within 30 minutes of antigen challenge as compared with control mice (Figure 4.3D). Notably, we observed no change in the expression of the transmembrane protein ZO-1 in jejunum of allergic mice following allergen exposure.

To determine whether the cleaved intestinal JP in the TJ, AJ and DM was associated with development of GI symptoms of food-induced anaphylaxis, we performed analyses on mice following the fifth food-challenge that do not demonstrate symptoms of food-induced anaphylaxis following challenge (post-5th challenge). We show that the level of TJ proteins, Claudin -1, -2, -3 and -5 were similar to that observed in naïve mice (Figure 4.3A; food-challenge #5). Furthermore, we observed full length E-cadherin and Dsg-2 and Dsc-2 in SI epithelial extracts from asymptomatic mice following 5th challenge (Figure 4.3B), albeit we detected the presence of cleaved cadherin fragments (E-cadherin and Dsg-2 and Dsc-2) (Figure 4.3B). Collectively these data suggest that cleavage of intestinal JP in the TJ, AJ and DM was associated with development of GI symptoms of food-induced anaphylaxis.

Given that we were able to detect cleaved cadherin fragments in the AJ and DM, we utilized the Dsg-2 western blot analyses as a surrogate marker to determine

whether a single dietary antigen-challenge induced rapid SI cadherin cleavage. To do this, we examined SI epithelial Dsg-2 in mice prior to (Pre-) and following (Post-) the 7th food-challenge. Notably, we observed loss of the native full length Dsg-2 following the 7th challenge. Additionally, we also observed decreased levels of the 50 kDa Dsg-2 cleavage fragment and accumulation of lower molecular weight (30kDa) Dsg-2 fragment (Figure 4.3C). These data indicate that a single allergen challenge is sufficient to induce a pronounced and rapid decrease in the full length high molecular weight Dsg-2 protein levels and increasing low molecular weight Dsg-2 cleavage products in mice that develop food-induced anaphylaxis.

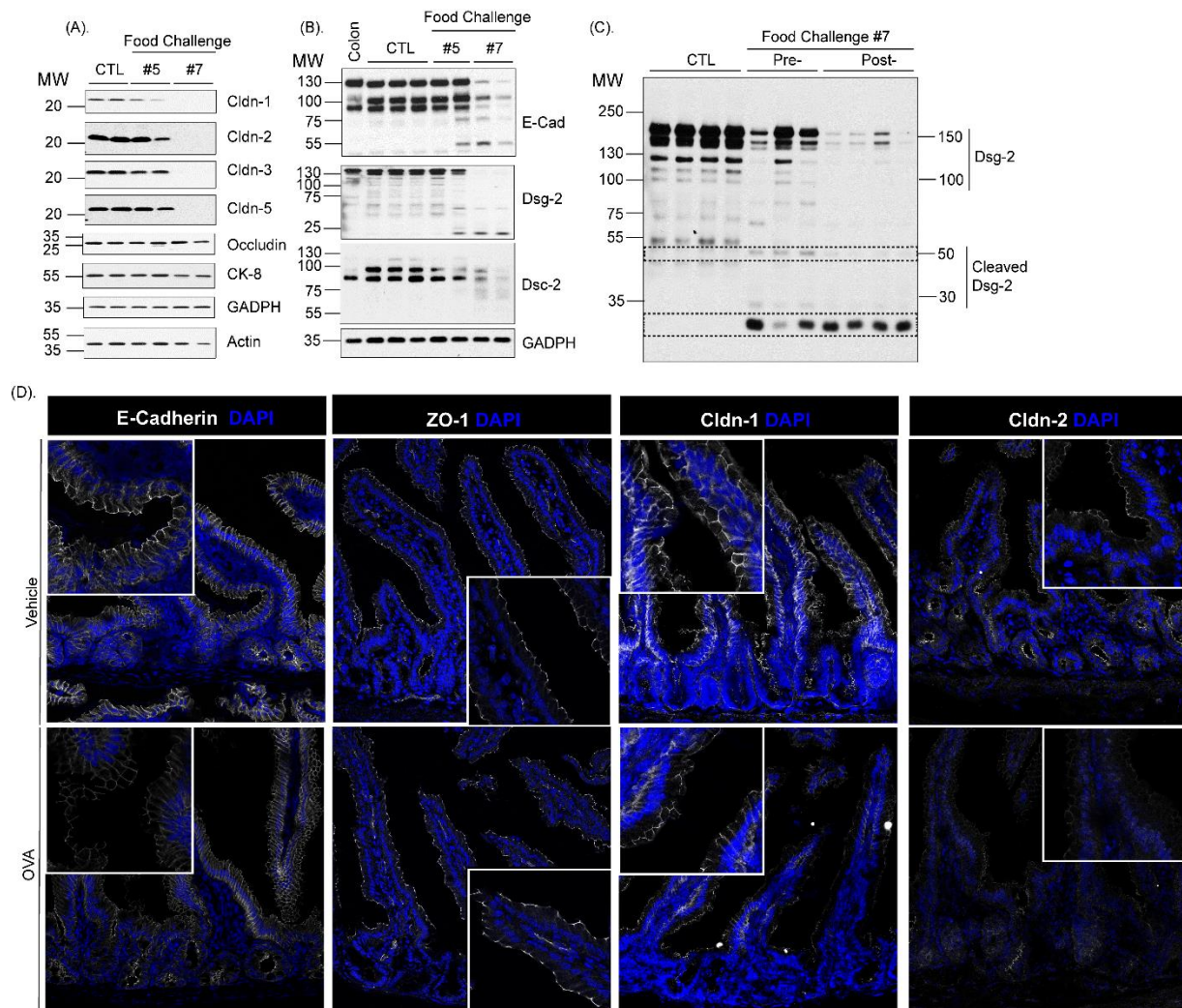


Figure 4.3: Oral antigen-induced SI para-cellular dysfunction is associated with degradation of adherence and tight junction proteins.

Assessment of intestinal junctional proteins expression: Western protein analysis of A Claudin-1, Claudin-2, Claudin-3, Claudin-5, Occludin, Keratin-8, GADPH and Actin and

B E-cadherin, Dsg-2, Dsc-2 and GAPDH in isolated jejunal epithelial cells from untreated (CTL) and OVA-sensitized mice 30 minutes following the 5th and 7th oral challenge.

C Western protein analysis of Dsg-2 in isolated jejunal epithelial cells from untreated (CTL) and OVA-sensitized mice prior to (Pre-) and 30 minutes following the 7th oral challenge (Post-) (A-C). Actin and GAPDH were used as a loading control. Colonic tissue was used as a positive control. MW, Molecular weight. Each column represents a single mouse D Immunofluorescence analysis of E-cadherin, ZO-1, Claudin-1 and Claudin-2 (white) in jejunum segments from Vehicle- and OVA-treated BALB/c WT mice within 30 minutes of the 7th OVA challenge. Nuclei are visualized with DAPI (blue).; (D). Representative photomicrographs of n = 5 - 7 mice per group and 5 serial SI sections per mouse.

To determine whether direct antigen exposure of the SI epithelium can induce the GI epithelial dysfunction, we exposed the apical surface of SI segments from naïve and food-allergic mice *ex vivo* to OVA in an Ussing Chamber system and assessed Isc and TER. *Ex vivo* exposure of OVA to the SI segment of a naïve animal did not induce any significant change in Isc or TER (Figure 4.4A). In contrast, OVA exposure of the SI segment from allergic mice stimulated an increase in Isc and a decrease in TER within 30 minutes (Figure 4.4A and B). The baseline Isc and TER of the SI segments from allergic mice was trending lower than that observed from naïve mice, however levels were not statistically significant (Figure 4.4A and B). These studies show that a single allergen challenge is sufficient to induce a pronounced and rapid decrease in intestinal epithelial barrier function that is related to enhanced ion transport and loss of intestinal epithelial barrier. To get insight into the temporal nature of the paracellular and transcellular epithelial dysfunction following allergen challenge, we monitored Isc and TER of SI segments from food allergic mice following the 7th OVA-challenge. We show that OVA-induced intestinal epithelial barrier dysfunction was maintained for at least 48 hours following dietary antigen challenge and returned to baseline levels by 72 hours (Figure 4.4 C and D). Collectively, these studies demonstrate that dietary antigen exposure of the SI mucosal epithelium is sufficient to induce SI barrier dysfunction that can be sustained for up to 48 hours following allergen exposure.

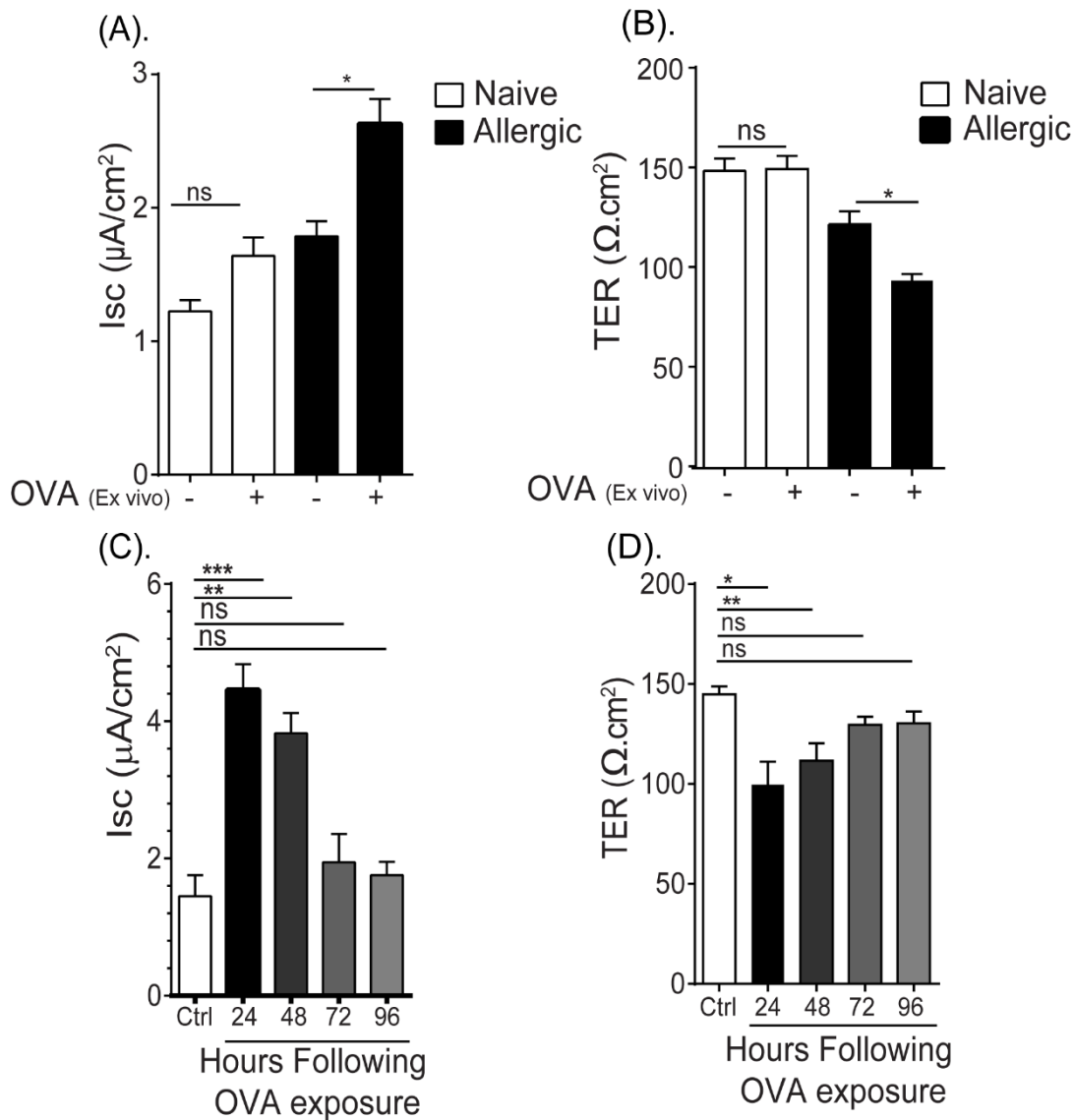


Figure 4.4: Oral antigen exposure leads to temporal loss of epithelial transcellular and paracellular dysfunction.

A Isc baseline and B TER of *ex vivo* jejunal segments from unsensitized (naïve) and OVA-sensitized and oral challenged mice (allergic) apically exposed to vehicle (PBS) or OVA in Ussing Chamber system.

C Isc and D TER of *ex vivo* jejunal segments from unsensitized (Ctrl) and OVA-sensitized and oral challenged mice 24 - 96 hours following the seventh oral challenge.

(A and B) Jejunum was removed from unsensitized (naïve) and OVA-sensitized and oral challenged mice (allergic- following 6th oral challenge) and mounted in a Ussing Chamber system and exposed to either PBS (-) or 1% OVA on the apical side and Isc and TER were recorded as described in the material and methods section. (C and D) Jejunum from unsensitized (Ctrl) and OVA-sensitized and oral challenged mice were removed 24, 48, 72 and 96 hours following seventh challenge and mounted in a Ussing Chamber system and Isc and TER were recorded as described in the material and methods section.

Data are represented as the mean \pm SD, n = 3 mice per group. **** P < 0.0001, *** P < 0.001, ** P < 0.01, * P < 0.05, ns > 0.05.

4. 4. 4 Dissection of mechanisms of oral antigen-induced transcellular and paracellular permeability:

To define the relationship between SI epithelial transcellular and paracellular barrier dysfunction and the development of the dietary antigen-induced GI symptom, secretory diarrhea, we examined the SI from allergic mice that did and did not develop diarrhea following the 7th challenge. The SI segment from mice that developed secretory diarrhea within 30 minutes of food allergen-challenge had a significant increase in I_{sc} (~3-fold) and dramatically decreased TER (~60% reduction) compared to vehicle-treated mice (Figure 4.5A and B). In contrary, the SI from mice that received antigen that failed to develop secretory diarrhea did not demonstrate evidence of altered I_{sc} but did show a significant reduction in TER (~26% reduction) compared to vehicle-treated mice (Figure 4.5A and B). These studies demonstrate a relationship between altered SI transcellular and paracellular permeability and the development of the food-induced symptom secretory diarrhea in food allergic mice.

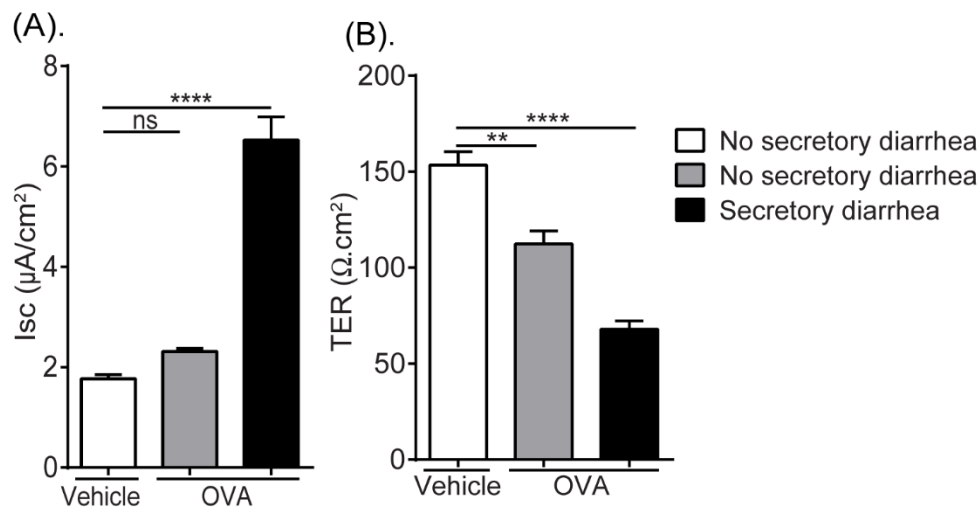


Figure 4.5: SI transcellular the paracellular permeability was associated with the development of oral antigen-induced secretory diarrhea.

A I_{sc} baseline and B TER measurements of jejunal segments from OVA-sensitized mice following Vehicle (Saline) or OVA oral challenge (7th challenge) and stratified according to secretory diarrhea development (60 minutes). OVA-sensitized mice were challenged with OVA (7th Challenge) and evidence of profuse liquid stool (diarrhea-positive) was examined. Following the 60 minutes diarrhea observation period, jejunal segments were removed and mounted in a Ussing Chamber system and I_{sc} and TER were recorded as described in the Material and Methods section.

Data are represented as the mean ± SD, n = 4 - 7 mice per group. **** P < 0.0001, *** P < 0.001, ** P < 0.01, * P < 0.05, ns > 0.05.

Given our demonstration of dietary antigen-induced enhanced Cl⁻ transport, and also paracellular barrier dysfunction associated with JP protein degradation and that this was associated with the GI symptom diarrhea, we hypothesized that the secretory diarrhea response was a consequence of CFTR-dependent Cl⁻ secretion and proteolytic-

activity. To test this hypothesis, mice that demonstrated a history of food-induced anaphylaxis (as confirmed by the 6th challenge) received either a chloride channel blocker (GlyH101) (o.g 15 minutes before OVA) or a protease inhibitor (AEBSF) (i.v 2h before OVA) alone or in combination prior to the 7th challenge and food allergen-induced SI epithelial transcellular and paracellular function was assessed (Figure 4.6A). As previously demonstrated, OVA-challenge of OVA-sensitized mice increased SI basal I_{sc}, forskolin-induced Δ I_{sc} response and FITC-dextran flux and reduced the TER compared to non-allergic (Vehicle) mice (Figure 4.2 and Figure 4.6 B and C). Pretreatment with GlyH101 alone, significantly attenuated OVA-induced amplification of forskolin-induced Δ I_{sc}, TER and FITC-dextran flux (Figure 4.6 B-E). Pretreatment with AEBSF alone, also significantly attenuated OVA-mediated induction of forskolin-induced Δ I_{sc}, TER and FITC-dextran flux, however SI forskolin-induced Δ I_{sc} was unaffected (Figure 4.6 B-E). Pretreatment with both GlyH101 and AEBS prior to the 7th OVA-challenge significantly attenuated OVA-induced dysregulation of both SI epithelial transcellular and paracellular function compared with OVA-treated mice that received vehicle (Figure 4.6 B-C). Importantly, pretreatment of mice with GlyH101 and AEBSF dramatically reduced the incidence of diarrhea in mice following the 7th OVA-challenge (Figure 4.7). Moreover, 10 of 10 of food allergic mice that received OVA developed secretory diarrhea following the 7th challenge. In contrast, only 8 of 18 mice who received GlyH101 and AEBSF developed secretory diarrhea following the 7th challenge (Figure 4.7). Collectively, the GI symptom of dietary antigen-induced anaphylaxis, secretory diarrhea, is a consequence of food antigen-induced transcellular and paracellular SI epithelial barrier function.

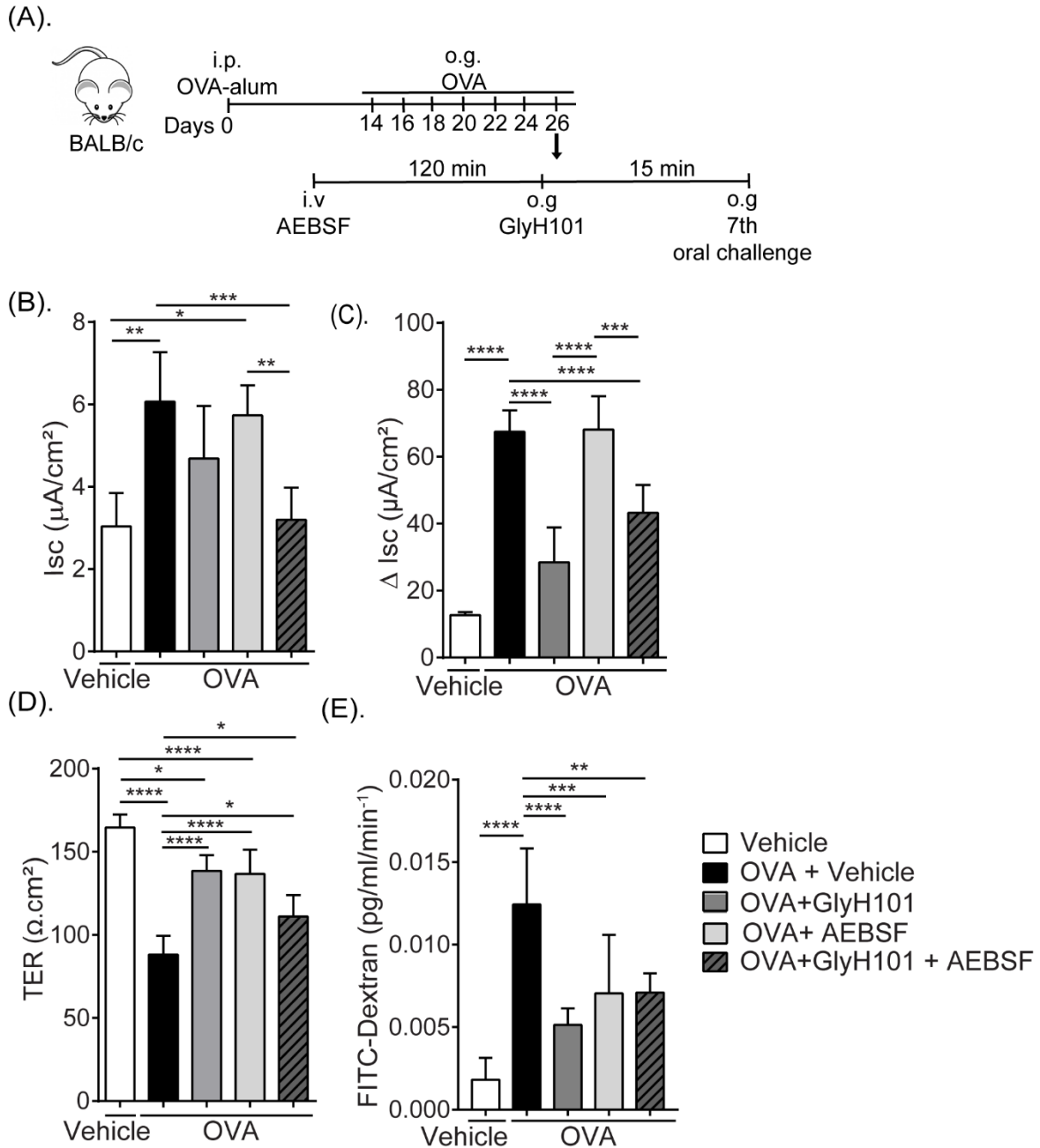


Figure 4.6: Inhibition of Cl⁻ secretory activity and proteolysis attenuated oral antigen-induced SI transcellular the paracellular permeability.

(A) Experimental regimen, (B) I_{sc} baseline and (C) Forskolin-induced I_{sc} responses (ΔI_{sc}), (D) TER, (E) FITC-dextran flux of jejunal segments from OVA-sensitized and oral challenged mice (7th Challenge) following pretreatment with GlyH101 and protease inhibitor (AEBSF) alone or in combination. OVA-sensitized mice received repeated OVA challenge (six challenges) and mice that demonstrated evidence of food allergy were stratified into indicated groups. Mice received either 0.5 mM GlyH101 (oral gavage) 15 minutes prior to the 7th OVA-challenge or 500 µg AEBSF (i.v.) 2 hours prior to 7th OVA-challenge, alone or in combination and subsequently received oral gavage (OVA). Following the 60 minutes observational period, jejunal segments were removed and mounted in a Ussing Chamber system and physiological measurements were recorded as described in the Material and Methods section. Vehicle represents unsensitized mice that received Vehicle oral gavage challenge. (C-E). Data are represented as the mean ± SD, n= 3 - 7 mice per group. **** P < 0.0001, *** P < 0.001, ** P < 0.01, * P < 0.05, ns > 0.05.

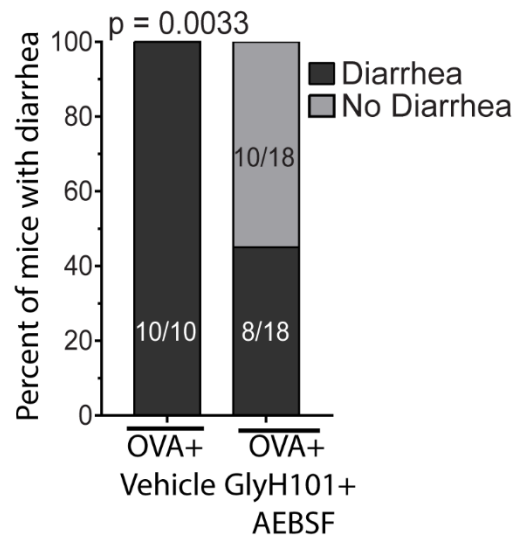


Figure 4.7: Inhibition of Cl⁻ secretory activity and proteolysis was associated with inhibition of GI symptoms of food-induced anaphylaxis.

Chi-square analysis of number of mice with/without secretory diarrhea. OVA-sensitized mice received repeated OVA challenge (six challenges) and mice that demonstrated evidence of food allergy were stratified into either Vehicle or GlyH101 + AEBSF groups. Mice received 500 µg AEBSF (i.v.) 2 hours prior to 7th OVA-challenge and 0.5 mM GlyH101 (oral gavage) 15 minutes prior to the 7th OVA-challenge and subsequently received oral gavage (OVA) and evidence for diarrhea was examined for a 60 minutes observational period.

4. 5. Discussion

In the present study, we show that: 1) the onset of GI symptoms of dietary antigen-induced anaphylaxis occurred with dietary antigen localized to the SI; 2) the symptom of diarrhea was associated with increased SI epithelial CFTR-dependent Cl⁻ secretion and epithelial JP degradation; 3) The transcellular and paracellular SI dysfunction occurred rapidly following food antigen exposure and persisted for up to 72 hours; 4) development of the intestinal symptom diarrhea in dietary antigen-induced anaphylaxis was linked to SI transcellular and paracellular dysfunction and 5) blockade of chloride channel and proteolytic activity attenuated the GI symptoms in dietary antigen-induced anaphylaxis.

The association between food allergy and diarrhea dates back to the 1930s³⁰⁸⁻³¹⁰. Rowe reported cases of diarrhea in 15% of 150 cases of GI allergy. Whether or not the symptom of diarrhea was associated with and acute-IgE-mediated reaction or part of some other allergic condition (e.g., allergic colitis or FPIES) was inconclusive, however the diarrhea phenotype was food-dependent, acute and often associated with other clinical signs and symptoms of food-induced anaphylaxis such as fatigue, toxemia and nervousness^{308,309}. More recent reports indicate that IgE-mediated anaphylactic reactions involving the GI tract including diarrhea occur in 30 to 45% of cases anaphylaxis^{311,312}.

Interestingly, antidotal data supports a role for GI symptoms in the severity of food induced anaphylaxis^{21,295}. Retrospective chart analyses of clinical features of acute generalized hypersensitivity reactions in 1,149 patients revealed that features of anaphylaxis, including vomiting and nausea, strongly correlated with anaphylaxis severity³⁷. In contrast, common skin features, including urticaria, erythema and angioedema, did not correlate with hypoxia and hypotension³⁷. Similarly, examination of the clinical history of 163 pediatric patients with food-induced anaphylaxis showed that relapsing GI symptoms increased the risk of hypotension and bradycardia or cardiac arrest²⁹⁴.

The molecular basis by which an eliciting dietary antigen induces GI symptoms in food-induced anaphylaxis is unclear. We have previously shown that oral antigen-induced anaphylaxis in mice is MC-dependent⁵⁸ and that heightened GI MC numbers correlate with intestinal and systemic anaphylaxis severity^{56,57}. Similarly, systemic mastocytosis patients can present with increased GI symptoms and have increased risk of severe anaphylaxis^{313,314} and administration of the MC stabilizing agent sodium cromoglycate protected food allergic individuals from food provocation-induced GI permeability and altered GI function³¹⁵. Herein, we demonstrate that the food allergen-induced GI symptom of diarrhea was associated with a rapid SI secretory response and epithelial barrier dysfunction and that suppression of the GI symptom required inhibition of both Cl⁻ channel activity and proteolysis. Several MC-derived mediators are known to modulate discrete components of the intestinal epithelial secretory and barrier function including histamine, prostaglandins and mast cell-derived proteases^{316,317}. Secretory diarrhea is generally a result of dysregulation of the coordinated GI epithelial secretory or absorptive processes leading to excessive accumulation of GI luminal fluid³¹⁸. The SI epithelial fluid secretion is predominantly mediated by transepithelial Cl⁻ flux from the basolateral to apical surface of the epithelium via coordinated chloride channels and transporters including Na/K/Cl symporter (NKCC1), Basolateral K⁺ channels (KCNQ1/KNE3 and KCNN4), the cyclic-nucleotide-activated cystic fibrosis transmembrane conductance regulator (CFTR) and Ca²⁺-activated Cl⁻ channels (CaCCs)³¹⁹. We show that dietary exposure of the SI of food-sensitized mice promoted an increase in basolateral to apical Cl⁻ secretion via CFTR-dependent mechanism. Histamine signaling through the H1R stimulates CFTR Cl⁻ ion

secretion through cAMP/PKA pathway^{320,321}. Similarly, prostaglandins and serotonin increase Cl⁻ secretion in human colon and jejunum samples respectively^{322,323}. However, experimental studies in *in vivo* animal model systems have demonstrated that while antihistamines may impact systemic symptoms, they do not impact the secretory diarrhea phenotype in food-induced anaphylaxis, and clinically antihistamines have been shown to be effective for the treatment of the cutaneous symptoms but not the gastrointestinal symptoms^{58,290}. A recent study reported an important role for MC-derived PGD₂ in the suppression of systemic symptom of shock (hypotension and hypothermia) during an anaphylactic reaction in mice³²⁴; however as the anaphylaxis model employed by the investigators did not induce GI symptoms, they were unable to assess the contribution of MC-derived PGD₂ to the secretory diarrhea response. Mast cell-derived cytokines such as IL-6, IL-8, IL-13 and TNF alpha have been shown to activate secondary messenger cascades including Ca²⁺ and cyclic nucleotides such as cAMP and cGMP to stimulate CFTR dependent Cl⁻ transport and also inhibition of the absorptive capacity of apical Na⁺ transporters and promote a secretory diarrhea phenotype^{214,318}. Furthermore, the pro-Type 2 cytokines associated with food-induced anaphylaxis such as IL-4 and IL-13 regulate SI CFTR expression and enhanced CFTR activity^{214,325,326}. However, IgE-FcεRI-induced release of cytokines from MCs generally occurs up to 1 hr following activation and we show that the dietary antigen-induced CFTR-dependent response occurred rapidly within minutes of allergen exposure suggesting that the CFTR dependent Cl⁻ transport is not likely MC-derived cytokine-mediated. We predict that the repetitive oral allergen challenge and stimulation of the SI CD4⁺ Th2 and ILC2 response is likely to drive SI CFTR mRNA and protein induction in the intestinal epithelium and that cAMP-inducing mast cell-derived mediators stimulate exaggerated intestinal epithelial CFTR activity and CFTR-dependent Cl⁻ secretion and as a consequence development of secretory diarrhea acutely following allergen exposure. The physiological significance of increased fluid secretion in the SI of food allergic mice is likely related to efforts to remove the food allergen from the SI surface epithelium and promote elimination of the food allergen from the host GI compartment. Analogous to this, helminth infestation of the GI tract is known to promote an anti-helminth host immune response known as the “weep and sweep”. The “weep and sweep” response involves induction of a GI CFTR-dependent secretory

response to increased luminal fluid (weep) and increased peristaltic contractility (sweep) which is thought to lead to detachment of the helminth parasite from the surface epithelia and promote parasite expulsion from the host³²⁷. Intriguingly, the anti-helminth host “weep and sweep” response is driven by a CD4⁺ Th2 and ILC2-dependent immune response similar to that observed in food allergic reactions^{327,328}.

The dietary antigen-induced SI epithelial barrier dysfunction was also associated with rapid degradation in the SI epithelial TJ and AJ proteins and increased paracellular leak. AJ and TJ proteins expressed by intestinal epithelial cells are critical of the establishment and maintenance of intestinal epithelial paracellular permeability and barrier function^{329,330}. Previous studies in rats have revealed increased intestinal permeability during an intestinal hypersensitivity reaction that was dependent on MC activation and release of MC proteases³³¹⁻³³³. IgE-crosslinking of FcεRI on MC promotes the rapid release of several proteases in both mouse and man³³⁴⁻³³⁷. In mice, IgE-mediated reactions are associated with the prodigious release of the chymotrypsin-like serine protease MCPT-1, however connective and mucosal MCs are known to express many additional proteases including MCPT-4 (chymotrypsin-like), MCPT-5 (Elastase-like), MCPT-6 and MCPT-7 (trypsin-like tryptases) and carboxypeptidase 3 (CPA3)³³⁸. Several of the MC proteases can disrupt TJ proteins and increase cellular permeability. MCPT-4, which possesses chymotryptic proteolytic activity, and the elastase-like MCPT-5 have been shown to disrupt epidermal TJ function, in particularly Claudin-4³³⁹. Studies in MCPT-1-deficient mice have revealed a role for MCPT-1 in the proteolytic degradation of Occludin³⁴⁰ and MCPT-4 induces disruption of SI epithelial Claudin-3 function via PAR-2-dependent process and altering SI intestinal permeability^{341,342}. Similarly, human trypsinase has been shown to regulate GI permeability via PAR-2-β-arrestin-dependent mechanism causing disruption of TJ, Claudin-1, ZO-1 and Occludin and perijunctional F-actin^{343,344}. Food-induced anaphylaxis in mice is associated with the accumulation and degranulation of intestinal mucosal MCs, and not connective tissue MCs, suggesting that mucosal MCs proteases such as MCPT-1 and MCPT-2 may drive the SI epithelial barrier dysfunction^{57,58}. Employing a rat model of anaphylaxis, investigators have previously reported a role for the mucosal mast cell granule chymase, rat mast cell protease-II (RMCP-II), in increased jejunal paracellular permeability^{333,345}. Notably, RMCP-II induces

loss of ZO-1 and Occludin in MDCK-II monolayers^{333,345}. Examination of *Mcpt1*^{-/-} mice on the BALB/c background, revealed no role for MCPT-1 in the incidence of diarrhea or severity of food-induced anaphylaxis (Incidence of Diarrhea; 8 / 10 vs 9 / 14; following the 7th oral (OVA) challenge of OVA-sensitized WT vs *Mcpt1*^{-/-} mice; n = 10 and 14 mice, respectively.) suggesting that other mucosal MC-derived proteases are likely to drive the SI epithelial barrier dysfunction.

In summary, by employing a murine model of dietary antigen-induced anaphylaxis with intestinal and systemic symptoms, we show that the dietary antigen-induced anaphylaxis is associated with an increase in SI transcellular and paracellular permeability. We show that the altered intestinal permeability and secretory diarrheal phenotype is rapidly induced by MC degranulation and can be inhibited by pharmacological blockade of proteolytic and CFTR-dependent Cl⁻ transport activity.

4. 6. Acknowledgements and Contributions

This work was supported by National Institutes of Health grants DK073553, DK090119, AI138177, and AI112626; Food Allergy Research & Education (FARE); Department of Defense grant W81XWH-15-1-051730; M-FARA; and the Mary H. Weiser Food Allergy Center supported (to S.P.H.)

Amnah Yamani, David Wu, Richard Ahrens and Lisa Waggoner performed experiments. Simon Hogan and Amnah Yamani analyzed the data and wrote the manuscript. Vicky Garcia-Hernandez and Asma Nusrat designed and assisted with some experiments. Taeko Noah, Nicholas W. Lukacs, Catherine Ptaschinski, Asma Nusrat, Charles A. Parkos manuscript revision and discussion. Simon Hogan study supervision and funding acquisition.

Chapter 5 Discussion and Future Directions

Summary for major findings:

- IL-4 enhanced the severity of food-induced anaphylaxis by exacerbation histamine-induced fluid extravasation and hypovolemic shock.
- IL-4 enhancement of murine models of food-induced anaphylaxis (histamine- and passive oral antigen-induced anaphylaxis) is dependent on the VE IL-4R α chain signaling.
- Histamine and IL-4 modulation of VE barrier dysfunction is ABL1 kinase-dependent.
- ABL kinase inhibitor attenuated pre-existing oral antigen-induced anaphylaxis.
- IL-4 enhancement of histamine-induced VE barrier dysfunction was associated with:
 - Enhanced histamine-induced intracellular calcium flux.
 - Modulated the kinetic of histamine-induced Rho GTPase activity.
 - Enhanced histamine-induced ABL1 kinase activity.
 - Dramatically modulate localization and decrease expression of VE-Cadherin upon histamine exposure.
- IL-4 enhanced histamine-induced VE barrier dysfunction through gene transcription, and IL-4-induced VE cell transcription was characterized by genes that possess putative STAT3 binding motif.
- In VE cells, IL-4/STAT3 dysregulates genes involved in barrier integrity and barrier signaling.
- VE STAT3 is required for IL-4 enhancement of histamine-induced VE barrier dysfunction.
- VE STAT3 is required for histamine- and IgE-MC-induced hypovolemic shock and IL-4 enhancement of the VE compartment.

- Oral antigen-challenge induced secretory diarrhea associated with a rapid transcellular and paracellular barrier dysfunction in the epithelium of the small intestine.
- Dietary antigen exposure increased intestinal epithelium CFTR-dependent Cl⁻ secretory response.
- Dietary antigen exposure modified the intestinal epithelium transmembrane proteins in the tight junction (claudin-1,2,3, 5 and junctional adhesion molecule-A) and epithelial cadherins in the adherens junction (E-cadherin) and desmosomes (Desmoglein 2 and desmocollin 2).
- Blockade of chloride channel and proteolytic activity attenuated secretory diarrhea in food-induced anaphylaxis.

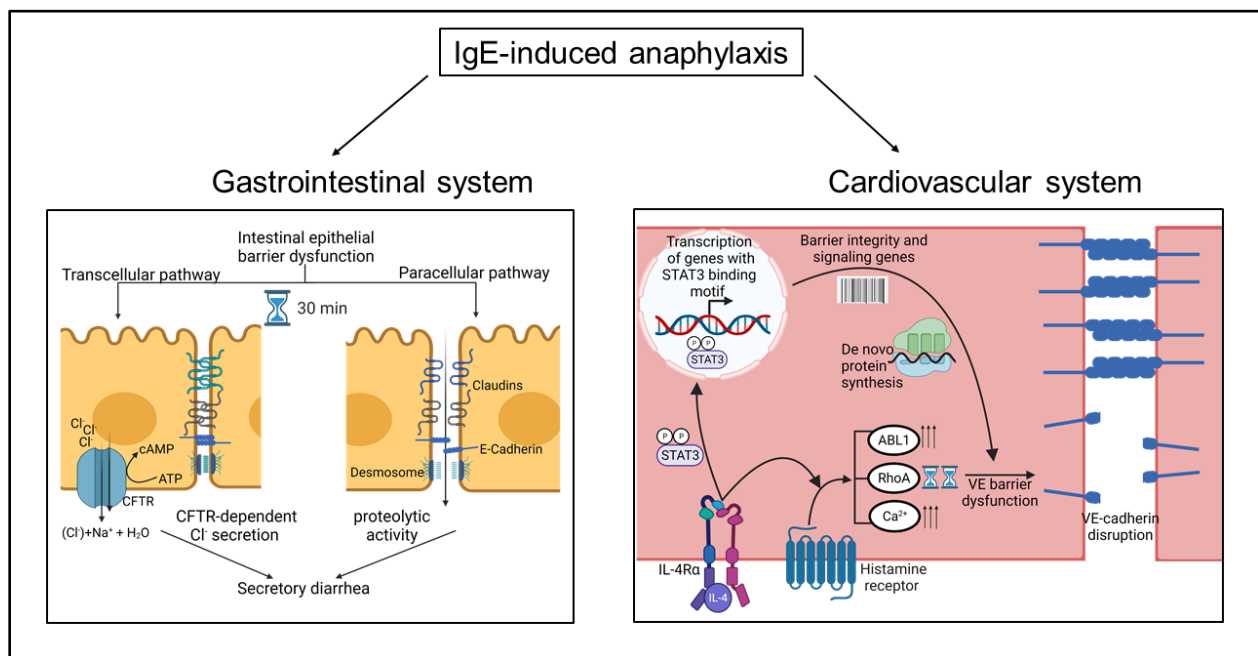


Figure 5.1: Summary for major findings

Chapter 2

In this dissertation, we aimed to understand underlying molecular processes that drive the severe food allergic phenotype. Previous studies have reported a relationship between severe anaphylaxis and hypovolemic shock^{23,30,34}. Experimental evidence from murine studies supports that food and oral antigen-induced anaphylaxis is IgE- mast cell (MC)-dependent^{55,56}. Notably, histamine is the primary MC mediator driving the systemic

symptoms in IgE-MC-mediated anaphylaxis^{55,56}. Experimental studies have revealed a role for IL-4 in the amplification of IgE-mediated anaphylaxis⁷⁵. However, the molecular mechanisms involved in IL-4 exacerbation of histamine-induced VE dysfunction and shock were unknown. Notably, hypovolemic shock is a consequence of VE barrier dysfunction and the movement of fluid from the blood vessels into the interstitial space. Therefore, we hypothesize that IL-4 acts on VE cells to enhance IgE-induced anaphylaxis and hypovolemic shock.

In Chapter 2, we demonstrate a positive correlation between the severity of anaphylaxis and hypovolemic shock. We show that IL-4 directly interacts with VE through the IL-4R α chain to enhance VE responsiveness in the context of histamine and oral-antigen mediated anaphylaxis. Indeed, we show that IL-4 amplifies histamine-induced VE barrier dysfunction.

Importantly, our study indicates that gain-of-function mutations in the IL-4R α chain that enhanced allergic inflammatory also affect the VE compartment. Moreover, this study support assessing the therapeutic potential for targeting VE barrier dysfunction pathways to reduce the severity of anaphylaxis and hypovolemic shock in case of accidental exposure to an allergen or adverse reaction during oral immunotherapy. IL-4R α chain can be target by the Food and Drug Administration (FDA)-approved human monoclonal antibody dupilumab, which is currently used for atopic dermatitis³⁴⁶. Dupilumab also has a significant positive effect in cases of persistent, moderate-to-severe asthma³⁴⁷. Moreover, dupilumab targets the IL-13 receptor since IL-13 signals through binding IL-13R α 1 chain then recruiting the IL-4R α chain. Although this study did not examine IL-13 role in enhancing IgE-mediated anaphylaxis, IL13 has been shown to enhance the murine model of anaphylaxis.

We show that IL-4 activates VE ABL1 kinase function and that pharmacological or genetic inhibition of ABL1 activity ablated histamine-induced VE dysfunction. Histamine and other permeability-inducing reagents directly or indirectly phosphorylate and disrupt VE-Cadherin and other components of AJs leading to gap formation between cells. The mechanism by which histamine induces barrier dysfunction via ABL1 is yet to be determined. ABL1 is required for histamine-induced [Ca²⁺]_i flux, suggesting that ABL1 can be involved in Calmodulin (CaM)-dependent myosin light chain kinase (MLCK)

activation. ABL kinases utilize their SH3 domain to bind several cytoskeleton-remodeling proteins, such as WASF4, WASF2 and ENAH, to drive cytoskeletal rearrangement, thus contributing to cell adhesion. Interestingly the tyrosine phosphatase PTPN6 is also an ABL kinases substrate. In chapter 3, we found that IL-4 dysregulated *PTPN6* in VE Cells; However, the role of PTPN6 and ABL kinases interaction in vascular permeability is unknown.

Notably, histamine can also utilize other kinases such as SRC kinase to phosphorylate the VE-cadherin complex. More studies are needed to understand kinases that might be activated by histamine, for example, Focal adhesion kinase (FAK). VEGF activated-FAK can phosphorylate β -catenin and subsequently induces β -catenin/VE-cadherin dissociation and increased junctional breakdown³⁴⁸. Several small molecule-based FAK tyrosine kinase inhibitors are currently undergoing pre-clinical and clinical testing and can be used as a combination therapy to attenuate histamine-induced anaphylaxis and hypovolemic shock³⁴⁸.

Another major finding of this study is that ABL kinase inhibitor attenuated pre-existing oral antigen-induced anaphylaxis. We used a dose of imatinib that does not affect MC degranulation through targeting c-KIT dependent tyrosine kinase signaling. Imatinib can indeed be used to also reduce MC degranulation to attenuate IgE/MC-mediated reactions. A clinical trial with imatinib on patients with refractor asthma showed reduced airway hyperresponsiveness and MC activation and numbers²⁴³. Imatinib was safe as the number of adverse events did not differ between the treated and placebo groups²⁴³. Notably, murine studies show that ABL kinases are required for the survival of mature B and T cells, but further studies are needed to delineate if imatinib can lower IgE concentration by target lymphocytes³⁴⁹. Therefore, imatinib can be safe and can hit immune and vascular compartments that contribute to anaphylaxis.

During anaphylactic shock, antihistamines medications do not relieve respiratory symptoms (upper or lower airway obstruction) or cardiovascular symptoms (hypotension), therefore they are not lifesaving³⁵⁰. A systematic review of the literature failed to find randomized-controlled trials that support the use of Histamine receptor 1 and 2 antagonists in anaphylaxis^{351,352}. Therefore, targeting histamine receptors during

anaphylaxis has a limited effect and further studies are needed to understand molecular pathways utilized by histamine to induce anaphylaxis.

This study raises important questions that should be addressed in the future including:

- Does IL-4 increase the severity of food-induced anaphylaxis in humans? if so, does blocking the IL-4 receptor alleviate severe symptoms of anaphylaxis?
- What are the sources of IL-4 that enhance anaphylaxis?
- What are the other mediators and factors that can enhance VE compartment to MC mediators leading to severe anaphylaxis?
- Can we find IL-4 induced biomarker to predict susceptibility to severe anaphylaxis?
- What are the molecular pathways of IL-4 + histamine-induced fluid extravasation and cardiovascular collapse leading to severe anaphylaxis?
- What are the kinases activated by histamine to induce hypovolemic shock? Can targeting these kinases attenuate hypovolemic shock?

Chapter 3

Our objective for this chapter was to extend the knowledge and delineate the molecular pathways that underlie IL-4 to enhance histamine-induced VE barrier dysfunction. Therefore, we examined the major signaling pathways driving histamine-induced endothelial barrier disruption (Figure 1.2). We show that IL-4 enhanced histamine-induced calcium flux and modulated the kinetic of histamine-induced Rho GTP activity in the EA.hy926 cell line. Chapter 2 showed that histamine-induced ABL1 kinase activity and IL-4 enhanced this activity. We also examined the kinetic of IL-4 enhancement of histamine-induced barrier VE dysfunction and formulated a module for barrier dysfunction where it is divided into an immediate phase then to a recovery phase. The immediate phase is the acute-initial response where histamine causes loss of barrier integrity and reaches its peak response. The recovery phase is when the VE barrier strength starts to be restored slowly. In this model, histamine causes an acute loss in barrier within ~20 minutes and then barrier strength is restored. We show that IL-4 pretreatment affects both the immediate phase and recovery phase of histamine-induced barrier dysfunction.

Janus kinase (JAK)/ signal transducer and activator of transcription (STAT) pathway is a well-characterized pathway that plays a crucial role in a wide range of cytokine signaling including interferons and interleukins¹³⁰. Following phosphorylation by JAK, STAT dimerizes and translocates to the nucleus to initiate gene transcription¹³⁰. Our findings are novel because we showed that IL-4 phosphorylated STAT3 in VE cells, while this has been shown before in fibroblast and keratinocytes^{131,353}. IL-4 is well known to activate STAT6, which in turn promotes transcription of immunoglobulin genes in B cells¹⁴³. We focused on STAT3 pathways in VE cells. We hypothesized that IL-4 signaling through VE STAT3 activates transcription and modulates the VE barrier function and the outcomes of IgE-MC-induced anaphylaxis. We employed both *in vivo* and *in vitro* RNA sequencing analysis to identify the specific VE transcriptome driven by IL-4/STAT3 that can modulate barrier function (Figure 3.9). These data show that IL-4 differentially expressed genes (DEGs) could affect the immediate phase of barrier dysfunction, such as Thrombospondin that phosphorylation adaptor molecules at adherence junction. IL-4 DEGs can also affect VE barrier recovery response, such as decreasing the phosphatase *PTPN6* that results in longer junctional protein phosphorylation and dissociation.

Excessive epithelial STAT3 activation within cancer cells promotes extracellular matrix (ECM) production and vascularization. Blood vessels that supply tumors have a defective VE-junction that makes vessels leaky with a sustained permeability³⁵⁴. The increase in permeability is because cancerous VE cells branch and sprout excessively leading to a defective endothelial monolayer, gap formation and loss of normal barrier function³⁵⁴. STAT3 is activated in the cancer microenvironment by IL-6 and vascular endothelial growth factor (VEGF)³⁵⁵. IL-6 causes acute vascular leakage by inducing phosphorylation of VE-cadherin via a MAPK/SRC-dependent pathway, and more chronic vascular leakage that depended on STAT3 activation and *de novo* protein synthesis³⁵⁶. Although IL-6 reduced VE-cadherin gene expression, protein expression was not decreased. IL-6 induced STAT3 transcriptome profile that leads to barrier dysfunction is unknown, but it includes increased VEGF-C expression, decreasing ZO-1 and Occludin expression. VEGF signaling via STAT3 drives VE cell barrier dysfunction and vascular leakiness²⁴⁹. VEGF activates various pathways such as PLC γ , eNOS and SRC kinase to induce permeability by changing localization of VE-Cadherin and occludin from cells

boarders³⁵⁷. In our data, we did not see genes known to be dysregulated by IL-6, such as VEGF and occludin, therefore, it is unlikely that the IL-4/STAT3 axis enhances barrier dysfunction indirectly via IL-6. Nevertheless, studies from cancer literature indicate that activation of STAT3 can drive a sustained vascular permeability. This is consistent with our study where we show that the IL-4/STAT3 axis contributes to sustained histamine-induced VE barrier dysfunction.

This study warrants further investigation into the role of non-transcriptional STAT3 activity in the histamine acute vascular response. It is not clear how histamine can induce STAT3^{S727} phosphorylation through its GPCR HR1. Another GPCR that can activate and phosphorylate STAT3 is Sphingosine-1 phosphate receptor 1 (S1P1) by binding JAK2 and SRC kinase³⁵⁸. Moreover, overexpressing of a constitutively activated mutant G α subunit in fibroblasts can activate STAT3 through SRC kinase³⁵⁹. Therefore, a GPCR can act as a docking site for STAT3 to be phosphorylated by kinases.

Through regulating mitochondrial function STAT3 is considered to play a key role in cellular metabolic homeostasis¹⁴⁹. STAT3^{S727} phosphorylation is required for mitochondrial localization, where it binds NADH oxidoreductase and succinate reductase in the electron transport chain¹⁵⁵. Mitochondria STAT3^{S727} is required for optimal ATP levels and oxidation rate¹⁵⁵. Since histamine-induced STAT3^{S727} phosphorylation, we speculate that histamine utilized mitochondrial STAT3 signaling to drive VE barrier dysfunction.

Adherens junction (AJs) are the key regulator of vascular permeability and barrier function⁸⁹. We, therefore, examined the IL-4 effect on VE-Cadherin and found that IL-4 decreases VE-Cadherin protein expression and localization upon histamine exposure. VE junctional complexes also contain tight junctions (TJs). We saw that IL-4 induced the dysregulation of TJ gene expression (e.g., claudin-5, claudin-16, JAM2) *in vitro* using venous cells. Further investigations are needed to understand the role of TJs *in vivo* during histamine and IgE-mediated hypovolemic shock. VE endothelial cell TJs are not as developed as epithelial cells. *In vivo*, the capillaries and postcapillary venules have loosely organized and discontinuous TJs¹⁰⁵. This junctional protein structure serves to maintain plasma protein extravasation, and mediate inflammatory responses¹⁰⁵. The blood-brain and blood-retina barrier contain VE cells with well-developed TJs³⁶⁰.

Consistent with this, Claudin-5 deficient mice showed a selective impairment of the blood-brain barrier for small molecules¹⁰⁷. Moreover, studies using cultured human VE cells showed that Claudin-5 expression and junctional organization control arteriolar-capillary paracellular barriers, whereas venular junctions use VE-cadherin¹⁰⁸.

Findings from this study have several important implications as understanding molecular pathways modulating VE barrier recovery response can help explain what happens during refractory anaphylaxis (defined as a failure of treating symptoms with at least two doses of epinephrine) and a biphasic anaphylaxis reaction. We speculate that failure of treating anaphylaxis can be from failing to trigger VE barrier recovery pathways.

This study raises important questions that should be addressed in the future including:

- How does IL-4 modulate the histamine-induced proteomics profile in VE cells? Does IL-4 enhance the activity of SRC kinases?
- What are the IL-4-mediated molecular pathways to enhanced histamine and MC mediator initial response?
- Can we block severe food-induced anaphylaxis by targeting the VE IL-4/STAT3 signaling axis?
- Can IL-6/STAT3 signaling enhance IgE-mediated anaphylaxis?
- What is the role of vascular TJ proteins in IgE-mediated hypovolemic shock and vascular dysfunction?

Chapter 4

Studies showed a correlation between gastrointestinal (GI) symptoms and the severity of food-induced anaphylaxis in human patients^{21,295}. The knowledge gap is the molecular processes that regulate the GI response. In chapter 5, we examined the sequential molecular processes associated with intestinal dysfunction and secretory diarrhea in mice during acute food-induced anaphylaxis.

Our major finding was that the onset of GI symptoms of dietary antigen-induced anaphylaxis occurred with dietary antigen localized to the small intestine (SI) but not the colon. Secretory diarrhea is the result of excessive secretion and/or impaired absorption of fluid and electrolytes across the intestinal epithelium. So, it is unclear what are the local colonic response leading to secretory diarrhea in the absence of antigen in the colon.

Notably, studies identified a population of SI epithelial cells (termed secretory antigen passages [SAPs]) that rapidly channel food antigens to mucosal MCs in sensitized mice and in human intestinal organoids²⁶⁰. Interestingly, activated MCs localized with neurons in the intestinal mucosa of patients with irritable bowel syndrome (IBS)³⁶¹. Moreover, a significant correlation was found between the proximity of MC to intestinal nerves and the severity of abdominal pain/discomfort³⁶². Indeed, hyperexcitability of the myenteric neurons in the jejunum (a major nerve that controls GI tract motility) has been associated with secretory diarrhea³⁶³. We speculate that activated MC can transfer signals via the enteric nervous system to promote GI symptoms. The MC preformed mediators histamine (through HR 3), serotonin (through 5-HT₃ receptor) and tryptase (through PAR1 receptor) have been shown to excite neurons of the enteric nervous system^{361,364,365}. Synergistic signaling by serotonin and PAF is required for experimental allergic diarrhea⁵⁸. However, it remains unknown if there is a contribution from serotonin and PAF signaling through the enteric nervous system.

In this study, we found that the symptom of diarrhea was associated with an acute increased in SI epithelial CFTR-dependent Cl⁻ secretion. Experimental data show that histamine drives the systemic manifestations of IgE-mediated anaphylaxis in mice^{58,185,301}, however the GI symptoms, while MC and IgE-dependent, are histamine independent (as tested by HR1 and HR2 antagonist)⁵⁸. Antihistamines (antihistamine receptors 1 and 2) also do not relieve gastrointestinal symptoms in humans^{312,350}. A question that remains unresolved is what immune signaling pathways modulate CFTR-dependent Cl⁻ secretion. We predict that this is a phasic response involving CFTR mRNA transcription and activation of CFTR function. The cytokine IL-13 has been shown to stimulate CFTR mRNA expression and secretory diarrhea by upregulation of CFTR and driving Cl⁻ secretion. MCs are unlikely the cellular source of IL-13 driving secretory diarrhea because IL-13 is not secreted immediately from MCs. Group 2 innate lymphoid cells (ILC2s) are a major source of IL-13 that is required for the onset of food allergy, however, it is unknown if IL-13 from ILC2s drives secretory diarrhea³²⁸.

We also show that the symptom of diarrhea was associated with an acute increase in epithelial JP degradation. Indeed several of the preformed MC mediators affect junctional integrity such as chymase (decreased occludin, ZO-1 and E-cadherin

expression), tryptase (induced ECM degradation and ZO-1 redistribution) and MMP (TJ integrity and ECM degradation)³⁶⁶.

Moreover, blockade of Cl⁻ channel and proteolytic activity attenuated the GI symptoms in dietary antigen-induced anaphylaxis. Notably, blocking IL-13 signaling via mAb to IL-4R α , during the effector phase of allergy, did not protect from diarrhea after a high-dose OVA challenge, but it decreased IgE and MC²³⁴. It is unclear if mAb to IL-4R α can block diarrhea with lower doses of allergens, as in the case of the initial phase of oral immunotherapy. In this case, our data suggest that proteolytic activity should also be blocked to see a positive outcome. More studies that identify causative agents of GI symptoms will help to find adjunctive and targeted therapies to attenuate GI symptoms during food-induced reactions.

In this chapter, our focus for GI symptoms was secretory diarrhea since we are using murine models. Interestingly, in humans with peanut-induced anaphylaxis, administration of intravenous fluids was associated with faster resolution of gastrointestinal symptoms (cramping and pain) and cardiovascular parameters²³. These data suggest that hypovolemic shock where fluid is redistributed is connected to the intestinal response. It will be interesting to study local VE cells in the intestine to examine their contribution to the response.

This study raises important questions that should be addressed in the future including:

- What are the individual contributions of MC mediators to intestinal epithelial barrier dysfunction?
- What are the local colonic responses that lead to secretory diarrhea in the absence of antigen in the colon?
- Can intestinal VE cells contribute to the severity of food-induced anaphylaxis?
- Can IL-13/IL-4 enhance GI symptoms during food-induced anaphylaxis?

Final Conclusions:

Previous studies have established that Food Allergy is associated with heightened systemic IL-4 and histamine levels²⁰⁴. Furthermore, IL-4 and histamine are associated with severe food allergic reactions²⁰⁴. However, the gap in knowledge is (i) the

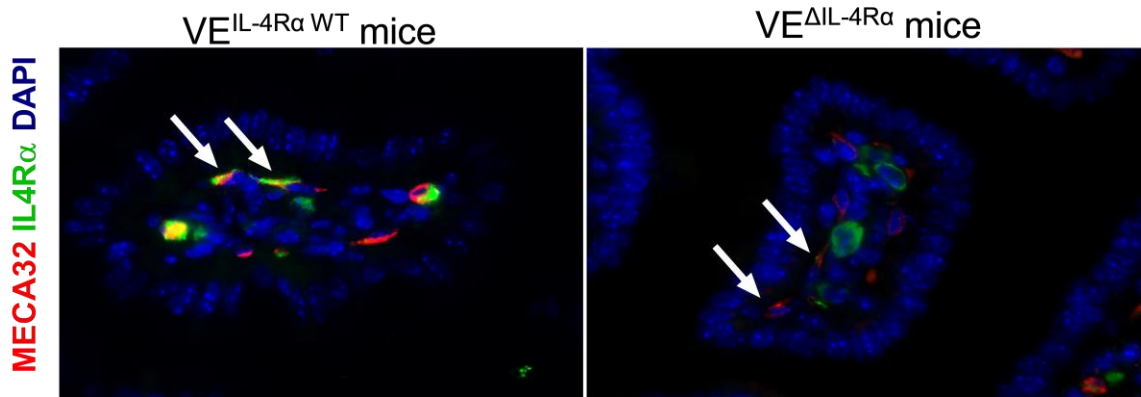
underlying molecular mechanisms involved in IL-4 and histamine induction of systemic and intestinal manifestations of severe IgE-mediated reactions. Based upon the findings described in this dissertation, we conclude that systemic IL-4 stimulates transcription with the vascular endothelium compartment via an IL-4/IL-4R α chain-dependent mechanism. Activation of the IL-4/IL-4R α chain leads to maximal activation and phosphorylation (Tyrosine 705 and Serine 727) of STAT3 which in turn upregulates barrier integrity and barrier signaling gene expression. Subsequent food allergen exposure leads to activation of the IgE-Fc ϵ RI-pathway on MC and release of preformed MC mediators including histamine. MC-derived histamine activates the IL-4-primed VE cells which stimulate intracellular signaling cascades including intracellular Ca²⁺ and Rho GTPase activation, which leads to degradation of VE-cadherin and increased paracellular permeability. The increased paracellular permeability permits vascular leak and movement of fluid from the peripheral blood into interstitial space leading to increased hemoconcentration and hypovolemic shock.

We also conclude that MC mediators including cytokines and proteases stimulate i) an increase in the small intestine intestinal epithelial CFTR-dependent Cl⁻ transport activity and 2) degradation of the epithelial intercellular junction proteins: claudin-1, 2, 3 and 5, E-cadherin and desmosomal cadherins. The increased basolateral-to-apical chloride movement and loss of the epithelial intercellular barrier proteins leads to increased paracellular permeability and accumulation of fluid in the small intestine lumen known as secretory diarrhea. The secretory diarrhea response is protease- and CFTR-dependent Cl⁻ transport-dependent.

These studies have identified key roles for IL-4 and histamine in the systemic symptoms and cytokines and MC proteases in the intestinal symptoms of food-induced anaphylaxis.

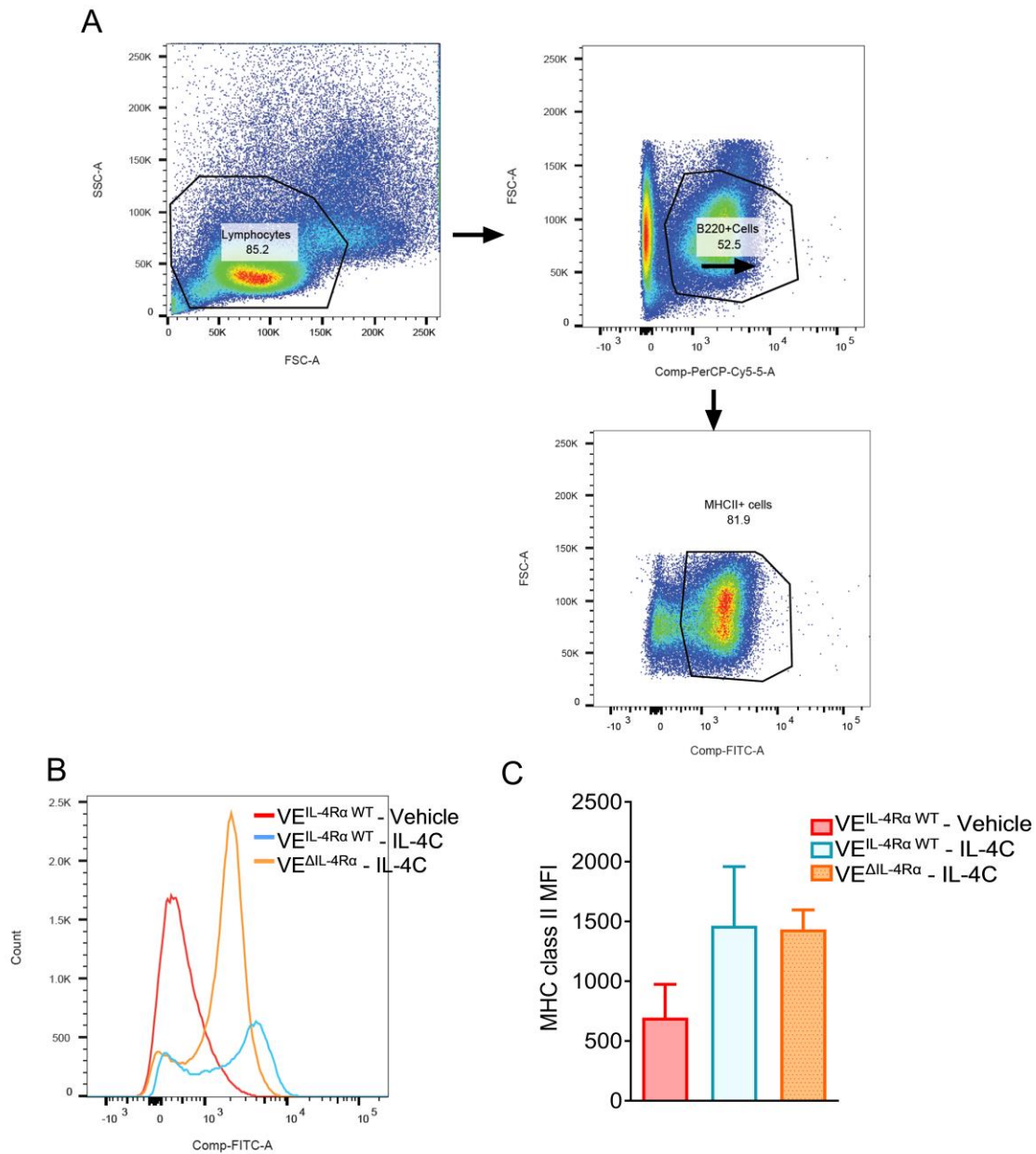
Appendices

Appendix 1: Chapter 2 Supplemental Figures



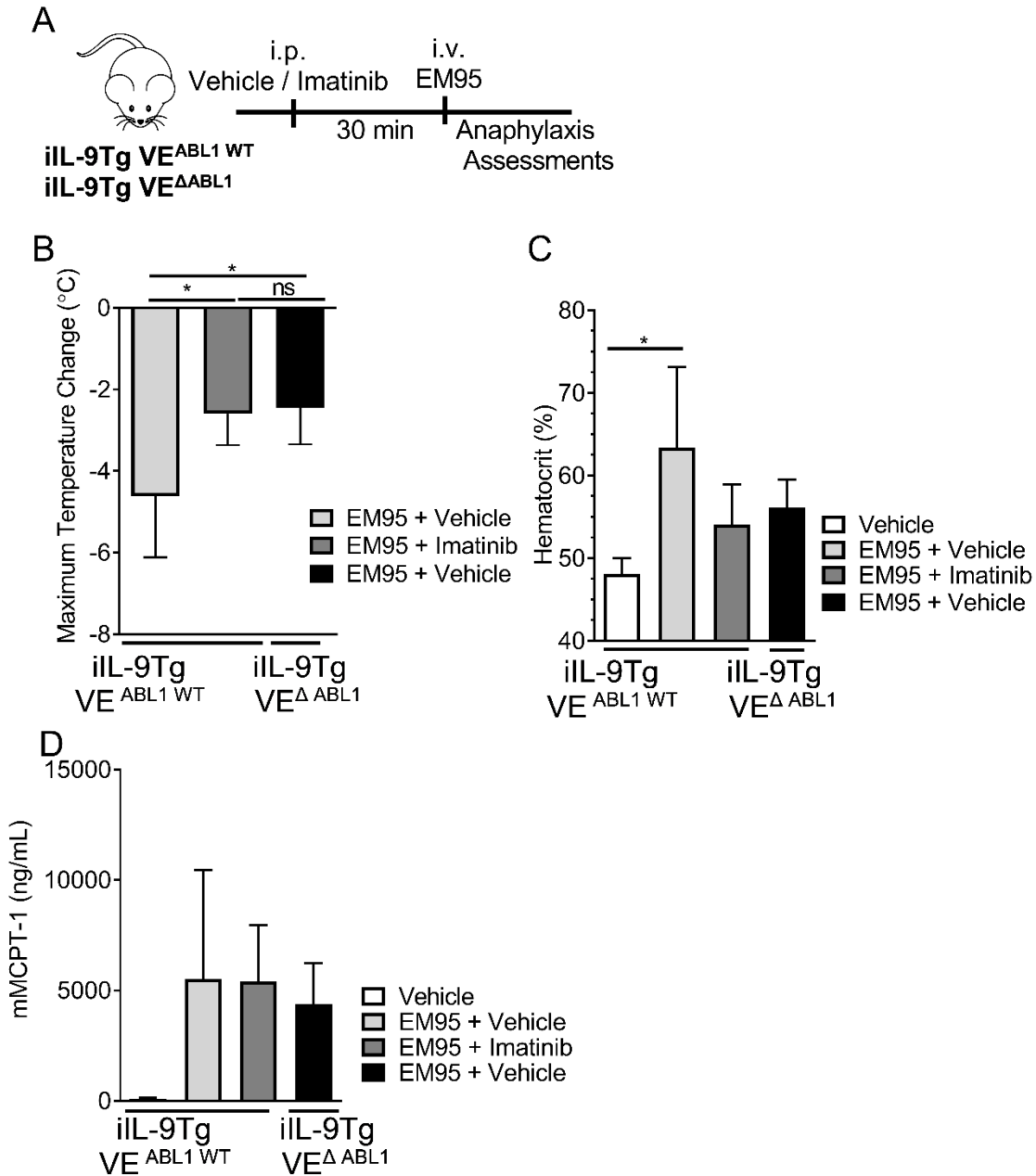
Supplementary Figure 2- 1: VE^{ΔIL-4Rα} mice lack IL-4Rα expression on VE cells.

Immunofluorescence images of jejunum from VE^{IL-4Rα} WT and VE^{ΔIL-4Rα} mice. Anti-panendothelial cell antigen staining with anti-rat PLVAP mAb (MECA32; red) identifies endothelial cells, anti-IL-4Rα staining (shown in green) was performed with anti-IL-4Rα (no. sc-28361; Santa Cruz Biotechnology), and 4'-6-diamidino-2-phenylindole (DAPI) staining is shown in blue. White arrows show the presence of IL-4Rα chain staining on endothelial cells of VE^{IL-4Rα} WT mice and its absence on endothelial cells of VE^{ΔIL-4Rα} mice.



Supplementary Figure 2- 2: IL-4C is biologically active in VE^{ΔIL-4Rα} mice.

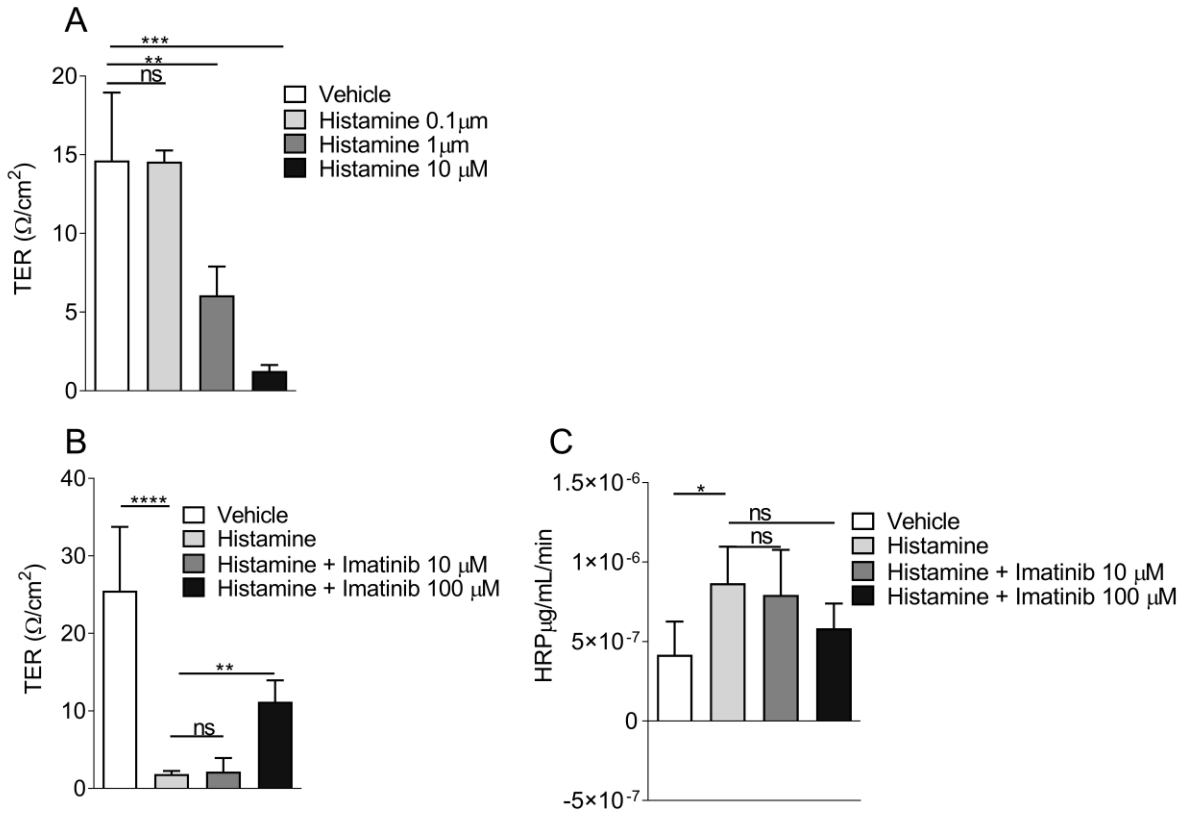
A, Representative flow plots show gating of the B220/ MHC class II population from lymphocytes. B, Histogram. C, Median fluorescence intensity (MFI) of fluorescein isothiocyanate (FITC) on peridinin-chlorophyll-protein complex (PerCP)/Cy5.51 cells determined by using flow cytometry. VE^{IL-4Rα}WT and VE^{ΔIL-4Rα} mice were injected intravenously (i.v.) with vehicle or IL-4C (1 mg of IL-4 plus 5 mg of anti-IL-4 mAb). Mice were killed the next day, and spleen cells were stained with anti-mouse MHC class II (I-A), FITC, and anti-mouse/human CD45R/B220 PerCP/Cy5.51 antibodies. Data are represented as means ± SDs (n = 2 mice per group from n = 1 experiment).



Supplementary Figure 2- 3: Effect of the VE IL-4R α chain on hypovolemic shock is MC and immunoglobulin independent.

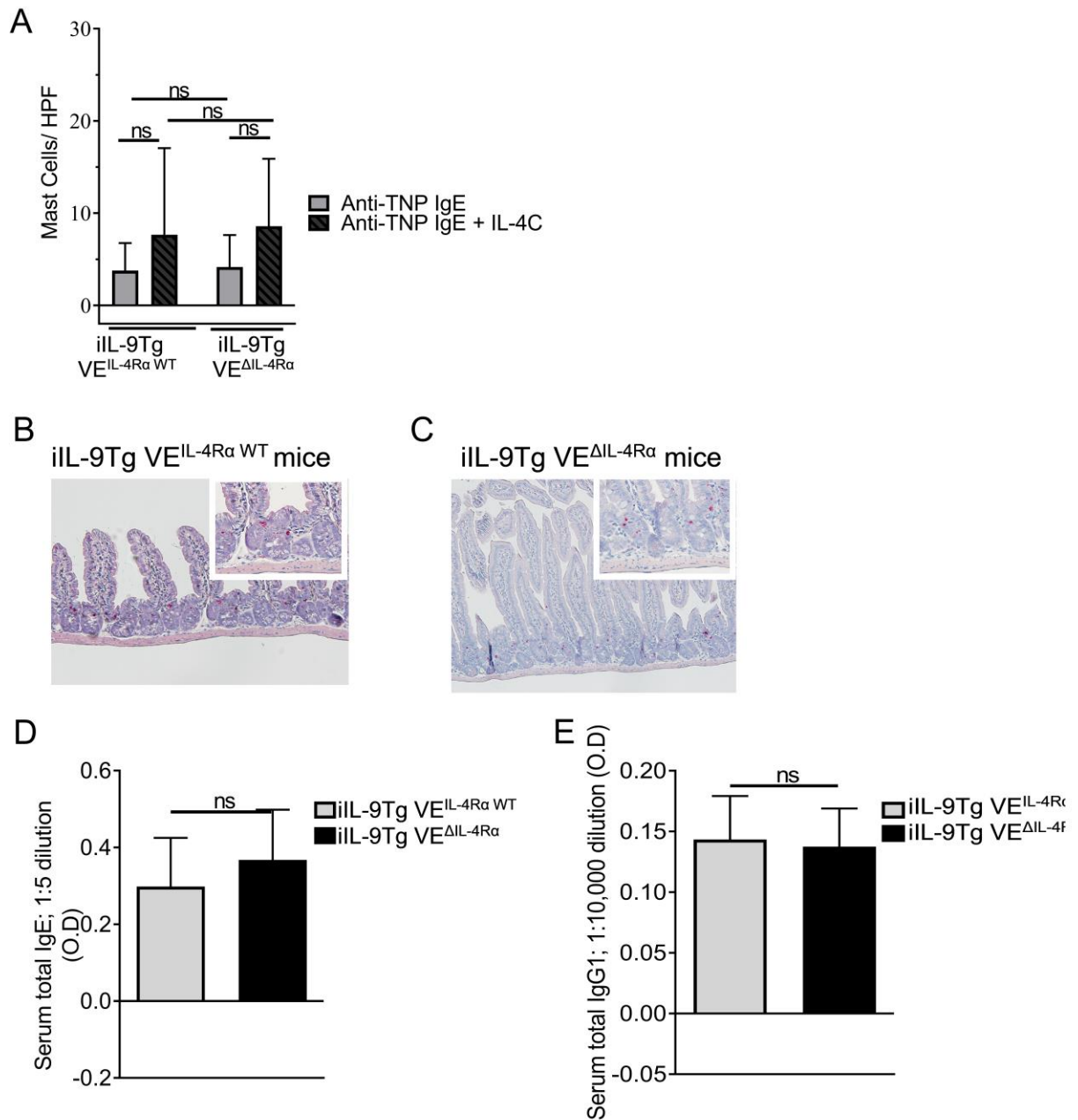
A-D, Intestinal MC counts (Fig E3, A), photomicrograph of chloroacetate esterase–stained intestinal section of iIL-9Tg VE^{IL-4R α WT} (Fig E3, B) and iIL-9Tg VE^{ΔIL-4R α} (Fig E3, C) mice, and total serum IgE levels (Fig E3, D). E, Total serum IgG1 levels of iIL-9Tg VE^{IL-4R α WT} and iIL-9Tg VE^{ΔIL-4R α} mice after treatment with anti-TNP IgE and IL-4C or vehicle and with TNP-OVA. Serum was collected from untreated iIL-9Tg VE^{IL-4R α WT} and iIL-9Tg VE^{ΔIL-4R α} mice. Data are represented as means \pm SDs (n = 4-5 mice per group [Fig E3, A, D, and E]). Photomicrograph = \times 10 magnification;

inset =X 40 magnification (Fig E3, B and C). ns, P > .05.



Supplementary Figure 2- 4: Histamine-induced VE permeability in EA.hy926 cells is inhibited by imatinib.

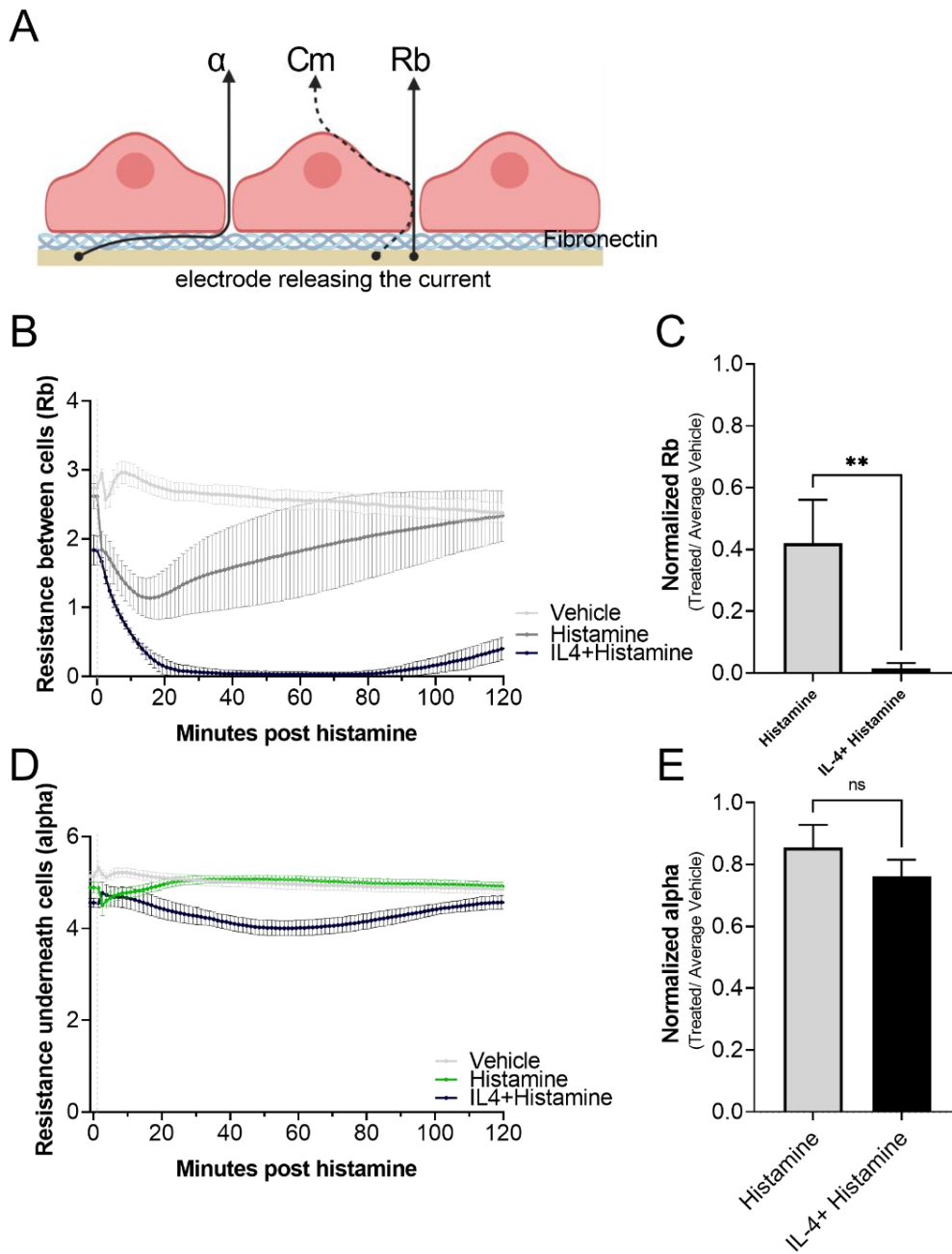
A, Confluent monolayers of cell line EA.hy296 cells (EVOM >100 ohms) were mounted in Ussing chambers and stimulated with different doses of histamine (0.1-10 $\mu\text{mol}/\text{L}$) for 30 minutes, and TER was determined by using Ohms law. B and C, EA.hy296 cells were pretreated with a different dose of imatinib (0-100 $\mu\text{mol}/\text{L}$) for 3 hours, mounted in Ussing chambers and treated with histamine (100 $\mu\text{mol}/\text{L}$ for 30 minutes), and TER (Fig E4, B) and HRP flux (Fig E4, C) were determined. Data are represented as means \pm SDs (n = 3 wells per group). *P < .05, **P < .01, ***P < .0001, and ****P < .0001. ns, P > .05.



Supplementary Figure 2- 5: Hypovolemic shock induced by EM95 is dependent on VE ABL1.

Experimental regimen (A), maximum temperature change (B), hematocrit percentage (C), and mMCPT-1 level (D) in iIL-9Tg VE^{ΔABL1} (iIL-9^{WT} Tie2^{cre} ABL1^{fl/fl}) and iIL-9^{Tg} VE^{ABL1 WT} (iIL-9^{WT} Tie2^{WT} Abl1^{fl/fl}; used as a WT control) mice treated intraperitoneally (i.p.) with vehicle or imatinib (1.25 mg/mice) 30 minutes before EM95 (2 mg/200 mL administered intravenously [i.v.]). iIL-9Tg VE^{ΔABL1} mice received EM95 only. Data are represented as means ± SDs (n = 4-6 mice per group from n = 3 experiments). *P < .05. ns, P > .05.

Appendix 2: Chapter 3 Supplemental Figures and Table



Supplementary Figure 3- 1:IL-4 and histamine modulated the resistance between the cells and not the resistance underneath the cells in VE cells

A diagram depicting type of the calculated resistance generated by ECIS® Z-Theta system. Resistance between cells (Rb) and the Resistance beneath the cells (alpha) Membrane capacitance (Cm).

B Rb within 2 hours of histamine treatment

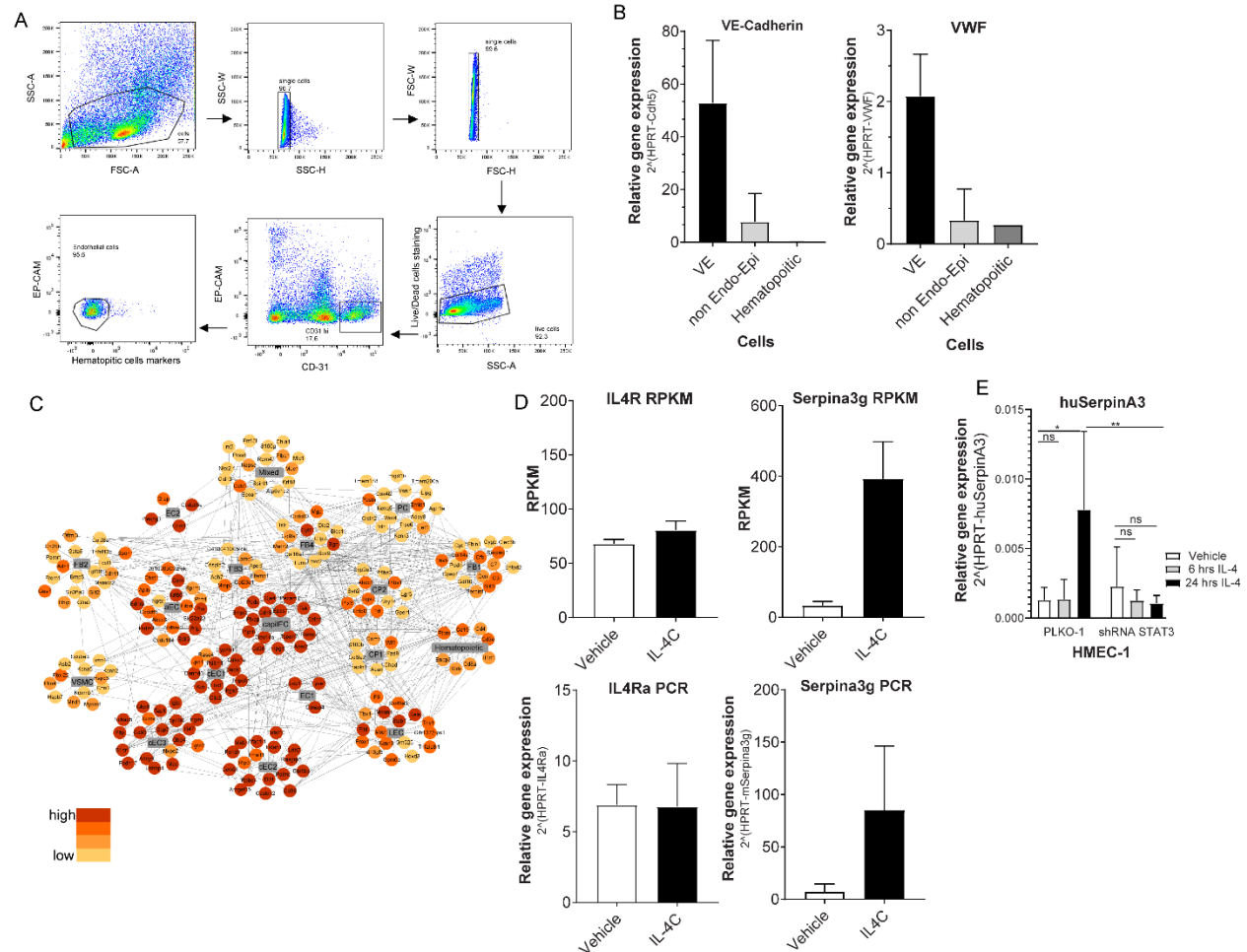
C maximum change in Rb normalized to vehicle treated cells

D alpha within 2 hours of histamine treatment

E maximum change in alpha normalized to vehicle treated cells

post-confluent EA.hy926 cells monolayer were pre-treated with Vehicle (PBS) or IL-4 (100 ng / mL; 24 hours) followed by removal of IL-4 then treatment with Vehicle (PBS) or histamine (100 μM; 2 hours) in ECIS® Z-Theta system.

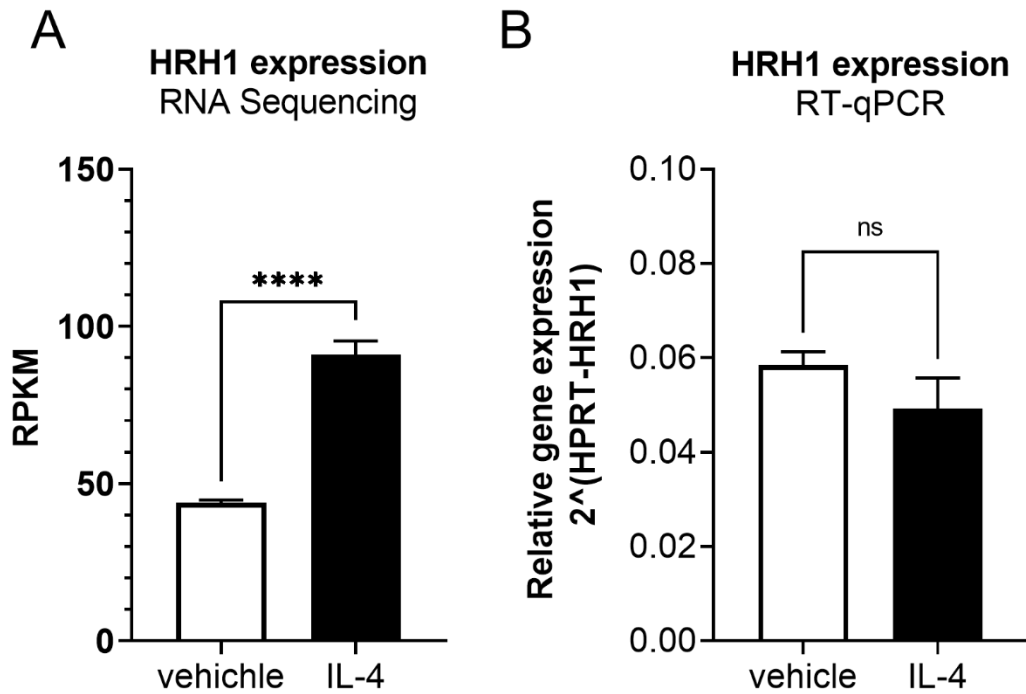
Data are represented as means ± SD; n=3-4 per group from a representative experiment that was done in triplicate. ****P < 0.0001, ***P < 0.001, **P < 0.01, *P < 0.05, ns > 0.05.



Supplementary Figure 3- 2: Sorted EP-CAM – CD31 hi Hematopoietic markers – cells show a distinct transcriptome profiles for endothelial cells.

A Gating strategy to identify endothelial cells from mice lungs: Forward and side scatter (FSC and SSC) gating on area (A), height (H), and width (W) excluded debris and non-single cells. A live/dead staining excluded dead cells. VE cells were identified as Ep-CAM- (CD326) and CD31 high. hematopoietic lineage markers - (CD45.2, Ly-6G, CD11c, ST2, CD11b, CD4, CD8 and B220). B Relative gene expression of VE-Cadherin genes and Von willebrand factor gene (VWF) normalized to the housekeeping gene HPRT: Endothelial Cells were collected from an independent experiment following FACS sorting, and RNA was used to generate cDNA for quantities PCR. C Gene expression data from mice lung sorted EC were mapped to the top markers from public data Single-cell RNA sequencing of mouse lung vascular and vessel-associated cell types. Highly expressed genes are shown in dark red color. aEC: arterial endothelial cells. CapillEC: capillary endothelial cells. EC1-2: endothelial cells type 1-2. cEC1-3 continuous endothelial cells. LEC: lymphatic endothelial cells.

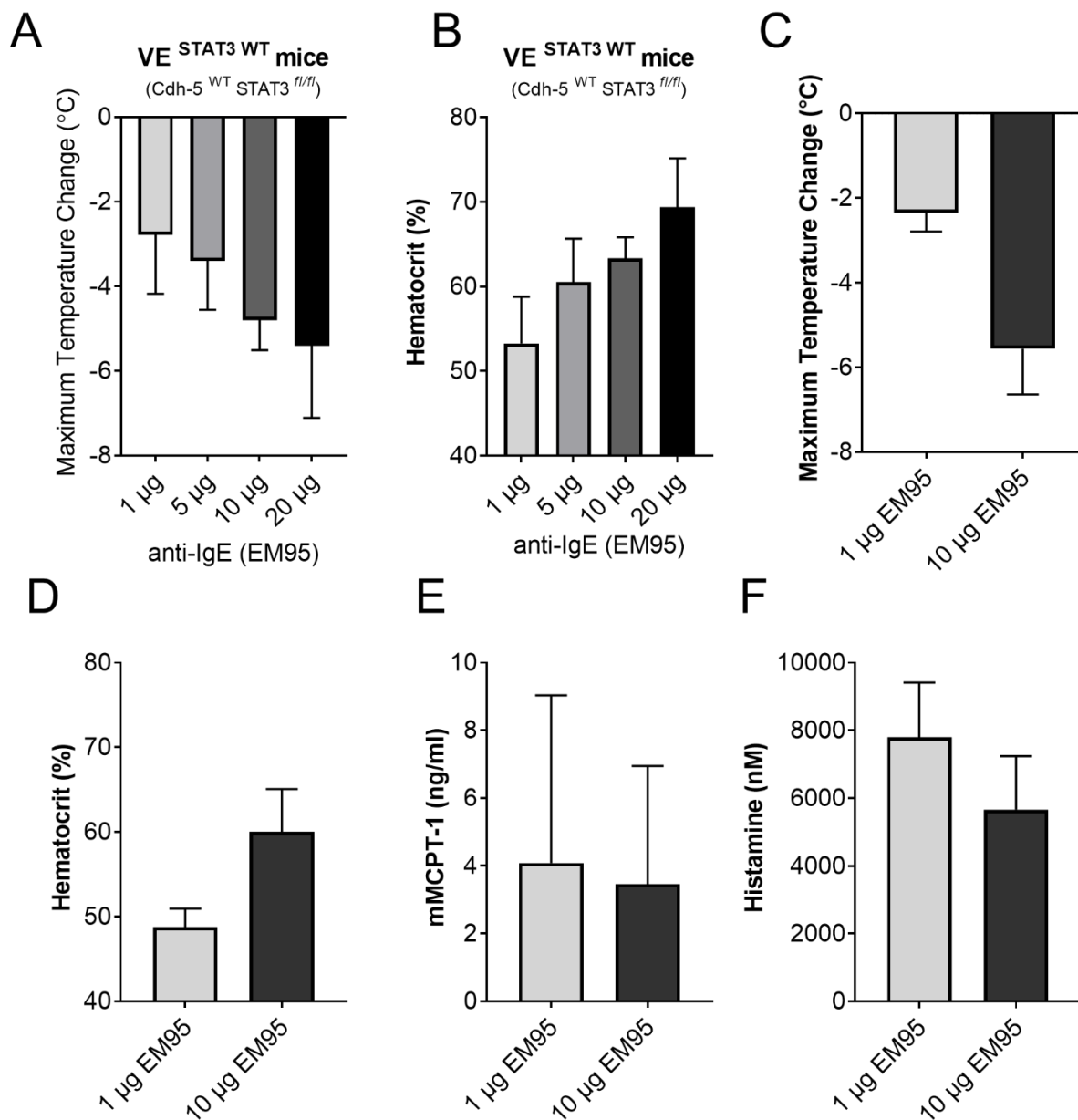
D Aliquot of RNA used from RNA sequencing was used separately to examine expression of IL-4ra, serpin3g, serpin3f and serpin3n by PCR (Top row). RPKM generated from RNA sequencing (Lower row). Data are represented as means \pm SD; n=3-4 (B), n=3 per group (D) from one experiment. *P < .05, **P < .01, and ****P < .0001. ns, P > .05. Relative gene expression of hu SerpinA3 genes normalized to the housekeeping gene HPRT following IL-4 treatment (100 ng / mL; 6-24 hours) from HUVEC (A), EA.hy926 (B), HMEC-1 WT (C). HMEC-1 Cells transduced with lentiviral particles carrying empty vector (PLKO-1; WT control) or lentiviral particles carrying STAT3 shRNA (D). Data are represented as means \pm SD; n=6-8 from duplicate experiments (A); n=6-9 from triplicate experiments (B); n=4-5 from one representative experiment (C-D); *P < .05, **P < .01, and ****P < .0001. ns, P > .05.



Supplementary Figure 3- 3: Histamine 1 receptor expression in EA.hy926 cells following IL-4 treatment.

A HRH1 genes expression express as RPKM, measured by RNA sequencing from figure 3.6.

B Relative gene expression of HRH1 genes normalized to the housekeeping gene HPRT. EA.hy926 WT cell were treated with IL-4 (100 ng / mL; 24 hours), then RNA was collected and isolated for RT-qPCR. n=3 wells per group (B). Data are represented as means \pm SD; n=3; *P < .05, **P < .01, and ****P < .0001. ns, P > .05.



Supplementary Figure 3- 4: Anti-IgE challenge in C57/B6 mice increase serum histamine levels.

A Maximum temperature change and B hematocrit from VE^{STAT3 WT} mice after intravenous (i.v.) injection with 1-20 µg / mice of anti-IgE mAb clone EM95

C Maximum temperature change, D hematocrit Percentage, E Serum mMCP1-1 and F Serum Histamine from C57/B6 mice after intravenous (i.v.) injection with 1 µg or 10 µg anti IgE mAb clone EM95. Serum was taken for histamine levels 10 - 15 minutes post anti-IgE mAb injections.

Data are represented as means ± SD; n=2-6 mice pre group (A-B), n=4-6 (C-E), n= 2-4 (F) from duplicates experiments. *P < .05, **P < .01, and ****P < .0001. ns, P > .05.

Normalized_RPKM

Ensembl ID	Gene Symbol	Liquin Markers	Veh_1	Veh_2	Veh_3	IL4_1	IL4_2	IL4_3
ENSMUSG00000025582	Nptx1	aEC	4.1	4.4	5.1	3.9	4.2	5.0
ENSMUSG00000029875	Ccdc184	aEC	4.5	7.2	5.4	6.8	4.5	5.2
ENSMUSG00000040152	Thbs1	CP2	8.3	7.9	8.5	10.9	10.6	11.2
ENSMUSG00000046215	Rprml	aEC	5.8	7.3	6.5	6.0	5.4	6.7
ENSMUSG00000079654	Prrt4	aEC	6.5	7.4	6.2	7.4	6.2	6.8
ENSMUSG00000079671	2610203C22Rik	aEC	7.6	8.1	7.4	8.1	7.4	7.7
ENSMUSG00000074971	Fibin	aEC	7.5	9.2	6.3	8.3	6.5	7.6
ENSMUSG00000027221	Chst1	aEC	7.6	9.3	6.9	8.7	6.8	8.0
ENSMUSG00000038903	Ccdc68	aEC	9.5	9.9	9.0	9.8	8.9	9.3
ENSMUSG00000079363	Gbp4	cEC3	13.0	12.7	13.8	14.7	14.8	15.1
ENSMUSG00000078853	Igtp	cEC3	10.3	10.0	11.5	11.9	12.3	12.5
ENSMUSG00000020865	Abcc3	aEC	9.2	10.3	9.1	9.8	8.4	9.0
ENSMUSG00000102697	Pcdhac2	aEC	9.3	10.9	8.6	10.3	9.1	10.1
ENSMUSG00000078921	Tgtp2	cEC3	9.3	8.9	9.9	10.6	10.7	11.1
ENSMUSG00000034488	Edil3	aEC	10.1	11.2	10.0	10.9	9.8	10.2
ENSMUSG00000037185	Krt80	aEC	10.2	11.5	10.0	10.9	9.7	10.2
ENSMUSG00000037010	Apln	aEC	9.1	12.1	8.7	10.9	8.4	9.5
ENSMUSG00000038267	Slc22a23	aEC	10.4	12.2	10.0	11.8	10.2	10.9
ENSMUSG00000038151	Prdm1	aEC	10.8	12.1	10.4	11.1	10.2	10.7
ENSMUSG00000053198	Prx	aEC	11.6	12.6	11.2	12.3	11.8	11.5
ENSMUSG00000022122	Ednrb	aEC	11.4	13.3	10.6	12.5	10.5	11.9
ENSMUSG00000000805	Car4	aEC	12.2	13.2	12.2	13.4	12.5	13.1
ENSMUSG00000050234	Gja4	capilEC	11.5	11.4	11.5	10.8	10.9	11.2
ENSMUSG00000034845	Plvap	capilEC	12.8	12.9	13.2	12.9	12.8	13.3
ENSMUSG00000046879	Irgm1	cEC3	10.0	9.9	10.6	11.3	11.2	11.4
ENSMUSG00000001240	Ramp2	capilEC	12.8	13.2	13.2	13.3	13.0	13.1
ENSMUSG00000058254	Tspan7	capilEC	14.2	14.5	14.5	14.3	14.0	14.4
ENSMUSG00000038007	Acer2	capilEC	14.6	14.3	14.6	14.8	14.8	14.9
ENSMUSG00000040253	Gbp7	cEC3	12.2	11.9	12.9	13.3	13.4	13.7
ENSMUSG00000031613	Hpgd	capilEC	14.5	14.9	14.2	14.2	13.3	14.0
ENSMUSG00000045930	Clec14a	capilEC	14.6	14.6	14.6	14.0	14.0	14.4
ENSMUSG00000025608	Podxl	capilEC	15.1	15.1	15.0	14.9	14.7	14.9
ENSMUSG00000020717	Pecam1	capilEC	15.1	15.2	15.0	15.4	15.2	15.6
ENSMUSG00000029298	Gbp9	cEC3	12.8	12.6	13.0	13.7	13.6	14.0
ENSMUSG00000006386	Tek	capilEC	15.5	14.9	15.4	14.8	14.9	15.2
ENSMUSG00000002944	Cd36	capilEC	16.1	16.1	16.0	16.3	15.9	16.8
ENSMUSG00000031871	Cdh5	capilEC	16.2	16.4	16.1	16.1	15.9	16.2
ENSMUSG00000067336	Bmpr2	capilEC	16.3	16.1	16.2	15.9	16.2	16.2

ENSMUSG00000024140	Epas1	capilEC	16.9	17.1	16.8	17.0	16.6	17.0
ENSMUSG00000059588	Calcl	capilEC	17.2	17.3	17.1	17.1	16.9	17.4
ENSMUSG00000020154	Ptprb	capilEC	17.4	17.0	17.3	16.9	17.3	17.2
ENSMUSG00000004952	Rasa4	cEC1	6.8	6.1	6.6	7.1	6.5	6.6
ENSMUSG00000020407	Upp1	cEC1	9.6	9.6	9.6	9.5	9.0	9.4
ENSMUSG00000030787	Lyve1	EC1	13.3	13.7	13.3	14.6	14.4	14.1
ENSMUSG00000055639	Dach1	cEC1	10.5	11.0	10.1	11.0	10.5	11.0
ENSMUSG00000055044	Pdlim1	cEC1	10.6	10.8	10.7	10.8	10.5	11.0
ENSMUSG00000003500	Impdh1	cEC1	11.1	11.7	11.3	11.3	10.9	11.0
ENSMUSG00000042812	Foxf1	cEC1	11.4	11.9	11.5	11.9	11.9	11.8
ENSMUSG00000001507	Itga3	cEC1	11.9	12.8	11.9	12.4	12.3	12.2
ENSMUSG00000036661	Dennd3	cEC1	12.4	11.9	12.4	12.4	12.8	12.4
ENSMUSG00000023067	Cdkn1a	cEC1	13.2	13.0	12.2	13.8	13.6	12.3
ENSMUSG00000028713	Cyp4b1	cEC1	13.0	13.8	12.9	13.3	12.6	12.9
ENSMUSG00000062960	Kdr	cEC1	14.1	14.9	13.6	14.4	13.5	14.0
ENSMUSG00000023959	Clic5	cEC1	14.4	14.5	14.1	14.6	14.1	14.4
ENSMUSG00000028347	Tmeff1	cEC2	9.8	9.8	9.9	9.9	10.0	10.0
ENSMUSG00000066319	Rtp3	cEC2	9.9	9.9	10.0	10.0	10.4	10.2
ENSMUSG00000027474	Ccm2l	cEC2	11.0	10.8	11.0	10.9	11.0	11.0
ENSMUSG00000028194	Ddah1	cEC2	10.9	11.8	10.7	11.3	10.6	10.7
ENSMUSG00000027314	Dll4	cEC2	11.5	11.5	11.5	11.1	11.2	11.6
ENSMUSG00000031824	6430548M 08Rik	cEC2	11.9	11.6	11.9	11.7	12.3	12.2
ENSMUSG00000029084	Cd38	cEC2	11.8	12.5	12.2	12.6	12.4	12.6
ENSMUSG00000034471	Caskin2	cEC2	12.4	12.4	12.3	12.5	12.6	12.6
ENSMUSG00000033377	Palmd	cEC2	12.7	12.4	12.5	12.2	12.3	12.7
ENSMUSG00000022579	Gpihbp1	cEC2	12.4	12.5	12.7	12.3	12.2	12.3
ENSMUSG00000032125	Robo4	cEC2	12.9	12.9	12.8	12.8	12.9	12.8
ENSMUSG00000000266	Mid2	cEC2	12.9	13.1	12.8	12.9	12.8	12.8
ENSMUSG00000033032	Afap1l1	cEC2	13.2	13.1	12.8	13.2	13.4	13.1
ENSMUSG00000052921	Arhgef15	cEC2	12.9	13.3	13.1	13.4	13.2	13.2
ENSMUSG00000097336	Fendrr	cEC2	14.3	13.2	14.0	14.0	14.6	13.8
ENSMUSG00000039706	Ldb2	cEC2	14.1	13.8	14.1	13.6	13.6	13.8
ENSMUSG00000071042	Rasgrp3	cEC2	14.1	14.1	14.0	14.3	14.1	14.3
ENSMUSG00000039304	Tnfsf10	cEC2	14.2	14.1	14.3	13.7	13.8	14.3
ENSMUSG00000032028	Nxpe2	cEC3	6.5	6.7	6.7	5.3	6.5	5.7
ENSMUSG00000027579	Srms	cEC3	7.3	7.8	7.6	7.3	7.6	7.6
ENSMUSG00000037321	Tap1	cEC3	10.2	9.8	11.0	11.2	11.3	11.5
ENSMUSG00000026222	Sp100	cEC3	11.4	11.0	11.4	11.7	11.6	11.6
ENSMUSG00000078920	Ifi47	cEC3	11.3	11.0	12.1	12.2	12.4	12.5
ENSMUSG00000022220	Adcy4	cEC3	12.7	12.4	12.7	12.6	13.0	12.8

ENSMUSG00000034911	Ushbp1	cEC3	13.0	12.8	13.1	13.0	13.1	12.9
ENSMUSG00000035566	Pcdh17	cEC3	13.1	13.4	12.9	13.1	12.4	13.3
ENSMUSG00000031775	Plip	aEC	10.6	10.7	10.5	10.1	9.9	10.0
ENSMUSG00000017754	Pltp	cEC3	13.4	13.3	13.3	13.1	13.2	13.3
ENSMUSG00000071856	Mcc	cEC3	13.3	13.6	13.3	13.4	12.9	13.5
ENSMUSG00000049690	Nckap5	cEC3	14.1	13.9	13.8	14.3	14.4	14.2
ENSMUSG00000045092	S1pr1	cEC3	14.4	14.5	14.5	14.6	14.3	14.6
ENSMUSG00000027435	Cd93	cEC3	16.4	16.4	16.4	16.4	16.3	16.4
ENSMUSG00000049551	Fzd9	CP1	3.5	2.5	3.2	3.1	3.0	3.8
ENSMUSG00000028626	Col9a2	CP1	2.8	4.0	3.1	4.5	3.4	4.1
ENSMUSG00000030607	Acan	CP1	4.3	3.6	2.7	2.9	2.7	2.7
ENSMUSG00000021613	Hapln1	CP1	3.1	4.8	2.5	4.2	3.6	3.5
ENSMUSG00000033208	S100b	CP1	4.5	3.2	3.4	4.0	4.7	4.8
ENSMUSG00000039084	Chad	CP1	5.2	4.5	4.8	3.7	4.1	5.2
ENSMUSG00000031849	Comp	CP1	5.5	5.0	5.1	6.2	5.5	5.0
ENSMUSG00000020218	Wif1	CP1	8.9	9.5	8.2	8.5	7.7	8.1
ENSMUSG00000042793	Lgr6	CP2	3.6	2.9	3.2	2.0	3.8	3.5
ENSMUSG00000025479	Cyp2e1	CP2	3.8	3.2	3.9	2.7	3.0	4.3
ENSMUSG00000051048	P4ha3	CP2	4.6	4.7	3.6	5.3	5.3	4.6
ENSMUSG00000053647	Gper1	CP2	4.5	5.0	4.1	5.2	5.6	5.1
ENSMUSG00000009394	Syn2	CP2	5.2	5.3	4.2	5.4	5.2	5.2
ENSMUSG00000036381	P2ry14	CP2	4.8	2.9	6.1	2.5	6.3	4.3
ENSMUSG00000027832	Ptx3	CP2	7.6	7.0	7.9	5.8	6.9	7.3
ENSMUSG00000037692	Ahdc1	CP2	7.4	7.8	7.3	7.6	7.9	7.7
ENSMUSG00000032554	Trf	CP2	8.4	8.2	8.4	7.4	8.5	7.0
ENSMUSG00000045312	Lhfpl2	CP2	8.6	9.3	8.1	9.3	8.3	8.8
ENSMUSG00000026360	Rgs2	CP2	9.1	8.4	10.0	8.1	9.8	7.8
ENSMUSG00000021998	Lcp1	EC1	11.9	12.2	12.4	12.0	12.5	11.8
ENSMUSG00000054435	Gimap4	EC1	12.1	12.6	11.8	12.6	11.7	12.5
ENSMUSG00000004837	Grap	EC2	9.2	10.0	9.8	10.1	10.0	9.8
ENSMUSG00000032878	Ccdc85a	EC2	12.1	11.9	11.9	11.9	11.9	12.1
ENSMUSG00000040624	Plekhg1	EC2	12.1	12.0	11.8	11.9	11.9	12.2
ENSMUSG00000024074	Crim1	EC2	12.1	12.0	12.4	11.7	12.2	12.4
ENSMUSG00000006369	Fbln1	FB1	2.3	3.4	2.9	3.4	4.2	3.5
ENSMUSG00000025784	Clec3b	FB1	3.6	3.8	3.2	3.1	3.2	3.3
ENSMUSG00000028600	Podn	FB1	2.5	4.7	3.5	2.7	4.2	2.4
ENSMUSG00000015085	Entpd2	FB1	2.0	5.1	2.9	4.3	2.7	2.7
ENSMUSG00000021943	Gdf10	FB1	3.5	5.2	3.6	3.6	3.6	3.8
ENSMUSG00000019278	Dpep1	FB1	4.7	4.4	5.1	4.0	4.3	3.1
ENSMUSG00000026574	Dpt	FB1	3.9	5.8	4.8	5.1	6.0	5.1
ENSMUSG00000079105	C7	FB1	4.1	5.4	5.6	4.6	4.7	4.6

ENSMUSG00000020810	Cygb	FB1	4.4	6.4	3.8	5.3	3.4	4.8
ENSMUSG00000000753	Serpinf1	FB1	5.3	6.0	5.3	5.9	5.2	5.2
ENSMUSG00000019929	Dcn	FB1	5.3	7.2	6.5	7.8	6.5	6.7
ENSMUSG00000090231	Cfb	FB1	6.9	7.0	7.4	7.1	6.7	7.1
ENSMUSG00000023224	Serping1	FB1	7.3	7.8	8.2	7.3	8.2	8.1
ENSMUSG00000022371	Col14a1	FB1	7.3	9.1	6.6	9.0	7.4	9.0
ENSMUSG00000024164	C3	FB1	7.8	7.8	9.1	8.0	9.1	8.4
ENSMUSG00000056427	Slit3	FB1	8.8	9.0	8.8	9.5	9.1	9.6
ENSMUSG00000033327	Tnxb	FB1	9.8	10.6	9.4	10.2	9.8	10.3
ENSMUSG00000015627	Gata5	FB2	2.0	2.0	2.7	2.0	3.8	3.6
ENSMUSG00000031497	Tnfsf13b	FB2	2.0	2.3	2.9	2.0	3.8	2.9
ENSMUSG00000097084	Foxl1	FB2	2.8	2.5	2.9	2.9	3.7	2.4
ENSMUSG00000020264	Slc36a2	FB2	2.8	3.0	3.1	3.1	3.8	2.0
ENSMUSG00000068794	Col28a1	FB2	2.9	4.1	2.5	3.2	3.0	2.7
ENSMUSG00000059049	Frem1	FB2	3.6	4.6	3.8	4.7	3.8	3.1
ENSMUSG00000033207	Mamdc2	FB2	4.5	3.8	4.5	4.3	3.8	4.6
ENSMUSG00000021732	Fgf10	FB2	3.3	5.4	3.6	3.1	3.6	3.1
ENSMUSG00000022103	Gfra2	FB2	4.2	3.3	5.5	4.8	5.0	2.0
ENSMUSG00000032179	Bmp5	FB2	4.6	3.8	5.2	4.5	4.6	4.3
ENSMUSG00000027188	Pamr1	FB2	4.0	5.9	4.1	5.1	4.2	4.9
ENSMUSG00000050370	Ch25h	FB2	5.4	5.4	5.0	6.0	5.2	6.9
ENSMUSG00000031673	Cdh11	FB2	5.2	6.2	5.7	6.0	5.8	5.6
ENSMUSG00000027848	Olfml3	FB2	6.4	6.8	6.8	6.3	6.9	7.1
ENSMUSG00000064325	Hhip	FB2	6.6	6.9	7.2	6.4	7.6	7.7
ENSMUSG00000031558	Slit2	FB2	6.9	7.7	5.8	8.0	6.5	7.4
ENSMUSG00000033066	Gas7	FB2	6.8	6.8	8.0	6.9	8.0	7.1
ENSMUSG00000074207	Adh1	FB2	6.6	8.3	6.3	7.4	6.9	6.9
ENSMUSG00000038156	Spon1	FB2	8.5	8.6	8.6	9.4	8.8	9.2
ENSMUSG00000068373	D430041D 05Rik	FB3	2.9	2.0	2.5	4.6	4.5	2.4
ENSMUSG00000055301	Adh7	FB3	3.3	3.4	2.7	4.3	3.7	3.3
ENSMUSG00000022548	Apod	FB3	3.1	3.5	3.8	2.7	3.4	4.6
ENSMUSG00000031825	Crispld2	FB3	3.8	3.5	3.6	4.0	3.7	2.7
ENSMUSG00000020467	Efemp1	FB3	5.3	4.7	5.8	4.9	5.7	4.5
ENSMUSG00000026840	Lamc3	FB3	5.2	6.1	4.0	6.2	4.7	4.6
ENSMUSG00000063564	Col23a1	FB3	7.7	7.6	7.5	7.3	7.9	7.8
ENSMUSG00000031740	Mmp2	FB3	7.4	8.6	7.0	8.6	7.7	7.8
ENSMUSG00000040690	Col16a1	FB4	2.3	3.3	2.9	3.1	3.7	2.7
ENSMUSG00000037206	Islr	FB4	2.9	4.3	2.0	3.2	4.0	2.7
ENSMUSG00000044006	Cilp2	FB4	3.4	3.9	3.1	3.2	2.0	3.6
ENSMUSG00000007682	Dio2	FB4	3.8	3.9	4.3	4.7	4.2	3.9

ENSMUSG00000036446	Lum	FB4	2.3	5.2	5.1	5.1	6.0	4.7
ENSMUSG00000014329	Bicc1	FB4	4.1	5.7	4.1	4.0	5.4	4.8
ENSMUSG00000046714	Foxc2	FB4	4.4	5.6	4.1	5.6	4.8	5.0
ENSMUSG00000000567	Sox9	FB4	2.3	6.4	2.7	5.7	2.4	3.5
ENSMUSG00000022324	Matn2	FB4	5.2	5.4	4.9	5.7	5.1	5.8
ENSMUSG00000068196	Col8a1	FB4	5.5	7.3	5.5	6.6	5.3	4.8
ENSMUSG00000022665	Ccdc80	FB4	6.5	7.5	5.8	8.3	6.2	7.6
ENSMUSG00000030218	Mgp	FB4	9.0	10.9	9.2	11.6	9.2	9.8
ENSMUSG00000031375	Bgn	FB4	10.0	10.7	9.4	10.5	9.7	10.0
ENSMUSG00000062329	Cyt11	FB4	9.9	11.0	9.8	10.7	9.2	9.8
ENSMUSG00000023274	Cd4	hematopoi etic	6.2	4.7	6.2	7.2	5.9	3.6
ENSMUSG00000026069	Il1rl1	hematopoi etic	5.9	2.9	6.8	3.7	7.5	2.0
ENSMUSG00000019989	Enpp3	hematopoi etic	6.2	6.7	6.4	6.1	7.1	6.6
ENSMUSG00000053977	Cd8a	hematopoi etic	6.4	5.5	7.1	7.8	7.3	4.0
ENSMUSG00000068227	Il2rb	hematopoi etic	6.6	5.6	8.6	6.5	9.2	3.1
ENSMUSG00000032093	Cd3e	hematopoi etic	7.8	6.5	8.3	8.2	8.5	2.9
ENSMUSG00000030724	Cd19	hematopoi etic	8.7	7.7	9.8	8.4	10.5	7.3
ENSMUSG00000026395	Ptprc	hematopoi etic	10.2	8.8	10.9	9.8	11.2	8.3
ENSMUSG00000079277	Hoxd3	LEC	4.7	4.7	3.8	4.0	3.8	4.9
ENSMUSG00000072553	Gm525	LEC	4.8	4.8	5.4	5.4	6.3	5.4
ENSMUSG00000030638	Sh3gl3	LEC	5.0	5.7	5.1	5.5	6.3	5.2
ENSMUSG00000046999	1110032F 04Rik	LEC	5.2	4.8	5.9	4.1	6.0	5.5
ENSMUSG00000009097	Tbx1	LEC	6.0	5.5	5.5	4.7	6.4	5.8
ENSMUSG00000026435	Slc45a3	LEC	7.1	7.6	7.5	7.0	7.9	7.1
ENSMUSG00000108218	Olf1372- ps1	LEC	8.3	7.1	8.2	7.4	8.7	7.9
ENSMUSG00000044469	Tnfaip8l1	LEC	7.8	7.9	8.3	7.6	7.8	7.9
ENSMUSG00000031517	Gpm6a	LEC	8.7	8.2	8.9	8.3	9.4	9.2
ENSMUSG00000031196	F8	LEC	8.6	8.6	9.1	8.3	9.5	9.4
ENSMUSG00000000794	Kcnn3	LEC	9.4	8.3	9.4	8.1	9.5	8.8
ENSMUSG00000026712	Mrc1	LEC	9.3	8.8	9.5	8.3	9.0	8.9
ENSMUSG00000010175	Prox1	LEC	9.5	9.8	9.7	9.8	10.2	9.9
ENSMUSG00000032011	Thy1	LEC	9.3	9.3	10.4	9.6	10.1	9.3
ENSMUSG00000042453	Reln	LEC	11.1	10.6	11.3	10.6	11.7	11.4
ENSMUSG00000054641	Mmrn1	LEC	12.3	11.7	12.4	11.5	12.8	12.4
ENSMUSG00000042286	Stab1	LEC	12.1	12.4	12.0	12.5	12.6	12.5
ENSMUSG00000020357	Flt4	LEC	13.2	13.4	13.5	13.1	13.6	13.3

ENSMUSG00000035805	Mlc1	Mixed	2.0	2.5	3.4	2.7	4.1	2.7
ENSMUSG00000001504	Irx2	Mixed	2.5	2.3	3.7	3.7	4.4	2.7
ENSMUSG00000023043	Krt18	Mixed	2.5	3.0	3.5	3.2	4.2	3.8
ENSMUSG00000045394	Epcam	Mixed	2.8	2.7	4.1	2.7	4.3	3.1
ENSMUSG00000047040	Prr15l	Mixed	2.8	3.0	4.6	4.1	3.2	2.7
ENSMUSG00000070473	Cldn3	Mixed	3.6	3.8	4.0	4.0	3.0	2.0
ENSMUSG00000027315	Spint1	Mixed	2.3	4.2	4.3	3.7	3.8	2.0
ENSMUSG00000070780	Rbm47	Mixed	3.4	4.3	4.9	3.6	4.8	2.4
ENSMUSG00000001496	Nkx2-1	Mixed	4.1	3.7	5.2	4.1	5.4	4.0
ENSMUSG00000040808	S100g	Mixed	4.2	3.8	5.2	4.6	4.4	3.3
ENSMUSG00000020566	Atp6v1c2	Mixed	4.8	4.4	4.7	4.1	5.9	3.9
ENSMUSG00000062778	Chia1	Mixed	3.6	5.1	5.0	5.2	5.4	2.4
ENSMUSG00000030800	Prss8	Mixed	5.5	4.5	4.4	4.3	5.5	4.5
ENSMUSG00000030214	Plbd1	Mixed	6.6	6.1	6.7	6.3	6.0	6.3
ENSMUSG00000002204	Napsa	Mixed	5.8	5.6	7.7	6.1	7.7	4.9
ENSMUSG00000042784	Muc1	Mixed	6.2	5.9	7.6	5.7	6.8	4.4
ENSMUSG00000000303	Cdh1	Mixed	8.6	5.6	9.3	6.8	9.2	3.9
ENSMUSG00000049420	Tmem200	PC	2.5	2.0	2.9	2.0	4.2	2.0
	a							
ENSMUSG00000049115	Agtr1a	PC	2.8	3.0	2.5	3.1	3.7	2.7
ENSMUSG00000017344	Vtn	PC	3.5	3.0	3.1	3.7	3.0	3.6
ENSMUSG00000031997	Trpc6	PC	3.8	3.3	2.9	3.8	3.4	2.9
ENSMUSG00000049265	Kcnk3	PC	3.1	3.7	3.7	3.2	3.6	2.9
ENSMUSG00000024245	Tmem178	PC	3.9	4.4	2.7	4.8	3.4	3.9
ENSMUSG00000053846	Lipg	PC	3.1	3.7	4.5	4.0	3.8	3.3
ENSMUSG00000009876	Cox4i2	PC	4.2	4.2	3.1	4.7	3.4	5.2
ENSMUSG00000022376	Adcy8	PC	4.2	3.2	4.4	3.5	4.3	3.1
ENSMUSG00000020928	Higd1b	PC	3.9	3.9	4.2	3.4	4.6	4.1
ENSMUSG00000032452	Clstn2	PC	4.1	3.9	4.1	4.9	3.6	4.1
ENSMUSG00000028033	Kcnq5	PC	3.3	3.4	5.4	4.8	5.5	3.5
ENSMUSG00000036856	Wnt4	PC	4.9	4.8	4.0	5.4	5.5	5.9
ENSMUSG00000054459	Vsnl1	PC	4.8	4.5	5.0	4.9	5.5	5.5
ENSMUSG00000027985	Lef1	PC	6.5	5.2	7.4	6.3	7.5	4.9
ENSMUSG00000034164	Emid1	PC	6.5	7.2	7.5	7.1	6.7	6.3
ENSMUSG00000027750	Postn	PC	7.3	7.7	7.6	8.5	7.6	6.7
ENSMUSG00000038319	Kcnh2	VSMC	2.8	2.5	2.5	3.8	4.3	2.4
ENSMUSG00000020155	Kcnmb1	VSMC	2.0	2.0	3.5	2.7	4.3	2.4
ENSMUSG00000045534	Kcna5	VSMC	2.3	3.9	2.9	4.3	3.6	2.0
ENSMUSG00000001349	Cnn1	VSMC	2.5	3.0	3.8	3.1	2.4	2.9
ENSMUSG00000006221	Hspb7	VSMC	2.8	3.2	3.9	2.7	2.7	2.7
ENSMUSG00000021200	Asb2	VSMC	3.5	3.0	3.9	3.1	2.4	2.0

ENSMUSG00000038677	Scube3	VSMC	3.4	3.5	4.4	4.2	4.2	4.0
ENSMUSG00000030317	Timp4	VSMC	3.4	5.0	3.9	5.6	5.2	3.6
ENSMUSG00000024049	Myom1	VSMC	5.4	5.5	5.3	4.9	4.8	4.6
ENSMUSG00000002831	Plin4	VSMC	5.7	5.4	5.3	6.1	6.8	6.4
ENSMUSG000000036854	Hspb6	VSMC	6.4	6.4	6.0	6.0	5.3	6.4
ENSMUSG00000005611	Mrv1	VSMC	6.1	6.5	6.2	7.5	7.4	6.6
ENSMUSG000000050503	Fbxl22	VSMC	8.0	7.0	7.0	7.3	7.7	7.6

Supplementary table 3- 1: cell specific subpopulation in sorted mouse pulmonary endothelial cells.

Symbol	RPKM								
	log2 FC	P_adj	Veh_1	Veh_2	Veh_3	IL4_1	IL4_2	IL4_3	
4930542D 17Rik	9.6 ↑	4.0E-33	4	6	6	851	841	1,076	
Rgs4	4.8 ↑	3.9E-14	11	27	14	557	124	432	
Arpp21	4.2 ↑	0.0126	4	11	9	186	38	14	
Ptges	3.6 ↑	1.9E-05	21	10	9	147	43	150	
Serpina3g	3.6 ↑	2.3E-31	667	1,261	1,360	11,897	9,985	16,861	
Thbs1	2.7 ↑	7.5E-27	309	244	358	1,895	1,506	2,392	
Serpina3f	2.7 ↑	2.5E-21	841	637	980	5,186	3,550	6,659	
Gbp11	2.6 ↑	1.5E-14	80	80	143	685	460	653	
Aldh1a7	2.6 ↑	0.0002	23	36	16	198	74	123	
Htr2a	2.1 ↑	0.0011	55	35	22	138	104	192	
Gbp6	2.0 ↑	2.9E-05	311	277	857	1,791	1,885	2,242	
Gbp10	2.0 ↑	0.0002	248	205	738	1,508	1,601	1,702	
F830016 B08Rik	1.8 ↑	0.0038	81	66	168	297	250	510	
Nlrc5	1.8 ↑	0.00079	570	338	1,192	1,889	2,806	2,484	
Spsb1	1.8 ↑	9.3E-06	96	72	76	367	222	220	
Tgtp1	1.7 ↑	0.0088	91	84	237	326	406	611	
Serpina3i	1.7 ↑	1.2E-06	487	320	407	1,476	836	1,608	
Gm12185	1.7 ↑	0.0022	221	211	497	651	908	1,334	
Gbp4	1.6 ↑	9.3E-06	8,077	6,575	14,708	25,759	28,884	35,004	
Gm4070	1.6 ↑	0.0002	162	122	260	437	514	625	
Igtp	1.5 ↑	0.0026	1,225	1,031	2,886	3,890	5,130	5,926	
A4galt	1.5 ↑	6.2E-08	264	217	237	574	603	872	
Ifi44	1.5 ↑	0.0012	491	609	664	2,504	952	1,424	
Ankrd6	1.5 ↑	2.3E-05	83	82	66	219	183	211	
P2ry2	1.4 ↑	0.0002	102	163	111	382	261	348	
Tgtp2	1.4 ↑	0.0003	637	464	976	1,552	1,627	2,236	
Ppt1	1.4 ↑	4.5E-05	3,588	5,311	3,991	13,626	7,285	12,464	
Gm5431	1.3 ↑	0.0453	50	36	64	134	96	133	
Oas2	1.3 ↑	0.0125	137	99	217	458	283	393	
Per2	1.3 ↑	0.0119	258	268	199	424	443	934	
Irgm2	1.3 ↑	0.0031	2,451	2,127	4,771	6,401	7,376	9,125	
Olf15l5	1.3 ↑	0.0457	51	72	86	151	126	215	

Adamts14	1.3	↑	0.0193	40	49	52	101	110	115
Oas1a	1.2	↑	0.0060	125	83	147	271	245	281
Deptor	1.2	↑	0.0002	193	170	222	357	422	511
Pola2	1.1	↑	5.4E-06	420	340	423	934	727	897
Slc35e4	1.1	↑	0.04573	55	56	59	112	108	134
Stat1	1.1	↑	4.2E-06	4,104	3,211	4,679	8,519	7,583	9,578
Irgm1	1.1	↑	4.6E-05	1,058	962	1,515	2,490	2,388	2,654
Plxnc1	1.1	↑	3.2E-09	765	842	793	1,549	1,656	1,888
Gbp7	1.1	↑	0.01038	4,555	3,727	7,681	9,967	10,634	13,044
Dnah8	1.1	↑	2.8E-06	1,439	1,190	1,468	2,738	3,282	2,463
Stat2	1.0	↑	0.00052	2,610	1,874	3,070	4,787	6,090	4,711
Ifit1	1.0	↑	0.01003	389	304	458	993	597	758
Gbp9	1.0	↑	3.2E-05	7,163	6,203	8,354	13,543	12,609	16,600
Hecw2	0.9	↑	9.3E-06	5,072	4,614	4,109	7,676	10,090	8,806
Lyve1	0.9	↑	0.00048	10,239	13,600	10,229	25,286	22,310	17,845
Kif13a	0.9	↑	1.2E-06	2,715	2,292	2,299	4,234	4,598	5,083
Oasl2	0.9	↑	0.00321	2,554	2,130	2,548	5,715	3,977	3,731
Nup210	0.9	↑	1.2E-06	3,511	4,050	3,600	7,571	6,431	6,547
Nrros	0.8	↑	0.00020	4,090	4,008	4,223	7,571	6,029	8,349
Mink1	0.8	↑	9.4E-06	1,100	1,142	1,288	2,104	1,982	2,081
Gm45837	0.8	↑	0.00172	541	731	655	1,124	1,083	1,121
Fmnl2	0.8	↑	0.00151	2,521	3,233	2,438	4,958	4,211	4,963
Nf1	0.8	↑	0.00163	5,171	4,148	3,770	7,147	8,092	7,094
Herc6	0.8	↑	0.02488	1597	1,114	1,534	2,257	2,758	2,164
Slfn5	0.7	↑	0.00025	13,006	12,607	11,494	21,481	17,955	21,668
Il6st	0.7	↑	0.04063	11,699	15,827	14,856	20,753	20,590	27,624
Unc45b	0.7	↑	0.02885	1,098	1,372	1,057	2,056	2,028	1,622
Fhl1	0.7	↑	0.00423	1,950	1,846	1,514	3,013	2,877	2,662
H2-T24	0.7	↑	0.00075	2,058	2,067	2,160	3,535	2,967	3,585
Ltbp1	0.7	↑	0.00823	2,041	2,191	1,807	3,364	2,788	3,407
Rnf213	0.7	↑	0.00211	13,299	11,226	13,159	21,551	18,071	19,787
Fam117b	0.6	↑	0.04532	4,468	3,790	3,801	6,109	5,285	7,236
Dusp16	0.6	↑	0.00147	960	984	1,002	1,497	1,477	1,490
Rin2	0.6	↑	0.0100	3,226	3,549	3,571	5,516	5,554	4,590
Znfx1	0.6	↑	0.0205	2,651	2,320	2,589	3,661	3,438	4,161
Tcn2	0.5	↑	0.0410	7,802	8,341	7,839	12,767	10,433	11,103
Ttc28	0.5	↑	0.0427	2,913	2,899	2,527	3,815	3,858	4,139
Plip	-0.6	↓	0.0185	1,502	1,702	1,453	1,100	965	1,020
Neto2	-0.7	↓	0.0248	595	518	512	339	305	360
Cxcl12	-0.8	↓	0.0008	17,539	17,171	18,056	11,312	8,201	11,073
Tril	-0.9	↓	0.0089	1,518	1,610	1,398	800	649	1,048
Map2k6	-0.9	↓	0.0453	305	306	297	207	134	145
Al197445	-1.0	↓	0.0406	603	604	367	309	238	270
Ntrk2	-1.0	↓	2.6E-10	4,388	3,974	4,218	2,108	2,112	2,276
Bmp4	-1.0	↓	0.0008	740	693	589	304	327	411
Edn1	-1.0	↓	0.0299	7,422	3,772	5,640	2,473	3,492	2,616
Glb1l2	-1.1	↓	0.00863	1,902	1,175	1,237	551	671	865

Slc6a6	-1.1 ↓	3.5E-07	14,030	11,256	11,828	6,343	5,033	6,407
Cxcr4	-1.1 ↓	9.4E-06	1,952	1,647	2,168	753	801	1,069
Esm1	-2.1 ↓	1.2E-15	2,022	2,194	1,707	617	358	440

Supplementary table 3- 2: IL-4C induced DEGs in lung endothelial cells

Term	Count	%	PValue	Genes
GO:0035458~cellular response to interferon-beta	11	15.7	1.07E-16	GBP6, TGTP2, F830016B08RIK, TGTP1, STAT1, IGTP, IRGM2, IRGM1, IFIT1, GM5431, GM12185
GO:0006952~defense response	8	11.4	1.37E-07	TGTP2, F830016B08RIK, TGTP1, IGTP, IRGM2, IRGM1, GM5431, GM12185
GO:0042832~defense response to protozoan	5	7.1	3.21E-06	GBP6, GBP10, GBP7, GBP9, IRGM2
GO:0034097~response to cytokine	6	8.6	8.43E-06	SERPINA3F, STAT1, IL6ST, SERPINA3G, SERPINA3I, PTGES
GO:0009615~response to virus	6	8.6	1.01E-05	TGTP2, TGTP1, OAS2, OAS1A, IFIT1, OASL2
GO:0071346~cellular response to interferon-gamma	5	7.1	8.66E-05	GBP6, GBP10, GBP7, GBP9, GBP4
GO:0051607~defense response to virus	6	8.6	2.68E-04	OAS2, STAT2, NLRC5, OAS1A, IFIT1, OASL2
GO:0002376~immune system process	8	11.4	3.27E-04	NRROS, OAS2, NLRC5, IRGM1, IFIT1, SERPINA3G, HERC6, OASL2
GO:0044406~adhesion of symbiont to host	3	4.3	4.10E-04	GBP6, GBP7, GBP9
GO:0045087~innate immune response	8	11.4	4.24E-04	NRROS, OAS2, NLRC5, IRGM1, OAS1A, IFIT1, HERC6, OASL2
GO:0043434~response to peptide hormone	4	5.7	0.0020	SERPINA3F, STAT1, SERPINA3G, SERPINA3I
GO:0006164~purine nucleotide biosynthetic process	3	4.3	0.0021	OAS2, OAS1A, OASL2
GO:0006955~immune response	6	8.6	0.0024	TGTP2, TGTP1, NRROS, OAS2, THBS1, OASL2
GO:0034341~response to interferon-gamma	3	4.3	0.0036	TGTP2, TGTP1, IRGM2
GO:0050830~defense response to Gram-positive bacterium	4	5.7	0.0040	GBP6, GBP10, GBP7, GBP9
GO:0001937~negative regulation of endothelial cell proliferation	3	4.3	0.0047	STAT1, NF1, THBS1
GO:0060337~type I interferon signaling pathway	2	2.9	0.0204	STAT1, STAT2
GO:0002544~chronic inflammatory response	2	2.9	0.0238	THBS1, PTGES
GO:0016525~negative regulation of angiogenesis	3	4.3	0.0254	STAT1, NF1, THBS1
GO:0050688~regulation of defense response to virus	2	2.9	0.0271	IFIT1, GBP4
GO:0001952~regulation of cell-matrix adhesion	2	2.9	0.0371	MINK1, NF1

GO:0035455~response to interferon-alpha 2 2.9 0.0404 TGTP2, TGTP1

Supplementary table 3- 3: GO analysis of IL-4 up regulated genes

Term	Coun t	%	PValue	Genes
GO:0030335~positive regulation of cell migration	4	30.8	2.15E-04	BMP4, EDN1, CXCL12, CXCR4
GO:0008284~positive regulation of cell proliferation	5	38.5	2.23E-04	BMP4, NTRK2, ESM1, EDN1, CXCL12
GO:0007281~germ cell development	3	23.1	2.59E-04	BMP4, CXCL12, CXCR4
GO:0001569~patterning of blood vessels	3	23.1	2.59E-04	EDN1, CXCL12, CXCR4
GO:0001764~neuron migration	3	23.1	0.0025	NTRK2, CXCL12, CXCR4
GO:0022029~telencephalon cell migration	2	15.4	0.0043	CXCL12, CXCR4
GO:0001667~ameboidal-type cell migration	2	15.4	0.0043	CXCL12, CXCR4
GO:0001934~positive regulation of protein phosphorylation	3	23.1	0.0053	BMP4, CXCR4, MAP2K6
GO:0008354~germ cell migration	2	15.4	0.0055	CXCL12, CXCR4
GO:0032308~positive regulation of prostaglandin secretion	2	15.4	0.0055	EDN1, MAP2K6
GO:0001666~response to hypoxia	3	23.1	0.0058	EDN1, CXCL12, CXCR4
GO:0090280~positive regulation of calcium ion import	2	15.4	0.0127	CXCL12, CXCR4
GO:0042098~T cell proliferation	2	15.4	0.0145	CXCL12, CXCR4
GO:0008045~motor neuron axon guidance	2	15.4	0.0169	CXCL12, CXCR4
GO:0051924~regulation of calcium ion transport	2	15.4	0.0223	CXCL12, CXCR4
GO:0019722~calcium-mediated signaling	2	15.4	0.0276	EDN1, CXCR4
GO:0060048~cardiac muscle contraction	2	15.4	0.0288	CXCR4, MAP2K6
GO:0001938~positive regulation of endothelial cell proliferation	2	15.4	0.0400	BMP4, CXCL12
GO:0030334~regulation of cell migration	2	15.4	0.0459	CXCL12, CXCR4
GO:0048661~positive regulation of smooth muscle cell proliferation	2	15.4	0.0476	BMP4, EDN1
GO:0051216~cartilage development	2	15.4	0.0488	BMP4, EDN1

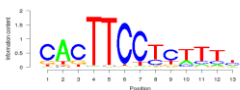
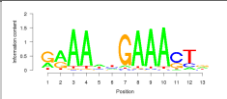
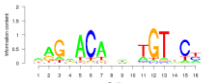
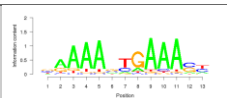
Supplementary table 3- 4: GO analysis of IL-4 down regulated genes

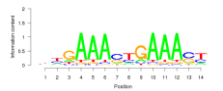
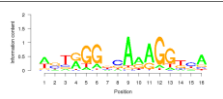
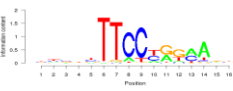
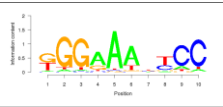
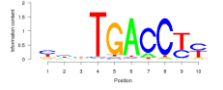
Sup table 4

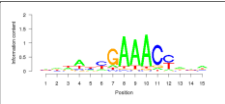
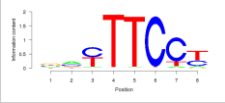
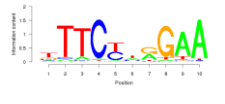
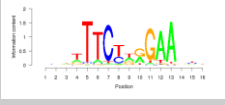
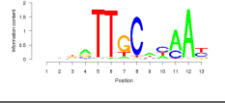
**Expression in Mice lung
ECs**

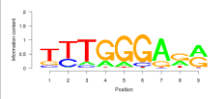
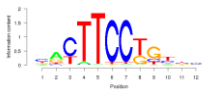
LISA top 20 TFs	Veh_1 (RPKM)	Veh_2 (RPKM)	Veh_3 (RPKM)	1st Sample p-value	2nd Sample p-value	3rd Sample p-value	4th Sample p-value	5th Sample p-value
STAT2	11.4	10.9	11.6	4.5E-22	2.0E-11	1.3E-09		
STAT1	12.0	11.6	12.2	2.0E-19	7.6E-18	1.4E-14	3.1E-14	3.5E-14
IRF8	5.4	5.1	6.9	2.1E-16	1.2E-90	4.4E-09	8.5E-09	9.7E-08
NR3C1	12.3	12.3	12.3	3.7E-15	1.8E-13	2.0E-13	9.4E-13	6.6E-08
SPI1	5.9	5.0	6.4	2.3E-12	5.5E-11	5.6E-11	6.9E-11	1.8E-10
ERG	11.5	11.7	11.3	9.8E-12	8.9E-06	2.2E-05	3.5E-05	1.9E-03
RELA	10.5	11.0	10.6	1.5E-10	6.3E-09	6.8E-09	5.2E-08	4.1E-07
PPARG	6.1	5.8	4.8	2.4E-10	2.3E-08	3.1E-08	5.5E-08	1.2E-07
STAT3	11.7	11.7	11.9	5.3E-10	3.0E-08	3.2E-08	8.1E-08	1.0E-07
IRF1	11.9	11.7	11.5	1.1E-09	2.1E-09	1.1E-08	3.1E-08	3.3E-08
STAT5A	8.2	7.6	8.1	3.0E-09	2.1E-07	2.9E-07	7.4E-05	1.8E-04
IRF4	6.3	6.3	7.8	9.6E-09	7.9E-08	2.1E-07	4.9E-07	8.2E-07
IKZF1	9.3	8.3	10.4	3.0E-08	6.9E-08	1.1E-07	2.2E-06	4.1E-04
RXRA	10.6	10.5	10.7	3.0E-08	8.3E-08	1.2E-07	1.3E-07	2.8E-07
STAT5B	9.1	9.5	9.6	1.5E-07	3.8E-06	2.2E-05	6.4E-05	6.6E-05
POLR2B	10.9	11.0	10.9	2.9E-07	2.9E-07	1.0E-06	1.1E-06	1.2E-06
BATF	3.8	2.9	5.3	4.3E-07	7.4E-05	1.0E-04	1.8E-04	2.0E-04
STAT6	10.9	10.7	11.0	4.7E-07	5.2E-07	1.9E-06	3.1E-06	4.6E-06
CEBPA	5.8	5.0	6.7	5.6E-07	1.3E-06	7.2E-05	1.5E-04	1.6E-04
BRD4	12.0	11.8	11.9	5.8E-07	1.1E-05	2.9E-04	3.6E-04	1.0E-03

Supplementary table 3- 5: TF program from endothelial cells

LISA top 20 TFs	Motif ID	Positional weight matrix (PWM)	Motif P-value	dbd	Species	Genes
Stat2	#N/A		0.000000289	Stat Protein Family	mus musculus	Stat1, Fam117b, Per2, Cxcr4, Fmnl2, Rin2, Ptges, Thbs1, Gbp7, Ifi44, Spsb1, Ppt1, Ttc28, Gbp4, Gbp9, Gbp10, Gbp6, Gbp11, Oasl2, Oas2, Oas1a, Nup210, Slc6a6, Dusp16, Herc6, P2ry2, Lyve1, Nlrc5, Pllp, Plxnc1, Stat2, Gm5431, Nf1, Map2k6, Tcn2, Slc35e4, Irgm1, Gm12185, Tgtp1, Olfr56, Tgtp2, Irgm2, Igtp, Mink1, Slfn5, Unc45b, Serpina3f, Serpina3i, Serpina3g, Serpina3h, Kif13a, Al197445, Edn1, Il6st, Htr2a, Deptor, 4930542D17Rik, Nrros, H2-T24, F830016B08Rik, Pola2, Ifit1
Spi1	MC00506		#N/A	Stat Protein Family	#N/A	Stat1, Gbp7, Gbp4, Gbp9, Gbp10, Gbp6, Gbp11, Oasl2, Oas2, Oas1a, Dusp16, Herc6, Stat2, Gm5431, Irgm1, Gm12185, Tgtp1, Tgtp2, Irgm2, Igtp, Serpina3f, Serpina3i, Serpina3g, Serpina3h, Nrros, H2-T24, F830016B08Rik, Ifit1
Stat1	MC00141		0.0000605	Stat Protein Family	Homo Sapiens	Stat1, Fam117b, Cxcr4, Fmnl2, Gbp7, Ifi44, Spsb1, Ppt1, Gbp4, Gbp9, Gbp10, Gbp6, Gbp11, Oasl2, Oas2, Oas1a, Nup210, Slc6a6, Dusp16, Herc6, P2ry2, Lyve1, Glb1l2, Plxnc1, Stat2, Gm5431, Nf1, Map2k6, Tcn2, Slc35e4, Irgm1, Gm12185, Tgtp1, Olfr56, Tgtp2, Irgm2, Igtp, Slfn5, Unc45b, Serpina3f, Serpina3g, Serpina3h, Edn1, Il6st, Htr2a, Deptor, 4930542D17Rik, Nrros, H2-T24, F830016B08Rik, Ifit1
Nr3c1	MC00396		0.252	Hormone-nuclear Receptor Family	mus musculus	Stat1, Fam117b, Per2, Cxcr4, Rgs4, Fmnl2, Rin2, Ptges, Thbs1, Znf1, Gbp7, Ifi44, Spsb1, Ppt1, Ttc28, Gbp4, Gbp9, Gbp10, Gbp6, Gbp11, Oasl2, Oas2, Nup210, Slc6a6, Cxcl12, Dusp16, Tril, Herc6, Gm4070, P2ry2, Lyve1, Nlrc5, Neto2, Pllp, Glb1l2, Adamts14, Plxnc1, Stat2, Gm5431, Nf1, Map2k6, Tcn2, Slc35e4, Irgm1, Tgtp1, Tgtp2, Irgm2, Igtp, Mink1, Slfn5, Unc45b, Serpina3f, Serpina3i, Serpina3g, Serpina3h, Kif13a, Ntrk2, Al197445, Edn1, Il6st, Esm1, Bmp4, Htr2a, Deptor, A4galt, Nrros, Dnah8, Ltbp1, H2-T24, Aldh1a7, Pola2, Ifit1, Fhl1
Irf1	M00062		0.00624	Interferon Regulatory Factor	mus musculus	Hecw2, Stat1, Fam117b, Per2, Cxcr4, Rgs4, Fmnl2, Rin2, Ptges, Thbs1, Znf1, Gbp7, Ifi44, Spsb1, Ankrd6, Ppt1, Ttc28, Gbp4, Gbp9, Gbp10, Gbp6, Gbp11, Oasl2, Oas2, Oas1a, Nup210, Slc6a6, Cxcl12, Dusp16, Tril, Herc6, Gm4070, P2ry2, Lyve1, Nlrc5, Neto2, Pllp, Arpp21,

						Glb1l2, Adamts14, Plxnc1, Stat2, Gm5431, Nf1, Map2k6, Tcn2, Slc35e4, Irgm1, Gm12185, Tgtp1, Olfr56, Tgtp2, Irgm2, Igtp, Mink1, Slfn5, Unc45b, Serpina3f, Serpina3i, Serpina3g, Serpina3h, Kif13a, Al197445, Edn1, Il6st, Esm1, Bmp4, Htr2a, Deptor, A4galt, 4930542D17Rik, Nrros, Dnah8, Ltbp1, H2-T24, F830016B08Rik, Aldh1a7, Pola2, Ifit1, Fhl1
Irf8	MS000 72		0.00135	Interferon Regulator y Factor	Homo Sapiens	NA
Pparg	MC001 30		0.102	Rel Homology Region Family	mus musculu s	Stat1, Fam117b, Per2, Cxcr4, Fmnl2, Rin2, Ptges, Thbs1, Znfx1, Gbp7, Ifi44, Spsb1, Ppt1, Gbp4, Gbp9, Gbp6, Gbp11, Oasl2, Oas2, Oas1a, Slc6a6, Cxcl12, Dusp16, Tril, Herc6, P2ry2, Lyve1, Nlrc5, Pllp, Glb1l2, Adamts14, Plxnc1, Stat2, Gm5431, Nf1, Map2k6, Tcn2, Slc35e4, Irgm1, Gm12185, Olfr56, Tgtp2, Irgm2, Igtp, Mink1, Slfn5, Unc45b, Serpina3f, Serpina3i, Serpina3g, Serpina3h, Kif13a, Al197445, Edn1, Il6st, Htr2a, Deptor, 4930542D17Rik, Nrros, H2-T24, Pola2, Ifit1
Stat3	MC001 40		0.178	Stat Protein Family	mus musculu s	Stat1, Fam117b, Per2, Cxcr4, Fmnl2, Rin2, Ptges, Thbs1, Znfx1, Gbp7, Spsb1, Ppt1, Gbp4, Gbp9, Gbp10, Gbp6, Gbp11, Oasl2, Nup210, Slc6a6, Cxcl12, Dusp16, Tril, Herc6, P2ry2, Lyve1, Nlrc5, Pllp, Glb1l2, Adamts14, Stat2, Nf1, Map2k6, Tcn2, Slc35e4, Irgm1, Irgm2, Igtp, Mink1, Slfn5, Unc45b, Serpina3f, Serpina3i, Serpina3g, Serpina3h, Kif13a, Ntrk2, Al197445, Il6st, Esm1, Deptor, A4galt, Nrros, Dnah8, Ltbp1, H2-T24, Aldh1a7, Pola2, Ifit1, Fhl1
Rela	MC001 35		0.0265	Rel Homology Region Family	mus musculu s	Stat1, Rin2, Gbp7, Spsb1, Ppt1, Gbp4, Gbp9, Gbp10, Gbp6, Gbp11, Oasl2, Oas2, Nup210, Dusp16, Herc6, P2ry2, Nlrc5, Pllp, Adamts14, Stat2, Map2k6, Irgm1, Gm12185, Tgtp1, Tgtp2, Irgm2, Igtp, Slfn5, Serpina3f, Serpina3i, Serpina3g, Serpina3h, Il6st, Deptor, Nrros, H2-T24, Ifit1
Rxra	MC004 71		0.0395	Interferon Regulator y Factor	Homo Sapiens	Hecw2, Stat1, Znfx1, Gbp7, Ifi44, Spsb1, Ppt1, Gbp4, Gbp9, Gbp10, Gbp6, Gbp11, Oasl2, Oas2, Oas1a, Nup210, Dusp16, Herc6, Plxnc1, Stat2, Gm5431, Irgm1, Gm12185, Tgtp1, Olfr56, Tgtp2, Irgm2, Igtp, Serpina3f, Serpina3g, Serpina3h, Deptor, 4930542D17Rik, Nrros, H2-T24, F830016B08Rik, Ifit1

Irf4	UP00018		0.0592	Interferon Regulator y Factor	mus musculus	Stat1, Per2, Fmnl2, Rin2, Ptges, Thbs1, Gbp7, Ifi44, Spsb1, Ppt1, Gbp4, Gbp9, Gbp6, Gbp11, Oasl2, Oas2, Oas1a, Nup210, Dusp16, Herc6, P2ry2, Nlrc5, Plip, Stat2, Gm5431, Nf1, Map2k6, Tcn2, Slc35e4, Irgm1, Tgtp1, Irgm2, Igtp, Mink1, Serpina3i, Serpina3h, Kif13a, Al197445, Edn1, Il6st, Esm1, Deptor, A4galt, Nrros, Ltbp1, H2-T24, Pola2, Ifit1, Fhl1
Polr2b	MC00505		0.00699	Interferon Regulator y Factor	mus musculus	Hecw2, Stat1, Fam117b, Per2, Cxcr4, Fmnl2, Rin2, Ptges, Thbs1, Gbp7, Ifi44, Spsb1, Ankrd6, Ppt1, Ttc28, Gbp4, Gbp9, Gbp10, Gbp6, Gbp11, Oasl2, Nup210, Slc6a6, Dusp16, Herc6, Nlrc5, Neto2, Plip, Adamts14, Plxnc1, Stat2, Gm5431, Nf1, Map2k6, Tcn2, Slc35e4, Irgm1, Gm12185, Tgtp1, Olfr56, Tgtp2, Irgm2, Igtp, Mink1, Slfn5, Unc45b, Serpina3f, Serpina3i, Serpina3g, Serpina3h, Kif13a, Al197445, Edn1, Il6st, Esm1, Htr2a, Deptor, A4galt, 4930542D17Rik, Nrros, Dnah8, Ltbp1, H2-T24, Pola2, Ifit1
Stat6	M00500		0.134	Stat Protein Family	Homo Sapiens	Stat1, Fam117b, Per2, Cxcr4, Gbp7, Spsb1, Ppt1, Gbp4, Gbp9, Gbp6, Oasl2, Oas2, Oas1a, Nup210, Slc6a6, Herc6, Plip, Plxnc1, Stat2, Gm5431, Nf1, Slc35e4, Irgm1, Tgtp1, Tgtp2, Irgm2, Igtp, Mink1, Slfn5, Unc45b, Serpina3f, Serpina3i, Serpina3g, Serpina3h, Il6st, Deptor, Nrros, H2-T24, Pola2, Ifit1
Stat5b	MC00204		0.246	Hormone-nuclear Receptor Family	mus musculus	Per2, Ptges, Gbp10, Gbp6, Gbp11, Slc6a6, Cxcl12, Lyve1, Adamts14, Stat2, Gm5431, Tcn2, Irgm2, Il6st, Deptor, A4galt, Dnah8, Aldh1a7
Stat5a	MC00205		0.148	Stat Protein Family	mus musculus	Hecw2, Stat1, Fam117b, Per2, Cxcr4, Fmnl2, Rin2, Ptges, Znfx1, Gbp7, Ifi44, Spsb1, Ankrd6, Ppt1, Ttc28, Gbp4, Gbp9, Gbp10, Gbp6, Gbp11, Oasl2, Oas2, Oas1a, Nup210, Slc6a6, Cxcl12, Dusp16, Herc6, P2ry2, Lyve1, Nlrc5, Plip, Glb1l2, Adamts14, Plxnc1, Stat2, Gm5431, Nf1, Map2k6, Tcn2, Slc35e4, Irgm1, Gm12185, Tgtp1, Olfr56, Tgtp2, Irgm2, Igtp, Mink1, Slfn5, Unc45b, Serpina3f, Serpina3i, Serpina3g, Serpina3h, Kif13a, Edn1, Il6st, Esm1, Bmp4, Htr2a, Deptor, A4galt, Nrros, Dnah8, H2-T24, F830016B08Rik, Aldh1a7, Pola2, Ifit1, Fhl1
Cebpa	MC00122		0.0337	DNA Polymerase-Beta Family	Homo Sapiens	NA

Ikzf1	M0014 1		0.378	Leucine zipper Family	mus musculus	Hecw2, Stat1, Fam117b, Per2, Cxcr4, Fmnl2, Rin2, Ptges, Thbs1, Znfx1, Gbp7, Ifi44, Spsb1, Ankrd6, Ppt1, Gbp4, Gbp9, Gbp10, Gbp6, Gbp11, Oasl2, Nup210, Slc6a6, Dusp16, Herc6, Nlrc5, Plip, Arpp21, Adamts14, Plxnc1, Stat2, Gm5431, Nf1, Map2k6, Slc35e4, Irgm1, Gm12185, Tgtp1, Olfr56, Tgtp2, Irgm2, Igtp, Mink1, Slfn5, Unc45b, Serpina3f, Serpina3i, Serpina3g, Serpina3h, Kif13a, Al197445, Il6st, Esm1, Htr2a, Deptor, A4galt, 4930542D17Rik, Nrros, Dnah8, H2-T24, Pola2, Ifit1
Batf	MC005 08		0.146	Stat Protein Family	Homo Sapiens	Stat1, Fam117b, Cxcr4, Fmnl2, Gbp7, Spsb1, Ppt1, Gbp4, Gbp9, Gbp10, Gbp6, Gbp11, Oasl2, Oas2, Oas1a, Nup210, Slc6a6, Dusp16, Herc6, Lyve1, Nlrc5, Plxnc1, Stat2, Gm5431, Map2k6, Slc35e4, Irgm1, Gm12185, Tgtp1, Tgtp2, Irgm2, Igtp, Mink1, Unc45b, Serpina3f, Serpina3i, Serpina3g, Serpina3h, Kif13a, Edn1, Il6st, Esm1, Htr2a, Deptor, A4galt, 4930542D17Rik, Nrros, Dnah8, H2-T24, Ifit1
Brd4	#N/A		0.875	Leucine Zipper Family	mus musculus	Stat1, Fam117b, Per2, Cxcr4, Fmnl2, Ptges, Thbs1, Gbp7, Ifi44, Spsb1, Ppt1, Gbp9, Gbp6, Gbp11, Oasl2, Nup210, Slc6a6, Cxcl12, Dusp16, Herc6, P2ry2, Lyve1, Nlrc5, Neto2, Plip, Plxnc1, Stat2, Nf1, Map2k6, Tcn2, Slc35e4, Irgm1, Olfr56, Tgtp2, Irgm2, Mink1, Slfn5, Unc45b, Serpina3f, Serpina3i, Serpina3g, Kif13a, Edn1, Il6st, Esm1, Htr2a, 4930542D17Rik, Nrros, H2-T24, Pola2, Ifit1
Erg	MC001 68		#N/A	#N/A	#N/A	NA

Supplementary table 3- 6: TF and motif information

Gene_name	log2F C	FC		padj	Veh1	Veh2	Veh3	IL4_1	IL4_2	IL4_3
CCL26	10.6	1519.0	↑	0	39	29	39	51,102	54,334	57,102
CSN1S1	9.8	875.0	↑	2.4E-219	5	11	7	6,607	6,438	7,080
SERPINB3	5.6	47.9	↑	1.8E-24	1	2	6	138	143	150
SERPINB4	5.5	45.6	↑	3.0E-46	8	5	5	265	248	308
NPPB	4.4	21.3	↑	6.3E-10	1	3	3	61	56	32
HAS3	4.3	19.9	↑	0	471	437	440	9,847	8,378	8,592
SUCNR1	4.1	17.7	↑	2.1E-94	26	21	42	482	551	542
PLA2G5	3.9	15.3	↑	5.1E-24	11	8	5	142	120	106
IRF6	3.8	14.3	↑	9.1E-24	7	6	12	118	111	129
HAS2	3.8	14.2	↑	8.7E-08	5	2	1	48	37	29
SERPINB2	3.8	13.8	↑	2.6E-114	50	53	44	689	594	741
CPA3	3.8	13.5	↑	5.6E-193	101	75	99	1,330	1,196	1,174
SLC7A8	3.7	13.0	↑	2.8E-134	74	56	52	839	757	764
FGL2	3.5	11.6	↑	1.8E-05	3	3	1	15	30	36
TNFAIP6	3.4	10.8	↑	1.1E-08	7	3	3	55	29	57
OTOGL	3.4	10.6	↑	6.8E-254	171	187	178	1,933	1,748	2,022
SCN9A	3.4	10.2	↑	9.5E-55	166	101	109	1,337	1,307	1,199
SELP	3.3	9.9	↑	0	3,106	2,724	2,869	30,871	27,890	27,265
EPHX4	3.2	9.3	↑	1.3E-08	5	7	3	35	57	47
CBSL	3.1	8.7	↑	0.0064	12	8	3	70	115	14
IL6	3.1	8.4	↑	5.5E-157	172	121	134	1,226	1,204	1,171
MMP7	3.1	8.3	↑	5.0E-23	116	59	118	733	844	864
CERS6	3.0	7.9	↑	0.0014	5	1	1	23	21	11
SESN3	2.9	7.4	↑	2.8E-08	5	7	7	49	39	52
ZNF474	2.9	7.2	↑	4.0E-17	12	13	17	108	94	102
SOCS1	2.8	7.0	↑	2.5E-138	147	197	186	1,292	1,144	1,267
MASP1	2.8	7.0	↑	1.0E-50	63	38	66	419	346	397
LOX	2.8	6.9	↑	0	4,652	4,021	4,843	31,425	29,978	31,572
HS3ST1	2.7	6.4	↑	1.8E-158	228	225	196	1,342	1,348	1,483
GCNT3	2.6	6.0	↑	1.0E-08	4	13	15	60	80	51
NTRK1	2.6	6.0	↑	7.2E-14	25	21	9	136	101	91
PI16	2.6	6.0	↑	5.6E-20	94	63	118	635	499	503
CSF2RB	2.6	5.9	↑	0	3,794	3,555	3,650	22,775	21,253	20,953
MMP28	2.6	5.9	↑	2.3E-29	29	46	38	202	255	209
TMEM71	2.6	5.9	↑	1.8E-20	22	35	19	158	156	133
KCNK3	2.5	5.8	↑	2.8E-08	10	5	13	55	51	57
VDR	2.5	5.6	↑	1.2E-222	566	484	510	3,043	2,784	2,880
PRSS35	2.4	5.4	↑	1.8E-12	19	13	19	109	82	82

SLC26A4	2.4	5.3	↑	1.4E-05	3	5	18	48	56	35
HAPLN1	2.4	5.2	↑	0.0084	2	3	5	22	23	7
CRYBG1	2.4	5.1	↑	3.9E-129	282	293	261	1,504	1,482	1,301
ST8SIA1	2.3	5.0	↑	9.8E-21	33	41	32	219	161	153
NABP1	2.2	4.7	↑	0	3,453	3,111	3,356	16,090	15,176	15,533
IL12RB1	2.2	4.7	↑	0.0029	3	5	5	19	19	23
SLC46A3	2.2	4.7	↑	1.3E-07	23	19	5	64	92	64
SFRP1	2.2	4.6	↑	4.4E-281	2,197	2,013	2,076	10,143	9,304	9,156
CCR7	2.2	4.5	↑	0.0029	11	3	3	28	14	35
TACR2	2.1	4.4	↑	0.0117	21	24	3	77	71	62
GGTLC4P	2.1	4.3	↑	0.0066	7	5	3	12	19	33
ADAM19	2.1	4.2	↑	5.3E-264	2,585	2,560	2,679	11,693	10,895	10,308
CYSLTR2	2.1	4.2	↑	7.8E-07	9	21	23	101	72	48
NKX2-3	2.1	4.2	↑	6.5E-49	209	125	188	707	740	725
PKD1L1	2.0	4.1	↑	3.4E-07	12	24	16	83	49	79
SCN3B	2.0	3.9	↑	3.4E-14	39	48	29	177	159	122
ATP2B2	2.0	3.9	↑	0.0001	7	13	9	40	33	41
SLC15A3	2.0	3.9	↑	0.0007	9	7	7	35	27	28
KLRD1	2.0	3.9	↑	0.0058	5	9	3	23	20	23
C5orf67	1.9	3.9	↑	1.6E-34	95	90	120	382	363	433
CLCN4	1.9	3.8	↑	9.3E-244	1,851	1,857	1,871	7,512	7,002	6,862
FNIP2	1.9	3.8	↑	5.8E-235	1,940	1,810	1,790	7,223	7,085	6,749
IL1RL1	1.9	3.8	↑	2.5E-148	1,722	1,529	1,528	5,677	5,793	6,662
ABI3BP	1.9	3.8	↑	6.1E-182	3,352	3,011	3,259	13,215	12,034	11,241
SLC8A1	1.9	3.8	↑	1.2E-38	126	121	162	582	475	484
ITGAV	1.9	3.8	↑	1.4E-236	35,667	31,259	35,949	131,908	125,829	128,877
OR2A5	1.9	3.7	↑	4.5E-07	12	18	28	79	61	76
JAM2	1.8	3.6	↑	0.0208	5	7	3	19	12	23
RTP4	1.8	3.6	↑	1.7E-17	45	48	63	187	197	176
HSPD1P16	1.8	3.5	↑	0.0412	1	5	7	15	13	18
ABCA9	1.8	3.5	↑	0.0003	9	13	16	32	63	38
ABCA6	1.8	3.5	↑	2.0E-08	20	41	22	94	95	99
AP1S3	1.8	3.4	↑	5.6E-157	772	771	796	2,703	2,706	2,658
CASP3	1.8	3.4	↑	2.2E-261	5,115	4,835	4,999	17,045	16,632	17,849
INHBA	1.8	3.4	↑	8.0E-174	3,415	2,974	3,406	11,735	10,837	11,107
TCP11	1.8	3.4	↑	0.0245	3	11	3	19	22	17
Z97198.1	1.8	3.4	↑	0.0011	6	15	14	38	56	25
PTGIS	1.8	3.4	↑	4.4E-44	185	163	171	622	591	533
BTBD11	1.7	3.3	↑	1.4E-27	108	101	116	354	321	411
PRSS3	1.7	3.3	↑	1.3E-32	127	110	110	388	379	389

SMIM14	1.7	3.3	↑	1.1E-138	1,379	1,498	1,596	4,792	4,710	5,164
RIMS1	1.7	3.3	↑	2.2E-77	352	330	358	1,133	1,180	1,095
MUC6	1.7	3.2	↑	0.0005	10	18	10	43	36	44
IL20RB	1.7	3.2	↑	5.4E-28	128	129	99	376	358	416
NUAK1	1.7	3.2	↑	4.2E-186	7,582	7,083	7,823	25,382	23,918	22,795
MEX3B	1.7	3.2	↑	8.4E-73	624	526	663	2,107	1,906	1,796
ABCG2	1.6	3.1	↑	3.5E-179	2,452	2,478	2,712	8,153	7,830	7,943
TMEM200A	1.6	3.1	↑	1.2E-106	766	738	667	2,278	2,271	2,205
TEX41	1.6	3.0	↑	0.0172	9	8	6	18	19	33
CD44-AS1	1.6	3.0	↑	0.0380	3	15	5	12	25	33
TNIK	1.6	3.0	↑	1.4E-125	2,572	2,649	2,599	8,681	7,764	7,269
LRRC32	1.6	3.0	↑	7.3E-91	1,016	825	944	2,860	2,782	2,686
DTX4	1.6	3.0	↑	1.4E-83	790	730	707	2,393	2,058	2,165
OPLAH	1.6	2.9	↑	0.0313	6	9	5	23	19	17
ARID5B	1.6	2.9	↑	4.1E-19	117	116	139	418	283	392
SCUBE3	1.6	2.9	↑	7.7E-07	32	29	40	124	100	72
GPR17	1.5	2.9	↑	0.0250	13	7	5	21	18	33
FZD8	1.5	2.9	↑	6.6E-89	841	781	881	2,540	2,287	2,338
ATXN1-AS1	1.5	2.9	↑	5.0E-10	69	40	52	162	136	162
SAMD3	1.5	2.8	↑	2.5E-06	27	28	43	76	90	110
RN7SKP106	1.5	2.8	↑	0.0382	14	10	2	32	23	18
MOV10L1	1.5	2.8	↑	2.0E-46	392	365	338	1,125	1,020	927
ATXN1	1.5	2.8	↑	5.0E-88	1,050	923	987	2,954	2,708	2,634
SHC3	1.5	2.8	↑	1.8E-121	2,268	2,149	2,385	6,672	6,248	6,015
FAM124B	1.5	2.8	↑	2.3E-25	255	180	238	663	530	660
ADAMTSL4	1.5	2.7	↑	4.7E-55	715	578	748	1,934	1,742	1,926
TJP2	1.4	2.7	↑	5.6E-05	35	48	17	112	71	90
CD55	1.4	2.7	↑	2.7E-175	7,902	7,895	7,341	21,293	20,414	21,186
NDST3	1.4	2.7	↑	1.9E-08	44	45	47	103	135	131
TMEM200C	1.4	2.7	↑	1.8E-104	2,202	2,028	2,168	5,895	5,294	6,014
GDF7	1.4	2.7	↑	1.6E-06	363	289	533	1,143	1,046	993
UOX	1.4	2.7	↑	0.0013	23	16	17	40	41	69
ANPEP	1.4	2.7	↑	1.5E-110	21,248	20,643	18,239	56,379	52,256	51,080
CLDN5	1.4	2.7	↑	0.0008	21	18	16	50	41	55
PRRG4	1.4	2.7	↑	0.0392	6	14	6	26	25	18
AQP11	1.4	2.6	↑	2.5E-22	142	147	152	370	434	364
KIAA0513	1.4	2.6	↑	1.2E-55	560	528	567	1,562	1,338	1,410
APOL6	1.4	2.6	↑	8.3E-50	595	601	529	1,589	1,540	1,333
FSIP2	1.4	2.6	↑	0.0008	15	26	19	53	51	51
TRPC4	1.4	2.6	↑	1.6E-05	71	28	44	151	112	104

FABP4	1.4	2.5	↑	1.8E-26	230	285	213	666	582	608
GREM1	1.3	2.5	↑	1.8E-12	95	85	92	245	191	254
IL17RA	1.3	2.5	↑	5.2E-79	972	1,000	1,010	2,674	2,396	2,466
SUSD6	1.3	2.5	↑	4.7E-102	2,318	2,165	2,046	5,663	5,423	5,359
KCTD4	1.3	2.5	↑	5.4E-17	122	137	115	282	331	329
LAMA3	1.3	2.5	↑	6.3E-84	8,047	7,939	7,997	21,783	20,633	17,677
PRAG1	1.3	2.5	↑	1.6E-103	5,431	4,783	5,356	13,635	12,772	12,551
LRRC4	1.3	2.5	↑	0.0276	25	6	11	37	44	24
RNF19B	1.3	2.5	↑	1.5E-121	4,114	4,057	3,818	10,456	9,619	9,881
LIPH	1.3	2.5	↑	0.0014	19	20	26	53	67	41
GCNT2	1.3	2.5	↑	3.4E-72	798	862	887	2,162	2,070	2,073
APOL1	1.3	2.5	↑	1.0E-40	493	522	436	1,281	1,218	1,090
MAGI2	1.3	2.5	↑	2.2E-14	109	95	108	276	246	248
IRF1-AS1	1.3	2.5	↑	5.4E-13	85	99	93	242	214	227
DUSP8	1.3	2.5	↑	1.7E-13	148	94	129	321	280	308
GATA6	1.3	2.4	↑	3.1E-47	1,492	1,174	1,454	3,700	3,142	3,247
UBE2R2-AS1	1.3	2.4	↑	0.0361	14	12	7	30	21	29
CCDC190	1.3	2.4	↑	2.4E-13	117	154	152	409	317	294
MBNL2	1.3	2.4	↑	1.5E-95	3,151	2,858	3,220	7,667	7,417	7,132
DENND4A	1.3	2.4	↑	1.2E-96	2,443	2,389	2,267	5,927	5,747	5,393
AMOT	1.3	2.4	↑	0.0484	9	17	7	28	32	19
XAF1	1.3	2.4	↑	0.0008	18	29	34	54	74	65
POSTN	1.3	2.4	↑	2.3E-17	159	196	241	502	438	480
KRT18P11	1.3	2.4	↑	0.0321	15	14	13	24	22	54
PIK3C2B	1.3	2.4	↑	4.1E-45	1,014	880	917	2,513	2,120	2,056
CCL2	1.2	2.4	↑	1.0E-57	710	658	722	1,722	1,606	1,641
DDO	1.2	2.4	↑	0.0002	29	37	63	126	73	106
DMD	1.2	2.4	↑	8.1E-58	1,225	1,113	1,340	3,070	2,842	2,774
TOX	1.2	2.3	↑	1.3E-79	2,789	2,420	2,718	6,425	6,117	5,980
C2orf27A	1.2	2.3	↑	2.2E-28	267	302	313	719	646	695
ARNTL2	1.2	2.3	↑	6.6E-130	12,110	12,643	11,928	29,515	27,453	28,609
APOL3	1.2	2.3	↑	5.5E-29	366	397	489	920	1,004	982
CREM	1.2	2.3	↑	2.1E-95	2,402	2,313	2,471	5,652	5,306	5,695
ABCA3	1.2	2.3	↑	1.9E-23	247	261	208	557	550	551
TNRC18P1	1.2	2.3	↑	0.0452	9	14	22	34	52	18
SHROOM2	1.2	2.3	↑	1.0E-40	687	589	642	1,608	1,455	1,369
NFIL3	1.2	2.3	↑	2.8E-22	426	290	374	905	800	809
SPHK1	1.2	2.3	↑	5.6E-79	7,611	7,809	7,344	18,966	15,932	17,579
MISP	1.2	2.3	↑	0.0020	40	22	27	92	50	63
CARD14	1.2	2.3	↑	0.0008	36	45	36	105	50	114

PPP1R3B	1.2	2.3	↑	1.4E-82	3,609	3,437	3,656	8,704	8,170	7,593
ITGB4	1.2	2.3	↑	3.1E-44	1,513	1,280	1,411	3,605	3,049	2,954
LRRRC8E	1.2	2.3	↑	0.0103	20	22	16	45	56	31
LGR4	1.2	2.3	↑	8.1E-64	1,311	1,151	1,262	2,728	2,800	2,906
BIK	1.2	2.2	↑	0.0148	24	23	10	37	44	47
CDC45	1.2	2.2	↑	5.4E-89	4,150	3,906	4,374	9,485	8,926	9,381
MEGF11	1.2	2.2	↑	0.0148	21	18	20	59	43	29
LIMD1-AS1	1.2	2.2	↑	0.0010	34	24	33	61	76	65
CDC42EP3	1.1	2.2	↑	9.1E-54	818	816	899	1,875	1,828	1,915
MAP3K14-AS1	1.1	2.2	↑	6.4E-06	58	66	102	206	140	155
RASSF2	1.1	2.2	↑	4.5E-47	606	646	648	1,391	1,376	1,439
NEDD4	1.1	2.2	↑	3.0E-115	5,750	5,594	5,532	12,773	12,229	12,168
MIR100HG	1.1	2.2	↑	1.9E-56	1,169	1,198	1,245	2,671	2,461	2,802
HK1	1.1	2.2	↑	3.5E-111	13,828	13,783	13,705	31,798	28,996	29,784
CALHM5	1.1	2.2	↑	8.2E-42	812	708	804	1,813	1,614	1,663
COL5A2	1.1	2.2	↑	6.5E-79	54,385	50,739	56,804	126,571	114,474	112,550
IRF1	1.1	2.2	↑	3.9E-41	980	1,210	1,218	2,589	2,414	2,438
LNCOG	1.1	2.2	↑	2.4E-53	856	845	834	1,881	1,757	1,887
LRP1B	1.1	2.2	↑	4.0E-31	378	393	367	845	798	836
WNT5A-AS1	1.1	2.2	↑	0.0426	11	18	16	44	30	24
ENSG00000234290	1.1	2.2	↑	0.0025	33	26	32	46	78	74
FGF12	1.1	2.2	↑	9.3E-09	143	159	101	348	283	244
SLC22A4	1.1	2.2	↑	8.5E-48	722	677	720	1,553	1,514	1,513
GDF6	1.1	2.2	↑	6.9E-76	2,093	1,962	2,113	4,566	4,445	4,293
SLIT2	1.1	2.2	↑	3.7E-68	13,671	13,944	12,714	31,537	28,334	26,983
FGD4	1.1	2.1	↑	2.5E-89	2,720	2,668	2,806	5,891	5,940	5,695
F5	1.1	2.1	↑	0.0088	50	18	44	97	49	92
GATA3	1.1	2.1	↑	1.4E-08	87	99	108	227	185	212
JAG1	1.1	2.1	↑	7.7E-77	13,457	12,326	12,740	29,210	26,395	26,103
SLC25A25	1.1	2.1	↑	6.2E-65	1,688	1,661	1,601	3,671	3,477	3,349
ARHGAP5-AS1	1.1	2.1	↑	4.9E-13	182	188	208	379	361	485
SMCO2	1.1	2.1	↑	0.0068	39	44	15	76	67	64
S1PR3	1.1	2.1	↑	2.7E-51	1,220	1,150	1,243	2,663	2,582	2,378
MAP3K14	1.1	2.1	↑	5.8E-79	2,575	2,383	2,445	5,269	5,090	5,253
RUNX2	1.1	2.1	↑	1.5E-10	112	124	118	248	254	241
SEMA3C	1.1	2.1	↑	2.6E-77	5,492	5,313	5,799	12,115	11,513	11,046
PDE3A	1.1	2.1	↑	1.0E-38	694	665	682	1,505	1,341	1,416
ANK3	1.1	2.1	↑	2.5E-16	301	370	290	760	651	591

TCAF2C	1.1	2.1	↑	0.0059	27	26	25	54	51	57
ZNF175	1.1	2.1	↑	8.9E-58	2,404	2,097	2,225	4,636	4,840	4,477
UFD1	1.1	2.1	↑	1.7E-94	5,557	5,483	5,794	11,649	11,323	11,892
ELK3	1.0	2.1	↑	5.5E-97	8,643	8,472	8,187	17,960	16,903	17,404
MICE	1.0	2.1	↑	0.0087	27	40	25	66	81	43
ANKRD29	1.0	2.1	↑	1.7E-13	192	220	192	470	402	375
PTGDR2	1.0	2.1	↑	0.0015	34	36	39	70	91	64
HRH1	1.0	2.1	↑	2.9E-68	3,196	3,064	3,126	6,843	6,137	6,312
PDCD1LG2	1.0	2.0	↑	2.5E-42	1,162	1,138	1,093	2,371	2,119	2,462
ZSWIM5	1.0	2.0	↑	0.0264	25	15	22	50	34	43
ABCB1	1.0	2.0	↑	2.2E-22	374	376	428	869	742	800
ARHGAP40	1.0	2.0	↑	0.0005	41	71	55	115	138	88
CTSO	1.0	2.0	↑	3.1E-16	243	326	316	608	568	630
MME	1.0	2.0	↑	3.9E-84	13,021	12,704	12,669	27,681	25,577	25,005
NIPAL4	1.0	2.0	↑	3.6E-36	728	706	822	1,535	1,539	1,510
IL18R1	1.0	2.0	↑	5.2E-06	87	69	69	140	168	148
ERCC6	1.0	2.0	↑	1.8E-77	5,832	5,591	5,705	12,043	11,630	10,938
CAPNS2	-1.0	-2.0	↓	0.0036	59	73	74	37	28	38
HLA-DPA1	-1.0	-2.0	↓	0.0117	40	69	65	27	28	32
STAC	-1.0	-2.0	↓	0.0176	38	53	52	23	27	21
TGFA	-1.0	-2.0	↓	1.6E-57	3,996	3,638	4,000	1,921	1,894	1,961
LCE2A	-1.0	-2.0	↓	6.0E-05	176	181	146	114	56	79
GDI2P2	-1.0	-2.0	↓	0.0203	56	48	42	19	19	34
HS1BP3-IT1	-1.0	-2.0	↓	0.0004	102	98	86	55	48	38
CST1	-1.0	-2.0	↓	1.3E-06	1,296	1,633	1,024	650	640	657
FAM24B	-1.0	-2.0	↓	5.1E-33	1,413	1,529	1,557	771	668	774
ROBO4	-1.0	-2.0	↓	1.5E-36	5,039	4,379	4,316	2,460	2,273	2,006
HHIP	-1.0	-2.0	↓	4.9E-53	12,562	11,483	12,104	6,077	5,319	6,329
PLPP4	-1.0	-2.0	↓	1.6E-12	371	452	514	210	213	232
NRARP	-1.0	-2.0	↓	7.7E-11	280	263	274	137	136	126
DRGX	-1.0	-2.1	↓	0.0486	48	32	25	17	17	17
COL5A1-AS1	-1.1	-2.1	↓	0.0278	43	36	35	18	21	16
FAM90A23P	-1.1	-2.1	↓	0.0366	40	66	50	18	13	44
NXF3	-1.1	-2.1	↓	0.0005	101	83	79	51	35	40
POU2F2	-1.1	-2.1	↓	1.1E-12	410	402	339	197	197	157
SDCBP2	-1.1	-2.1	↓	3.8E-16	415	450	468	215	228	194
NTM	-1.1	-2.1	↓	4.2E-10	253	243	243	130	118	105
MAF	-1.1	-2.1	↓	0.0097	48	43	83	29	28	26
EIF2B5-DT	-1.1	-2.1	↓	0.0237	36	36	40	19	17	17
HSD17B6	-1.1	-2.1	↓	0.0024	66	61	78	23	34	40

ZNF704	-1.1	-2.1	↓	2.8E-11	257	315	292	147	129	132
LONRF2	-1.1	-2.1	↓	0.0404	39	57	48	40	9	19
KCNN3	-1.1	-2.1	↓	1.3E-10	295	300	297	147	164	110
DRP2	-1.1	-2.1	↓	2.9E-09	312	304	220	135	117	142
CD93	-1.1	-2.1	↓	4.0E-50	15,427	16,117	13,846	7,810	7,096	6,471
FAM131C	-1.1	-2.1	↓	0.0218	42	43	45	31	13	17
SP6	-1.1	-2.1	↓	0.0356	47	39	25	13	22	17
USHBP1	-1.1	-2.1	↓	3.4E-18	645	664	593	345	297	248
GPR4	-1.1	-2.1	↓	1.5E-12	423	358	311	174	176	160
SSTR2	-1.1	-2.1	↓	0.0482	35	50	20	19	14	16
GIMAP4	-1.1	-2.1	↓	4.8E-27	830	777	736	355	354	383
NLRC3	-1.1	-2.1	↓	1.2E-13	402	389	384	213	148	186
CD177	-1.1	-2.1	↓	8.6E-07	158	154	163	84	56	81
KLK6	-1.1	-2.2	↓	0.0191	56	35	36	24	16	19
SMN1	-1.1	-2.2	↓	0.0479	2,108	1,452	697	651	679	634
KLHL6	-1.1	-2.2	↓	0.0027	66	69	82	31	20	49
CLEC2B	-1.1	-2.2	↓	0.0013	66	92	97	54	39	24
CCRL2	-1.1	-2.2	↓	4.2E-07	189	212	153	102	85	67
ADGRG1	-1.1	-2.2	↓	7.0E-67	1,476	16,417	15,313	8,138	7,239	7,062
SPRY1	-1.1	-2.2	↓	1.0E-08	274	328	344	166	171	96
HES7	-1.1	-2.2	↓	5.2E-16	361	375	346	158	172	162
OR7E96P	-1.1	-2.2	↓	0.0020	73	54	60	25	25	35
LAMB3	-1.1	-2.2	↓	3.3E-66	7,915	8,510	7,251	3,759	3,527	3,464
TTLL11-IT1	-1.1	-2.2	↓	0.0005	81	139	74	49	48	36
BHLHE41	-1.2	-2.2	↓	2.1E-05	124	98	96	48	50	45
BAIAP3	-1.2	-2.2	↓	0.0240	43	39	27	12	17	20
LTF	-1.2	-2.2	↓	0.0475	32	21	36	18	12	10
SH2D3C	-1.2	-2.2	↓	2.3E-20	630	506	603	277	243	261
MIR126	-1.2	-2.2	↓	2.2E-07	237	207	263	112	68	137
KDR	-1.2	-2.2	↓	8.4E-49	1,697	1,862	1,736	822	813	736
CLDN16	-1.2	-2.2	↓	0.0235	33	33	37	16	19	11
FAM43A	-1.2	-2.2	↓	5.7E-58	7,822	7,190	8,176	3,820	3,200	3,311
TXLNB	-1.2	-2.3	↓	0.0107	39	36	51	18	22	16
PSG4	-1.2	-2.3	↓	6.9E-43	1,619	1,668	1,926	742	780	793
LCT	-1.2	-2.3	↓	0.0255	32	48	26	18	13	16
TMEM156	-1.2	-2.3	↓	0.0093	38	65	62	22	14	37
EFCC1	-1.2	-2.3	↓	0.0326	41	30	40	16	26	7
LCNL1	-1.2	-2.3	↓	0.0215	41	52	25	19	21	12
TNFSF15	-1.2	-2.3	↓	1.2E-46	1,214	1,260	1,239	556	529	551
NRROS	-1.2	-2.3	↓	0.0492	35	20	32	11	8	19

MYL2	-1.2	-2.3	↓	0.0068	46	42	41	19	22	15
GSTM4	-1.2	-2.3	↓	0.0007	81	102	78	59	30	24
TUBA5P	-1.2	-2.3	↓	0.0079	38	55	48	15	16	30
MYH16	-1.2	-2.3	↓	1.3E-09	210	226	187	108	75	86
GIMAP7	-1.2	-2.3	↓	7.7E-09	165	159	175	75	63	77
DHRS2	-1.2	-2.3	↓	6.8E-76	4,035	3,678	3,996	1,735	1,587	1,720
CYP1A1	-1.2	-2.3	↓	2.0E-11	278	230	333	109	126	127
VWA5B2	-1.2	-2.3	↓	0.0310	29	38	24	14	9	16
LFNG	-1.3	-2.4	↓	4.3E-35	1,465	1,324	1,456	686	504	582
EFNB1	-1.3	-2.4	↓	2.4E-101	4,727	4,527	4,518	1,993	1,892	1,859
PLAC8	-1.3	-2.4	↓	0.0028	49	41	72	16	28	23
ARC	-1.3	-2.4	↓	5.7E-16	440	444	509	233	142	198
RASGRP3	-1.3	-2.4	↓	0.0095	45	46	31	12	13	25
SORL1	-1.3	-2.4	↓	0.0164	21	45	44	17	11	17
FCN3	-1.3	-2.5	↓	1.0E-09	194	175	176	57	81	84
GRAMD1B	-1.3	-2.5	↓	3.2E-55	3,841	4,265	3,704	1,810	1,554	1,444
CD34	-1.3	-2.5	↓	2.6E-57	2,266	2,007	2,317	853	852	964
SIRPB2	-1.3	-2.5	↓	4.3E-77	2,934	2,793	2,746	1,196	1,058	1,173
DMBT1L1	-1.3	-2.5	↓	0.0423	34	33	20	19	12	4
MPZL2	-1.3	-2.5	↓	1.1E-118	5,910	5,512	5,723	2,290	2,211	2,334
ADGRB3	-1.3	-2.5	↓	4.5E-48	1,476	1,614	1,338	620	586	548
COL13A1	-1.3	-2.5	↓	4.2E-49	1,542	1,529	1,532	684	529	604
RFPL2	-1.4	-2.6	↓	0.0009	52	55	64	24	13	30
CXCL2	-1.4	-2.6	↓	1.9E-10	190	205	167	66	64	90
FAM90A14P	-1.4	-2.6	↓	0.0003	69	55	78	34	28	17
ZG16B	-1.4	-2.6	↓	3.3E-05	69	77	74	27	29	30
CYB5R2	-1.4	-2.6	↓	0.0029	36	46	46	21	14	15
TRAC	-1.4	-2.6	↓	0.0008	42	52	58	20	20	19
ADORA1	-1.4	-2.6	↓	1.8E-48	959	916	972	370	375	358
EXOC3L1	-1.4	-2.6	↓	3.0E-11	222	183	196	91	80	61
PFKP-DT	-1.4	-2.6	↓	0.0453	19	18	33	5	12	10
MOBP	-1.4	-2.6	↓	2.2E-34	930	882	1,077	402	320	392
DDIT4	-1.4	-2.6	↓	1.6E-36	899	779	977	358	335	329
PTPN6	-1.4	-2.6	↓	0.0499	26	21	21	14	3	9
HR	-1.4	-2.6	↓	6.7E-05	76	82	73	39	32	17
MT2A	-1.4	-2.7	↓	6.6E-117	46,099	39,961	40,711	16,594	15,839	15,264
ANKRD20A1	-1.4	-2.7	↓	3.0E-06	101	101	75	34	30	40
PRR29-AS1	-1.4	-2.7	↓	0.0006	50	53	45	18	16	21
DUSP5-DT	-1.5	-2.7	↓	1.5E-11	212	190	164	81	56	70
INSL4	-1.5	-2.7	↓	5.7E-07	155	94	198	67	44	52

MT1E	-1.5	-2.7	↓	4.7E-95	3,728	4,010	4,297	1,538	1,457	1,392
RAET1E	-1.5	-2.8	↓	0.0007	41	47	49	13	19	17
EWSAT1	-1.5	-2.8	↓	0.0225	34	19	23	13	9	5
CHGA	-1.5	-2.9	↓	0.0240	27	14	36	13	7	7
CPNE5	-1.5	-2.9	↓	3.0E-09	165	118	152	55	35	60
CST4	-1.6	-2.9	↓	0.0001	67	63	52	11	29	22
SYN1	-1.6	-2.9	↓	0.0369	23	14	19	6	7	6
CUBNP2	-1.6	-3.0	↓	0.0374	22	17	23	13	4	4
LST1	-1.6	-3.0	↓	0.0293	39	16	16	8	5	11
CHST2	-1.6	-3.0	↓	2.4E-129	4,733	4,632	4,647	1,656	1,445	1,631
SHE	-1.6	-3.0	↓	0.0122	20	30	33	7	6	15
MT2P1	-1.6	-3.0	↓	8.5E-23	2,537	2,381	2,557	684	809	988
NLRP11	-1.6	-3.0	↓	0.0113	21	22	33	6	9	10
CMKLR1	-1.6	-3.1	↓	0.0003	44	41	54	18	16	11
PATJ	-1.6	-3.1	↓	0.0171	32	17	19	7	7	8
BCAS1	-1.6	-3.1	↓	0.0021	39	34	27	13	9	10
FREM3	-1.7	-3.1	↓	0.0195	26	20	20	3	7	11
PIWIL1	-1.7	-3.1	↓	0.0145	39	16	30	3	15	9
FAM90A21P	-1.7	-3.2	↓	0.0252	16	17	24	6	7	5
RPL7P15	-1.7	-3.2	↓	0.0385	25	16	13	3	5	9
MT1X	-1.7	-3.2	↓	5.3E-36	574	506	498	145	184	165
FGD5	-1.7	-3.3	↓	0.0122	18	37	23	9	12	3
B3GAT1-DT	-1.7	-3.3	↓	0.0006	36	34	39	11	9	13
CCM2L	-1.7	-3.3	↓	3.6E-44	760	715	712	266	198	193
ATP1A3	-1.7	-3.3	↓	0.0181	15	20	25	8	6	4
PSMD10P2	-1.7	-3.4	↓	0.0463	14	16	17	6	1	7
MYLK2	-1.8	-3.4	↓	8.6E-107	1,786	1,869	1,897	587	546	513
RNVU1-15	-1.8	-3.4	↓	0.0040	35	39	18	6	14	7
SLIT3	-1.8	-3.5	↓	1.1E-06	104	68	125	18	22	46
HID1	-1.8	-3.5	↓	5.6E-05	65	43	55	11	11	25
KSR2	-1.8	-3.5	↓	1.3E-22	265	257	254	86	60	77
JPH2	-1.8	-3.5	↓	0.0012	38	27	50	7	7	19
CYGB	-1.8	-3.5	↓	0.0334	22	14	27	14	1	3
GABBR2	-1.8	-3.5	↓	2.1E-08	79	100	77	25	21	27
CAPN11	-1.9	-3.7	↓	4.5E-08	144	113	73	17	37	36
CYP2B7P	-1.9	-3.7	↓	4.5E-28	330	321	290	93	70	93
LIPG	-1.9	-3.8	↓	1.0E-146	5,287	4,830	5,092	1,245	1,285	1,510
HMG2P28	-1.9	-3.8	↓	0.0076	27	22	15	5	5	7
BDH1	-1.9	-3.8	↓	0.0187	11	35	15	3	4	9
KCNJ12	-2.0	-3.9	↓	1.8E-14	183	165	118	38	36	45
VSTM1	-2.0	-4.1	↓	0.0006	43	24	27	7	7	9

SDR42E1	-2.0	-4.1	↓	3.3E-14	129	127	118	35	25	31
FAM172BP	-2.1	-4.1	↓	2.1E-09	114	74	102	34	21	15
ITGB2-AS1	-2.1	-4.2	↓	1.9E-09	87	70	120	21	17	28
CCL23	-2.1	-4.2	↓	0.0009	28	29	23	5	7	7
ANKRD2	-2.1	-4.2	↓	0.0001	39	32	43	7	15	5
PCDH19	-2.1	-4.2	↓	0.0210	15	6	34	3	5	5
NOG	-2.1	-4.3	↓	1.5E-20	302	235	287	53	45	95
HSD17B2	-2.1	-4.3	↓	1.7E-11	88	132	97	30	19	24
CEACAMP10	-2.2	-4.5	↓	0.0070	22	10	26	4	5	4
ZNF114	-2.2	-4.6	↓	1.7E-13	92	121	137	30	21	25
ENSG00000204282	-2.2	-4.6	↓	0.0038	15	24	21	5	5	3
TRPM3	-2.2	-4.6	↓	0.0146	6	24	21	3	3	5
APLN	-2.2	-4.7	↓	5.8E-200	11,537	11,646	10,109	2,643	2,242	2,252
KRTAP2-3	-2.3	-4.8	↓	0.0035	22	52	13	1	5	12
CNBD2	-2.4	-5.2	↓	0.0030	32	23	13	9	3	1
CRLF2	-2.4	-5.3	↓	2.5E-07	61	54	54	16	3	13
DMBT1	-2.5	-5.6	↓	2.2E-49	357	350	354	67	63	60
PLEK2	-2.6	-6.0	↓	5.7E-12	89	114	66	21	13	11
LILRB5	-2.6	-6.2	↓	0.0028	17	11	28	1	3	5
C11orf96	-2.6	-6.2	↓	0.0057	13	9	28	1	3	4
ADGRG5	-2.7	-6.4	↓	0.0068	18	7	26	6	1	1
CSF2	-2.7	-6.6	↓	2.4E-05	36	34	23	4	7	3
IVL	-2.7	-6.7	↓	3.2E-11	65	85	77	9	19	6
KRT81	-3.0	-8.0	↓	7.3E-106	1,034	1,034	853	103	110	154
AFAP1L2	-3.4	-10.3	↓	6.1E-05	20	23	29	1	1	5

Supplementary table 3- 7: IL-4 DEGs in EA.hy926^{PLKO-1} cells

Term	Count	%	PValue	Genes
GO:0042493~response to drug	15	7.4	2.32E-06	NTRK1, ABCB1, SEMA3C, ABCA3, GATA6, GATA3, INHBA, SLC8A1, IL6, SFRP1, LOX, CASP3, PDE3A, KCNK3, ABCG2
GO:0048468~cell development	6	3.0	4.68E-05	GATA6, ARID5B, IRF6, INHBA, GDF6, GDF7
GO:0071356~cellular response to tumor necrosis factor	8	4.0	1.19E-04	IL6, SFRP1, POSTN, FABP4, CCL2, HAS2, GATA3, CCL26
GO:0030198~extracellular matrix organization	10	5.0	1.60E-04	POSTN, LOX, ITGB4, ADAMTSL4, ABI3BP, LAMA3, COL5A2, ITGAV, HAPLN1, JAM2
GO:0071347~cellular response to interleukin-1	6	3.0	7.22E-04	IL6, SFRP1, PTGIS, CCL2, HAS2, CCL26
GO:0006869~lipid transport	6	3.0	9.84E-04	APOL6, ABCA6, ABCA3, ABCA9, APOL1, APOL3

GO:0070374~positive regulation of ERK1 and ERK2 cascade	8	4.0	0.0019	NTRK1, IL6, CYSLTR2, GCNT2, CCL2, CCR7, PLA2G5, CCL26
GO:0019221~cytokine-mediated signaling pathway	7	3.5	0.0020	IL6, SOCS1, LRRC4, IL20RB, CCL2, IL12RB1, IL17RA
GO:0045893~positive regulation of transcription, DNA-templated	14	6.9	0.0021	GATA6, GATA3, INHBA, GDF6, ARNTL2, RUNX2, ELK3, GDF7, IL6, SFRP1, IRF1, HAS3, IRF6, LGR4
GO:0030335~positive regulation of cell migration	8	4.0	0.0025	SERPINB3, SEMA3C, TNFAIP6, SPHK1, GCNT2, HAS2, ITGAV, CCL26
GO:0032689~negative regulation of interferon-gamma production	4	2.0	0.0027	IL1RL1, IL20RB, GATA3, PDCD1LG2
GO:0071773~cellular response to BMP stimulus	4	2.0	0.0033	SFRP1, GATA6, GATA3, RUNX2
GO:0060395~SMAD protein signal transduction	5	2.5	0.0034	MAGI2, BTBD11, INHBA, GDF6, GDF7
GO:0006955~immune response	12	5.9	0.0035	IL1RL1, IL6, CYSLTR2, SEMA3C, NFIL3, PTGDR2, CCL2, CCR7, PDCD1LG2, MAP3K14, IL18R1, CCL26
GO:0045892~negative regulation of transcription, DNA-templated	13	6.4	0.0045	VDR, GATA6, CREM, ARID5B, GATA3, RUNX2, ELK3, GREM1, SFRP1, ATXN1, FABP4, IRF1, LGR4
GO:0006508~proteolysis	13	6.4	0.0045	CPA3, MMP7, MME, FGL2, F5, CTSO, SFRP1, ADAMTSL4, ANPEP, CASP3, MMP28, MASP1, PRSS3
GO:0006954~inflammatory response	11	5.4	0.0049	SELP, IL6, HRH1, TNFAIP6, SPHK1, SCN9A, CCL2, CCR7, S1PR3, APOL3, CCL26
GO:0046849~bone remodeling	3	1.5	0.0052	IL6, RASSF2, LGR4
GO:0045766~positive regulation of angiogenesis	6	3.0	0.0060	NTRK1, GREM1, CYSLTR2, PTGIS, SPHK1, GATA6
GO:0050710~negative regulation of cytokine secretion	3	1.5	0.0061	IL6, LRRC32, LGR4
GO:0043116~negative regulation of vascular permeability	3	1.5	0.0061	PDE3A, SLIT2, AMOT
GO:0070588~calcium ion transmembrane transport	6	3.0	0.0069	TRPC4, PKD1L1, ITGAV, ATP2B2, SLC8A1, SLC25A25
GO:0003215~cardiac right ventricle morphogenesis	3	1.5	0.0072	JAG1, SEMA3C, GATA3
GO:0050892~intestinal absorption	3	1.5	0.0084	VDR, GCNT3, TJP2
GO:0042060~wound healing	5	2.5	0.0085	IL6, SERPINB2, LOX, CASP3, ELK3
GO:0032924~activin receptor signaling pathway	3	1.5	0.0109	INHBA, GDF6, GDF7
GO:0055085~transmembrane transport	8	4.0	0.0116	SLC46A3, ABCB1, ABCA6, ABCA3, ABCA9, CSN1S1, SLC15A3, SLC25A25
GO:0010466~negative regulation of peptidase activity	3	1.5	0.0123	SERPINB3, SERPINB4, PI16

GO:0010765~positive regulation of sodium ion transport	3	1.5	0.0152	ANK3, SCN3B, FGF12
GO:0071456~cellular response to hypoxia	5	2.5	0.0158	SFRP1, PTGIS, GATA6, KCNK3, SLC8A1
GO:0042346~positive regulation of NF-kappaB import into nucleus	3	1.5	0.0184	GREM1, SPHK1, IL18R1

Supplementary table 3- 8: GO analysis based on the biological process on IL-4-up-regulated genes in EA.hy926^{PLKO-1}

Sup table 8

Term	Count	%	PValue	Genes
GO:0045926~negative regulation of growth	3	1.9	0.008	MT2A, MT1X, MT1E
GO:0071294~cellular response to zinc ion	3	1.9	0.008	MT2A, MT1X, MT1E
GO:0002026~regulation of the force of heart contraction	3	1.9	0.008	CHGA, MYL2, APLN
GO:0006955~immune response	9	5.6	0.010	CCL23, CSF2, NRROS, TNFSF15, LST1, CXCL2, CMKLR1, HLA-DPA1, APLN
GO:0070098~chemokine-mediated signaling pathway	4	2.5	0.014	CCL23, CCRL2, CXCL2, CMKLR1
GO:0036018~cellular response to erythropoietin	2	1.2	0.014	MT2A, MT1X
GO:1902367~negative regulation of Notch signaling pathway involved in somitogenesis	2	1.2	0.014	LFNG, NRARP
GO:0008283~cell proliferation	8	4.9	0.015	LIPG, DDIT4, BHLHE41, CYP1A1, TGFA, PTPN6, CD34, INSL4
GO:0031295~T cell costimulation	4	2.5	0.018	EFNB1, TRAC, PTPN6, HLA-DPA1
GO:0008285~negative regulation of cell proliferation	8	4.9	0.023	CCL23, ADGRG1, ADORA1, PTPN6, SLIT3, SPRY1, SSTR2, DHRS2
GO:0055114~oxidation-reduction process	10	6.2	0.025	CYB5R2, SDR42E1, NLRP11, BDH1, HHIP, HSD17B2, CYP1A1, HR, HSD17B6, DHRS2
GO:0043407~negative regulation of MAP kinase activity	3	1.9	0.027	PTPN6, SPRY1, SORL1
GO:0016048~detection of temperature stimulus	2	1.2	0.028	TRPM3, DRGX
GO:1901215~negative regulation of neuron death	3	1.9	0.033	CHGA, CD34, SORL1
GO:0001895~retina homeostasis	3	1.9	0.033	ZG16B, CST4, LTF
GO:0007267~cell-cell signaling	6	3.7	0.035	EFNB1, CCL23, ADGRG1, ADORA1, SSTR2, INSL4
GO:0016337~single organismal cell-cell adhesion	4	2.5	0.035	CD93, COL13A1, CD34, MPZL2
GO:0060048~cardiac muscle contraction	3	1.9	0.040	MYLK2, MYL2, ATP1A3
GO:0003158~endothelium development	2	1.2	0.042	KDR, CD34
GO:0045908~negative regulation of vasodilation	2	1.2	0.042	CHGA, ADORA1

GO:0014807~regulation of somitogenesis	2	1.2	0.049	LFNG, HES7
--	---	-----	-------	------------

Supplementary table 3- 9: GO analysis based on the biological process on IL-4–down-regulated genes in EA.hy926^{PLKO-1}

Term	EA,hy926 (RPKM)	Count	%	PValue	Genes
BACH1	2,715	173	47.5	2.04E-05	EXOC3L1, FCN3, PATJ, NRROS, CSF2, CPNE5, HHIP, LST1, HR, ANKRD20A1, SLC8A1, HID1, AMOT, ELK3, NIPAL4, RIMS1, DMBT1, NDST3, LIPG, SCN9A, ADORA1, AP1S3, PRSS3, TCP11, MBNL2, MAGI2, ARID5B, ANK3, MIR100HG, SDCBP2, RUNX2, ADAM19, SFRP1, LCE2A, PLPP4, TXLNB, LOX, PPP1R3B, ADGRB3, DDIT4, TNIK, MASP1, TOX, C11ORF96, SHC3, ABCB1, COL13A1, NTM, IL20RB, TGFA, CSF2RB, GATA3, DTX4, PCDH19, KLK6, CYB5R2, EFNB1, SCUBE3, ADGRG1, NUAK1, HRH1, ATXN1, SOCS1, MOBP, ZNF704, ADGRG5, PLEK2, KCNN3, SCN3B, NKX2-3, TRPM3, ANKRD29, AFAP1L2, JAG1, DENND4A, ZG16B, ST8SIA1, STAC, VDR, BTBD11, INHBA, GDF6, POU2F2, LRP1B, MEX3B, COL5A2, PDE3A, SP6, CYP2B7P, MAP3K14, FGF12, ROBO4, ITGB4, MEGF11, LRRC4, SIRPB2, NRARP, LRRC32, LFNG, ADAMTSL4, CASP3, MMP28, CCR7, ANKRD2, CERS6, SERPINB2, MMP7, MME, TRPC4, SPHK1, NOG, SH2D3C, SHROOM2, KSR2, DUSP8, SYN1, F5, GREM1, BDH1, SLC7A8, IRF1, CDC42EP3, IRF6, ZNF474, GRAMD1B, SEMA3C, LAMA3, PKD1L1, NLRC3, TMEM71, DRP2, PRRG4, KIAA0513, CDC45, NFIL3, HSD17B2, GCNT2, HAS3, HAS2, SUSD6, S1PR3, SLIT3, DMD, KRTAP2-3, SLIT2, IL12RB1, APOL1, FNIP2, ZSWIM5, LRRC8E, SLC25A25, APOL3, SAMD3, DRGX, MUC6, NTRK1, GABBR2, LAMB3, KCNJ12, ATP2B2, SORL1, HS3ST1, APLN, BAIAP3, TMEM156, FABP4, CLCN4, FAM131C, MAP3K14-AS1, PTPN6, ERCC6, KCNK3, TJP2
SOX9	3.67	154	42.3	5.70E-05	EXOC3L1, PATJ, CPNE5, TMEM200A, HHIP, HR, SLC8A1, HID1, AMOT, ELK3, RIMS1, RASSF2, SESN3, DMBT1, CAPNS2, LIPG, SCN9A, AP1S3, MBNL2, CD93, MAGI2, ARID5B, ANK3, VWA5B2, KCTD4, MIR100HG, RUNX2, ADAM19, CLDN5, SFRP1, PLPP4, MAF, TXLNB, PPP1R3B, ADGRB3, TNIK, MASP1, TOX, SHC3, ABCB1, COL13A1, NTM, CREM, IL20RB, TGFA, DTX4, PCDH19, RASGRP3, EFNB1, SCUBE3, ATXN1, ZNF704, MOV10L1, KCNN3, SLC15A3, TRPM3, ANKRD29, GPR17, JAG1, ST8SIA1, STAC, ABCA6, VDR, ABCA9, FZD8, BTBD11, INHBA, POU2F2, LRP1B, SELP, MEX3B, COL5A2, PDE3A, SP6, FGF12, RTP4, ITGB4, MEGF11, BHLHE41, LRRC4, NRARP, HK1, PIK3C2B, LFNG, ADAMTSL4, MMP28, ITGAV, CCR7, ANKRD2, CD34, BCAS1, SMIM14, SERPINB3, SERPINB4, CERS6, SERPINB2, MMP7, MME, TRPC4, SPHK1, NOG, SH2D3C, SHROOM2, KSR2, PDCD1LG2, SYN1, F5, GREM1, SLC7A8, IRF1, CDC42EP3, IRF6, LCT, KRT81, GRAMD1B, SEMA3C, LAMA3, CCM2L, PKD1L1, TMEM71, DRP2, FGD4, FGD5, CDC45, NXF3, NFIL3, ABI3BP, HSD17B2, GCNT2, HAS2, SUSD6, S1PR3, SLIT3, DMD, SLIT2, FNIP2, ZSWIM5, APOL3, SAMD3, DRGX, GABBR2, LAMB3, KCNJ12, GPR4, ATP2B2, SORL1, APLN, FABP4, FAM131C, NEDD4, SPRY1, PTPN6, LGR4, KCNK3
NF1	3,926	131	36.0	1.67E-04	MYLK2, EXOC3L1, NRROS, CSF2, CPNE5, HHIP, TMEM200C, HR, SLC8A1, AMOT, ELK3, NPPB, LCNL1, SESN3, ANPEP, LIPG, SCN9A, ADORA1, AP1S3, CMKLR1, MBNL2, MAGI2, ARID5B, VWA5B2, MIR100HG, RUNX2, ARC, LOX, TNIK, MASP1, TOX,

					ABCG2, SHC3, ABCB1, COL13A1, USHBP1, NTM, GATA6, IL20RB, DTX4, PCDH19, RASGRP3, CYB5R2, EFNB1, SCUBE3, ADGRG1, NUAK1, ATXN1, SOCS1, PLEK2, KCNN3, NKX2-3, TRPM3, ANKRD29, GPR17, JAG1, ZG16B, ST8SIA1, STAC, TNFSF15, VDR, ABCA9, BTBD11, GDF6, POU2F2, LRP1B, SELP, PDE3A, SP6, SLC26A4, EFCC1, FGF12, ITGB4, MEGF11, PTGDR2, LRRC4, NRARP, LRRC32, LFNG, JPH2, ADAMTSL4, BCAS1, MME, SPHK1, NOG, SH2D3C, KSR2, PDCD1LG2, DUSP8, F5, GREM1, SLC7A8, IRF6, CHST2, GRAMD1B, SEMA3C, PKD1L1, ATP1A3, CYGB, FGD5, ABI3BP, HAS3, CCL2, S1PR3, SLIT3, DMD, SLIT2, FNIP2, ZSWIM5, LRRC8E, SLC25A25, DRGX, GABBR2, CCL23, LAMB3, KCNJ12, GPR4, ATP2B2, DHRS2, SORL1, APLN, BAIAP3, CAPN11, CLCN4, FAM131C, NEDD4, PTPN6, ERCC6, LGR4, KCNK3, UOX
NFE2	4.67	124	34.1	2.98E-04	EXOC3L1, FCN3, PATJ, CSF2, CPNE5, HHIP, LST1, HR, ANKRD20A1, SLC8A1, HID1, ELK3, ANPEP, SCN9A, ADORA1, SMCO2, CMKLR1, HES7, MBNL2, MAGI2, ARID5B, ANK3, VWA5B2, MIR100HG, SDCBP2, RUNX2, ADAM19, ARC, TXLNB, PPP1R3B, ADGRB3, TNIK, TOX, C11ORF96, SHC3, ABCB1, USHBP1, NTM, GATA6, IL20RB, TGFA, GATA3, PCDH19, CYB5R2, C2ORF27A, EFNB1, SCUBE3, ADGRG1, NUAK1, ATXN1, SOCS1, PLEK2, KCNN3, SLC15A3, SCN3B, TRPM3, JAG1, DENND4A, ZG16B, FZD8, BTBD11, POU2F2, LRP1B, GDF7, PDE3A, MAP3K14, FGF12, ROBO4, ITGB4, MEGF11, LRRC4, CXCL2, PIK3C2B, LFNG, SHE, ADAMTSL4, MMP28, ITGAV, BCAS1, MME, SPHK1, SH2D3C, KSR2, BDH1, SLC7A8, IRF1, IRF6, CLDN16, IVL, GRAMD1B, LAMA3, CCM2L, PKD1L1, ATP1A3, CYGB, DRP2, FGD4, CDC45, NXF3, ABI3BP, GCNT2, HAS3, HAS2, SUSD6, SLIT3, DMD, SLIT2, FNIP2, ZSWIM5, LRRC8E, SLC25A25, MPZL2, NTRK1, GABBR2, PRSS35, GPR4, ATP2B2, SORL1, HS3ST1, BAIAP3, NLRP11, KLHL6, MAP3K14-AS1, LGR4
BACH2	3.67	143	39.3	9.93E-04	EXOC3L1, FCN3, NRROS, CPNE5, HHIP, LST1, HR, SLC8A1, HID1, AMOT, ELK3, NIPAL4, NDST3, LIPG, SCN9A, ADORA1, CMKLR1, MBNL2, MAGI2, ARID5B, ANK3, VWA5B2, MIR100HG, SDCBP2, RUNX2, ADAM19, SFRP1, LCE2A, MAF, LOX, PPP1R3B, ADGRB3, DDIT4, TNIK, TOX, C11ORF96, SHC3, ABCB1, NTM, IL20RB, TGFA, GATA3, PLA2G5, PCDH19, KLK6, EFNB1, SCUBE3, ADGRG1, NUAK1, HRH1, ATXN1, MOBP, FAM43A, KCNN3, SCN3B, LONRF2, TRPM3, ANKRD29, JAG1, DENND4A, ZG16B, ST8SIA1, STAC, VDR, BTBD11, INHBA, GDF6, POU2F2, LRP1B, MEX3B, COL5A2, CYP1A1, PDE3A, SP6, CYP2B7P, SLC26A4, MAP3K14, FGF12, ROBO4, ITGB4, MEGF11, LRRC4, NRARP, LRRC32, CXCL2, HAPLN1, LFNG, ADAMTSL4, MMP28, ITGAV, CCR7, HLA-DPA1, BCAS1, CERS6, SERPINB2, MMP7, MME, SPHK1, NOG, SH2D3C, SHROOM2, KSR2, SSTR2, SYN1, F5, SLC7A8, IRF1, IRF6, CLDN16, KRT81, GRAMD1B, SEMA3C, LAMA3, NLRC3, HSD17B6, ARNTL2, KIAA0513, FGD4, NFIL3, ABI3BP, GCNT2, HAS2, SUSD6, SLIT3, DMD, KRTAP2-3, SLIT2, FNIP2, ZSWIM5, LRRC8E, NTRK1, GABBR2, KCNJ12, SORL1, HS3ST1, APLN, BAIAP3, TMEM156, KLHL6, FAM131C, PTPN6, KCNK3, TJP2

GATA3	98.00	85	23.4	0.001	SLC46A3, EXOC3L1, MYLK2, PATJ, NRROS, ITGB4, MEGF11, LRRC4, NRARP, HR, LRRC32, SLC8A1, HAPLN1, PIK3C2B, HID1, RIMS1, CAPNS2, ADAMTSL4, NDST3, LIPG, ADORA1, CCR7, CD177, POSTN, MBNL2, SPHK1, MAGI2, ARID5B, KSR2, PDCD1LG2, DUSP8, MIR100HG, RUNX2, ARC, SLC7A8, PPP1R3B, ADGRB3, CCDC190, TOX, GRAMD1B, KRT81, SEMA3C, NTM, ATP1A3, DTX4, PCDH19, CYGB, RASGRP3, DRP2, EFNB1, SCUBE3, HRH1, ADGRG1, FGD5, ATXN1, CDC45, NFIL3, HAS3, SUSD6, SLIT3, DMD, KRTAP2-3, ZSWIM5, LRRC8E, TRPM3, NTRK1, GABBR2, AFAP1L2, EPHX4, ABCA9, ATP2B2, INHBA, GDF6, POU2F2, SORL1, HS3ST1, LRP1B, APLN, CAPN11, CLCN4, COL5A2, MAP3K14-AS1, ERCC6, MAP3K14, LGR4
SOX5	11.00	156	42.9	0.001	SLC46A3, PATJ, NRROS, CPNE5, HHIP, RNF19B, HR, SLC8A1, AMOT, ELK3, NIPAL4, RIMS1, RASSF2, SESN3, DMBT1, CAPNS2, NDST3, SCN9A, AP1S3, POSTN, MBNL2, MAGI2, ARID5B, ANK3, VWA5B2, KCTD4, MIR100HG, RUNX2, ADAM19, CLDN5, SFRP1, PLPP4, MAF, TXLNB, LOX, ADGRB3, DDIT4, TNIK, MASP1, TOX, ABCG2, SHC3, ABCB1, COL13A1, NTM, GATA6, CREM, TGFA, GATA3, DTX4, PCDH19, KLK6, RASGRP3, EFNB1, SCUBE3, FAM124B, ATXN1, ZNF704, MOV10L1, PLEK2, KCNN3, SCN3B, TRPM3, GPR17, JAG1, DENND4A, ST8SIA1, STAC, ABCA6, TNFSF15, ABCA3, FZD8, BTBD11, INHBA, POU2F2, LRP1B, SELP, MEX3B, RAET1E, COL5A2, PDE3A, NABP1, SLC26A4, MAP3K14, EFCC1, FGF12, ITGB4, MEGF11, LRRC4, NRARP, HAPLN1, HK1, PIK3C2B, LFNG, ADAMTSL4, ITGAV, BCAS1, SMIM14, SERPINB3, SERPINB4, CERS6, PTGIS, SERPINB2, MME, TRPC4, NOG, SH2D3C, SHROOM2, KSR2, ARHGAP5-AS1, SYN1, SLC7A8, IRF1, CDC42EP3, CLDN16, CHST2, ZNF474, GRAMD1B, SEMA3C, LAMA3, PKD1L1, ARNTL2, DRP2, KIAA0513, FGD4, FGD5, CDC45, NXF3, NFIL3, ABI3BP, HSD17B2, GCNT2, CCL2, HAS2, S1PR3, SLIT3, DMD, SLIT2, ZSWIM5, SAMD3, DRGX, GABBR2, GPR4, ATP2B2, SORL1, HS3ST1, APLN, BAIAP3, NEDD4, AQP11, SPRY1, PTPN6, ERCC6, LGR4, UOX, TJP2
HSF2	1,074	137	37.6	0.002	MYLK2, EXOC3L1, PATJ, NRROS, CPNE5, HHIP, TMEM200C, HR, ANKRD20A1, AMOT, ELK3, RIMS1, SESN3, CAPNS2, NDST3, LIPG, SMCO2, AP1S3, CMKLR1, HES7, POSTN, MBNL2, CD93, MAGI2, ARID5B, ANK3, VWA5B2, KCTD4, MIR100HG, RUNX2, CLDN5, SFRP1, PLPP4, PPP1R3B, ADGRB3, DDIT4, TNIK, TOX, C11ORF96, SHC3, ABCB1, NTM, TGFA, GATA3, PLA2G5, RASGRP3, EFNB1, SCUBE3, NUA1K1, HRH1, ATXN1, SOCS1, MOBP, ZNF704, ADGRG5, MOV10L1, PLEK2, KCNN3, SCN3B, NKX2-3, TRPM3, JAG1, DENND4A, ST8SIA1, ABCA3, BTBD11, GDF6, LRP1B, MEX3B, CYP1A1, PDE3A, NABP1, CYP2B7P, SLC26A4, FGF12, ROBO4, ITGB4, MEGF11, LRRC4, OPLAH, HAPLN1, PIK3C2B, LFNG, SHE, JPH2, ADAMTSL4, ITGAV, ANKRD2, BCAS1, CERS6, PTGIS, SERPINB2, SH2D3C, SHROOM2, KSR2, ARHGAP5-AS1, F5, IL17RA, BDH1, SLC7A8, CDC42EP3, IRF6, CLDN16, LCT, IVL, CHST2, SEMA3C, LAMA3, PKD1L1, FGD5, CDC45, ABI3BP, GCNT2, HAS3, HAS2, S1PR3, SLIT3, DMD, SLIT2, IL12RB1, SLC25A25, APOL3, MUC6, NTRK1, CHGA, GABBR2, PRSS35, ATP2B2, SORL1, BAIAP3, TMEM156, NEDD4, PTPN6, ERCC6, PI16, LGR4, TJP2

HLF	6.00	132	36.3	0.004	SLC46A3, MYLK2, EXOC3L1, PATJ, HHIP, TMEM200C, RNF19B, HR, SLC8A1, AMOT, RIMS1, RASSF2, ARHGAP40, SESN3, CAPNS2, ANPEP, NDST3, SCN9A, ADORA1, SMCO2, AP1S3, PRSS3, HES7, POSTN, MBNL2, FAM24B, MAGI2, ARID5B, ANK3, MIR100HG, RUNX2, MAF, TXLNB, LOX, ADGRB3, TNIK, TOX, SLC22A4, SUCNR1, SHC3, ABCB1, NTM, GATA6, GATA3, DTX4, PCDH19, RASGRP3, SCUBE3, NUAK1, HRH1, ATXN1, MOBP, ZNF704, FAM43A, KCNN3, TRPM3, ANKRD29, JAG1, DENND4A, STAC, TNFSF15, VDR, ABCA9, EPHX4, BTBD11, INHBA, LRP1B, SELP, IL6, COL5A2, PDE3A, SP6, MAP3K14, FGF12, TNFAIP6, MEGF11, BHLHE41, LRRC4, NRARP, HAPLN1, PIK3C2B, LFNG, ITGAV, BCAS1, SMIM14, SERPINB2, MME, TRPC4, NOG, SHROOM2, KSR2, ARHGAP5-AS1, SYN1, F5, GREM1, BDH1, SLC7A8, CLDN16, CHST2, ZNF474, KRT81, LAMA3, CYGB, DDO, DRP2, FGD4, NFIL3, ABI3BP, HAS3, GCNT3, SUSD6, SLIT3, DMD, SLIT2, FNIP2, ZSWIM5, APOL3, SAMD3, NTRK1, GABBR2, GPR4, ATP2B2, SORL1, LILRB5, BAIAP3, FABP4, KLHL6, NEDD4, MAP3K14-AS1, ERCC6, LGR4, TJP2
STAT	#N/A	115	31.6	0.006	PATJ, CPNE5, HHIP, LST1, RNF19B, MT1X, HR, SLC8A1, AMOT, ELK3, RIMS1, MT2A, NDST3, SCN9A, ADORA1, SMCO2, MBNL2, MAGI2, ARID5B, ANK3, KCTD4, MIR100HG, SDCBP2, RUNX2, ADAM19, CNBD2, MAF, LOX, PPP1R3B, ADGRB3, TNIK, TOX, MT1E, ABCB1, COL13A1, NTM, GATA6, CREM, IL20RB, TGFA, DTX4, PCDH19, RASGRP3, ATXN1, SOCS1, ZNF704, MOV10L1, KCNN3, SLC15A3, TRPM3, ANKRD29, GPR17, JAG1, DENND4A, STAC, VDR, ABCA3, GDF6, LRP1B, SELP, EWSAT1, COL5A2, PDE3A, XAF1, MAP3K14, EFCC1, FGF12, MEGF11, PTGDR2, LRRC4, OPLAH, HAPLN1, PIK3C2B, ADAMTSL4, CCR7, CERS6, MMP7, MME, TRPC4, SPHK1, SHROOM2, KSR2, F5, GREM1, IRF1, IRF6, GRAMD1B, LAMA3, PKD1L1, CYGB, DDO, FGD5, NFIL3, ABI3BP, GCNT2, CCL2, SUSD6, SLIT3, DMD, SLIT2, ZSWIM5, MPZL2, NTRK1, GABBR2, LAMB3, BIK, KCNJ12, GPR4, SORL1, HS3ST1, KLHL6, NEDD4, ERCC6, LGR4, KCNK3
LHX3	6.00	120	33.0	0.006	FCN3, PATJ, CPNE5, HHIP, TMEM200C, GIMAP4, SLC8A1, AMOT, ELK3, RIMS1, RASSF2, SESN3, NDST3, SCN9A, AP1S3, CMKLR1, POSTN, MBNL2, MAGI2, ARID5B, ANK3, VWA5B2, MIR100HG, RUNX2, PLPP4, MAF, TXLNB, ADGRB3, TNIK, TOX, ABCG2, SLC22A4, SUCNR1, SHC3, ABCB1, COL13A1, NTM, IL20RB, GATA3, DTX4, PCDH19, RASGRP3, EFNB1, NUAK1, HRH1, ATXN1, SOCS1, ZNF704, PLEK2, FAM43A, KCNN3, SCN3B, TRPM3, GSTM4, SDR42E1, JAG1, DENND4A, ST8SIA1, STAC, TNFSF15, ABCA9, EPHX4, BTBD11, INHBA, GDF6, LRP1B, PDE3A, SLC26A4, FGF12, RTP4, MEGF11, BHLHE41, LRRC4, HAPLN1, HK1, SHE, BCAS1, CERS6, SERPINB2, MME, TRPC4, SPHK1, SH2D3C, KSR2, ARHGAP5-AS1, SYN1, F5, GREM1, BDH1, CDC42EP3, CLDN16, CHST2, SEMA3C, LAMA3, TMEM71, PRRG4, FGD5, NFIL3, ABI3BP, GCNT2, HAS2, SLIT3, DMD, SLIT2, FNIP2, ZSWIM5, CD55, SAMD3, DRGX, NTRK1, GABBR2, CCL23, SORL1, HS3ST1, TMEM156, SPRY1, PTPN6, ERCC6, LGR4, KCNK3

NFKB	#N/A	157	43.1	0.007	MYLK2, FCN3, PATJ, NRROS, CSF2, CPNE5, TMEM200A, LST1, TMEM200C, MT1X, HR, SLC8A1, NIPAL4, RIMS1, RASSF2, ANPEP, NDST3, LIPG, SCN9A, ADORA1, KDR, SMCO2, AP1S3, HES7, MBNL2, CD93, MAGI2, ARID5B, ANK3, VWA5B2, SDCBP2, RUNX2, ADAM19, CLDN5, SFRP1, PLPP4, MAF, ADGRB3, DDIT4, TNIK, MASP1, TOX, SHC3, COL13A1, USHBP1, NTM, IL20RB, TGFA, CSF2RB, GATA3, DTX4, PCDH19, KLK6, RASGRP3, EFNB1, SCUBE3, ATXN1, SOCS1, ADGRG5, FAM43A, KCNN3, SCN3B, NKX2-3, TRPM3, GSTM4, GPR17, AFAP1L2, JAG1, DENND4A, ST8SIA1, TNFSF15, ABCA3, BTBD11, INHBA, GDF6, POU2F2, LRP1B, GDF7, SELP, IL6, PDE3A, SP6, MAP3K14, FGF12, ROBO4, ITGB4, MEGF11, LRRC4, LRRC32, CXCL2, HAPLN1, HK1, PIK3C2B, JPH2, CTSO, ADAMTSL4, CSN1S1, ANKRD2, CD34, BCAS1, CERS6, MME, SPHK1, RFPL2, SH2D3C, SHROOM2, KSR2, PDCD1LG2, SYN1, F5, IL17RA, SLC7A8, IRF1, CDC42EP3, LCT, LTF, ZNF474, GRAMD1B, SEMA3C, LAMA3, CCM2L, ATP1A3, CYGB, TMEM71, DRP2, IL1RL1, FGD5, CDC45, ABI3BP, HAS3, CCL2, HAS2, SUSD6, SLIT3, DMD, SLIT2, IL12RB1, FNIP2, ZSWIM5, MISP, LRRC8E, DRGX, NTRK1, GABBR2, CCL23, LAMB3, KCNJ12, GPR4, ATP2B2, TMEM156, NLRP11, FAM131C, MAP3K14-AS1, AQP11, SPRY1, PTPN6, IL18R1
GATA6	1,373	57	15.7	0.021	PATJ, CSF2, HHIP, BHLHE41, HAPLN1, PIK3C2B, LFNG, NDST3, SCN9A, TRPC4, SPHK1, MAGI2, NOG, ARID5B, ANK3, MIR100HG, RUNX2, F5, ADAM19, ADGRB3, IRF1, CDC42EP3, TNIK, MASP1, ABCB1, SEMA3C, COL13A1, NTM, GATA6, GATA3, RASGRP3, DRP2, CYB5R2, SCUBE3, ADGRG1, ATXN1, NFIL3, ZNF704, ABI3BP, SLIT3, DMD, SLIT2, KCNN3, FNIP2, CHGA, DENND4A, BIK, ABCA3, BTBD11, INHBA, GDF6, LRP1B, GDF7, PDE3A, SP6, SPRY1, LGR4
TBP	1,439	112	30.8	0.023	SLC46A3, PATJ, HHIP, LST1, RNF19B, SLC8A1, ELK3, RIMS1, RASSF2, SESN3, CAPNS2, NDST3, SCN9A, KDR, HES7, MBNL2, MAGI2, ARID5B, ANK3, VWA5B2, RUNX2, CLDN5, PLPP4, MAF, TXLNB, ADGRB3, MYL2, TNIK, MASP1, TOX, ABCG2, SHC3, ABCB1, NTM, TGFA, DTX4, PCDH19, RASGRP3, SCUBE3, NUAK1, FAM124B, ATXN1, KCNN3, NKX2-3, TRPM3, ANKRD29, JAG1, ST8SIA1, STAC, TNFSF15, VDR, EPHX4, FZD8, INHBA, LRP1B, GDF7, SELP, MEX3B, IL6, COL5A2, PDE3A, XAF1, FGF12, RTP4, MEGF11, LRRC4, HAPLN1, HK1, SMIM14, CERS6, MME, RFPL2, SHROOM2, DUSP8, F5, SLC7A8, IRF1, CDC42EP3, CLDN16, LCT, CHST2, ZNF474, SEMA3C, PKD1L1, TMEM71, DRP2, FGD4, FGD5, CDC45, NXF3, ABI3BP, HAS3, S1PR3, SLIT3, DMD, KRTAP2-3, SLIT2, ZSWIM5, SAMD3, GABBR2, CCL23, PRSS35, ATP2B2, DHRS2, HS3ST1, APLN, BAIAP3, TMEM156, NEDD4, ERCC6, LGR4, TJP2
FOXD3	1.67	108	29.7	0.024	PATJ, HHIP, SLC8A1, AMOT, RIMS1, NDST3, SCN9A, TCP11, POSTN, MBNL2, CD93, MAGI2, ARID5B, ANK3, MIR100HG, RUNX2, ADAM19, PLPP4, MAF, TXLNB, PPP1R3B, ADGRB3, MYL2, TNIK, MASP1, TOX, ABCG2, SHC3, ABCB1, COL13A1, NTM, CREM, PCDH19, SCUBE3, NUAK1, ATXN1, MOB1, ZNF704, MOV10L1, PLEK2, KCNN3, LONRF2, TRPM3, JAG1, DENND4A, ST8SIA1, STAC, ABCA6, BTBD11, INHBA, LRP1B, GDF7, RAET1E, COL5A2, CYP1A1, PDE3A, SP6, FGF12, MEGF11, NRARP, HAPLN1, PIK3C2B, SHE, CASP3, BCAS1, SMIM14, CERS6, MME, TRPC4, NOG, SH2D3C, KSR2,

					ARHGAP5-AS1, PDCD1LG2, SSTR2, F5, CCDC190, CLDN16, SEMA3C, LAMA3, FGL2, NLRC3, DRP2, FGD4, IL1RL1, CDC45, NXF3, NFIL3, ABI3BP, HSD17B2, GCNT2, SUSD6, S1PR3, SLIT3, DMD, SLIT2, FNIP2, APOL3, DRGX, CHGA, GABBR2, ATP2B2, HS3ST1, TMEM156, NEDD4, SPRY1, ERCC6, LGR4
ZIC3	1.00	121	33.2	0.025	PATJ, NRROS, CSF2, CPNE5, HHIP, TMEM200C, HR, SLC8A1, ELK3, NPPB, RIMS1, LCNL1, SESN3, ANPEP, CCRL2, ADORA1, AP1S3, PRSS3, CPA3, HES7, CD93, FAM24B, MAGI2, ARID5B, ANK3, VWA5B2, MIR100HG, RUNX2, CLDN5, ARC, MAF, PPP1R3B, ADGRB3, MASP1, TOX, SHC3, COL13A1, USHBP1, NTM, GATA6, GATA3, PCDH19, KLK6, CYB5R2, EFNB1, SCUBE3, NUAKE1, ATXN1, MOBP, ZNF704, KCNN3, SLC15A3, NKX2-3, GSTM4, JAG1, ZG16B, ABCA6, ABCA9, POU2F2, LRP1B, MEX3B, SP6, MAP3K14, ROBO4, ITGB4, MEGF11, LRRC4, LRRC32, OPLAH, HAPLN1, PIK3C2B, LFNG, ADAMTSL4, ITGAV, CCR7, ANKRD2, CD34, BCAS1, CERS6, MME, SPHK1, NOG, SH2D3C, KSR2, SSTR2, SYN1, IL17RA, SLC7A8, CCDC190, SEMA3C, CCM2L, ATP1A3, NLRC3, CYGB, DRP2, FGD5, CDC45, ABI3BP, HAS3, GCNT3, HAS2, SUSD6, SLIT3, DMD, ZSWIM5, MISP, LRRC8E, SLC25A25, MPZL2, NTRK1, LAMB3, KCNJ12, GPR4, ATP2B2, CAPN11, CLCN4, NEDD4, MAP3K14-AS1, PTPN6, LGR4, KCNK3
STAT1	7,994	124	34.1	0.026	SLC46A3, MYLK2, EXOC3L1, FCN3, PATJ, NRROS, CPNE5, HHIP, LST1, TMEM200C, RNF19B, HR, GIMAP7, SLC8A1, AMOT, ELK3, NPPB, MT2A, CYSLTR2, CAPNS2, ADORA1, CMKLR1, CPA3, HES7, MBNL2, MAGI2, ARID5B, ANK3, MIR100HG, RUNX2, ADAM19, CNBD2, CLDN5, SFRP1, ADGRB3, TNIK, TOX, MT1E, ABCB1, COL13A1, USHBP1, NTM, GATA6, TGFA, GATA3, PCDH19, EFNB1, SCUBE3, ADGRG1, HRH1, FAM124B, ATXN1, FAM43A, KCNN3, SMN1, SCN3B, NKX2-3, TRPM3, GPR17, JAG1, DENND4A, STAC, VDR, INHBA, GDF6, POU2F2, LRP1B, GDF7, EWSAT1, MEX3B, SLC26A4, MAP3K14, PIWIL1, ROBO4, ITGB4, MEGF11, LRRC4, OPLAH, HK1, PIK3C2B, ADAMTSL4, MMP28, ITGAV, CD34, SPHK1, NOG, SH2D3C, KSR2, SYN1, GREM1, SLC7A8, IRF6, GRAMD1B, LAMA3, FGL2, CYGB, TMEM71, DRP2, CDC45, ABI3BP, GCNT2, HAS3, HAS2, SLIT3, DMD, SLIT2, FNIP2, ZSWIM5, LRRC8E, CD55, MPZL2, GABBR2, BIK, ATP2B2, DHRS2, SORL1, APLN, BAIAP3, CAPN11, CLCN4, MAP3K14-AS1, PTPN6, LGR4, TJP2
MEIS1	613	142	39.0	0.033	SLC46A3, MYLK2, PATJ, CSF2, TMEM200A, HHIP, LST1, SLC8A1, AMOT, NIPAL4, NPPB, RIMS1, LCNL1, RASSF2, DMBT1, CAPNS2, NDST3, LIPG, SCN9A, ADORA1, AP1S3, MBNL2, MAGI2, ARID5B, ANK3, VWA5B2, MIR100HG, SDCBP2, RUNX2, SFRP1, MAF, PPP1R3B, ADGRB3, MYL2, DDIT4, TNIK, MASP1, TOX, ABCB1, COL13A1, USHBP1, NTM, GATA6, CREM, IL20RB, TGFA, GATA3, DTX4, PCDH19, KLK6, RASGRP3, C2ORF27A, EFNB1, SCUBE3, ADGRG1, NUAKE1, HRH1, ATXN1, FAM43A, KCNN3, SLC15A3, TRPM3, GSTM4, JAG1, DENND4A, STAC, ABCA9, BTBD11, INHBA, LRP1B, EWSAT1, COL5A2, CYP1A1, PDE3A, SP6, NABP1, SLC26A4, MAP3K14, FGF12, RTP4, MEGF11, LRRC4, SIRPB2, OPLAH, HAPLN1, PIK3C2B, SHE, JPH2, ADAMTSL4, CCR7, BCAS1, TRPC4, RFPL2, NOG, KSR2, PDCD1LG2, SYN1,

GREM1, BDH1, SLC7A8, CDC42EP3, LCT, GRAMD1B, SEMA3C, LAMA3, CCM2L, PKD1L1, ATP1A3, CYGB, ARNTL2, TMEM71, DRP2, FGD4, FGD5, CDC45, ABI3BP, GCNT2, HAS3, SUSD6, SLIT3, DMD, SLIT2, FNIP2, ZSWIM5, SLC25A25, DRGX, NTRK1, GABBR2, LAMB3, ATP2B2, SORL1, HS3ST1, LILRB5, APLN, BAIAP3, KLHL6, FAM131C, MAP3K14-AS1, PTPN6, LGR4, KCNK3, UOX

ZIC2	47.00	76	20.9	0.038	ROBO4, FCN3, CPNE5, ITGB4, HHIP, BHLHE41, LRRC4, HR, PIK3C2B, AMOT, JPH2, ARHGAP40, CAPNS2, ANKRD2, HES7, MBNL2, MME, SPHK1, MAGI2, NOG, SH2D3C, KSR2, SDCBP2, SYN1, RUNX2, ARC, MAF, PPP1R3B, TNIK, MT1E, NTM, GATA6, ATP1A3, NLRC3, GATA3, PCDH19, CYGB, DRP2, CYB5R2, KIAA0513, SCUBE3, NUA1, ATXN1, MOBP, ZNF704, PLEK2, SLIT3, DMD, SLIT2, SMN1, SCN3B, FNIP2, MISP, LRRC8E, TRPM3, NKX2-3, DRGX, NTRK1, GPR17, JAG1, DENND4A, VDR, ABCA3, GPR4, ATP2B2, GDF7, FAM131C, NEDD4, COL5A2, PDE3A, SP6, PTPN6, PI16, CYP2B7P, FGF12, LGR4
------	-------	----	------	-------	---

Supplementary table 3- 10: TF binding by IL-4 DEGs in EA.hy926^{PLKO-1}

Term	Count	%	P-Value	Genes
GO:0030198--extracellular matrix organization	9	5.4	2.8E-04	COL13A1, LAMB3, LOX, ITGB4, ADAMTSL4, ABI3BP, LAMA3, ITGAV, HAPLN1
GO:0042493--response to drug	11	6.5	2.8E-04	NTRK1, IL6, SFRP1, SEMA3C, LOX, ABCA3, GATA6, TGFA, GATA3, INHBA, SLC8A1
GO:0048468--cell development	5	3.0	3.6E-04	MAF, GATA6, ARID5B, IRF6, INHBA
GO:0006869--lipid transport	6	3.6	4.7E-04	APOL6, ABCA6, ABCA3, APOL1, SORL1, APOL3
GO:0001525--angiogenesis	9	5.4	6.5E-04	ADGRG1, ROBO4, JAG1, ANPEP, FZD8, CCL2, TGFA, ITGAV, ELK3
GO:0006955--immune response	12	7.1	9.6E-04	IL1RL1, IL6, CSF2, SEMA3C, NFIL3, TNFSF15, CCL2, CCR7, PDCD1LG2, CXCL2, MAP3K14, CCL26
GO:0035987--endodermal cell differentiation	4	2.4	0.0015	LAMB3, LAMA3, ITGAV, INHBA
GO:0006954--inflammatory response	11	6.5	0.0015	IL6, HRH1, TNFAIP6, SPHK1, ADORA1, CCL2, CCR7, S1PR3, CXCL2, APOL3, CCL26
GO:0032689--negative regulation of interferon-gamma production	4	2.4	0.0017	IL1RL1, IL20RB, GATA3, PDCD1LG2
GO:0008285--negative regulation of cell proliferation	11	6.5	0.0021	NTRK1, IL6, SFRP1, ADGRG1, VDR, IRF1, ADORA1, PTPN6, IRF6, GATA3, INHBA
GO:0070588--calcium ion transmembrane transport	6	3.6	0.0035	TRPC4, PKD1L1, ITGAV, ATP2B2, SLC8A1, SLC25A25
GO:0031581--hemidesmosome assembly	3	1.8	0.0045	LAMB3, ITGB4, LAMA3
GO:0042060--wound healing	5	3.0	0.0048	IL6, SERPINB2, LOX, TGFA, ELK3
GO:0003215--cardiac right ventricle morphogenesis	3	1.8	0.0053	JAG1, SEMA3C, GATA3
GO:0050892--intestinal absorption	3	1.8	0.0061	VDR, GCNT3, TJP2
GO:0008584--male gonad development	5	3.0	0.0085	SFRP1, GATA6, ARID5B, GATA3, INHBA
GO:0010466--negative regulation of peptidase activity	3	1.8	0.0090	SERPINB3, SERPINB4, PI16
GO:0045892--negative regulation of transcription, DNA-templated	11	6.5	0.0104	SFRP1, ATXN1, VDR, IRF1, GATA6, BHLHE41, ARID5B, HR, GATA3, LGR4, ELK3
GO:0002026--regulation of the force of heart contraction	3	1.8	0.0112	CHGA, MYL2, SLC8A1
GO:0071294--cellular response to zinc ion	3	1.8	0.0112	MT2A, MT1X, MT1E
GO:0045926--negative regulation of growth	3	1.8	0.0112	MT2A, MT1X, MT1E
GO:0006959--humoral immune response	4	2.4	0.0127	IL6, CCL2, GATA3, POU2F2
GO:0045893--positive regulation of transcription, DNA-templated	11	6.5	0.0128	IL6, SFRP1, IRF1, GATA6, HAS3, IRF6, GATA3, INHBA, LGR4, ARNTL2, ELK3
GO:0071356--cellular response to tumor necrosis factor	5	3.0	0.0145	IL6, SFRP1, CCL2, GATA3, CCL26

GO:0061290~canonical Wnt signaling pathway involved in metanephric kidney development	2	1.2	0.0170	GATA3, LGR4
GO:0036018~cellular response to erythropoietin	2	1.2	0.0170	MT2A, MT1X
GO:0051602~response to electrical stimulus	3	1.8	0.0176	NTRK1, IL6, TACR2
GO:0030335~positive regulation of cell migration	6	3.6	0.0207	SERPINB3, SEMA3C, TNFAIP6, SPHK1, ITGAV, CCL26
GO:0071347~cellular response to interleukin-1	4	2.4	0.0227	IL6, SFRP1, CCL2, CCL26
GO:0009791~post-embryonic development	4	2.4	0.0244	SEMA3C, MYL2, ARID5B, GATA3
GO:0071549~cellular response to dexamethasone stimulus	3	1.8	0.0252	IL6, DDIT4, CCL2
GO:0032651~regulation of interleukin-1 beta production	2	1.2	0.0253	SPHK1, S1PR3
GO:0019221~cytokine-mediated signaling pathway	5	3.0	0.0257	IL6, LRRRC4, IL20RB, CCL2, IL12RB1
GO:0071773~cellular response to BMP stimulus	3	1.8	0.0268	SFRP1, GATA6, GATA3
GO:0030216~keratinocyte differentiation	4	2.4	0.0271	LCE2A, JAG1, IRF6, IVL
GO:0006508~proteolysis	10	6.0	0.0274	FCN3, SFRP1, CAPN11, MME, CAPNS2, ADAMTSL4, ANPEP, MMP28, PRSS3, F5
GO:0010332~response to gamma radiation	3	1.8	0.0285	CCL2, GATA3, ERCC6
GO:0046718~viral entry into host cell	4	2.4	0.0309	SERPINB3, ANPEP, ITGAV, CD55
GO:0010574~regulation of vascular endothelial growth factor production	2	1.2	0.0336	IL6, CCL2
GO:0048565~digestive tract development	3	1.8	0.0357	ITGB4, GATA3, LGR4
GO:0007165~signal transduction	17	10.1	0.0384	SHC3, TNFAIP6, TNFSF15, STAC, VDR, SPHK1, ANK3, GATA3, SORL1, ELK3, IL1RL1, CDC42EP3, ADORA1, CCL2, IL12RB1, APOL3, CCL26
GO:0042157~lipoprotein metabolic process	3	1.8	0.0415	APOL6, APOL1, APOL3
GO:0045578~negative regulation of B cell differentiation	2	1.2	0.0419	SFRP1, INHBA
GO:0098735~positive regulation of the force of heart contraction	2	1.2	0.0419	MYL2, SLC8A1
GO:0007155~cell adhesion	9	5.4	0.0428	ADGRG1, LAMB3, TNFAIP6, ITGB4, LAMA3, HAS3, CCL2, ITGAV, HAPLN1
GO:0000122~negative regulation of transcription from RNA polymerase II promoter	12	7.1	0.0438	HES7, MAF, NFIL3, VDR, GATA6, BHLHE41, FZD8, ARID5B, NRARP, GATA3, ANKRD2, FNIP2
GO:1901215~negative regulation of neuron death	3	1.8	0.0455	CHGA, IL6, SORL1
GO:0045599~negative regulation of fat cell differentiation	3	1.8	0.0497	IL6, JAG1, GATA3

GO:0002548-monocyte chemotaxis 3 1.8 0.0497 IL6, CCL2, CCL26

Supplementary table 3- 11: GO on biological process by IL-4 DEGs with STAT3 TFBM in EA.hy^{PLKO-1}

Gene_name	log2FC	FC	padj	Veh1	Veh2	Veh3	IL4_1	IL4_2	IL4_3
CCL26	11.1	2183.4	1.3E-192	26	21	48	62,963	76,339	68,394
CSN1S1	9.4	675.4	3.5E-140	10	5	9	4,431	6,822	4,981
HAS3	4.2	18.1	4.9E-82	441	316	363	5,646	8,155	6,423
SLC7A8	4.0	16.1	2.2E-63	61	79	86	1,016	1,432	1,205
HS3ST1	3.2	9.5	1.2E-55	176	168	181	1,430	1,888	1,654
SELP	3.1	8.7	4.3E-49	4,182	2,943	3,582	26,983	36,889	29,424
SERPINB2	4.9	29.4	3.1E-47	15	9	22	400	560	394
LOX	2.9	7.3	4.6E-43	4,236	3,188	3,901	23,437	32,542	26,274
SUCNR1	3.6	11.8	1.0E-38	41	30	34	362	478	403
OTOGL	3.4	10.4	1.7E-37	152	116	190	1,256	2,108	1,408
IL6	3.1	8.8	4.0E-36	105	105	160	939	1,308	991
MMP28	3.6	12.2	7.2E-34	46	33	25	338	509	420
SOCS1	2.8	7.1	1.7E-31	203	118	165	1,001	1,244	1,222
IL1RL1	2.3	5.0	3.9E-30	955	938	834	3,885	5,428	4,421
PI16	2.9	7.4	5.5E-30	123	94	123	634	1,034	848
SCN9A	3.2	9.0	1.3E-29	133	87	149	924	1,503	887
CSF2RB	2.5	5.6	5.3E-29	4,539	3,274	4,190	18,860	27,767	20,873
CPA3	3.2	8.9	6.6E-29	145	61	123	894	1,101	939
APLN	-2.4	-5.3	5.6E-27	8,765	6,289	9,130	1,356	1,813	1,352
NABP1	2.4	5.2	6.2E-27	3,464	2,704	3,304	13,931	20,445	14,607
SERPINB4	5.5	46.1	2.5E-26	7	5	1	158	257	185
VDR	2.5	5.6	2.5E-26	534	389	525	2,193	3,353	2,549
RIMS1	2.2	4.7	6.9E-24	225	203	261	959	1,273	1,025
MMP7	2.8	6.8	6.5E-23	73	63	73	347	626	458
KRT81	-2.3	-4.8	3.4E-22	555	482	527	103	127	96
CRYBG1	2.4	5.3	7.1E-22	405	261	350	1,527	2,308	1,576
PRSS3	2.4	5.4	7.0E-21	68	52	69	304	370	347
MASP1	2.7	6.4	1.6E-20	94	54	79	377	614	462
NKX2-3	2.4	5.3	2.7E-19	188	100	152	703	918	710
AP1S3	2.0	3.9	4.2E-18	702	610	598	2,073	3,144	2,279
SFRP1	2.1	4.3	6.0E-18	1,809	1,199	1,786	5,546	8,267	6,606
ADAM19	1.9	3.9	4.0E-17	3,082	2,405	2,939	9,047	13,879	9,627

SPHK1	1.8	3.4	1.0E-16	4,748	3,817	4,396	11,926	16,485	15,430
CYSLTR2	1.9	3.7	2.4E-16	184	179	206	631	823	639
LIPG	-1.8	-3.4	2.9E-16	4,837	3,759	4,341	1,144	1,515	1,184
CLCN4	1.9	3.6	3.4E-16	2,199	1,737	2,147	5,916	9,158	7,117
FZD8	1.8	3.6	5.7E-16	918	673	754	2,269	3,216	2,906
INHBA	1.9	3.7	6.9E-16	2,723	2,091	2,581	7,306	11,447	8,481
MYLK2	-1.8	-3.5	3.1E-15	2,102	1,551	1,846	421	612	520
FNIP2	1.9	3.7	4.0E-15	2,176	1,635	2,135	5,861	9,460	6,832
CASP3	1.8	3.4	4.5E-15	5,291	4,126	5,069	13,839	20,570	15,205
SERPINB3	5.7	51.3	5.0E-15	4	1	1	105	107	96
AQP11	2.0	3.9	8.4E-15	163	118	170	492	687	587
SMIM14	1.7	3.2	1.1E-14	1,500	1,261	1,471	3,839	5,554	4,301
TMEM200A	1.8	3.5	1.8E-14	644	450	673	1,786	2,419	2,037
DMBT1	-2.5	-5.7	6.6E-14	220	177	293	26	50	44
ANPEP	1.6	2.9	8.6E-14	16,393	12,721	15,563	40,130	50,417	40,929
ABI3BP	1.8	3.4	2.0E-13	3,300	2,659	3,200	8,499	13,795	9,155
ITGAV	1.7	3.3	2.6E-13	43,080	33,522	41,427	108,863	163,902	112,887
CCM2L	-1.8	-3.4	3.6E-13	967	685	819	202	281	242
PTGIS	1.6	3.1	4.2E-13	279	234	262	695	791	879
PRSS35	2.6	6.1	1.2E-12	33	15	33	164	195	132
CD55	1.6	3.0	2.6E-12	6,714	5,216	6,382	15,505	22,094	16,838
ST8SIA1	2.2	4.6	3.4E-12	40	34	53	188	227	167
ABCG2	1.6	3.1	6.3E-12	2,938	2,253	2,927	6,972	10,337	7,569
NTRK1	2.7	6.6	8.0E-12	20	19	14	91	150	110
NUAK1	1.6	3.0	1.0E-11	8,666	7,004	9,191	20,613	31,074	23,105
ZNF114	-2.5	-5.7	1.0E-11	124	130	108	22	26	16
DDIT4	-1.6	-3.0	1.1E-11	1,026	744	918	249	313	320
IRF6	2.6	6.2	1.8E-11	46	19	19	137	167	218
KCNK3	4.0	15.8	2.5E-11	7	1	5	61	72	73
IL20RB	1.6	3.1	4.3E-11	111	122	110	326	380	343
TMEM200C	1.6	2.9	5.1E-11	1,846	1,303	1,819	4,035	5,617	4,908
MPZL2	-1.5	-2.8	6.1E-11	6,492	4,811	6,162	1,785	2,468	1,907
DHRS2	-1.4	-2.7	7.2E-11	5,393	4,232	4,970	1,468	2,034	1,852
RNF19B	1.5	2.9	7.7E-11	3,573	2,693	3,760	8,014	11,449	9,319
MEX3B	1.7	3.2	1.1E-10	719	470	643	1,508	2,460	1,985
LNCOG	1.5	2.9	1.1E-10	724	508	737	1,666	2,155	1,871
FAM124B	1.6	3.1	1.3E-10	365	252	264	809	1,106	822
ADORA1	-1.5	-2.9	2.3E-10	959	704	923	291	345	267
FABP4	1.5	2.9	2.3E-10	404	297	343	941	1,192	871
ADAMTSL4	1.5	2.9	2.6E-10	836	673	743	1,776	2,748	1,976

ZNF474	2.9	7.4	2.7E-10	17	17	5	89	118	83
MMP1	1.4	2.7	4.1E-10	8,528	6,582	7,883	18,068	25,378	18,584
TMEM158	1.5	2.9	4.7E-10	204	156	217	485	614	585
MOV10L1	1.6	3.0	5.2E-10	407	374	474	1,036	1,654	1,103
BTBD11	1.8	3.5	6.2E-10	69	79	103	250	362	270
TMEM71	2.6	6.0	7.3E-10	17	12	29	87	145	117
SHC3	1.5	2.8	7.4E-10	2,403	1,945	2,426	5,086	7,978	5,861
MT1X	-1.6	-3.0	2.0E-09	487	324	478	146	146	134
CCL2	1.4	2.7	2.2E-09	434	339	441	941	1,277	1,039
SES3	3.7	12.7	2.6E-09	9	1	5	49	84	58
GATA6	1.3	2.5	3.3E-09	1,438	1,234	1,364	2,767	4,042	3,410
CHST2	-1.4	-2.6	3.8E-09	4,791	3,551	4,511	1,366	1,871	1,749
KSR2	-1.8	-3.5	3.8E-09	348	260	314	61	116	89
TNIK	1.4	2.7	3.8E-09	3,218	2,623	3,254	6,570	10,485	7,599
IVL	-3.3	-9.9	4.2E-09	69	62	56	3	11	5
TNFAIP6	5.1	33.5	5.1E-09	1	3	1	45	77	46
PRAG1	1.4	2.6	7.0E-09	5,897	4,367	5,250	11,191	16,071	12,538
ATXN1	1.5	2.7	7.5E-09	1,068	885	952	2,114	3,485	2,388
IRF1	1.3	2.5	1.0E-08	1,064	823	994	2,057	2,725	2,296
SIRPB2	-1.4	-2.6	1.4E-08	2,962	2,254	2,875	860	1,279	965
ADGRB3	-1.4	-2.6	1.5E-08	1,089	848	975	319	455	338
MT2P1	-1.5	-2.9	2.1E-08	2,684	1,559	2,052	825	796	586
PLPP3	1.3	2.5	3.7E-08	896	726	737	1,656	2,387	1,829
GCNT2	1.4	2.6	4.1E-08	816	681	778	1,611	2,510	1,750
MOBP	-1.4	-2.6	4.9E-08	1,178	781	1,103	348	448	373
KIAA0513	1.5	2.8	5.0E-08	536	431	675	1,265	1,898	1,367
HAS2	4.9	28.9	5.1E-08	1	3	1	47	64	34
CCDC190	1.7	3.2	6.3E-08	92	84	90	225	393	242
DTX4	1.3	2.5	6.5E-08	1,136	824	955	2,059	2,909	2,277
UFD1	1.3	2.5	6.9E-08	5,326	4,023	5,165	9,739	14,470	11,541
HK1	1.3	2.4	7.8E-08	13,296	9,959	12,923	24,026	33,665	28,932
SUSD6	1.3	2.4	9.4E-08	2,358	1,894	2,369	4,478	6,371	4,941
ZNF704	-1.4	-2.6	1.6E-07	450	457	448	143	219	160
IGFBP3	-1.2	-2.4	1.9E-07	7,685	5,865	7,211	2,409	3,510	2,834
PKD1L1	2.4	5.1	2.2E-07	18	11	17	69	100	67
CD34	-1.4	-2.6	2.4E-07	2,301	1,685	2,209	619	1,015	771
ARNTL2	1.3	2.5	2.6E-07	10,443	8,342	10,576	20,146	31,937	21,212
S1PR3	1.2	2.4	2.6E-07	1,086	949	1,225	2,118	3,098	2,509
MT1E	-1.2	-2.3	2.7E-07	3,090	2,470	3,263	1,022	1,428	1,310
APOL6	1.3	2.4	4.0E-07	727	502	639	1,258	1,801	1,514

CREM	1.3	2.4	4.5E-07	2,121	1,577	1,974	3,695	5,584	4,315
GATA3	1.4	2.6	4.6E-07	127	100	89	263	286	283
UCP2	-1.1	-2.2	5.6E-07	2,718	2,074	2,723	1,073	1,146	1,223
MIR100HG	1.3	2.5	6.5E-07	1,368	1,159	1,274	2,620	4,171	2,597
TOX	1.2	2.3	8.9E-07	2,491	2,127	2,530	4,438	6,812	5,178
COL13A1	-1.2	-2.3	9.9E-07	1,185	1,110	1,160	458	626	432
CDC45	1.2	2.3	1.0E-06	3,980	2,991	3,592	6,524	10,152	8,100
IL17RA	1.2	2.3	1.0E-06	1,014	823	1,005	1,754	2,737	2,187
APOL3	1.3	2.5	1.1E-06	446	336	461	884	1,364	905
EFNB1	-1.2	-2.3	1.1E-06	5,581	4,045	4,919	1,712	2,501	2,086
MT2A	-1.2	-2.4	1.2E-06	41,362	25,467	37,841	15,913	12,600	15,524
CYP2B7P	-1.3	-2.5	1.3E-06	240	234	249	81	105	98
ITGB4	1.2	2.2	1.4E-06	2,116	1,545	1,813	3,444	4,740	4,066
KCTD4	1.6	3.1	1.4E-06	65	44	61	139	216	173
HSD17B2	-1.9	-3.8	1.5E-06	115	87	94	24	20	34
SLC8A1	1.6	2.9	1.7E-06	186	136	171	332	683	435
LAMA3	1.2	2.4	1.8E-06	8,564	7,070	8,719	14,950	24,790	17,686
HKDC1	1.3	2.4	2.1E-06	136	116	122	272	346	291
NEDD4	1.2	2.3	2.1E-06	5,536	4,559	5,509	10,097	15,623	10,421
TPST1	1.2	2.3	2.6E-06	1,339	1,002	1,237	2,209	3,311	2,642
RTP4	1.6	3.0	3.3E-06	91	65	77	172	321	212
ATXN1-AS1	1.7	3.2	3.4E-06	34	55	39	109	157	149
KLK6	-1.9	-3.8	4.0E-06	104	74	123	21	34	25
DMD	1.3	2.4	4.0E-06	1,260	920	1,281	2,240	3,657	2,494
DIO2	-1.2	-2.2	4.1E-06	5,609	4,640	5,558	1,919	2,980	2,165
LFNG	-1.2	-2.2	4.9E-06	1,572	1,281	1,571	515	783	676
DUSP5-DT	-1.6	-2.9	5.0E-06	170	139	171	40	68	55
SLC25A25	1.2	2.2	5.0E-06	1,429	1,203	1,507	2,537	3,890	2,843
TNFSF15	-1.3	-2.4	5.4E-06	1,715	1,118	1,592	611	747	500
APOL1	1.2	2.3	5.5E-06	578	400	463	899	1,285	1,130
NPPB	4.3	19.8	5.6E-06	3	5	1	26	71	82
NOG	-1.5	-2.9	5.8E-06	258	207	214	65	61	111
CD93	-1.1	-2.2	5.9E-06	14,589	11,531	14,131	5,158	7,536	6,027
SAMD3	2.1	4.4	6.0E-06	33	15	13	93	110	67
DUSP8	1.3	2.5	6.6E-06	135	100	105	228	332	305
AFAP1L2	-4.1	-17.7	6.7E-06	40	19	47	1	2	3
EPHX4	2.9	7.4	6.9E-06	5	7	5	46	47	33
MAGED4	1.6	3.0	8.2E-06	81	55	47	222	136	198
KCNJ12	-1.5	-2.9	9.4E-06	135	114	126	41	50	37
HRH1	1.1	2.2	1.1E-05	3,165	2,355	2,917	5,091	7,701	5,734

CALHM5	1.1	2.1	1.3E-05	830	670	722	1,342	1,804	1,467
GREM1	1.5	2.7	1.5E-05	76	69	69	141	244	203
LRRC32	1.1	2.1	1.6E-05	1,211	900	1,119	1,892	2,592	2,309
SH2D3C	-1.2	-2.3	1.6E-05	579	421	553	213	270	206
GDF6	1.1	2.1	1.7E-05	2,541	1,811	2,292	3,919	5,552	4,705
C5orf67	1.4	2.7	1.7E-05	102	87	69	178	305	223
ROBO4	-1.0	-2.1	1.7E-05	5,201	3,907	4,737	1,879	2,560	2,262
SLC22A4	1.1	2.1	1.7E-05	710	550	736	1,253	1,692	1,318
GRAMD1B	-1.2	-2.3	1.8E-05	3,607	2,681	3,641	1,193	1,903	1,187
MAP3K14	1.2	2.3	1.9E-05	2,403	2,070	2,502	4,115	7,263	4,644
SLIT2	1.1	2.1	2.0E-05	13,650	11,575	14,491	23,331	35,335	25,510
ANKRD29	1.2	2.3	2.0E-05	181	137	200	369	444	367
MAGI2	1.3	2.5	2.4E-05	111	77	125	227	301	255
ARHGAP40	1.6	3.0	2.7E-05	40	51	63	124	202	132
PDGFB	-1.1	-2.1	2.8E-05	5,890	3,981	5,196	1,982	2,694	2,448
GCNT3	2.0	4.0	2.8E-05	18	14	15	68	61	58
PITRM1	1.1	2.1	2.9E-05	10,244	7,967	10,203	16,218	23,813	18,971
CDC42EP3	1.1	2.2	4.0E-05	792	609	896	1,362	2,065	1,618
SORL1	-2.0	-4.1	4.0E-05	62	63	83	10	16	25
TOM1L2	1.1	2.1	4.0E-05	4,039	2,961	3,676	6,020	9,126	7,331
ATP2B2	3.1	8.6	4.3E-05	7	4	3	19	61	41
CCR7	3.2	9.3	4.3E-05	6	2	3	24	44	34
LRP1B	1.2	2.3	4.4E-05	247	251	220	438	751	485
MEF2C	-1.1	-2.1	4.8E-05	2,732	2,058	2,710	1,046	1,469	1,070
ITGB2-AS1	-2.1	-4.2	4.8E-05	89	53	78	9	19	25
PTGS1	-1.2	-2.4	5.7E-05	779	452	671	266	322	220
EVA1A	1.0	2.1	5.7E-05	3,173	2,310	2,830	4,746	6,830	5,483
NFIL3	1.2	2.2	5.9E-05	421	269	416	767	1,000	718
GDF7	1.1	2.1	6.1E-05	476	381	508	800	1,129	922
ANK3	1.2	2.3	6.2E-05	273	238	340	560	827	544
ARID5B	1.4	2.6	6.2E-05	125	93	151	243	426	284
MYO7A	1.2	2.3	6.5E-05	176	116	146	270	387	366
FAM43A	-1.0	-2.1	7.0E-05	9,222	6,261	8,428	3,185	4,399	4,011
FGL2	4.3	19.6	7.0E-05	1	1	3	39	50	9
JAG1	1.1	2.1	7.3E-05	14,110	10,525	13,364	21,422	33,139	24,561
GBP4	1.1	2.1	7.6E-05	451	380	413	713	1,078	808
PLEK2	-2.0	-3.9	7.6E-05	66	72	64	13	27	12
RASSF2	1.1	2.1	7.8E-05	992	654	890	1,558	2,082	1,667
COL5A2	1.0	2.0	0.0001	55,128	43,464	54,059	84,663	129,496	95,191

ERCC6	1.1	2.1	0.0001	6,345	5,356	6,346	9,897	16,547	11,223
GPR4	-1.1	-2.2	0.0001	361	292	422	144	173	179
GLIPR1	1.0	2.0	0.0001	9,828	7,192	9,105	14,781	21,521	16,355
ABCA6	1.8	3.5	0.0001	22	13	32	77	95	65
PIK3C2B	1.1	2.2	0.0001	1,402	978	1,338	2,125	3,560	2,421
SCN3B	1.5	2.8	0.0002	73	39	51	129	202	129
MBNL2	1.1	2.1	0.0002	3,904	2,706	3,566	5,805	9,359	6,446
ZG16B	-1.8	-3.5	0.0002	65	61	65	23	19	12
DYSF	-1.0	-2.1	0.0002	10,666	8,111	10,559	3,650	5,992	4,597
DENND4A	1.1	2.1	0.0002	2,728	2,047	2,742	4,338	7,234	4,559
CLDN5	2.3	4.8	0.0002	9	7	22	40	88	54
TGFA	-1.0	-2.0	0.0002	3,682	2,891	3,393	1,301	2,090	1,532
ALDH1A3	1.0	2.0	0.0002	590	443	499	888	1,269	937
SLC46A3	1.7	3.2	0.0002	33	22	25	65	113	77
ZNF175	1.0	2.0	0.0003	2,755	2,304	2,871	4,305	6,930	4,784
ADRA1B	-1.1	-2.2	0.0003	267	204	237	90	124	110
PTHLH	1.1	2.2	0.0003	311	213	285	491	764	508
SHROOM2	1.0	2.0	0.0003	768	580	725	1,098	1,748	1,359
TACR2	2.3	4.8	0.0004	15	14	6	49	90	30
SLCO2A1	1.1	2.1	0.0004	291	205	213	412	623	466
CAPN11	-1.4	-2.7	0.0005	102	95	119	26	45	46
PPP1R3B	1.0	2.0	0.0006	4,027	3,101	4,023	5,849	9,705	6,777
EXOC3L1	-1.2	-2.3	0.0006	251	172	217	72	112	97
NEXN	1.1	2.1	0.0006	246	176	238	362	574	455
MICE	1.6	3.0	0.0006	25	25	38	60	117	91
KCNJ2-AS1	1.2	2.2	0.0007	217	112	175	357	435	329
MIR126	-1.1	-2.1	0.0008	303	204	279	103	139	127
ABCA9	1.9	3.7	0.0009	20	13	13	47	84	41
FAM90A24P	-1.3	-2.4	0.0009	173	288	161	69	107	80
GABBR2	-1.7	-3.3	0.0010	47	61	71	17	24	13
TJP2	1.6	3.0	0.0010	35	38	27	79	152	69
PLA2G5	3.7	12.9	0.0011	17	1	7	75	134	114
SLC40A1	1.0	2.1	0.0011	232	211	279	387	637	458
NDST3	1.4	2.7	0.0012	45	31	36	115	117	69
VIT	1.1	2.2	0.0013	194	158	159	290	509	305
F5	1.1	2.1	0.0017	84	85	95	169	224	162
HAPLN1	3.6	12.2	0.0019	1	3	1	21	26	14
OTX1	1.0	2.0	0.0020	177	136	207	324	444	297
KLRD1	2.6	6.1	0.0025	3	5	5	36	21	22
NOTCH4	-1.0	-2.0	0.0026	394	299	344	129	221	161

IRF1-AS1	1.1	2.2	0.0029	117	134	154	232	426	231
TXLNB	-1.7	-3.3	0.0031	83	49	51	11	29	15
KRT8P41	1.4	2.6	0.0037	42	43	31	84	140	75
AIF1L	-1.0	-2.0	0.0042	429	310	417	134	244	192
ATP6V0D2	2.4	5.2	0.0044	2	7	8	22	25	42
SLIT3	-1.2	-2.4	0.0046	84	77	88	34	40	31
CSF2	-1.8	-3.4	0.0053	37	41	39	11	9	14
FGF1	1.1	2.1	0.0057	280	134	190	322	549	426
SPRR2A	-2.9	-7.6	0.0058	18	18	25	5	1	2
HS1BP3-IT1	-1.4	-2.5	0.0058	107	58	110	29	44	35
MEG9	1.0	2.1	0.0060	205	173	217	321	589	314
NTM	-1.1	-2.1	0.0085	199	136	176	54	105	79
C6orf201	1.3	2.5	0.0093	30	27	31	66	94	58
RTL3	-1.1	-2.2	0.0096	142	83	134	55	62	46
MRO	2.4	5.4	0.0101	5	5	3	15	31	24
FAM172BP	-2.2	-4.7	0.0101	93	102	155	11	45	18
ARNTL2-AS1	2.8	6.8	0.0114	4	3	2	12	32	17
LRRC4	2.5	5.6	0.0128	11	11	7	23	98	43
BHLHE41	-1.1	-2.2	0.0133	106	90	108	41	62	37
SELPLG	1.0	2.1	0.0133	102	75	82	128	235	169
POSTN	1.0	2.0	0.0144	181	134	142	264	432	218
HID1	-1.6	-3.0	0.0153	50	29	52	15	13	16
HYAL4	-2.3	-4.9	0.0153	17	29	27	3	9	3
PCDH19	-1.8	-3.4	0.0155	31	27	61	15	9	11
SMCO2	1.4	2.7	0.0155	37	19	22	49	103	59
MYO7B	1.2	2.3	0.0160	32	29	34	56	92	74
CMKLR1	-1.8	-3.5	0.0166	80	22	45	9	12	21
CCL23	-1.9	-3.6	0.0177	35	24	32	5	9	11
CRLF2	-1.9	-3.7	0.0189	36	32	27	14	8	4
CARD14	1.2	2.4	0.0198	52	45	47	65	175	101
DUOXA1	1.6	2.9	0.0203	10	15	21	47	56	32
KLHL6	-1.2	-2.3	0.0228	80	62	79	22	44	29
RAET1E	-1.7	-3.1	0.0240	47	38	25	15	9	11
RFPL2	-1.5	-2.8	0.0249	42	44	56	9	24	18
CPNE5	-1.0	-2.0	0.0261	165	118	113	49	81	67
TYRP1	-1.0	-2.0	0.0270	140	107	113	47	80	50
LTF	-1.5	-2.8	0.0274	51	33	59	11	22	19
MISP	1.3	2.5	0.0280	19	20	18	40	52	52
PITRM1-AS1	1.6	3.0	0.0289	44	53	50	101	246	98
RARS1P1	2.6	5.9	0.0294	1	3	5	16	23	14

NEXN-AS1	1.3	2.4	0.0297	28	27	30	40	93	74
KCNK2	-1.2	-2.3	0.0314	62	63	67	27	37	20
SLC26A4	1.7	3.2	0.0315	14	6	11	31	30	37
HSPD1P16	2.5	5.7	0.0317	5	2	5	9	45	14
CD200R1	1.9	3.7	0.0341	5	6	17	17	53	35
TRPC4	1.1	2.1	0.0356	37	47	37	65	103	86
PDE7B	1.3	2.5	0.0369	23	18	36	53	98	45
SHE	-1.8	-3.5	0.0392	28	24	25	10	7	5
PDE10A	1.3	2.5	0.0415	28	22	12	41	60	55
TREH	1.0	2.0	0.0419	76	91	95	105	250	172
VSTM1	-1.9	-3.7	0.0424	23	21	29	4	7	9
DRGX	-1.9	-3.8	0.0458	22	18	36	3	7	10
CLEC12B	-1.0	-2.0	0.0460	82	113	93	35	60	48
RBMXP4	-2.2	-4.6	0.0462	26	13	25	1	8	5
INSL4	-1.1	-2.1	0.0476	148	75	96	44	64	46
SYNC	1.4	2.6	0.0476	11	16	24	48	55	32
PRICKLE2	1.6	3.0	0.0478	18	7	12	24	42	44
TMOD1	2.0	4.1	0.0484	11	2	5	19	34	20
ADGRG4	-2.2	-4.5	0.0490	32	18	13	3	8	3

Supplementary table 3- 12: IL-4 induced DEGs in EA.hy926^{STAT3 shRNA}

Common IL-4 DEGs (231 genes)

IRF6	ABI3BP	GDF6	ANK3	CCL26
DRGX	PTGIS	MOBP	MAP3K14	RIMS1
KLK6	HAS3	CDC42EP3	TMEM200C	CRLF2
AFAP1L2	ST8SIA1	CASP3	HK1	CYP2B7P
SLC26A4	RFPL2	TGFA	APOL3	CPNE5
SORL1	PIK3C2B	VDR	CD55	SLIT3
CPA3	MASP1	KSR2	MISP	ARHGAP40
GCNT3	ADAM19	SHC3	NABP1	SPHK1
SUCNR1	COL5A2	ITGB2-AS1	TJP2	MICE
TXLNB	DUSP5-DT	SERPINB4	TACR2	HS3ST1
IVL	IL17RA	MAGI2	ANKRD29	AQP11
SLC46A3	APOL1	MEX3B	ANPEP	NOG
LRRC32	KLHL6	ABCA6	NTRK1	PLEK2
C5orf67	NPPB	TMEM71	COL13A1	KLRD1
SCN3B	SFRP1	SOCS1	VSTM1	SAMD3
ZG16B	NUAK1	BHLHE41	MT2A	HSPD1P16
CSN1S1	LAMA3	PRAG1	LIPG	PRSS3
GDF7	RASSF2	ZNF474	S1PR3	KRT81
SLC8A1	APOL6	DMD	MIR100HG	FGL2
HS1BP3-IT1	SUSD6	CARD14	IRF1	SESN3
EPHX4	CALHM5	ERCC6	FAM124B	CLDN5
LTF	IL20RB	GATA6	CCL2	CSF2
ZNF114	SIRPB2	CREM	FABP4	HAS2
ZNF704	CSF2RB	CRYBG1	PRSS35	CCR7
TRPC4	CLCN4	EFNB1	ATXN1-AS1	MMP28
MMP7	MYLK2	IL6	TMEM200A	SERPINB2
DTX4	TNFSF15	DUSP8	EXOC3L1	ATP2B2
POSTN	CD34	GCNT2	AP1S3	LRRC4

RTP4	ADGRB3	MIR126	HSD17B2	HAPLN1
PLA2G5	DMBT1	CDC45	CHST2	KCNK3
SHE	ZNF175	BTBD11	RNF19B	TNFAIP6
DHRS2	NFIL3	ADAMTSL4	CCL23	
DDIT4	NTM	NEDD4	HID1	
ITGAV	CCM2L	LOX	MT1E	
APLN	ABCG2	MT1X	UFD1	
PPP1R3B	ITGB4	GABBR2	KCTD4	
FAM172BP	OTOGL	SLC25A25	PI16	
SCN9A	FNIP2	MT2P1	GATA3	
ARID5B	ATXN1	KIAA0513	PCDH19	
SHROOM2	JAG1	GRAMD1B	SLC7A8	
SELP	TOX	ABCA9	FZD8	
CMKLR1	SLIT2	HRH1	PKD1L1	
MBNL2	ROBO4	LFNG	NKX2-3	
CYSLTR2	SMIM14	LRP1B	SMCO2	
MPZL2	GPR4	ARNTL2	INSL4	
RAET1E	CD93	SERPINB3	LNCOG	
IRF1-AS1	F5	INHBA	IL1RL1	
DENND4A	SH2D3C	MOV10L1	KCNJ12	
TNIK	SLC22A4	GREM1	CCDC190	
ADORA1	NDST3	FAM43A	CAPN11	

Unique IL-4 DEGs in EA.hy 926^{PLKO-1} (151 genes)

CBSL	BIK	PLPP4	KDR	CHGA
CERS6	MEGF11	NRARP	CLDN16	CST4
IL12RB1	LIMD1-AS1	COL5A1-AS1	PSG4	SYN1
GGTLC4P	MAP3K14-AS1	FAM90A23P	LCT	CUBNP2
SLC15A3	WNT5A-AS1	NXF3	TMEM156	LST1
	ENSG00000234			
OR2A5	290	POU2F2	EFCC1	NLRP11
JAM2	FGF12	SDCBP2	LCNL1	PATJ
TCP11	FGD4	MAF	NRROS	BCAS1
Z97198.1	ARHGAP5-AS1	EIF2B5-DT	MYL2	FREM3
MUC6	RUNX2	HSD17B6	GSTM4	PIWIL1
TEX41	SEMA3C	LONRF2	TUBA5P	FAM90A21P
CD44-AS1	PDE3A	KCNN3	MYH16	RPL7P15
OPLAH	TCAF2C	DRP2	GIMAP7	FGD5
SCUBE3	ELK3	FAM131C	CYP1A1	B3GAT1-DT
GPR17	PTGDR2	SP6	VWA5B2	ATP1A3
RN7SKP106	PDCD1LG2	USHBP1	PLAC8	PSMD10P2
UOX	ZSWIM5	SSTR2	ARC	RNVU1-15
PRRG4	ABCB1	GIMAP4	RASGRP3	JPH2
FSIP2	CTSO	NLRC3	FCN3	CYGB
LIPH	MME	CD177	DMBT1L1	HMG2P28
UBE2R2-AS1	NIPAL4	SMN1	CXCL2	BDH1
AMOT	IL18R1	CLEC2B	FAM90A14P	SDR42E1
XAF1	CAPNS2	CCRL2	CYB5R2	ANKRD2
KRT18P11	HLA-DPA1	ADGRG1	TRAC	CEACAMP10
				ENSG00000204
DDO	STAC	SPRY1	PFKP-DT	282
C2orf27A	LCE2A	HES7	PTPN6	TRPM3
ABCA3	GDI2P2	OR7E96P	HR	KRTAP2-3
TNRC18P1	CST1	LAMB3	ANKRD20A1	
LRRC8E	FAM24B	TLL11-IT1	PRR29-AS1	
LGR4	HHIP	BAIAP3	EWSAT1	
ADGRG5	C11orf96	LILRB5	CNBD2	

Unique IL-4 DEGs in EA.hy 926^{shRNA STAT3} (60 genes)

TMOD1	KRT8P41	HKDC1	PDE7B	DIO2
-------	---------	-------	-------	------

ATP6V0D2	PITRM1	SELPLG	MRO	IGFBP3
PRICKLE2	EVA1A	SLC40A1	CD200R1	PTGS1
TPST1	DUOXA1	PTHLH	RBMXP4	UCP2
TOM1L2	PITRM1-AS1	ALDH1A3	FAM90A24P	MEF2C
GLIPR1	MMP1	MYO7B	RARS1P1	KCNK2
FGF1	NEXN	MAGED4	ADRA1B	PDGFB
TREH	KCNJ2-AS1	PDE10A	SPRR2A	CLEC12B
PLPP3	GBP4	OTX1	TYRP1	DYSF
ARNTL2-AS1	TMEM158	SYNC	RTL3	ADGRG4
VIT	SLCO2A1	NEXN-AS1	NOTCH4	HYAL4
MYO7A	C6orf201	MEG9	AIF1L	113374946

Unique IL-4 DEGs in EA.hy 926^{PLKO-1} (21 genes; FC ≥ 1.25 in EA.hy926^{PLKO-1} vs EA.hy926^{shRNA STAT3} group)

C5orf67	GCNT3	LRRC32	SLC46A3
CAPN11	GDF7	NOG	SLIT3
CPNE5	INSL4	PLEK2	TRPC4
CRLF2	IRF6	POSTN	
CSF2	KCNJ12	SCN3B	
CYP2B7P	KRT81	SLC26A4	

Validated STAT3 dependent genes (55 genes)

IL12RB1	ARHGAP5-AS1	SDCBP2	MYL2	ANKRD2
TEX41	SEMA3C	MAF	GSTM4	C11orf96
OPLAH	ELK3	USHBP1	MYH16	CAPN11
UOX	PDCD1LG2	GIMAP4	FCN3	CPNE5
PRRG4	MME	CD177	CXCL2	CSF2
LIPH	NIPAL4	CLEC2B	CYB5R2	GCNT3
ABCA3	CAPNS2	ADGRG1	PTPN6	IRF6
LRRC8E	STAC	HES7	HR	KRT81
LGR4	LCE2A	LAMB3	CHGA	SLC26A4
LIMD1-AS1	NRARP	CLDN16	JPH2	SLC46A3
FGD4	POU2F2	TMEM156	CYGB	TRPC4

Supplementary table 3- 13: Gene list identified by comparison and *in silico* analysis

Term	Count	%	PValue	Genes
GO:0006955~immune response	9	5.6	0.008	CSF2, NRROS, SEMA3C, PTGDR2, LST1, PDCD1LG2, CXCL2, IL18R1, HLA-DPA1
GO:0031295~T cell costimulation	4	2.5	0.016	TRAC, PTPN6, PDCD1LG2, HLA-DPA1
GO:0048468~cell development	3	1.9	0.030	MAF, IRF6, GDF7
GO:0060048~cardiac muscle contraction	3	1.9	0.037	MYL2, ATP1A3, SCN3B
GO:0032729~positive regulation of interferon-gamma production	3	1.9	0.038	IL12RB1, IL18R1, HLA-DPA1
GO:0055114~oxidation-reduction process	9	5.6	0.046	CYB5R2, SDR42E1, NLRP11, BDH1, HHIP, CYP1A1, HR, HSD17B6, DDO
GO:0006935~chemotaxis	4	2.5	0.049	PTGDR2, CCRL2, CXCL2, AMOT

Supplementary table 3- 14: GO analysis based on the biological process on IL-4-dyregulated and STAT3 dependent genes

Term	Count	%	PValue	Genes
GO:0019825~oxygen binding	3	1.9	0.037	CBSL, CYP1A1, CYGB

GO:0016491~oxidoreductase activity	5	3.1	0.041	CYB5R2, BDH1, CYP1A1, HR, HSD17B6
hsa04530:Tight junction	4	2.5	0.029	PATJ, MYL2, CLDN16, JAM2
GO:0005923~bicellular tight junction	4	2.5	0.040	PATJ, CLDN16, JAM2, AMOT
GO:0005886~plasma membrane	42	25.9	0.004	PATJ, NRROS, ABCB1, PTGDR2, TRAC, ATP1A3, ANKRD20A1, RASGRP3, DRP2, JPH2, CAPNS2, ADGRG5, LIPH, CCRL2, KDR, KCNN3, IL12RB1, SCN3B, LRRC8E, TRPM3, JAM2, CD177, HLA-DPA1, GPR17, MME, TRPC4, KCNJ12, ABCA3, PDCD1LG2, SSTR2, SDCBP2, ARC, PLPP4, CLEC2B, SPRY1, CLDN16, OR2A5, LCT, SLC26A4, LGR4, IL18R1, CRLF2

Supplementary table 3- 15: GO analysis on IL-4-dyregulated and STAT3 dependent genes

Bibliography

- 1 Bloom, B., Cohen, R. A. & Freeman, G. Summary health statistics for U.S. children: National Health Interview Survey, 2010. *Vital Health Stat* **10**, 1-80 (2011).
- 2 Sicherer, S. H. & Sampson, H. A. Food allergy: Epidemiology, pathogenesis, diagnosis, and treatment. *J Allergy Clin Immunol* **133**, 291-307; quiz 308, doi:10.1016/j.jaci.2013.11.020 (2014).
- 3 Boyce, J. A. *et al.* Guidelines for the diagnosis and management of food allergy in the United States: report of the NIAID-sponsored expert panel. *J Allergy Clin Immunol* **126**, S1-58, doi:10.1016/j.jaci.2010.10.007 (2010).
- 4 Sicherer, S. H. Epidemiology of food allergy. *J Allergy Clin Immunol* **127**, 594-602, doi:10.1016/j.jaci.2010.11.044 (2011).
- 5 Ben-Shoshan, M. *et al.* Is the prevalence of peanut allergy increasing? A 5-year follow-up study in children in Montreal. *J Allergy Clin Immunol* **123**, 783-788, doi:10.1016/j.jaci.2009.02.004 (2009).
- 6 Nicolaou, N. *et al.* Allergy or tolerance in children sensitized to peanut: prevalence and differentiation using component-resolved diagnostics. *J Allergy Clin Immunol* **125**, 191-197 e191-113, doi:10.1016/j.jaci.2009.10.008 (2010).
- 7 Branum, A. M. & Lukacs, S. L. Food allergy among children in the United States. *Pediatrics* **124**, 1549-1555, doi:10.1542/peds.2009-1210 (2009).
- 8 Sampson, H. A. Anaphylaxis and emergency treatment. *Pediatrics* **111**, 1601-1608 (2003).
- 9 Ross, M. P. *et al.* Analysis of food-allergic and anaphylactic events in the national electronic injury surveillance system. *J. Allergy Clin. Immunol.* **121**, 166-171 (2008).
- 10 De Smit, V., Cameron, P. A. & Rainer, T. H. Anaphylaxis presentations to an emergency department in Hong Kong: incidence and predictors of biphasic reactions. *J. Emerg. Med.* **28**, 381-388 (2005).
- 11 Simons, E. R., Chad, Z. H. & Gold, M. in *Allergy Frontiers and Futures: Proceedings of the 24th Symposium of the Collegium Internationale Allergologicum*. Vol. Supplement 1 (eds J. Bienenstock, J. Ring, & A. Togias) 242 (Hogrefe & Huber Publishers, 2004).
- 12 Rudders, S. A., Arias, S. A. & Camargo, C. A., Jr. Trends in hospitalizations for food-induced anaphylaxis in US children, 2000-2009. *J Allergy Clin Immunol* **134**, 960-962 e963, doi:10.1016/j.jaci.2014.06.018 (2014).
- 13 Liew, W. K., Williamson, E. & Tang, M. L. Anaphylaxis fatalities and admissions in Australia. *J Allergy Clin Immunol* **123**, 434-442, doi:10.1016/j.jaci.2008.10.049 (2009).

- 14 Gupta, R. *et al.* The economic impact of childhood food allergy in the United States. *JAMA Pediatr* **167**, 1026-1031, doi:10.1001/jamapediatrics.2013.2376 (2013).
- 15 Cherkaoui, S. *et al.* Accidental exposures to peanut in a large cohort of Canadian children with peanut allergy. *Clin Transl Allergy* **5**, 16, doi:10.1186/s13601-015-0055-x (2015).
- 16 Yu, J. W. *et al.* Accidental ingestions in children with peanut allergy. *J Allergy Clin Immunol* **118**, 466-472, doi:10.1016/j.jaci.2006.04.024 (2006).
- 17 Yeung, J. P., Kloda, L. A., McDevitt, J., Ben-Shoshan, M. & Alizadehfar, R. Oral immunotherapy for milk allergy. *Cochrane Database Syst Rev* **11**, CD009542, doi:10.1002/14651858.CD009542.pub2 (2012).
- 18 Kemp, S. F., Lockey, R. F., Simons, F. E. & World Allergy Organization ad hoc Committee on Epinephrine in, A. Epinephrine: the drug of choice for anaphylaxis—a statement of the world allergy organization. *World Allergy Organ J* **1**, S18-26, doi:10.1097/WOX.0b013e31817c9338 (2008).
- 19 Simons, F. E. First-aid treatment of anaphylaxis to food: focus on epinephrine. *J Allergy Clin Immunol* **113**, 837-844, doi:10.1016/j.jaci.2004.01.769 (2004).
- 20 Pumphrey, R. S. & Nicholls, J. M. Epinephrine-resistant food anaphylaxis. *Lancet* **355**, 1099, doi:10.1016/s0140-6736(05)72220-0 (2000).
- 21 Sampson, H. A., Mendelson, L. & Rosen, J. P. Fatal and near-fatal anaphylactic reactions to food in children and adolescents. *N Engl J Med* **327**, 380-384 (1992).
- 22 Bock, S. A., Munoz-Furlong, A. & Sampson, H. A. Further fatalities caused by anaphylactic reactions to food, 2001-2006. *J Allergy Clin Immunol* **119**, 1016-1018, doi:S0091-6749(06)03814-0 [pii] 10.1016/j.jaci.2006.12.622 [doi] (2007).
- 23 Ruiz-Garcia, M. *et al.* Cardiovascular changes during peanut-induced allergic reactions in human subjects. *J Allergy Clin Immunol* **147**, 633-642, doi:10.1016/j.jaci.2020.06.033 (2021).
- 24 Sampson, H. A. Food Allergy. *J. Allergy Clin. Immunol.* **111**, S540-547 (2003).
- 25 Sampson, H. A. *et al.* Second symposium on the definition and management of anaphylaxis: summary report--second National Institute of Allergy and Infectious Disease/Food Allergy and Anaphylaxis Network symposium. *Ann Emerg Med* **47**, 373-380, doi:S0196-0644(06)00083-7 [pii] 10.1016/j.annemergmed.2006.01.018 [doi] (2006).
- 26 Boyce, J. A. *et al.* Guidelines for the diagnosis and management of food allergy in the United States: summary of the NIAID-sponsored expert panel report. *Nutr Res* **31**, 61-75, doi:10.1016/j.nutres.2011.01.001 (2011).
- 27 Sicherer, S. H. Clinical aspects of gastrointestinal food allergy in childhood. *Pediatrics* **111**, 1609-1616 (2003).
- 28 Cianferoni, A. *et al.* Clinical features of acute anaphylaxis in patients admitted to a university hospital: an 11-year retrospective review (1985-1996). *Ann Allergy Asthma Immunol* **87**, 27-32, doi:10.1016/s1081-1206(10)62318-6 (2001).
- 29 Novembre, E. *et al.* Anaphylaxis in children: clinical and allergologic features. *Pediatrics* **101**, E8 (1998).
- 30 Fisher, M. M. Clinical observations on the pathophysiology and treatment of anaphylactic cardiovascular collapse. *Anaesth Intensive Care* **14**, 17-21 (1986).

- 31 Brown, S. G. A. Cardiovascular aspects of anaphylaxis: Implications for treatment and diagnosis. *Curr. Opin. Allergy and Clin. Immunol.* **5**, 359-264 (2005).
- 32 Brown, S. G. The pathophysiology of shock in anaphylaxis. *Immunol Allergy Clin North Am* **27**, 165-175, doi:10.1016/j.iac.2007.03.003 (2007).
- 33 Darwish, A. & Lui, F. in *StatPearls* (2021).
- 34 Black, J. H. & Kemp, H. A. Blood density in anaphylaxis in hay fever artificially induced. *Am J Clin Pathol* **7**, 300 (1937).
- 35 Sonin, L., Grammer, L. C., Greenberger, P. A. & Patterson, R. Idiopathic anaphylaxis. A clinical Summary. *Annals Intern Med* **99**, 634-635 (1983).
- 36 Fisher, M. Blood volume replacement in acute anaphylactic cardiovascular collapse related to anaesthesia. *Br J Anaesth* **49**, 1023-1026, doi:10.1093/bja/49.10.1023 (1977).
- 37 Brown, S. G. Clinical features and severity grading of anaphylaxis. *The Journal of allergy and clinical immunology* **114**, 371-376, doi:10.1016/j.jaci.2004.04.029 (2004).
- 38 Cianferoni, A. & Muraro, A. Food-induced Anaphylaxis. *Immunol Allergy Clin North Am* **32**, 165-195 (2012).
- 39 Young, M. C., Munoz-Furlong, A. & Sicherer, S. H. Management of food allergies in schools: a perspective for allergists. *J Allergy Clin Immunol* **124**, 175-182, 182 e171-174; quiz 183-174, doi:10.1016/j.jaci.2009.04.004 (2009).
- 40 Smith, S. G. *et al.* Increased numbers of activated group 2 innate lymphoid cells in the airways of patients with severe asthma and persistent airway eosinophilia. *J Allergy Clin Immunol* **137**, 75-86.e78, doi:10.1016/j.jaci.2015.05.037 (2016).
- 41 Ishizaka, T. *et al.* Preferential differentiation of inflammatory cells by recombinant human interleukins. *Int Arch Allergy Appl Immunol* **88**, 46-49 (1989).
- 42 Galli, S. J. *et al.* Mast cells as "tunable" effector and immunoregulatory cells: recent advances. *Annu Rev Immunol* **23**, 749-786, doi:10.1146/annurev.immunol.21.120601.141025 (2005).
- 43 Strait, R. T., Morris, S. C., Yang, M., Qu, X. W. & Finkelman, F. D. Pathways of anaphylaxis in the mouse. *J Allergy Clin Immunol* **109**, 658-668. (2002).
- 44 Stone, S. F. & Brown, S. G. Mediators released during human anaphylaxis. *Curr Allergy Asthma Rep* **12**, 33-41, doi:10.1007/s11882-011-0231-6 (2012).
- 45 Kemp, S. F. & Lockey, R. F. Anaphylaxis: A review of causes and mechanisms. *J. Allergy Clin. Immunol.* **110**, 341-348 (2002).
- 46 Lin, R. Y. *et al.* Histamine and tryptase levels in patients with acute allergic reactions: An emergency department-based study. *J Allergy Clin Immunol* **106**, 65-71 (2000).
- 47 Bjornsson, H. M. & Graffeo, C. S. Improving diagnostic accuracy of anaphylaxis in the acute care setting. *West J Emerg Med* **11**, 456-461 (2010).
- 48 Enrique, E., Garcia-Ortega, P., Sotorra, O., Gaig, P. & Richart, C. Usefulness of UniCAP-Tryptase fluoroimmunoassay in the diagnosis of anaphylaxis. *Allergy* **54**, 602-606, doi:10.1034/j.1398-9995.1999.00882.x (1999).
- 49 Wongkaewpothong, P. *et al.* The utility of serum tryptase in the diagnosis of food-induced anaphylaxis. *Allergy Asthma Immunol Res* **6**, 304-309, doi:10.4168/aaair.2014.6.4.304 (2014).

- 50 Schwartz, L. B., Metcalfe, D. D., Miller, J. S., Earl, H. & Sullivan, T. Tryptase levels as an indicator of mast-cell activation in systemic anaphylaxis and mastocytosis. *N. Eng. J. Med.* **316**, 1622-1626 (1987).
- 51 Dombrowicz, D., Flamand, V., Brigman, K. K., Koller, B. H. & Kinetic, J. P. Abolition of anaphylaxis by targeted disruption of the high affinity immunoglobulin E receptor alpha chain gene. *Cell* **75**, 969-976 (1993).
- 52 Khodoun, M. V., Orekhova, T., Potter, C., Morris, S. & Finkelman, F. D. Basophils initiate IL-4 production during a memory T-dependent response. *J Exp Med* **200**, 857-870 (2004).
- 53 Madden, K. B. *et al.* Role of STAT6 and mast cells in IL-4- and IL-13-induced alterations in murine intestinal epithelial cell function. *J Immunol* **169**, 4417-4422. (2002).
- 54 Khodoun, M. V., Strait, R., Armstrong, L., Yanase, N. & Finkelman, F. D. Identification of markers that distinguish IgE- from IgG-mediated anaphylaxis. *Proc Natl Acad Sci U S A* **108**, 12413-12418, doi:10.1073/pnas.1105695108 (2011).
- 55 Osterfeld, H. *et al.* Differential roles for the IL-9/IL-9 receptor alpha-chain pathway in systemic and oral antigen-induced anaphylaxis. *J Allergy Clin Immunol* **125**, 469-476 e462, doi:10.1016/j.jaci.2009.09.054 (2010).
- 56 Ahrens, R. *et al.* Intestinal mast cell levels control severity of oral antigen-induced anaphylaxis in mice. *Am J Pathol* **180**, 1535-1546, doi:10.1016/j.ajpath.2011.12.036 (2012).
- 57 Forbes, E. E. *et al.* IL-9- and mast cell-mediated intestinal permeability predisposes to oral antigen hypersensitivity. *J Exp Med* **205**, 897-913 (2008).
- 58 Brandt, E. B. *et al.* Mast cells are required for experimental oral allergen-induced diarrhea. *J Clin Invest* **112**, 1666-1677, doi:10.1172/jci200319785 (2003).
- 59 Makabe-Kobayashi, Y. *et al.* The control effect of histamine on body temperature and respiratory function in IgE-dependent systemic anaphylaxis. *J Allergy Clin Immunol* **110**, 298-303 (2002).
- 60 Oettgen, H. C. *et al.* Active anaphylaxis in IgE-deficient mice. *Nature* **370**, 367-370 (1994).
- 61 Jonsson, F. *et al.* Mouse and human neutrophils induce anaphylaxis. *J Clin Invest* **121**, 1484-1496, doi:10.1172/jci45232 (2011).
- 62 Karasuyama, H., Tsujimura, Y., Obata, K. & Mukai, K. Role for basophils in systemic anaphylaxis. *Chem Immunol Allergy* **95**, 85-97, doi:10.1159/000315939 (2010).
- 63 Smit, J. J. *et al.* Contribution of classic and alternative effector pathways in peanut-induced anaphylactic responses. *PLoS One* **6**, e28917, doi:10.1371/journal.pone.0028917 (2011).
- 64 Jonsson, F., Mancardi, D. A., Albanesi, M. & Bruhns, P. Neutrophils in local and systemic antibody-dependent inflammatory and anaphylactic reactions. *J Leukoc Biol* **94**, 643-656, doi:10.1189/jlb.1212623 (2013).
- 65 Miyajima, I. *et al.* Systemic anaphylaxis in the mouse can be mediated largely through IgG1 and Fc gammaRIII. Assessment of the cardiopulmonary changes, mast cell degranulation, and death associated with active or IgE- or IgG1-dependent passive anaphylaxis. *J Clin Invest* **99**, 901-914 (1997).

- 66 Tsujimura, Y. *et al.* Basophils play a pivotal role in immunoglobulin-G-mediated but not immunoglobulin-E-mediated systemic anaphylaxis. *Immunity* **28**, 581-589 (2008).
- 67 Hogan, S. P., Wang, Y. H., Strait, R. & Finkelman, F. D. Food-induced anaphylaxis: mast cells as modulators of anaphylactic severity. *Semin Immunopathol* **34**, 643-653, doi:10.1007/s00281-012-0320-1 (2012).
- 68 Kanagaratham, C., El Ansari, Y. S., Lewis, O. L. & Oettgen, H. C. IgE and IgG Antibodies as Regulators of Mast Cell and Basophil Functions in Food Allergy. *Front Immunol* **11**, 603050, doi:10.3389/fimmu.2020.603050 (2020).
- 69 Keet, C. A. *et al.* The safety and efficacy of sublingual and oral immunotherapy for milk allergy. *J Allergy Clin Immunol* (2011).
- 70 Jones, S. M. *et al.* Clinical efficacy and immune regulation with peanut oral immunotherapy. *J Allergy Clin Immunol* **124**, 292-300, 300 e291-297, doi:10.1016/j.jaci.2009.05.022 (2009).
- 71 Burks, A. W. *et al.* Oral immunotherapy for treatment of egg allergy in children. *N Engl J Med* **367**, 233-243, doi:10.1056/NEJMoa1200435 (2012).
- 72 Ruitter, B. *et al.* Maintenance of tolerance to cow's milk in atopic individuals is characterized by high levels of specific immunoglobulin G4. *Clin Exp Allergy* **37**, 1103-1110, doi:10.1111/j.1365-2222.2007.02749.x (2007).
- 73 Savilahti, E. M. *et al.* Early recovery from cow's milk allergy is associated with decreasing IgE and increasing IgG4 binding to cow's milk epitopes. *J Allergy Clin Immunol* **125**, 1315-1321 e1319, doi:10.1016/j.jaci.2010.03.025 (2010).
- 74 James, J. M. & Sampson, H. A. Immunologic changes associated with the development of tolerance in children with cow milk allergy. *J Pediatr* **121**, 371-377 (1992).
- 75 Strait, R. T., Morris, S. C., Smiley, K., Urban, J. F., Jr. & Finkelman, F. D. IL-4 exacerbates anaphylaxis. *J Immunol* **170**, 3835-3842 (2003).
- 76 Fulton, J. D., Harris, W. E. & Craft, C. E. Hematocrit change as indication of anaphylactic shock in the mouse. *Proc Soc Exp Biol Med* **95**, 625-627 (1957).
- 77 Sampson, H. A. *et al.* Symposium on the definition and management of anaphylaxis: summary report. *J Allergy Clin Immunol* **115**, 584-591, doi:S0091674905000886 [pii] 10.1016/j.jaci.2005.01.009 [doi] (2005).
- 78 Nowak-Wegrzyn, A. *et al.* Work Group report: oral food challenge testing. *J Allergy Clin Immunol* **123**, S365-383, doi:S0091-6749(09)00562-4 [pii] 10.1016/j.jaci.2009.03.042 [doi] (2009).
- 79 Muller, U. & Haeberli, G. The problem of anaphylaxis and mastocytosis. *Curr Allergy Asthma Rep* **9**, 64-70 (2009).
- 80 Munoz, J. & Bergman, R. K. MECHANISM OF ANAPHYLACTIC DEATH IN THE MOUSE. *Nature* **205**, 199-200 (1965).
- 81 Bergmann, R. K. & Munoz, J. Circulatory changes in anaphylaxis and histamine toxicity in mice. *J Immunol* **95**, 1-8 (1965).
- 82 Osher, E., Weisinger, G., Limor, R., Tordjman, K. & Stern, N. The 5 lipoxygenase system in the vasculature: emerging role in health and disease. *Mol Cell Endocrinol* **252**, 201-206, doi:10.1016/j.mce.2006.03.038 (2006).

- 83 Williams, T. J. & Morley, J. Prostaglandins as potentiators of increased vascular permeability in inflammation. *Nature* **246**, 215-217, doi:10.1038/246215a0 (1973).
- 84 Campbell, R. L. *et al.* Emergency department diagnosis and treatment of anaphylaxis: a practice parameter. *Ann Allergy Asthma Immunol* **113**, 599-608, doi:10.1016/j.anai.2014.10.007 (2014).
- 85 Ashina, K. *et al.* Histamine Induces Vascular Hyperpermeability by Increasing Blood Flow and Endothelial Barrier Disruption In Vivo. *PLoS One* **10**, e0132367, doi:10.1371/journal.pone.0132367 (2015).
- 86 Mendez-Barbero, N. *et al.* The TNF-like weak inducer of the apoptosis/fibroblast growth factor-inducible molecule 14 axis mediates histamine and platelet-activating factor-induced subcutaneous vascular leakage and anaphylactic shock. *J Allergy Clin Immunol* **145**, 583-596 e586, doi:10.1016/j.jaci.2019.09.019 (2020).
- 87 Wallez, Y. & Huber, P. Endothelial adherens and tight junctions in vascular homeostasis, inflammation and angiogenesis. *Biochim Biophys Acta* **1778**, 794-809, doi:10.1016/j.bbamem.2007.09.003 (2008).
- 88 Trani, M. & Dejana, E. New insights in the control of vascular permeability: vascular endothelial-cadherin and other players. *Curr Opin Hematol* **22**, 267-272, doi:10.1097/MOH.000000000000137 (2015).
- 89 Bazzoni, G. & Dejana, E. Endothelial cell-to-cell junctions: molecular organization and role in vascular homeostasis. *Physiol Rev* **84**, 869-901, doi:10.1152/physrev.00035.2003 (2004).
- 90 Vandenbroucke, E., Mehta, D., Minshall, R. & Malik, A. B. Regulation of endothelial junctional permeability. *Ann N Y Acad Sci* **1123**, 134-145, doi:10.1196/annals.1420.016 (2008).
- 91 Dejana, E., Orsenigo, F., Molendini, C., Baluk, P. & McDonald, D. M. Organization and signaling of endothelial cell-to-cell junctions in various regions of the blood and lymphatic vascular trees. *Cell Tissue Res* **335**, 17-25, doi:10.1007/s00441-008-0694-5 (2009).
- 92 Corada, M. *et al.* Vascular endothelial-cadherin is an important determinant of microvascular integrity in vivo. *Proc Natl Acad Sci U S A* **96**, 9815-9820, doi:10.1073/pnas.96.17.9815 (1999).
- 93 Gonzalez-Mariscal, L., Tapia, R. & Chamorro, D. Crosstalk of tight junction components with signaling pathways. *Biochim Biophys Acta* **1778**, 729-756, doi:10.1016/j.bbamem.2007.08.018 (2008).
- 94 Wolburg, H. & Lippoldt, A. Tight junctions of the blood-brain barrier: development, composition and regulation. *Vascul Pharmacol* **38**, 323-337, doi:10.1016/s1537-1891(02)00200-8 (2002).
- 95 Duong, C. N. *et al.* Interference With ESAM (Endothelial Cell-Selective Adhesion Molecule) Plus Vascular Endothelial-Cadherin Causes Immediate Lethality and Lung-Specific Blood Coagulation. *Arterioscler Thromb Vasc Biol* **40**, 378-393, doi:10.1161/ATVBAHA.119.313545 (2020).
- 96 Dejana, E. & Orsenigo, F. Endothelial adherens junctions at a glance. *J Cell Sci* **126**, 2545-2549, doi:10.1242/jcs.124529 (2013).

- 97 Claesson-Welsh, L., Dejana, E. & McDonald, D. M. Permeability of the Endothelial Barrier: Identifying and Reconciling Controversies. *Trends Mol Med* **27**, 314-331, doi:10.1016/j.molmed.2020.11.006 (2021).
- 98 Lampugnani, M. G. *et al.* A novel endothelial-specific membrane protein is a marker of cell-cell contacts. *J Cell Biol* **118**, 1511-1522, doi:10.1083/jcb.118.6.1511 (1992).
- 99 Xiao, K. *et al.* Mechanisms of VE-cadherin processing and degradation in microvascular endothelial cells. *J Biol Chem* **278**, 19199-19208, doi:10.1074/jbc.M211746200 (2003).
- 100 Cattelino, A. *et al.* The conditional inactivation of the beta-catenin gene in endothelial cells causes a defective vascular pattern and increased vascular fragility. *J Cell Biol* **162**, 1111-1122, doi:10.1083/jcb.200212157 (2003).
- 101 Hox, V. *et al.* Diminution of signal transducer and activator of transcription 3 signaling inhibits vascular permeability and anaphylaxis. *J Allergy Clin Immunol* **138**, 187-199, doi:10.1016/j.jaci.2015.11.024 (2016).
- 102 Wessel, F. *et al.* Leukocyte extravasation and vascular permeability are each controlled in vivo by different tyrosine residues of VE-cadherin. *Nat Immunol* **15**, 223-230, doi:10.1038/ni.2824 (2014).
- 103 Orsenigo, F. *et al.* Phosphorylation of VE-cadherin is modulated by haemodynamic forces and contributes to the regulation of vascular permeability in vivo. *Nat Commun* **3**, 1208, doi:10.1038/ncomms2199 (2012).
- 104 Simionescu, M., Simionescu, N. & Palade, G. E. Characteristic endothelial junctions in different segments of the vascular system. *Thromb Res* **8**, 247-256, doi:10.1016/0049-3848(76)90067-0 (1976).
- 105 Aird, W. C. Endothelial cell heterogeneity. *Cold Spring Harb Perspect Med* **2**, a006429, doi:10.1101/cshperspect.a006429 (2012).
- 106 Gunzel, D. & Yu, A. S. Claudins and the modulation of tight junction permeability. *Physiol Rev* **93**, 525-569, doi:10.1152/physrev.00019.2012 (2013).
- 107 Nitta, T. *et al.* Size-selective loosening of the blood-brain barrier in claudin-5-deficient mice. *J Cell Biol* **161**, 653-660, doi:10.1083/jcb.200302070 [doi] jcb.200302070 [pii] (2003).
- 108 Kluger, M. S., Clark, P. R., Tellides, G., Gerke, V. & Pober, J. S. Claudin-5 controls intercellular barriers of human dermal microvascular but not human umbilical vein endothelial cells. *Arterioscler Thromb Vasc Biol* **33**, 489-500, doi:10.1161/ATVBAHA.112.300893 (2013).
- 109 Kakogiannos, N. *et al.* JAM-A Acts via C/EBP-alpha to Promote Claudin-5 Expression and Enhance Endothelial Barrier Function. *Circ Res* **127**, 1056-1073, doi:10.1161/CIRCRESAHA.120.316742 (2020).
- 110 Aurrand-Lions, M., Johnson-Leger, C., Wong, C., Du Pasquier, L. & Imhof, B. A. Heterogeneity of endothelial junctions is reflected by differential expression and specific subcellular localization of the three JAM family members. *Blood* **98**, 3699-3707, doi:10.1182/blood.v98.13.3699 (2001).
- 111 Simon, A. M. & Goodenough, D. A. Diverse functions of vertebrate gap junctions. *Trends Cell Biol* **8**, 477-483, doi:10.1016/s0962-8924(98)01372-5 (1998).

- 112 Yin, J. *et al.* Connexin 40 regulates lung endothelial permeability in acute lung injury via the ROCK1-MYPT1-MLC20 pathway. *Am J Physiol Lung Cell Mol Physiol* **316**, L35-L44, doi:10.1152/ajplung.00012.2018 (2019).
- 113 Gardner, T. W. *et al.* Histamine reduces ZO-1 tight-junction protein expression in cultured retinal microvascular endothelial cells. *Biochem J* **320 (Pt 3)**, 717-721 (1996).
- 114 Laakkonen, J. P. *et al.* Differential regulation of angiogenic cellular processes and claudin-5 by histamine and VEGF via PI3K-signaling, transcription factor SNAI2 and interleukin-8. *Angiogenesis* **20**, 109-124, doi:10.1007/s10456-016-9532-7 (2017).
- 115 Shen, Q., Rigor, R. R., Pivetti, C. D., Wu, M. H. & Yuan, S. Y. Myosin light chain kinase in microvascular endothelial barrier function. *Cardiovasc Res* **87**, 272-280, doi:10.1093/cvr/cvq144 (2010).
- 116 Mikelis, C. M. *et al.* RhoA and ROCK mediate histamine-induced vascular leakage and anaphylactic shock. *Nat Commun* **6**, 6725, doi:10.1038/ncomms7725 (2015).
- 117 Hubbard, K. B. & Hepler, J. R. Cell signalling diversity of the Gqalpha family of heterotrimeric G proteins. *Cell Signal* **18**, 135-150, doi:10.1016/j.cellsig.2005.08.004 (2006).
- 118 Griner, E. M. & Kazanietz, M. G. Protein kinase C and other diacylglycerol effectors in cancer. *Nat Rev Cancer* **7**, 281-294, doi:10.1038/nrc2110 (2007).
- 119 Vandembroucke St Amant, E. *et al.* PKCalpha activation of p120-catenin serine 879 phospho-switch disassembles VE-cadherin junctions and disrupts vascular integrity. *Circ Res* **111**, 739-749, doi:10.1161/CIRCRESAHA.112.269654 (2012).
- 120 Gavard, J. & Gutkind, J. S. VEGF controls endothelial-cell permeability by promoting the beta-arrestin-dependent endocytosis of VE-cadherin. *Nat Cell Biol* **8**, 1223-1234, doi:10.1038/ncb1486 (2006).
- 121 Jia, L. & Wong, H. In vitro and in vivo assessment of cellular permeability and pharmacodynamics of S-nitrosylated captopril, a nitric oxide donor. *Br J Pharmacol* **134**, 1697-1704, doi:10.1038/sj.bjp.0704431 (2001).
- 122 Thors, B., Halldorsson, H. & Thorgeirsson, G. Thrombin and histamine stimulate endothelial nitric-oxide synthase phosphorylation at Ser1177 via an AMPK mediated pathway independent of PI3K-Akt. *FEBS Lett* **573**, 175-180, doi:10.1016/j.febslet.2004.07.078 (2004).
- 123 Di Lorenzo, A. *et al.* eNOS-derived nitric oxide regulates endothelial barrier function through VE-cadherin and Rho GTPases. *J Cell Sci* **126**, 5541-5552, doi:10.1242/jcs.115972 (2013).
- 124 Deambrosis, I. *et al.* Inhibition of CD40-CD154 costimulatory pathway by a cyclic peptide targeting CD154. *J Mol Med* **87**, 181-197, doi:10.1007/s00109-008-0416-1 [doi] (2009).
- 125 Andriopoulou, P., Navarro, P., Zanetti, A., Lampugnani, M. G. & Dejana, E. Histamine induces tyrosine phosphorylation of endothelial cell-to-cell adherens junctions. *Arterioscler Thromb Vasc Biol* **19**, 2286-2297 (1999).
- 126 Chislock, E. M. & Pendergast, A. M. Abl family kinases regulate endothelial barrier function in vitro and in mice. *PLoS One* **8**, e85231, doi:10.1371/journal.pone.0085231 (2013).

- 127 Greuber, E. K., Smith-Pearson, P., Wang, J. & Pendergast, A. M. Role of ABL family kinases in cancer: from leukaemia to solid tumours. *Nat Rev Cancer* **13**, 559-571, doi:10.1038/nrc3563 (2013).
- 128 Zandy, N. L., Playford, M. & Pendergast, A. M. Abl tyrosine kinases regulate cell-cell adhesion through Rho GTPases. *Proc Natl Acad Sci U S A* **104**, 17686-17691, doi:10.1073/pnas.0703077104 (2007).
- 129 Nieuwenhuizen, N., Herbert, D. R., Lopata, A. L. & Brombacher, F. CD4+ T cell-specific deletion of IL-4 receptor alpha prevents ovalbumin-induced anaphylaxis by an IFN-gamma-dependent mechanism. *J Immunol* **179**, 2758-2765, doi:179/5/2758 [pii] (2007).
- 130 Leonard, W. J. & Lin, J. X. Cytokine receptor signaling pathways. *J Allergy Clin Immunol* **105**, 877-888, doi:10.1067/mai.2000.106899 (2000).
- 131 Wery-Zennaro, S., Letourneur, M., David, M., Bertoglio, J. & Pierre, J. Binding of IL-4 to the IL-13Ralpha(1)/IL-4Ralpha receptor complex leads to STAT3 phosphorylation but not to its nuclear translocation. *FEBS Lett* **464**, 91-96, doi:S0014-5793(99)01680-4 [pii] (1999).
- 132 Gessner, A. & Rollinghoff, M. Biologic functions and signaling of the interleukin-4 receptor complexes. *Immunobiology* **201**, 285-307, doi:10.1016/S0171-2985(00)80084-4 (2000).
- 133 Jiang, H., Harris, M. B. & Rothman, P. IL-4/IL-13 signaling beyond JAK/STAT. *J Allergy Clin Immunol* **105**, 1063-1070 (2000).
- 134 Park, L. S., Friend, D., Sassenfeld, H. M. & Urdal, D. L. Characterization of the human B cell stimulatory factor 1 receptor. *J Exp Med* **166**, 476-488, doi:10.1084/jem.166.2.476 (1987).
- 135 Lowenthal, J. W. *et al.* Expression of high affinity receptors for murine interleukin 4 (BSF-1) on hemopoietic and nonhemopoietic cells. *J Immunol* **140**, 456-464 (1988).
- 136 Murata, T., Taguchi, J. & Puri, R. K. Interleukin-13 receptor alpha' but not alpha chain: a functional component of interleukin-4 receptors. *Blood* **91**, 3884-3891 (1998).
- 137 Andrews, A. L., Holloway, J. W., Holgate, S. T. & Davies, D. E. IL-4 receptor alpha is an important modulator of IL-4 and IL-13 receptor binding: implications for the development of therapeutic targets. *J Immunol* **176**, 7456-7461 (2006).
- 138 Geha, R. S., Jabara, H. H. & Brodeur, S. R. The regulation of immunoglobulin E class-switch recombination. *Nat Rev Immunol* **3**, 721-732, doi:10.1038/nri1181 (2003).
- 139 Miloux, B. *et al.* Cloning of the human IL-13R alpha1 chain and reconstitution with the IL4R alpha of a functional IL-4/IL-13 receptor complex. *FEBS Lett* **401**, 163-166. (1997).
- 140 Matthews, D. J. *et al.* Function of the interleukin-2 (IL-2) receptor gamma-chain in biologic responses of X-linked severe combined immunodeficient B cells to IL-2, IL-4, IL-13, and IL-15. *Blood* **85**, 38-42 (1995).
- 141 Witthuhn, B. A. *et al.* Involvement of the Jak-3 Janus kinase in signalling by interleukins 2 and 4 in lymphoid and myeloid cells. *Nature* **370**, 153-157, doi:10.1038/370153a0 (1994).

- 142 Warren, W. D., Roberts, K. L., Linehan, L. A. & Berton, M. T. Regulation of the germline immunoglobulin Cgamma1 promoter by CD40 ligand and IL-4: dual role for tandem NF-kappaB binding sites. *Mol Immunol* **36**, 31-44, doi:10.1016/s0161-5890(98)00114-x (1999).
- 143 Stutz, A. M. & Woisetschlager, M. Functional synergism of STAT6 with either NF-kappa B or PU.1 to mediate IL-4-induced activation of IgE germline gene transcription. *J Immunol* **163**, 4383-4391 (1999).
- 144 Quelle, F. W. *et al.* Cloning of murine Stat6 and human Stat6, Stat proteins that are tyrosine phosphorylated in responses to IL-4 and IL-3 but are not required for mitogenesis. *Molecular & Cellular Biology* **15**, 3336-3343 (1995).
- 145 Ryan, J. J. *et al.* Growth and gene expression are predominantly controlled by distinct regions of the human IL-4 receptor. *Immunity* **4**, 123-132 (1996).
- 146 Busch-Dienstfertig, M. & Gonzalez-Rodriguez, S. IL-4, JAK-STAT signaling, and pain. *JAKSTAT* **2**, e27638, doi:10.4161/jkst.27638 (2013).
- 147 Orchansky, P. L., Kwan, R., Lee, F. & Schrader, J. W. Characterization of the cytoplasmic domain of interleukin-13 receptor-alpha. *J Biol Chem* **274**, 20818-20825 (1999).
- 148 Umeshita-Suyama, R. *et al.* Characterization of IL-4 and IL-13 signals dependent on the human IL-13 receptor alpha chain 1: redundancy of requirement of tyrosine residue for STAT3 activation. *Int Immunol* **12**, 1499-1509, doi:10.1093/intimm/12.11.1499 (2000).
- 149 Yu, H., Lee, H., Herrmann, A., Buettner, R. & Jove, R. Revisiting STAT3 signalling in cancer: new and unexpected biological functions. *Nat Rev Cancer* **14**, 736-746, doi:10.1038/nrc3818 (2014).
- 150 Takeda, K. *et al.* Targeted disruption of the mouse Stat3 gene leads to early embryonic lethality. *Proc Natl Acad Sci U S A* **94**, 3801-3804, doi:10.1073/pnas.94.8.3801 (1997).
- 151 Pickert, G. *et al.* STAT3 links IL-22 signaling in intestinal epithelial cells to mucosal wound healing. *J Exp Med* **206**, 1465-1472, doi:10.1084/jem.20082683 (2009).
- 152 Grimbacher, B., Holland, S. M. & Puck, J. M. Hyper-IgE syndromes. *Immunol Rev* **203**, 244-250, doi:10.1111/j.0105-2896.2005.00228.x (2005).
- 153 Johnston, P. A. & Grandis, J. R. STAT3 signaling: anticancer strategies and challenges. *Mol Interv* **11**, 18-26, doi:10.1124/mi.11.1.4 (2011).
- 154 Tripathi, S. K. *et al.* Genome-wide Analysis of STAT3-Mediated Transcription during Early Human Th17 Cell Differentiation. *Cell Rep* **19**, 1888-1901, doi:10.1016/j.celrep.2017.05.013 (2017).
- 155 Wegrzyn, J. *et al.* Function of mitochondrial Stat3 in cellular respiration. *Science* **323**, 793-797, doi:10.1126/science.1164551 (2009).
- 156 Feissner, R. F., Skalska, J., Gaum, W. E. & Sheu, S. S. Crosstalk signaling between mitochondrial Ca²⁺ and ROS. *Front Biosci (Landmark Ed)* **14**, 1197-1218, doi:10.2741/3303 (2009).
- 157 Davidson, S. M. & Duchon, M. R. Endothelial mitochondria: contributing to vascular function and disease. *Circ Res* **100**, 1128-1141, doi:10.1161/01.RES.0000261970.18328.1d (2007).

- 158 Wang, L. M. *et al.* IRS-1: essential for insulin- and IL-4-stimulated mitogenesis in hematopoietic cells. *Science* **261**, 1591-1594 (1993).
- 159 Junttila, I. S. Tuning the Cytokine Responses: An Update on Interleukin (IL)-4 and IL-13 Receptor Complexes. *Front Immunol* **9**, 888, doi:10.3389/fimmu.2018.00888 (2018).
- 160 Chatila, T. A. Interleukin-4 receptor signaling pathways in asthma pathogenesis. *Trends Mol Med* **10**, 493-499, doi:S1471-4914(04)00212-6 [pii] 10.1016/j.molmed.2004.08.004 [doi] (2004).
- 161 Keegan, A., Nelms, K. & Paul, W. E. The IL-4 receptor--signaling mechanisms. *Adv Exp Med Biol* **365**, 211-215 (1994).
- 162 Wurster, A. L., Withers, D. J., Uchida, T., White, M. F. & Grusby, M. J. Stat6 and IRS-2 cooperate in interleukin 4 (IL-4)-induced proliferation and differentiation but are dispensable for IL-4-dependent rescue from apoptosis. *Mol Cell Biol* **22**, 117-126 (2002).
- 163 Katagiri, S. *et al.* Overexpressing IRS1 in Endothelial Cells Enhances Angioblast Differentiation and Wound Healing in Diabetes and Insulin Resistance. *Diabetes* **65**, 2760-2771, doi:10.2337/db15-1721 (2016).
- 164 Kubota, T., Kubota, N. & Kadowaki, T. The role of endothelial insulin signaling in the regulation of glucose metabolism. *Rev Endocr Metab Disord* **14**, 207-216, doi:10.1007/s11154-013-9242-z (2013).
- 165 Lee, Y. W., Eum, S. Y., Chen, K. C., Hennig, B. & Toborek, M. Gene expression profile in interleukin-4-stimulated human vascular endothelial cells. *Mol Med* **10**, 19-27, doi:10.2119/2004-00024.lee (2004).
- 166 Kong, D. H., Kim, Y. K., Kim, M. R., Jang, J. H. & Lee, S. Emerging Roles of Vascular Cell Adhesion Molecule-1 (VCAM-1) in Immunological Disorders and Cancer. *Int J Mol Sci* **19**, doi:10.3390/ijms19041057 (2018).
- 167 Cerutti, C. & Ridley, A. J. Endothelial cell-cell adhesion and signaling. *Exp Cell Res* **358**, 31-38, doi:10.1016/j.yexcr.2017.06.003 (2017).
- 168 Alon, R. *et al.* The integrin VLA-4 supports tethering and rolling in flow on VCAM-1. *J Cell Biol* **128**, 1243-1253, doi:10.1083/jcb.128.6.1243 (1995).
- 169 van Wetering, S. *et al.* VCAM-1-mediated Rac signaling controls endothelial cell-cell contacts and leukocyte transmigration. *Am J Physiol Cell Physiol* **285**, C343-352, doi:10.1152/ajpcell.00048.2003 (2003).
- 170 Wittchen, E. S. Endothelial signaling in paracellular and transcellular leukocyte transmigration. *Front Biosci (Landmark Ed)* **14**, 2522-2545, doi:10.2741/3395 (2009).
- 171 Toi, M., Harris, A. L. & Bicknell, R. Interleukin-4 Is a Potent Mitogen for Capillary Endothelium. *Biochemical and Biophysical Research Communications* **174**, 1287-1293, doi:Doi 10.1016/0006-291x(91)91561-P (1991).
- 172 Klein, N. J., Rigley, K. P. & Callard, R. E. IL-4 regulates the morphology, cytoskeleton, and proliferation of human umbilical vein endothelial cells: relationship between vimentin and CD23. *Int Immunol* **5**, 293-301, doi:10.1093/intimm/5.3.293 (1993).
- 173 Lee, I. Y. *et al.* Interleukin-4 inhibits the vascular endothelial growth factor- and basic fibroblast growth factor-induced angiogenesis in vitro. *Mol Cells* **14**, 115-121 (2002).

- 174 Kim, J. *et al.* IL-4 inhibits cell cycle progression of human umbilical vein endothelial cells by affecting p53, p21(Waf1), cyclin D1, and cyclin E expression. *Mol Cells* **16**, 92-96 (2003).
- 175 Atkins, M. B. *et al.* Phase I evaluation of thrice-daily intravenous bolus interleukin-4 in patients with refractory malignancy. *J Clin Oncol* **10**, 1802-1809, doi:10.1200/JCO.1992.10.11.1802 (1992).
- 176 Tulpule, A. *et al.* Interleukin-4 in the treatment of AIDS-related Kaposi's sarcoma. *Ann Oncol* **8**, 79-83, doi:10.1023/a:1008205424763 (1997).
- 177 Sosman, J. A., Fisher, S. G., Kefer, C., Fisher, R. I. & Ellis, T. M. A phase I trial of continuous infusion interleukin-4 (IL-4) alone and following interleukin-2 (IL-2) in cancer patients. *Ann Oncol* **5**, 447-452, doi:10.1093/oxfordjournals.annonc.a058878 (1994).
- 178 Prendiville, J. *et al.* Recombinant human interleukin-4 (rhu IL-4) administered by the intravenous and subcutaneous routes in patients with advanced cancer--a phase I toxicity study and pharmacokinetic analysis. *Eur J Cancer* **29A**, 1700-1707, doi:10.1016/0959-8049(93)90108-r (1993).
- 179 Kotowicz, K., Callard, R. E., Klein, N. J. & Jacobs, M. G. Interleukin-4 increases the permeability of human endothelial cells in culture. *Clin Exp Allergy* **34**, 445-449, doi:10.1111/j.1365-2222.2004.01902.x (2004).
- 180 Chalubinski, M. *et al.* IL-33 and IL-4 impair barrier functions of human vascular endothelium via different mechanisms. *Vascul Pharmacol* **73**, 57-63, doi:10.1016/j.vph.2015.07.012 (2015).
- 181 Skaria, T., Burgener, J., Bachli, E. & Schoedon, G. IL-4 Causes Hyperpermeability of Vascular Endothelial Cells through Wnt5A Signaling. *PLoS One* **11**, e0156002, doi:10.1371/journal.pone.0156002 (2016).
- 182 Bakker, R. A., Timmerman, H. & Leurs, R. Histamine receptors: specific ligands, receptor biochemistry, and signal transduction. *Clin Allergy Immunol* **17**, 27-64 (2002).
- 183 Thurmond, R. L., Gelfand, E. W. & Dunford, P. J. The role of histamine H1 and H4 receptors in allergic inflammation: the search for new antihistamines. *Nat Rev Drug Discov* **7**, 41-53, doi:10.1038/nrd2465 (2008).
- 184 Jutel, M., Akdis, M. & Akdis, C. A. Histamine, histamine receptors and their role in immune pathology. *Clin Exp Allergy* **39**, 1786-1800, doi:10.1111/j.1365-2222.2009.03374.x (2009).
- 185 Wechsler, J. B., Schroeder, H. A., Byrne, A. J., Chien, K. B. & Bryce, P. J. Anaphylactic responses to histamine in mice utilize both histamine receptors 1 and 2. *Allergy* **68**, 1338-1340, doi:10.1111/all.12227 (2013).
- 186 Takeda, T., Yamashita, Y., Shimazaki, S. & Mitsui, Y. Histamine decreases the permeability of an endothelial cell monolayer by stimulating cyclic AMP production through the H2-receptor. *J Cell Sci* **101 (Pt 4)**, 745-750 (1992).
- 187 Parsons, M. E. & Ganellin, C. R. Histamine and its receptors. *Br J Pharmacol* **147 Suppl 1**, S127-135, doi:10.1038/sj.bjp.0706440 (2006).
- 188 Lovenberg, T. W. *et al.* Cloning and functional expression of the human histamine H3 receptor. *Mol Pharmacol* **55**, 1101-1107 (1999).
- 189 Toyota, H. *et al.* Behavioral characterization of mice lacking histamine H(3) receptors. *Mol Pharmacol* **62**, 389-397, doi:10.1124/mol.62.2.389 (2002).

- 190 Nakayama, T., Yao, L. & Tosato, G. Mast cell-derived angiopoietin-1 plays a critical role in the growth of plasma cell tumors. *J Clin Invest* **114**, 1317-1325, doi:10.1172/jci22089 (2004).
- 191 Gantner, F. *et al.* Histamine h(4) and h(2) receptors control histamine-induced interleukin-16 release from human CD8(+) T cells. *J Pharmacol Exp Ther* **303**, 300-307, doi:10.1124/jpet.102.036939 (2002).
- 192 O'Reilly, M. *et al.* Identification of a histamine H4 receptor on human eosinophils -role in eosinophil chemotaxis. *J Recept Signal Transduct Res* **22**, 431-448, doi:10.1081/rrs-120014612 (2002).
- 193 Hofstra, C. L., Desai, P. J., Thurmond, R. L. & Fung-Leung, W. P. Histamine H4 receptor mediates chemotaxis and calcium mobilization of mast cells. *J Pharmacol Exp Ther* **305**, 1212-1221, doi:10.1124/jpet.102.046581 (2003).
- 194 Sampson, H. A. Food-induced anaphylaxis. *Novartis Found Symp* **257**, 161-171; discussion 171-166, 207-110, 276-185 (2004).
- 195 Silverman, H. J., Van Hook, C. & Haponik, E. F. Hemodynamic changes in human anaphylaxis. *Am J Med* **77**, 341-344, doi:0002-9343(84)90717-4 [pii] (1984).
- 196 Beaupre, P. N. *et al.* Hemodynamic and two-dimensional transesophageal echocardiographic analysis of an anaphylactic reaction in a human. *Anesthesiology* **60**, 482-484, doi:10.1097/00000542-198405000-00017 (1984).
- 197 Lum, H. & Malik, A. B. Regulation of vascular endothelial barrier function. *Am J Physiol* **267**, L223-241 (1994).
- 198 Gavard, J. Endothelial permeability and VE-cadherin: a wacky comradeship. *Cell Adh Migr* **8**, 158-164 (2014).
- 199 Carmeliet, P. *et al.* Targeted deficiency or cytosolic truncation of the VE-cadherin gene in mice impairs VEGF-mediated endothelial survival and angiogenesis. *Cell* **98**, 147-157, doi:10.1016/s0092-8674(00)81010-7 (1999).
- 200 Crosby, C. V. *et al.* VE-cadherin is not required for the formation of nascent blood vessels but acts to prevent their disassembly. *Blood* **105**, 2771-2776, doi:10.1182/blood-2004-06-2244 (2005).
- 201 Yuan, L. *et al.* RhoJ is an endothelial cell-restricted Rho GTPase that mediates vascular morphogenesis and is regulated by the transcription factor ERG. *Blood* **118**, 1145-1153, doi:10.1182/blood-2010-10-315275 (2011).
- 202 Aman, J. *et al.* Effective treatment of edema and endothelial barrier dysfunction with imatinib. *Circulation* **126**, 2728-2738, doi:10.1161/circulationaha.112.134304 (2012).
- 203 Ogawa, Y. & Grant, J. A. Mediators of anaphylaxis. *Immunol. Allergy Clin North Am* **27**, 249-260 (2007).
- 204 Stone, S. F. *et al.* Elevated serum cytokines during human anaphylaxis: Identification of potential mediators of acute allergic reactions. *The Journal of allergy and clinical immunology* **124**, 786-792 e784, doi:10.1016/j.jaci.2009.07.055 (2009).
- 205 Finkelman, F. D. Anaphylaxis: lessons from mouse models. *J. Allergy Clin. Immunol.* **120**, 506-515 (2007).

- 206 Tachdjian, R. *et al.* In vivo regulation of the allergic response by the IL-4 receptor alpha chain immunoreceptor tyrosine-based inhibitory motif. *J Allergy Clin Immunol* **125**, 1128-1136 e1128, doi:10.1016/j.jaci.2010.01.054 (2010).
- 207 Alva, J. A. *et al.* VE-Cadherin-Cre-recombinase transgenic mouse: a tool for lineage analysis and gene deletion in endothelial cells. *Dev Dyn* **235**, 759-767, doi:10.1002/dvdy.20643 (2006).
- 208 Kisanuki, Y. Y. *et al.* Tie2-Cre transgenic mice: a new model for endothelial cell-lineage analysis in vivo. *Dev Biol* **230**, 230-242, doi:10.1006/dbio.2000.0106 (2001).
- 209 Baniyash, M. & Eshhar, Z. Inhibition of IgE binding to mast cells and basophils by monoclonal antibodies to murine IgE. *Eur J Immunol* **14**, 799-807 (1984).
- 210 Finkelman, F. D. *et al.* Anti-cytokine antibodies as carrier proteins. Prolongation of in vivo effects of exogenous cytokines by injection of cytokine-anti-cytokine antibody complexes. *Journal of immunology* **151**, 1235-1244 (1993).
- 211 Bouis, D., Hospers, G. A., Meijer, C., Molema, G. & Mulder, N. H. Endothelium in vitro: a review of human vascular endothelial cell lines for blood vessel-related research. *Angiogenesis* **4**, 91-102, doi:10.1023/a:1012259529167 (2001).
- 212 Edgell, C. J., McDonald, C. C. & Graham, J. B. Permanent cell line expressing human factor VIII-related antigen established by hybridization. *Proc Natl Acad Sci U S A* **80**, 3734-3737, doi:10.1073/pnas.80.12.3734 (1983).
- 213 Dudek, S. M. *et al.* Abl tyrosine kinase phosphorylates nonmuscle Myosin light chain kinase to regulate endothelial barrier function. *Mol Biol Cell* **21**, 4042-4056, doi:10.1091/mbc.E09-10-0876 (2010).
- 214 Wu, D. *et al.* Interleukin-13 (IL-13)/IL-13 Receptor α 1 (IL-13R α 1) Signaling Regulates Intestinal Epithelial Cystic Fibrosis Transmembrane Conductance Regulator Channel-dependent Cl⁻ Secretion*. *J Biol Chem* **286**, 13357-13369, doi:10.1074/jbc.M110.214965 (2011).
- 215 Noah, T. K., Kazanjian, A., Whitsett, J. & Shroyer, N. F. SAM pointed domain ETS factor (SPDEF) regulates terminal differentiation and maturation of intestinal goblet cells. *Exp Cell Res* **316**, 452-465, doi:10.1016/j.yexcr.2009.09.020 (2010).
- 216 Sandford, A. J. *et al.* Polymorphisms in the IL4, IL4RA, and FCER1B genes and asthma severity. *J Allergy Clin Immunol* **106**, 135-140 (2000).
- 217 Howard, T. D. *et al.* Gene-gene interaction in asthma: IL4RA and IL13 in a Dutch population with asthma. *Am J Hum Genet* **70**, 230-236, doi:S0002-9297(07)61296-8 [pii] 10.1086/338242 [doi] (2002).
- 218 Hershey, G. K., Friedrich, M. F., Esswein, L. A., Thomas, M. L. & Chatila, T. A. The association of atopy with a gain-of-function mutation in the alpha subunit of the interleukin-4 receptor. *N Engl J Med* **337**, 1720-1725. (1997).
- 219 Faffe, D. S. *et al.* IL-13 and IL-4 promote TARC release in human airway smooth muscle cells: role of IL-4 receptor genotype. *Am J Physiol Lung Cell Mol Physiol* **285**, L907-914, doi:10.1152/ajplung.00120.2003 [doi] 00120.2003 [pii] (2003).
- 220 Risma, K. A. *et al.* V75R576 IL-4 receptor alpha is associated with allergic asthma and enhanced IL-4 receptor function. *J Immunol* **169**, 1604-1610 (2002).

- 221 Wenzel, S. E. *et al.* IL4R alpha mutations are associated with asthma exacerbations and mast cell/IgE expression. *Am J Respir Crit Care Med* **175**, 570-576, doi:10.1164/rccm.200607-909OC (2007).
- 222 Lyseng-Williamson, K. & Jarvis, B. Imatinib. *Drugs* **61**, 1765-1774; discussion 1775-1766, doi:10.2165/00003495-200161120-00007 (2001).
- 223 Iwaki, S. *et al.* Btk plays a crucial role in the amplification of Fc epsilonRI-mediated mast cell activation by kit. *J Biol Chem* **280**, 40261-40270, doi:10.1074/jbc.M506063200 (2005).
- 224 Brown, S. G. *et al.* Anaphylaxis: clinical patterns, mediator release, and severity. *J Allergy Clin Immunol* **132**, 1141-1149 e1145, doi:10.1016/j.jaci.2013.06.015 (2013).
- 225 Tachdjian, R. *et al.* Pathogenicity of a disease-associated human IL-4 receptor allele in experimental asthma. *J Exp Med* **206**, 2191-2204, doi:10.1084/jem.20091480 (2009).
- 226 Mathias, C. B. *et al.* IgE-mediated systemic anaphylaxis and impaired tolerance to food antigens in mice with enhanced IL-4 receptor signaling. *J Allergy Clin Immunol* **127**, 795-805 e791-796, doi:10.1016/j.jaci.2010.11.009 (2011).
- 227 Blaeser, F. *et al.* Targeted inactivation of the IL-4 receptor alpha chain I4R motif promotes allergic airway inflammation. *J Exp Med* **198**, 1189-1200, doi:10.1084/jem.20030471 (2003).
- 228 Sledd, J. *et al.* Loss of IL-4Ralpha-mediated PI3K signaling accelerates the progression of IgE/mast cell-mediated reactions. *Immun Inflamm Dis* **3**, 420-430, doi:10.1002/iid3.80 (2015).
- 229 Burton, O. T. *et al.* Direct effects of IL-4 on mast cells drive their intestinal expansion and increase susceptibility to anaphylaxis in a murine model of food allergy. *Mucosal Immunol*, doi:10.1038/mi.2012.112 (2012).
- 230 Chen, C. Y. *et al.* Induction of Interleukin-9-producing Mucosal Mast cells Promotes Susceptibility to IgE-mediated Experimental Food Allergy. *Immunity* **43**, 788-802, doi:10.1016/j.immuni.2015.08.020 (2015).
- 231 Lee, J. *et al.* IL-25 and CD4+ Th2 cells enhance ILC2-derived IL-13 production that promotes IgE-mediated experimental food allergy. *JACI* **accepted**. (2015).
- 232 Chen, L. *et al.* RSRC1 SUMOylation enhances SUMOylation and inhibits transcriptional activity of estrogen receptor beta. *FEBS Lett* **589**, 1476-1484, doi:10.1016/j.febslet.2015.04.035 (2015).
- 233 Sullivan, B. M. *et al.* Genetic analysis of basophil function in vivo. *Nat Immunol* **12**, 527-535, doi:10.1038/ni.2036 (2011).
- 234 Brandt, E. B. *et al.* Targeting IL-4/IL-13 signaling to alleviate oral allergen-induced diarrhea. *J Allergy Clin Immunol* **123**, 53-58, doi:10.1016/j.jaci.2008.10.001 (2009).
- 235 Noelle, R., Krammer, P. H., Ohara, J., Uhr, J. W. & Vitetta, E. S. Increased expression of Ia antigens on resting B cells: an additional role for B-cell growth factor. *Proc Natl Acad Sci U S A* **81**, 6149-6153, doi:10.1073/pnas.81.19.6149 (1984).
- 236 Bhasin, M. *et al.* Bioinformatic identification and characterization of human endothelial cell-restricted genes. *BMC Genomics* **11**, 342, doi:10.1186/1471-2164-11-342 (2010).

- 237 Jabbour, E., Kantarjian, H. & Cortes, J. Use of second- and third-generation tyrosine kinase inhibitors in the treatment of chronic myeloid leukemia: an evolving treatment paradigm. *Clin Lymphoma Myeloma Leuk* **15**, 323-334, doi:10.1016/j.clml.2015.03.006 (2015).
- 238 Aikawa, Y. *et al.* PU.1-mediated upregulation of CSF1R is crucial for leukemia stem cell potential induced by MOZ-TIF2. *Nat Med* **16**, 580-585, 581p following 585, doi:10.1038/nm.2122 (2010).
- 239 Mol, C. D. *et al.* Structural basis for the autoinhibition and STI-571 inhibition of c-Kit tyrosine kinase. *J Biol Chem* **279**, 31655-31663, doi:10.1074/jbc.M403319200 (2004).
- 240 Heinrich, M. C. *et al.* Inhibition of c-kit receptor tyrosine kinase activity by STI 571, a selective tyrosine kinase inhibitor. *Blood* **96**, 925-932 (2000).
- 241 Tuveson, D. A. *et al.* STI571 inactivation of the gastrointestinal stromal tumor c-KIT oncoprotein: biological and clinical implications. *Oncogene* **20**, 5054-5058, doi:10.1038/sj.onc.1204704 (2001).
- 242 Cerny-Reiterer, S. *et al.* Long-term treatment with imatinib results in profound mast cell deficiency in Ph+ chronic myeloid leukemia. *Oncotarget* **6**, 3071-3084, doi:10.18632/oncotarget.3074 (2015).
- 243 Cahill, K. N. *et al.* KIT Inhibition by Imatinib in Patients with Severe Refractory Asthma. *N Engl J Med* **376**, 1911-1920, doi:10.1056/NEJMoa1613125 (2017).
- 244 Gupta, R. S. *et al.* The Public Health Impact of Parent-Reported Childhood Food Allergies in the United States. *Pediatrics* **142**, doi:10.1542/peds.2018-1235 (2018).
- 245 Sampson, H. A. 9. Food allergy. *J Allergy Clin Immunol* **111**, S540-547, doi:S0091674902912534 [pii] (2003).
- 246 Yamani, A. *et al.* The vascular endothelial specific IL-4 receptor alpha-ABL1 kinase signaling axis regulates the severity of IgE-mediated anaphylactic reactions. *J Allergy Clin Immunol* **142**, 1159-1172 e1155, doi:10.1016/j.jaci.2017.08.046 (2018).
- 247 Majno, G., Palade, G. E. & Schoefl, G. I. Studies on inflammation. II. The site of action of histamine and serotonin along the vascular tree: a topographic study. *J Biophys Biochem Cytol* **11**, 607-626 (1961).
- 248 Alsaffar, H., Martino, N., Garrett, J. P. & Adam, A. P. Interleukin-6 promotes a sustained loss of endothelial barrier function via Janus kinase-mediated STAT3 phosphorylation and de novo protein synthesis. *Am J Physiol Cell Physiol* **314**, C589-C602, doi:10.1152/ajpcell.00235.2017 (2018).
- 249 Wang, L. *et al.* Suppressing STAT3 activity protects the endothelial barrier from VEGF-mediated vascular permeability. *bioRxiv*, doi:10.1101/2020.10.27.358374 (2020).
- 250 Moh, A. *et al.* Role of STAT3 in liver regeneration: survival, DNA synthesis, inflammatory reaction and liver mass recovery. *Lab Invest* **87**, 1018-1028, doi:10.1038/labinvest.3700630 (2007).
- 251 Singer, B. D. *et al.* Flow-cytometric method for simultaneous analysis of mouse lung epithelial, endothelial, and hematopoietic lineage cells. *Am J Physiol Lung Cell Mol Physiol* **310**, L796-801, doi:10.1152/ajplung.00334.2015 (2016).

- 252 Qin, Q. *et al.* Lisa: inferring transcriptional regulators through integrative modeling of public chromatin accessibility and ChIP-seq data. *Genome Biol* **21**, 32, doi:10.1186/s13059-020-1934-6 (2020).
- 253 He, L. *et al.* Single-cell RNA sequencing of mouse brain and lung vascular and vessel-associated cell types. *Sci Data* **5**, 180160, doi:10.1038/sdata.2018.160 (2018).
- 254 Giaever, I. & Keese, C. R. Micromotion of mammalian cells measured electrically. *Proc Natl Acad Sci U S A* **88**, 7896-7900, doi:10.1073/pnas.88.17.7896 (1991).
- 255 Dejana, E., Orsenigo, F. & Lampugnani, M. G. The role of adherens junctions and VE-cadherin in the control of vascular permeability. *J Cell Sci* **121**, 2115-2122, doi:10.1242/jcs.017897 (2008).
- 256 Kugelmann, D. *et al.* Histamine causes endothelial barrier disruption via Ca(2+)-mediated RhoA activation and tension at adherens junctions. *Sci Rep* **8**, 13229, doi:10.1038/s41598-018-31408-3 (2018).
- 257 Gokal, P. K., Cavanaugh, A. H. & Thompson, E. A., Jr. The effects of cycloheximide upon transcription of rRNA, 5 S RNA, and tRNA genes. *J Biol Chem* **261**, 2536-2541 (1986).
- 258 Nolop, K. B. & Ryan, U. S. Enhancement of tumor necrosis factor-induced endothelial cell injury by cycloheximide. *Am J Physiol* **259**, L123-129, doi:10.1152/ajplung.1990.259.2.L123 (1990).
- 259 Huang da, W., Sherman, B. T. & Lempicki, R. A. Systematic and integrative analysis of large gene lists using DAVID bioinformatics resources. *Nat Protoc* **4**, 44-57, doi:10.1038/nprot.2008.211 (2009).
- 260 Noah, T. K. *et al.* IL-13-induced intestinal secretory epithelial cell antigen passages are required for IgE-mediated food-induced anaphylaxis. *J Allergy Clin Immunol* **144**, 1058-1073 e1053, doi:10.1016/j.jaci.2019.04.030 (2019).
- 261 Dalal, P. J., Muller, W. A. & Sullivan, D. P. Endothelial Cell Calcium Signaling during Barrier Function and Inflammation. *Am J Pathol* **190**, 535-542, doi:10.1016/j.ajpath.2019.11.004 (2020).
- 262 Wierzbicki, T. *et al.* IL-4 primes human endothelial cells for secondary responses to histamine. *J Leukoc Biol* **74**, 420-427 (2003).
- 263 Schnyder, B. *et al.* Interleukin-4 (IL-4) and IL-13 bind to a shared heterodimeric complex on endothelial cells mediating vascular cell adhesion molecule-1 induction in the absence of the common gamma chain. *Blood* **87**, 4286-4295 (1996).
- 264 Harrison, A. R. *et al.* Lyssavirus P-protein selectively targets STAT3-STAT1 heterodimers to modulate cytokine signalling. *PLoS Pathog* **16**, e1008767, doi:10.1371/journal.ppat.1008767 (2020).
- 265 Maretzky, T. *et al.* ADAM10 mediates E-cadherin shedding and regulates epithelial cell-cell adhesion, migration, and beta-catenin translocation. *Proc Natl Acad Sci U S A* **102**, 9182-9187, doi:10.1073/pnas.0500918102 (2005).
- 266 Aghababaei, M., Hogg, K., Perdu, S., Robinson, W. P. & Beristain, A. G. ADAM12-directed ectodomain shedding of E-cadherin potentiates trophoblast fusion. *Cell Death Differ* **22**, 1970-1984, doi:10.1038/cdd.2015.44 (2015).

- 267 Patel, A. *et al.* Histamine induces the production of matrix metalloproteinase-9 in human astrocytic cultures via H1-receptor subtype. *Brain Struct Funct* **221**, 1845-1860, doi:10.1007/s00429-015-1007-x (2016).
- 268 Gschwandtner, M. *et al.* Histamine upregulates keratinocyte MMP-9 production via the histamine H1 receptor. *J Invest Dermatol* **128**, 2783-2791, doi:10.1038/jid.2008.153 (2008).
- 269 Gulati, A. Vascular Endothelium and Hypovolemic Shock. *Curr Vasc Pharmacol* **14**, 187-195, doi:10.2174/1570161114666151202210221 (2016).
- 270 Lee, Y. W., Kuhn, H., Hennig, B. & Toborek, M. IL-4 induces apoptosis of endothelial cells through the caspase-3-dependent pathway. *FEBS Lett* **485**, 122-126, doi:10.1016/s0014-5793(00)02208-0 (2000).
- 271 Childs, E. W., Tharakan, B., Hunter, F. A., Tinsley, J. H. & Cao, X. Apoptotic signaling induces hyperpermeability following hemorrhagic shock. *Am J Physiol Heart Circ Physiol* **292**, H3179-3189, doi:10.1152/ajpheart.01337.2006 (2007).
- 272 Wojciak-Stothard, B., Potempa, S., Eichholtz, T. & Ridley, A. J. Rho and Rac but not Cdc42 regulate endothelial cell permeability. *J Cell Sci* **114**, 1343-1355 (2001).
- 273 Duluc, L. & Wojciak-Stothard, B. Rho GTPases in the regulation of pulmonary vascular barrier function. *Cell Tissue Res* **355**, 675-685, doi:10.1007/s00441-014-1805-0 (2014).
- 274 Goldblum, S. E., Young, B. A., Wang, P. & Murphy-Ullrich, J. E. Thrombospondin-1 induces tyrosine phosphorylation of adherens junction proteins and regulates an endothelial paracellular pathway. *Mol Biol Cell* **10**, 1537-1551, doi:10.1091/mbc.10.5.1537 (1999).
- 275 Hu, Y. *et al.* Identification and functional characterization of a novel human misshapen/Nck interacting kinase-related kinase, hMINK beta. *J Biol Chem* **279**, 54387-54397, doi:10.1074/jbc.M404497200 (2004).
- 276 Daulat, A. M. *et al.* Mink1 regulates beta-catenin-independent Wnt signaling via Prickle phosphorylation. *Mol Cell Biol* **32**, 173-185, doi:10.1128/MCB.06320-11 (2012).
- 277 Schnoor, M., Betanzos, A., Weber, D. A. & Parkos, C. A. Guanylate-binding protein-1 is expressed at tight junctions of intestinal epithelial cells in response to interferon-gamma and regulates barrier function through effects on apoptosis. *Mucosal Immunol* **2**, 33-42, doi:10.1038/mi.2008.62 (2009).
- 278 Konno, T. *et al.* Guanylate binding protein-1-mediated epithelial barrier in human salivary gland duct epithelium. *Exp Cell Res* **371**, 31-41, doi:10.1016/j.yexcr.2018.07.033 (2018).
- 279 Tripal, P. *et al.* Unique features of different members of the human guanylate-binding protein family. *J Interferon Cytokine Res* **27**, 44-52, doi:10.1089/jir.2007.0086 (2007).
- 280 Belgrano, A. *et al.* Multi-tasking role of the mechanosensing protein Ankrd2 in the signaling network of striated muscle. *PLoS One* **6**, e25519, doi:10.1371/journal.pone.0025519 (2011).
- 281 Alluri, H. *et al.* Attenuation of Blood-Brain Barrier Breakdown and Hyperpermeability by Calpain Inhibition. *J Biol Chem* **291**, 26958-26969, doi:10.1074/jbc.M116.735365 (2016).

- 282 Victorino, G. P., Newton, C. R. & Curran, B. Endothelin-1 decreases microvessel permeability after endothelial activation. *J Trauma* **56**, 832-836, doi:10.1097/01.ta.0000057228.45839.3c (2004).
- 283 Abraham, D. & Dashwood, M. Endothelin--role in vascular disease. *Rheumatology (Oxford)* **47 Suppl 5**, v23-24, doi:10.1093/rheumatology/ken282 (2008).
- 284 Farrugia, A. J. & Calvo, F. The Borg family of Cdc42 effector proteins Cdc42EP1-5. *Biochem Soc Trans* **44**, 1709-1716, doi:10.1042/BST20160219 (2016).
- 285 Kouklis, P., Konstantoulaki, M., Vogel, S., Broman, M. & Malik, A. B. Cdc42 regulates the restoration of endothelial barrier function. *Circ Res* **94**, 159-166, doi:10.1161/01.RES.0000110418.38500.31 [doi] 01.RES.0000110418.38500.31 [pii] (2004).
- 286 McCole, D. F. Phosphatase regulation of intercellular junctions. *Tissue Barriers* **1**, e26713, doi:10.4161/tisb.26713 (2013).
- 287 Cheung, Y. P. *et al.* A Critical Role for Perivascular Cells in Amplifying Vascular Leakage Induced by Dengue Virus Nonstructural Protein 1. *mSphere* **5**, doi:10.1128/mSphere.00258-20 (2020).
- 288 Potter, M. D., Barbero, S. & Cheresh, D. A. Tyrosine phosphorylation of VE-cadherin prevents binding of p120- and beta-catenin and maintains the cellular mesenchymal state. *J Biol Chem* **280**, 31906-31912, doi:10.1074/jbc.M505568200 (2005).
- 289 Xu, X., Kasembeli, M. M., Jiang, X., Tweardy, B. J. & Tweardy, D. J. Chemical probes that competitively and selectively inhibit Stat3 activation. *PLoS One* **4**, e4783, doi:10.1371/journal.pone.0004783 (2009).
- 290 Wang, J. & Sampson, H. A. Food anaphylaxis. *Clin. Exp. Allergy* **37**, 651-660 (2007).
- 291 Schrandt, J. J., Unsalan-Hooyan, R. W., Forget, P. P. & Jansen, J. [51Cr]EDTA intestinal permeability in children with cow's milk tolerance. *J. pediatr. Gastroenterol. Nutr.* **10**, 189-192 (1990).
- 292 Troncone, R., Caputo, N., Florio, G. & Finelli, E. Increased intestinal sugar permeability after challenge in children with cow's milk allergy or intolerance. *Allergy* **49**, 142-146 (1994).
- 293 Van Elburg, R., Heymans, H. S. & De, M. J. Effect of disodium cromoglycate on intestinal permeability changes and clinical response during cow's milk challenge. *Source (Bibliographic Citation): Pediatr Allergy Immunol* **4**, 79-85 (1993).
- 294 Calvani M Fau - Cardinale, F. *et al.* Risk factors for severe pediatric food anaphylaxis in Italy. *Pediatr Allergy Immunol* **22**, 813-819 LID - 810.1111/j.1399-3038.2011.01200.x [doi] (2011).
- 295 Brown, S. G. A. Clinical features and severity grading of anaphylaxis. *J Allergy Clin Immunol* **114**, 371-376 (2004).
- 296 Galli, S. J. *et al.* Mast cells as "tunable" effector and immunoregulatory cells: recent advances. *Annu. Rev. Immunol.* **23**, 749-786 (2005).
- 297 Lorentz, A., Schwengberg, S., Mierke, C., Manns, M. P. & Bischoff, S. C. Human intestinal mast cells produce IL-5 in vitro upon IgE receptor cross-linking and in vivo in the course of intestinal inflammatory disease. *Eur J Immunol* **29**, 1496-1503 (1999).

- 298 Santos, J., Benjamin, M., Yang, P. C., Prior, T. & Perdue, M. H. Chronic stress impairs rat growth and jejunal epithelial barrier function: role of mast cells. *Am J Physiol Gastrointest Liver Physiol* **278**, G847-854 (2000).
- 299 Kelefiotis, D. & Vakirtzi-Lemonias, C. In vivo responses of mouse blood cells to platelet-activating factor (PAF): role of the mediators of anaphylaxis. *Agents Actions* **40**, 150-156 (1993).
- 300 Lorentz, A., Schwengberg, S., Sellge, G., Manns, M. P. & Bischoff, S. C. Human intestinal mast cells are capable of producing different cytokine profiles: Role of IgE receptor cross-linking and IL-4. *J. Immunol.* **164**, 43-48 (2000).
- 301 Wang, M. *et al.* Combined blockade of the histamine H1 and H4 receptor suppresses peanut-induced intestinal anaphylaxis by regulating dendritic cell function. *Allergy* **71**, 1561-1574, doi:10.1111/all.12904 (2016).
- 302 Capaldo, C. T. *et al.* Proinflammatory cytokine-induced tight junction remodeling through dynamic self-assembly of claudins. *Mol Biol Cell* **25**, 2710-2719, doi:10.1091/mbc.E14-02-0773 (2014).
- 303 Akiho, H., Blennerhassett, P., Deng, Y. & Collins, S. M. Role of IL-4, IL-13, and STAT6 in inflammation-induced hypercontractility of murine smooth muscle cells. *Am J Physiol Gastrointest Liver Physiol* **282**, G226-232, doi:10.1152/ajpgi.2002.282.2.G226 (2002).
- 304 Akiho, H., Ihara, E., Motomura, Y. & Nakamura, K. Cytokine-induced alterations of gastrointestinal motility in gastrointestinal disorders. *World J Gastrointest Pathophysiol* **2**, 72-81 (2011).
- 305 Akiho, H. *et al.* Interleukin-4- and -13-induced hypercontractility of human intestinal muscle cells-implication for motility changes in Crohn's disease. *Am J Physiol Gastrointest Liver Physiol* **288**, G609-615, doi:10.1152/ajpgi.00273.2004 (2005).
- 306 Khan, W. I. *et al.* Modulation of intestinal muscle contraction by interleukin-9 (IL-9) or IL-9 neutralization: correlation with worm expulsion in murine nematode infections. *Infect Immun* **71**, 2430-2438 (2003).
- 307 Zhao, A. *et al.* Dependence of IL-4, IL-13, and nematode-induced alterations in murine small intestinal smooth muscle contractility on Stat6 and enteric nerves. *J Immunol* **171**, 948-954, doi:10.4049/jimmunol.171.2.948 (2003).
- 308 Rowe, A., Jr., Rowe, A. H., Uyeyama, K. & Young, E. J. Diarrhea caused by food allergy. *J Allergy* **27**, 424-436, doi:10.1016/0021-8707(56)90102-2 (1956).
- 309 Rowe, A. H. [Food allergy and its clinical manifestations]. *Rev Clin Esp* **62**, 366-373 (1956).
- 310 Rowe, A. H. Abdominal Food Allergy: Its History, Symptomatology, Diagnosis and Treatment. *Cal West Med* **29**, 317-322 (1928).
- 311 Simons, F. E. & Sheikh, A. Anaphylaxis: the acute episode and beyond. *Bmj* **346**, f602, doi:10.1136/bmj.f602 (2013).
- 312 Lieberman, P. *et al.* The diagnosis and management of anaphylaxis practice parameter: 2010 update. *J Allergy Clin Immunol* **126**, 477-480 e471-442, doi:10.1016/j.jaci.2010.06.022 (2010).
- 313 Soter, N. A., Austen, K. F. & Wasserman, S. I. Oral disodium cromoglycate in the treatment of systemic mastocytosis. *N Engl J Med* **301**, 465-469, doi:10.1056/nejm197908303010903 (1979).

- 314 Horan, R. F., Sheffer, A. L. & Austen, K. F. Cromolyn sodium in the management of systemic mastocytosis. *J Allergy Clin Immunol* **85**, 852-855 (1990).
- 315 Andre, C., Andre, F., Colin, L. & Cavagna, S. Measurement of intestinal permeability to mannitol and lactulose as a means of diagnosing food allergy and evaluating therapeutic effectiveness of disodium cromoglycate. *Ann Allergy* **59**, 127-130 (1987).
- 316 Perdue, M. H., Masson, S., Wershil, B. K. & Galli, S. J. Role of mast cells in ion transport abnormalities associated with intestinal anaphylaxis. Correction of the diminished secretory response in genetically mast cell-deficient W/W^v mice by bone marrow transplantation. *J Clin Invest* **87**, 687-693 (1991).
- 317 Crowe, S. E., Sestini, P. & Perdue, M. H. Allergic reactions of rat jejunal mucosa. Ion transport responses to luminal antigen and inflammatory mediators. *Gastroenterology* **99**, 74-82 (1990).
- 318 Thiagarajah, J. R., Donowitz, M. & Verkman, A. S. Secretory diarrhoea: mechanisms and emerging therapies. *Nat Rev Gastroenterol Hepatol* **12**, 446-457, doi:10.1038/nrgastro.2015.111 (2015).
- 319 Barrett, K. E. & Keely, S. J. Chloride secretion by the intestinal epithelium: Molecular basis and Regulatory Aspects. *Ann. Rev. Physiol.* **62**, 535-572 (2000).
- 320 Homaidan, F. R., Tripodi, J., Zhao, L. & Burakoff, R. Regulation of ion transport by histamine in mouse cecum. *Eur. J. Pharmacol.* **331**, 199-204 (1997).
- 321 Kim, J. E. *et al.* Diosgenin effectively suppresses skin inflammation induced by phthalic anhydride in IL-4/Luc/CNS-1 transgenic mice. *Biosci Biotechnol Biochem* **80**, 891-901, doi:10.1080/09168451.2015.1135040 (2016).
- 322 Kellum, J. M., Budhoo, M. R., Siriwardena, A. K., Smith, E. P. & Jebraili, S. A. Serotonin induces Cl⁻ secretion in human jejunal mucosa in vitro via a nonneural pathway at a 5-HT₄ receptor. *Am J Physiol* **267**, G357-363, doi:10.1152/ajpgi.1994.267.3.G357 (1994).
- 323 Collins, D., Hogan, A. M., Skelly, M. M., Baird, A. W. & Winter, D. C. Cyclic AMP-mediated chloride secretion is induced by prostaglandin F₂α in human isolated colon. *Br J Pharmacol* **158**, 1771-1776, doi:10.1111/j.1476-5381.2009.00464.x (2009).
- 324 Nakamura, T. *et al.* Mast cell-derived prostaglandin D₂ attenuates anaphylactic reactions in mice. *J Allergy Clin Immunol* **140**, 630-632 e639, doi:10.1016/j.jaci.2017.02.030 (2017).
- 325 Galletta, L. J. *et al.* IL-4 is a potent modulator of ion transport in the human bronchial epithelium in vitro. *J Immunol* **168**, 839-845 (2002).
- 326 Zund, G., Madara, J. L., Dzus, A. L., Awtrey, C. S. & Colgan, S. P. Interleukin-4 and Interleukin-13 differentially regulate epithelial chloride secretion. *J Biol Chem* **271**, 7460-7464 (1996).
- 327 Anthony, R. M., Rutitzky, L. I., Urban, J. F., Jr., Stadecker, M. J. & Gause, W. C. Protective immune mechanisms in helminth infection. *Nat Rev Immunol* **7**, 975-987, doi:10.1038/nri2199 (2007).
- 328 Lee, J. B. *et al.* IL-25 and CD4(+) TH₂ cells enhance type 2 innate lymphoid cell-derived IL-13 production, which promotes IgE-mediated experimental food allergy. *J Allergy Clin Immunol* **137**, 1216-1225 e1215, doi:10.1016/j.jaci.2015.09.019 (2016).

- 329 Groschwitz, K. R. & Hogan, S. P. Intestinal barrier function: molecular regulation and disease pathogenesis. *J Allergy Clin Immunol* **124**, 3-20; quiz 21-22, doi:S0091-6749(09)00864-1 [pii]
10.1016/j.jaci.2009.05.038 [doi] (2009).
- 330 Turner, J. R. Intestinal mucosal barrier function in health and disease. *Nat Rev Immunol* **9**, 799-809, doi:nri2653 [pii]
10.1038/nri2653 [doi] (2009).
- 331 Turner, M. W. *et al.* Intestinal hypersensitivity reactions in the rat. I. Uptake of intact protein, permeability to sugars and their correlation with mucosal mast-cell activation. *Immunology* **63**, 119-124 (1988).
- 332 King, S. J., Miller, H. R., Newlands, G. F. & Woodbury, R. G. Depletion of mucosal mast cell protease by corticosteroids: effect on intestinal anaphylaxis in the rat. *Proc Natl Acad Sci U S A* **82**, 1214-1218 (1985).
- 333 Scudamore, C. L., Thornton, E. M., McMillan, L., Newlands, G. F. & Miller, H. R. Release of the mucosal mast cell granule chymase, rat mast cell protease-II, during anaphylaxis is associated with the rapid development of paracellular permeability to macromolecules in rat jejunum. *J Exp Med* **182**, 1871-1881 (1995).
- 334 Yu, L. C. & Perdue, M. H. Role of mast cells in intestinal mucosal function: studies in models of hypersensitivity and stress. *Immunol Rev* **179**, 61-73 (2001).
- 335 Bischoff, S. C. & Manns, M. P. [The scientific basis for food allergy]. *Med Klin (Munich)* **91**, 389-395 (1996).
- 336 Gurish, M. F. & Austen, K. F. The diverse roles of mast cells. *The Journal of experimental medicine* **194**, F1-5 (2001).
- 337 Galli, S. J., Maurer, M. & Lantz, C. S. Mast cells as sentinels of innate immunity. *Curr Opin Immunol* **11**, 53-59 (1999).
- 338 Pejler, G., Abrink, M., Ringvall, M. & Wernersson, S. Mast cell proteases. *Adv Immunol* **95**, 167-255, doi:S0065-2776(07)95006-3 [pii]
10.1016/S0065-2776(07)95006-3 [doi] (2007).
- 339 Bankova, L. G. *et al.* Mouse mast cell proteases 4 and 5 mediate epidermal injury through disruption of tight junctions. *J Immunol* **192**, 2812-2820, doi:10.4049/jimmunol.1301794 (2014).
- 340 Lawrence, C. E., Paterson, Y. Y., Wright, S. H., Knight, P. A. & Miller, H. R. Mouse mast cell protease-1 is required for the enteropathy induced by gastrointestinal helminth infection in the mouse. *Gastroenterology* **127**, 155-165, doi:S0016508504006092 [pii] (2004).
- 341 Groschwitz, K. R. *et al.* Mast cells regulate homeostatic intestinal epithelial migration and barrier function by a chymase/Mcpt4-dependent mechanism. *Proc Natl Acad Sci U S A* **106**, 22381-22386, doi:0906372106 [pii]
10.1073/pnas.0906372106 [doi] (2009).
- 342 Groschwitz, K. R., Wu, D., Osterfeld, H., Ahrens, R. & Hogan, S. P. Chymase-mediated intestinal epithelial permeability is regulated by a protease-activating receptor/matrix metalloproteinase-2-dependent mechanism. *Am J Physiol Gastrointest Liver Physiol* **304**, G479-489, doi:10.1152/ajpgi.00186.2012 (2013).

- 343 Jacob, C. *et al.* Mast cell tryptase controls paracellular permeability of the intestine. Role of protease-activated receptor 2 and beta-arrestins. *J Biol Chem* **280**, 31936-31948, doi:10.1074/jbc.M506338200 (2005).
- 344 Wilcz-Villega, E. M., McClean, S. & O'Sullivan, M. A. Mast cell tryptase reduces junctional adhesion molecule-A (JAM-A) expression in intestinal epithelial cells: implications for the mechanisms of barrier dysfunction in irritable bowel syndrome. *Am J Gastroenterol* **108**, 1140-1151, doi:10.1038/ajg.2013.92 (2013).
- 345 Scudamore, C. L. *et al.* Basal secretion and anaphylactic release of rat mast cell protease-II (RMCP-II) from ex vivo perfused rat jejunum: translocation of RMCP-II into the gut lumen and its relation to mucosal histology. *Gut* **37**, 235-241 (1995).
- 346 Woodcock, J. *Center for Drug Evaluation and Research Advancing Health Through Innovation 2017 New Drug Therapy Approvals*, <<https://www.fda.gov/media/110526/download>> (2018).
- 347 Wenzel, S. E., Wang, L. & Pirozzi, G. Dupilumab in persistent asthma. *N Engl J Med* **369**, 1276, doi:10.1056/NEJMc1309809 (2013).
- 348 Lee, B. Y., Timpson, P., Horvath, L. G. & Daly, R. J. FAK signaling in human cancer as a target for therapeutics. *Pharmacol Ther* **146**, 132-149, doi:10.1016/j.pharmthera.2014.10.001 (2015).
- 349 Hardin, J. D. *et al.* Bone marrow B lymphocyte development in c-abl-deficient mice. *Cell Immunol* **165**, 44-54, doi:10.1006/cimm.1995.1185 (1995).
- 350 Simons, F. E. *et al.* World Allergy Organization Anaphylaxis Guidelines: 2013 update of the evidence base. *Int Arch Allergy Immunol* **162**, 193-204, doi:10.1159/000354543 (2013).
- 351 Sheikh, A., Ten Broek, V., Brown, S. G. & Simons, F. E. H1-antihistamines for the treatment of anaphylaxis: Cochrane systematic review. *Allergy* **62**, 830-837, doi:10.1111/j.1398-9995.2007.01435.x (2007).
- 352 Nurmatov, U. B., Rhatigan, E., Simons, F. E. & Sheikh, A. H2-antihistamines for the treatment of anaphylaxis with and without shock: a systematic review. *Ann Allergy Asthma Immunol* **112**, 126-131, doi:10.1016/j.anai.2013.11.010 (2014).
- 353 Doucet, C., Jasmin, C. & Azzarone, B. Unusual interleukin-4 and -13 signaling in human normal and tumor lung fibroblasts. *Oncogene* **19**, 5898-5905 (2000).
- 354 Dudley, A. C. Tumor endothelial cells. *Cold Spring Harb Perspect Med* **2**, a006536, doi:10.1101/cshperspect.a006536 (2012).
- 355 Wei, L. H. *et al.* Interleukin-6 promotes cervical tumor growth by VEGF-dependent angiogenesis via a STAT3 pathway. *Oncogene* **22**, 1517-1527, doi:10.1038/sj.onc.1206226 (2003).
- 356 Lo, C. W. *et al.* IL-6 trans-signaling in formation and progression of malignant ascites in ovarian cancer. *Cancer Res* **71**, 424-434, doi:10.1158/0008-5472.can-10-1496 (2011).
- 357 Bates, D. O. Vascular endothelial growth factors and vascular permeability. *Cardiovasc Res* **87**, 262-271, doi:10.1093/cvr/cvq105 (2010).
- 358 Lee, H. *et al.* STAT3-induced S1PR1 expression is crucial for persistent STAT3 activation in tumors. *Nat Med* **16**, 1421-1428, doi:10.1038/nm.2250 (2010).

- 359 Ram, P. T., Horvath, C. M. & Iyengar, R. Stat3-mediated transformation of NIH-3T3 cells by the constitutively active Q205L Galphao protein. *Science* **287**, 142-144, doi:10.1126/science.287.5450.142 (2000).
- 360 Naylor, A., Hopkins, A., Hudson, N. & Campbell, M. Tight Junctions of the Outer Blood Retina Barrier. *Int J Mol Sci* **21**, doi:10.3390/ijms21010211 (2019).
- 361 Buhner, S. & Schemann, M. Mast cell-nerve axis with a focus on the human gut. *Biochim Biophys Acta* **1822**, 85-92, doi:10.1016/j.bbadis.2011.06.004 (2012).
- 362 Barbara, G. *et al.* Activated mast cells in proximity to colonic nerves correlate with abdominal pain in irritable bowel syndrome. *Gastroenterology* **126**, 693-702, doi:10.1053/j.gastro.2003.11.055 (2004).
- 363 Koussoulas, K., Gwynne, R. M., Foong, J. P. P. & Bornstein, J. C. Cholera Toxin Induces Sustained Hyperexcitability in Myenteric, but Not Submucosal, AH Neurons in Guinea Pig Jejunum. *Front Physiol* **8**, 254, doi:10.3389/fphys.2017.00254 (2017).
- 364 Peiris, M. *et al.* Human visceral afferent recordings: preliminary report. *Gut* **60**, 204-208, doi:10.1136/gut.2010.221820 (2011).
- 365 Michel, K. *et al.* Serotonin excites neurons in the human submucous plexus via 5-HT₃ receptors. *Gastroenterology* **128**, 1317-1326, doi:10.1053/j.gastro.2005.02.005 (2005).
- 366 Pastwinska, J., Zelechowska, P., Walczak-Drzewiecka, A., Brzezinska-Blaszczyk, E. & Dastyk, J. The Art of Mast Cell Adhesion. *Cells* **9**, doi:10.3390/cells9122664 (2020).